MOLECULAR AND PHYSIOLOGICAL RESPONSES OF SOYBEAN (*GLYCINE MAX*) TO COLD AND THE STRESS HORMONE ETHYLENE

A Dissertation

Submitted to the Faculty

of

Purdue University

by

Jennifer Dawn Robison

In Partial Fulfillment of the

Requirements for the Degree

of

Doctor of Philosophy

May 2019

Purdue University

Indianapolis, Indiana

THE PURDUE UNIVERSITY GRADUATE SCHOOL
STATEMENT OF COMMITTEE APPROVAL

Dr. Stephen K. Randall, Chair

Department of Biology

Dr. Lata Balakrishnan

Department of Biology

Dr. John C. Watson

Department of Biology

Dr. Brenda J. Blacklock

Department of Chemistry and Chemical Biology

Approved by:

Dr. Theodore R. Cummins

Head of the Graduate Program

This dissertation is dedicated to my grandfather Dr. Richard Wayne Robison. Thanks for being my lifelong educational inspiration. I hope someday my students remember me as "Professor Robi" as fondly as they remember you.

ACKNOWLEDGMENTS

First and foremost, I wish to acknowledge my son Wayne for his support and help during long days and nights in lab with rarely a complaint. He spent many hours planting, watering, racking tips, and doing other general lab work to help my projects go faster. His support and encouragement have meant so much. Love you so much Boo!

My parents, Wayne and Debbie, were instrumental in this achievement, providing more behind the scenes help than anyone fully realizes, without them this would never have been possible. I am forever grateful for their selflessness to support me through this endeavor. Many thanks to my closest friends, Skye S., Melissa D., and Kent D., who have listened to me vent and encouraged me through the "why did I decide to do this!" phases of my PhD. Abundant gratitude to my unofficial editors Beronda M., Nick T., Allison B., Ian S., and Paul B. for sacrificing their time to offer feedback and advice to improve my many written projects during this dissertation.

I am thankful for the mentoring and support provided by Dr. Stephen Randall and the members of my committee. Their guidance and constructive comments have increased the quality of this work immensely. Specific thanks to Dr. Lata Balakrishnan and Dr. Catherine Njeri for their assistance and training for the protein purification and DNA binding activity work in Chapter 7. This work would not have been possible with the support of the IUPUI Biology Department, especially Dr. A.J. Baucum for allowing the use of his LI-COR Odyssey, Dr. Gregory Anderson for the use of his spectrophotometer, and last, but certainly not least, Rick Frey and Angela Longfellow who were always available to help troubleshoot all laboratory issues. The impact on my teaching strategies and abilities by Dr. John Watson, Dr. Robert Yost, Dr. Patricia Clark, and Dr. Anusha Rao can never be fully expressed. Working in Dr. Randall's laboratory was enhanced by an atmosphere laughter and joy created by all

of my current and former labmates, especially Gage K., Yuji Y., and Zach D. Without the selfless training and support of Gage and Yuji I would never have become a proficient laboratory scientist. This work would not have been possible without the generous donation of 1-MCP from Allan Green at Agrofresh and the loan of the Hansatech Handy-PEA from Tim Doyle at PP Systems.

And finally, I wish to acknowledge all of my supporters and followers on Twitter for providing motivation, amusement, and commiseration over the past 5 years. With special thanks to: @BerondaM, @asiekmanbarnes, @IHStreet, @tomeopaste, @heydebigale, @RishiMasalia, @sciencegurlz0, @melfoxphd, @vivrosati, @dr_carina_c, @PlantTeaching, @MaddieGrant, @JenniferMach2, @4Binder, @SusanCato, @Campbell_JD_PhD, @BeckSamBar, @ejfphd, @RunPipetRepeat, @ErinSparksPhD, @HJ_Thompson, @UNKBiol106, @PP_Systems, and @Conviron.

TABLE OF CONTENTS

Page

Page

Page

LIST OF TABLES

LIST OF FIGURES

Figure Page

Figure Page

Figure Page

Figure Page

Figure Page

Figure Page

Figure Page

Figure Page

ABBREVIATIONS

ψE_o	Quantum yield of electron transport
ϕE_o	Probability of electron transport into photosynthesis
γRC	Probability that a cholorphyll molecule is acting as a PSII reaction center
1-MCP	1-Methylcyclopropene
ABA	Abscisic acid
ABRE	ABA-responsive element
ABS	Absorbance
ACC	1-Aminocyclopropane-1-carboxylic acid
At	*Arabidopsis thaliana*
AVG	Aminoethoxyvinylglycine
BAM	β -amylase
bHLH	Basic helix loop helix
BR	Brassinosteroid hormones
BZR1	Brassinazole-resistant 1
CAMTA3	Calmodulin binding transcriptional activator 3
CBF/DREB	C-repeat binding factor / Dehydration responsive element binding protein
cDNA	Complementary deoxyribonucleic acid
CES	CESTA
Col-0	*Arabidopsis thaliana* ecotype Columbia
COR	Cold-regulated genes
COR15a	Cold-regulated gene 15a
COR47	Cold-regulated gene 47

CRISPR/Cas9	Clustered regularly interspaced short palindromic repeats/CRISPR-associated protein 9
CRLK1	Calcium/calmodulin-regulated receptor-like kinase 1
CRT/DRE	C-repeat/Dehydration-responsive element
CS	Cross-section
CTR1	Constitutive triple response 1
d	Days
DAK	Diacylglycerol kinase
DI_o	Dissipation of photons away from photosynthesis
DTT	Dithiothreitol
E. coli	*Escherichia coli*
EBF1/2	EIN3 binding F protein 1/2
EIN2	Ethylene-insensitive 2
EIN3	Ethylene-insensitive 3
ERD10	Early responsive to dehydration 10
ERD14	Early responsive to dehydration 14
ET_o	Electron transport
ETR1	Ethylene receptor 1
ETR	Electron transport rate
FPLC	Fast protein liquid chromatography
F_v/F_m	Quantum yield of light dependent photosynthesis
GA	Gibberellic acid
GC/MS	Gas chromatography-mass spectrometry
GFP	Green fluorescence protein
Gm	*Glycine max*
GEO	Gene Expression Omnibus
GO	Gene ontology
GUS	β-glucuronidase
HOS1	High expression of osmotically responsive genes

ICE1	Inducer of CBF expression 1
IPTG	Isopropyl-β-D-1-thiogalactopyranoside
JA	Jasmonic acid
JAZ	Jasmonate ZIM-domain
LB	Luria broth
LB+Kan	Luria broth with kanamycin sulfate
LHCII	Light harvesting complex II
MBS	MYB binding site
MCA1/2	Mid1-complementing activity 1/2
MDA	Malondialdehyde
MEKK1	Mitogen-activated protein kinase kinase kinase 1
MKK2/4/6	Mitogen-activated protein kinase kinase 2/4/6
mRNA	Messenger RNA
MUG	4-Methylumbelliferyl-β-D-glucuronide dihydrate
MW	Molecular weight
NPQ	Nonphotochemical quenching
OST	Open stomata 1
PBS	Phosphate buffered saline
PCR	Polymerase chain reaction
PI_{ABS}	Performance index of photosystem II
phyB	Phytochrome B
pI	Isoelectric point
PIF3	Phytochrome interacting factor
PNK	Polynucleotide kinase
PIP	Plasma membrane intrinsic proteins
PQ	Plastoquinone
prom	Promoter
PSI	Photosystem I
PSII	Photosystem II

qE	High energy quenching
qI	Photoinhibition
qPCR	Quantitative real time polymerase chain reaction
qT	State transition quenching
RAB18	Responsive to ABA 18
RbohF	Respiratory burst oxidase homologues F
RC	Reaction center
RNASeq	RNA sequencing
ROS	Reactive oxygen species
RT-PCR	Reverse transcription polymerase chain reaction
SDS	Sodium dodecyl sulfate
SDS-PAGE	Sodium dodecyl sulfate polyacrylamide gel electrophoresis
SSB	SDS-PAGE sample buffer
SFR2	sensitive to freezing 2
SFR6/MED16	sensitive to freezing 6/mediator 16 subunit
SIZ1	SUMO E3 ligase
SOC media	Super optimal broth with catabolite repression media
STS	Silver thiosulfate ($AgNa_3O_6S_4$)
SUMO	Small ubiquitin-like modifier
T1	First transgenic generation
T2	Second transgenic generation
T3	Third transgenic generation
TAIR	The Arabidopsis Information Resource, `www.arabidopsis.org`
TR_o	Photon trapping
WT	Wild-Type
w/v	Weight per volume
VAZ	Violaxanthin antheraxanthin zeaxanthin cycle
v/v	volume per volume
ZT	Zeitgeber Time

ABSTRACT

Robison, Jennifer Dawn Ph.D., Purdue University, May 2019. Molecular and Physiological Responses of Soybean (*Glycine max*) to Cold and the Stress Hormone Ethylene. Major Professor: Stephen K. Randall.

Abiotic stresses, such as cold, are serious agricultural problems resulting in substantial crop and revenue losses. Soybean (*Glycine max*) is an important worldwide crop for food, feed, fuel, and other products. Soybean has long been considered to be cold-intolerant and incapable of cold acclimation. In contrast to these reports, this study demonstrates that cold acclimation improved freezing tolerance in the domestic soybean cultivar Williams 82 with 50% enhancement of freezing tolerance after 5.2 ± 0.6 days of cold exposure. Decreases in light dependent photosynthetic function and efficiency accompanied cold treatment. These decreases were due to an increase in photon dissipation likely driven by a decrease in plastoquinone (PQ) pool size limiting electron flow from photosystem II (PSII) to photosystem I (PSI). Cold-induced damage to operational photosynthesis began at 25 minutes of cold exposure and maximal photosynthesis was disrupted after 6 to 7 hours of cold exposure. Cold exposure caused severe photodamage leading to the loss of PSII reaction centers and photosynthetic efficiency.

Comparisons of eight cultivars of *G. max* demonstrated a weak correlation between cold acclimation and northern cultivars versus southern cultivars. In the non-domesticated soybean species *Glycine soja*, the germination rate after cold imbibition was positively correlated with seedling cold acclimation potential. However, the overall cold acclimation potential in *G. soja* was equal to that of domestic soybean *G. max* reducing the enthusiasm for the "wild" soybean as an additional source of genetic diversity for cold tolerance.

Despite being relatively cold intolerant, the soybean genome possesses homologs of the major cold responsive CBF/DREB1 transcription factors. These genes are cold-induced in soybean in a similar pattern to that of the cold tolerant model plant species *Arabidopsis thaliana*. In Arabidopsis, EIN3, a major component of the ethylene signaling pathway, is a negative transcriptional regulator of CBF/DREB1. In contrast to *AtEIN3* transcript levels which do not change during cold treatment in Arabidopsis, we observed a cold-dependent 3.6 fold increase in *GmEIN3* transcript levels in soybean. We hypothesized that this increase could prevent effective *CBF/DREB1* cold regulation in soybean. Analysis of our newly developed cold responsive reporter (*AtRD29Aprom::GFP/GUS*) soybean transgenic lines demonstrated that inhibition of the ethylene pathway via foliar sprays (AVG, 1-MCP, and silver nitrate) resulted in significant cold-induced GUS activity. Transcripts of *GmEIN3A;1* increased in response to ethylene pathway stimulation (ACC and ethephon) and decreased in response to ethylene pathway inhibition in the cold. Additionally, in the cold, inhibition of the ethylene pathway resulted in a significant increase in transcripts of *GmDREB1A;1* and *GmDREB1A;2* and stimulation of the ethylene pathway led to a decrease in *GmDREB1A;1* and *GmDREB1B;1* transcripts. To assess the physiological effects of these transcriptional changes; electrolyte leakage, lipid oxidation, free proline content, and photosynthesis were examined. Improvement in electrolyte leakage, a measure of freezing tolerance, was seen only under silver nitrate treatment. Only 1-MCP treatment resulted in significantly decreased lipid oxidation. Transcripts for *CBF/DREB1* downstream targets (containing the consensus CRT/DRE motifs) significantly decreased in plants treated with ethylene pathway stimulators in the cold; however, ethylene pathway inhibition generally produced no increase over basal cold levels.

To identify if GmEIN3A;1 was capable of binding to *GmDREB1* promoters, the negative regulator GmEIN3A;1 and the positive regulator GmICE1A were cloned and expressed in *Escherichia coli (E. coli)*. Preliminary binding results indicated that GmEIN3A;1 can bind to a double stranded section of the *GmDREB1A;1* pro-

moter containing putative EIN3 and ICE1 binding sites. GmICE1A is capable of binding to the same section of the *GmDREB1A;1* promoter, though only when single stranded. Additional experiments will be required to demonstrate that GmEIN3A;1 and GmICE1A are capable of binding to the *GmDREB1A;1* promoter and this work provides the tools to answer these questions.

Overall, this work provides evidence that the ethylene pathway transcriptionally inhibits the CBF/DREB1 pathway in soybean through the action of GmEIN3A;1. Yet when *GmCBF/DREB1* transcripts are upregulated by ethylene pathway inhibition, no consistent change in downstream targets was observed. These data indicate that the limitation in cold tolerance in soybean is due to a yet unidentified target downstream of *CBF/DREB1* transcription.

1. INTRODUCTION

Plants must adapt to a wide variety of environmental stresses such as fluctuating temperatures, water content, and osmotic pressure. Some plants, such as Arabidopsis, are considered cold-tolerant, meaning they have the ability to acclimate to cold temperatures via changes in gene expression (Thomashow, 1999). Other plants, for example tomato (Zhang et al., 2004), peanut (Zhang et al., 2016), and soybean (Littlejohns and Tanner, 1976), are considered to be cold-intolerant and unable to acclimate to cold temperature. The physiological mechanisms that plants use to survive decreasing temperatures are of great interest to researchers with the hopes of potentially transferring cold-tolerance strategies to non-tolerant species.

Molecular responses to the cold are the result of two different pathways: abscisic acid (ABA)-dependent and ABA-independent. The ABA-dependent pathway is regulated by the phytohormone ABA which is derived from xanthoxin, a xanthophyll, and results in the activation of genes containing the ABA responsive element (ABRE) found in the promoter of some cold responsive genes (Tuteja, 2007). Cold treatment results in an increase of ABA in some plants and some cold responsive genes (those that contain an ABRE); however, the ABA-independent pathway has been demonstrated to have a greater impact on cold tolerance (Pirzadah et al., 2014; Roychoudhury et al., 2013; Sah et al., 2016; Thomashow, 1999).

The ABA-independent pathway is primarily driven by the CBF/DREB (C repeat binding factor/dehydration response element binding factor) cold responsive pathway (Figure 1.1). *CBF/DREB* gene family members encode AP2 transcription factors that regulate cold and drought responses (Medina et al., 1999; Stockinger et al., 1997). Arabidopsis has four CBF genes, *AtCBF1*, *AtCBF2*, *AtCBF3* (also known as *AtDREB1B, AtDREB1C, AtDREB1A* respectively) and *AtCBF4* (*AtDREB1D*). *AtCBF1 - 3* are in tandem on chromosome 4 (Gilmour et al., 1998) and *AtCBF4* is on

chromosome 5 (Haake et al., 2002). Cold stress induces the up-regulation of *AtCBF1 - 3* (Medina et al., 1999), while *AtCBF4* is more responsive to drought stress (Haake et al., 2002; Liu et al., 1998). Overexpression of *AtCBF1 - 3* in Arabidopsis leads to an increase of downstream transcripts and enhanced freezing survival (Jaglo-Ottosen et al., 1998). Conversely, when *AtCBF1 - 3* were knocked out via CRISPR/Cas9, Arabidopsis seedlings were hypersensitive to cold stress (Jia et al., 2016).

Transcriptome analysis via RNASeq revealed 414 CBF-regulated genes in Arabidopsis, with 346 up-regulated and 68 down-regulated (Zhao et al., 2016) during cold stress. AtCBF1 - 3 directly regulate the expression of about 15% of cold responsive genes, collectively known as the CBF regulon (Fowler and Thomashow, 2002; Park et al., 2015; Vogel et al., 2005), demonstrating the importance of this pathway.

1.1 The CBF/DREB1 Cold Pathway

When plants encounter low temperatures, the earliest detected effects are a decrease in membrane fluidity and a transient increase in cytosolic calcium (Knight et al., 1991; Orvar et al., 2000). This transient cytosolic calcium pulse is thought to trigger kinase cascades that may be important in the activation of transcription factors (Figure 1.1). Recent work in Arabidopsis identified two mechanosensitive channels, MCA1 and MCA2, which are critical for the cold-induced calcium influx (Mori et al., 2018). Calcium is required for the phosphorylation of MEKK1 by CRLK1 during the early cold response in Arabidopsis (Furuya et al., 2013). MEKK1 phosphorylates a MAP kinase cascade, MKK2-MKK4/6, resulting in the expression of cold responsive genes (Teige et al., 2004). The pathway between kinase activation and CBF activation remains murky. However, it is known that CAMTA3 (calmodulin binding transcriptional activator 3) transcriptionally regulates *AtCBF1* and *AtCBF2* genes (Doherty et al., 2009), while AtICE1 (inducer of CBF expression) regulates primarily *AtCBF3* and to a lesser extent *AtCBF1* and *AtCBF2* (Chinnusamy et al., 2003).

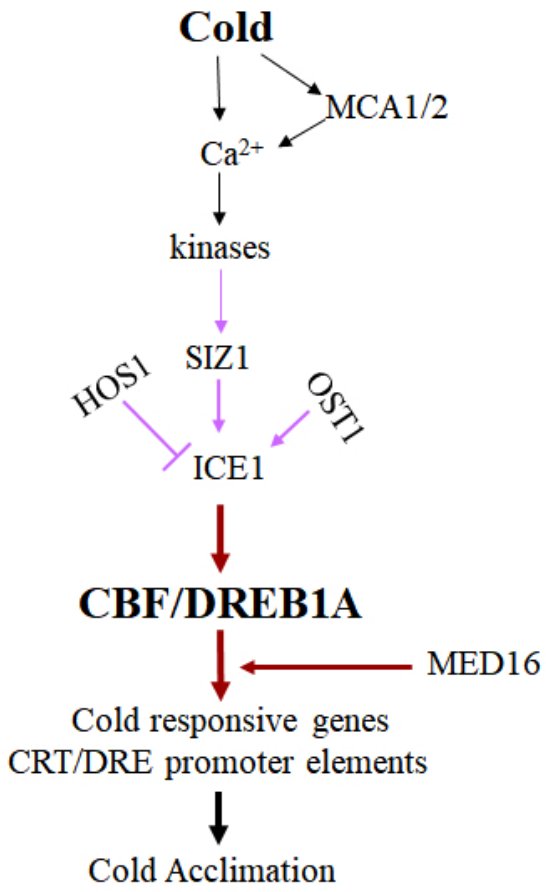

Fig. 1.1. Illustration of the CBF/DREB1 Cold-Responsive Pathway. Purple arrows indicate post-translational regulation, red arrows indicate transcriptional regulation. See text for full description.

AtICE1 (Figure 1.1) is on chromosome 3 and codes a predicted protein of 494 amino acids with a molecular mass of 53.5 kDa and contains a MYC-like bHLH domain in the C-terminal region (Chinnusamy et al., 2003). AtICE1 is constitutively produced in the cell but ubiquitination by HOS1 (high expression of osmotically responsive gene 1) results in degradation thus preventing ICE1 activation of its downstream targets (Dong et al., 2006). Conversely, sumoylation by SIZ1, a SUMO E3 ligase, stabilizes ICE1 allowing it to activate *AtCBF3* (Miura et al., 2007). Another layer of regulation of ICE1 is provided by OST1 (open stomata 1), a Ser/Thr ki-

nase, which phosphorylates ICE1 stabilizing the protein (Ding et al., 2015). OST1 also binds the C-terminus of HOS1 preventing the binding of ICE1 and its subsequent ubiquitination (Ding et al., 2015). AtICE1 binds to the MYC-recognition sites (CANNTG) found in the promoters of *AtCBF1 - 3* (Chinnusamy et al., 2003). AtICE2 is regulated similarly to AtICE1 and is likely to be redundant as it also regulates *AtCBF1 - 3* (Kim et al., 2015).

It has been suggested that ICE1 and ICE2 regulate all three CBFs based on a study of *ice1/2* knockouts (Kim et al., 2015). In Arabidopsis seedlings that were not acclimated to cold, there was no change in survival rate or electrolyte leakage between wild-type and the *ice* knockouts. However, when seedlings were cold acclimated, both *ice1* single and *ice1/ice2* double knockout had significantly lower survival rates and higher electrolyte leakage indicating ICE1 plays a role in cold acclimation but not basal freezing tolerance. Additionally, *CBF3* and *CBF2* expression were markedly reduced in *ice1* mutants while *CBF2* was the only CBF to be markedly reduced in the *ice2* mutant. Kim et al. (2015) have suggested that ICE2 plays a role in attenuating the cold response by creating a feedback loop to ensure the upregulation of *AtCBF2*. Supporting this contention that CBF2 is a negative regulator of the CBF/DREB cold pathway, increased freezing tolerance is observed in *cbf2* knockout mutants (Novillo et al., 2004). Additionally, a significant increase in *CBF1* and *CBF3* transcripts were observed in the *cbf2* knockouts leading to increased downstream targets and cold tolerance (Novillo et al., 2004). These data support the hypothesis that ICE2 and CBF2 attenuate the cold response.

Cold stress induces significant upregulation of *AtCBF1, AtCBF2*, and *AtCBF3* (Figure 1.1) transcripts within 15 minutes with maximal expression between 2 - 4 h (Gilmour et al., 1998). *CBF1 - 3* transcript levels remain elevated, though lower than maximal, for 21 days (Zarka et al., 2003). *CBF* transcripts are turned over rapidly with an estimated half-life of 7.5 minutes (Zarka et al., 2003). The CBF protein (Figure 1.1) binds to the CRT/DRE (C-repeat/dehydration responsive element) consensus sequence CCGAC, which is found in the promoter of many cold respon-

sive genes (Jaglo-Ottosen et al., 1998; Stockinger et al., 1997). These CRT/DRE containing target transcripts significantly increase between 4 - 24 h after on-set of cold (Gilmour et al., 1998). The regulation of CRT/DRE genes by CBF requires the mediator 16 (MED16) subunit of the mediator complex (Hemsley et al., 2014; Knight et al., 2009, 1999) for successful RNA polymerase recruitment and transcription of downstream target genes (Figure 1.1).

Overexpression of *CBF1* or *CBF3* in Arabidopsis induces cold responsive transcripts in the absence of cold, as well as increases cold tolerance as evidenced by decreased electrolyte leakage and increased freezing survival (Gilmour et al., 2000; Jaglo-Ottosen et al., 1998). In addition to increased cold tolerance, overexpression of CBFs results in biochemical and physiological changes. Dwarfism occurs due to increased GA2-oxidase expression which inactivates gibberellic acid (GA) leading to the accumulation of DELLA proteins which repress plant bolting and leaf expansion (Achard et al., 2008; Lee et al., 2002; Peng et al., 1997; Silverstone et al., 1998). Exogenous application of GA rescues dwarfism resulting from CBF overexpression (Achard et al., 2008). Late flowering has been observed with CBF overexpression (Gilmour et al., 2004; Liu et al., 1998; Seo et al., 2009) and linked with increased FLC (flowering locus c) which suppresses flowering (Seo et al., 2009). Plants overexpressing CBF genes have lower seed production compared to wild type (Gilmour et al., 2000; Liu et al., 1998). Conversely, when all 3 *CBF* (*cbf123*) genes are knocked out in wild-type Arabidopsis via CRISPR/Cas9, the mutant plants had significantly lower germination, shorter roots, and smaller leaves, but no difference was noted in fresh weight (Jia et al., 2016; Zhao et al., 2016). These mutants were more sensitive to freezing stress after acclimation with 0% survival at -7 °C compared to 60% survival for wild type (Jia et al., 2016). These results indicate CBF transcription factors must be tightly regulated to balance plant growth with cold survival.

The circadian clock also impacts *CBF* regulation. Under normal conditions, CBF transcript levels are regulated by central clock transcription factors, peaking 8 hours after dawn (ZT8) (Lee and Thomashow, 2012). Plants grown under short days have a

3 - 5 fold higher *CBF* transcript levels versus long day plants (Lee and Thomashow, 2012). Chloroplast signaling also contributes to the circadian expression of CBFs (Norn et al., 2016). Diurnal cycling of tetrapyrrole levels within the plastid begin a signaling pathway that leads to the repression of *CBF*s (Norn et al., 2016). During cold stress, there are greater levels of *CBF* transcript produced during daylight hours (Fowler et al., 2005).

In addition to the circadian clock, light plays a role in cold sensing via photoreceptors (Jung et al., 2016; Kurepin et al., 2013; Legris et al., 2016; Maibam et al., 2013). PhytochromeB (phyB) is activated by red light and inactivated by far red light and warm temperatures (Legris et al., 2016). As the temperature decreases, the proportion of active phyB increases leading to the activation of cold responsive genes (Jung et al., 2016). Conversely, PIF3 (phytochrome-interacting factor3) negatively regulates the CBF pathway by directly binding to *CBF* promoters downregulating their expression (Jiang et al., 2017).

Finally, hormone signaling regulates CBF-dependent cold signaling. Brassinosteroid (BR) hormones play an important role in regulating plant growth, development, and metabolism (Zhu et al., 2013). These hormones activate a suite of transcription factors, two of which directly control transcription of *CBF* (Eremina et al., 2016; Li et al., 2017). Treatment with BR increases cold tolerance due to the BR-induced post-translational modification of CES (Eremina et al., 2016) and/or BZR1 (Li et al., 2017). The phytohormone jasmonate also positively regulates cold tolerance. Exogenous application of jasmonate increases cold tolerance and upregulates *CBF* and its downstream targets (Hu et al., 2013). The interaction of jasmonate signaling and CBF signaling occurs at ICE1. JAZ (jasmonate ZIM-domain) proteins are negative regulators of the jasmonate signaling pathway. JAZ proteins directly interact with ICE1 repressing the transcriptional functionality of ICE1 and decreasing the activation of CBF signaling. In the cold, endogenous jasmonate production results in degradation of JAZ proteins relieving the inhibition of ICE1 and increasing the CBF pathway (Hu et al., 2013).

The role of salicylic acid in cold treatment is still under investigation. In tomato, salicylic acid treatment protects the fruit from chilling injury by regulating GA and increasing *CBF1* expression resulting in the degradation of DELLA proteins indicating a positive role of salicylic acid to cold stress (Ding et al., 2016). However in watermelon, CBF levels were decreased by salicylic acid treatment during chilling stress indicating a negative role of salicylic acid in CBF signaling (Cheng et al., 2016). It was also noted in watermelon that while CBF levels decreased, photosynthetic yield and electrolyte leakage were improved by salicylic acid suggesting a positive role for salicylic acid in cold signaling that is controlled by a non-CBF dependent pathway (Cheng et al., 2016).

The phytohormone ethylene negatively regulates cold tolerance. *AtCBF1 - 3* are negatively regulated by EIN3, a transcription factor within the ethylene synthesis pathway, as evidenced by the increase in CBF transcripts in *ein3* knockout mutants (Shi et al., 2012). In the ethylene signaling pathway EBF1/2 target EIN3 and PIF3 for proteasome-mediated degradation (Street and Schaller, 2016; Jiang et al., 2017). These results indicate that EBF1 and 2 are important for the maintenance of cold signaling due to their role in the degradation of two transcriptional inhibitors of CBF.

Important downstream targets of CBF include several members of the dehydrin family, for example, *ERD10, ERD14, RAB18,* and *COR47* (Koehler et al., 2007; Nylander et al., 2001). Dehydrins are group 2 late embryogenesis abundant (LEA) proteins with varying numbers of 3 conserved motifs, K, S and Y, with the distributions K_n, SK_n, K_nS, Y_nSK_n, and Y_nK_n and 90 - 95% intrinsically disordered structure (Close, 1996; Hannah et al., 2006). Overexpression of dehydrins in Arabidopsis results in increased freezing tolerance in both cold-acclimated and noncold-acclimated, plants (Puhakainen et al., 2004). The exact mechanisms of freezing tolerance conferred by dehydrins is unknown, but ERD14 and ERD10 have been suggested to have chaperone and membrane stabilizing roles *in vitro* (Kovacs et al., 2008). Phosphorylation of ERD14 is important to regulate binding of calcium and other ions which may play a role in membrane interactions, buffering, or removing the calcium signaling pathway

to down-regulate CBF (Alsheikh et al., 2003, 2005; Chacha, 2014). Regardless of the mechanism, CBF-controlled dehydrin expression is important for successful cold tolerance making dehydrins important aspects of research.

Additionally, carbohydrate metabolic genes play an important role in cold tolerance. Galactinol synthases (GolS) have been shown to be important for cold and other abiotic stress tolerance. In Arabidopsis, GolS3 regulates the levels of galactinol, raffinose, and stachyose (Taji et al., 2002). Overexpression of *AtCBF1 - 3* results in significant increases in *GolS3* transcripts and sugar production (Gilmour et al., 2004). When *TaGolS* from wheat (*Triticum aestivum* is constitutively expressed in rice (*Oryza sativa*), it confers increased cold-tolerance (Shimosaka and Ozawa, 2015) likely due to the increased sugar content.

The CBF/DREB1 cold pathway is also involved in the regulation of other transcription factors. In *cbfs* triple knockout plants, 39 transcription factors decrease in the cold compared to wild-type Arabidopsis (Zhao et al., 2016). Eleven of these transcription factors were AP2-type transcription factors and 7 were involved in hormonal signaling (Zhao et al., 2016). These results suggest that CBF/DREB1 is controlling an extensive network of cellular pathways via transcription factor regulation.

Beyond dehydrins, GolS, and other transcription factors, CBF/DREB1 also regulates cell wall modification, chloroplast processes, oxidative stress response, and lipid metabolism (Zhao et al., 2016). Considering the CBF/DREB1 cold pathway directly controls 15% of cold responsive genes (Park et al., 2015), only a select few were reviewed above.

1.2 Physiological responses of cold treated plants

The exact mechanisms by which cold tolerance occurs remain incompletely characterized but cellular and metabolic changes have been reported. Photosynthesis is disrupted by cold temperatures, exhibiting decreased electron transport rates, increased closed photosystem II (PSII) reaction centers, and decreased photosystem

I (PSI) activity (Savitch et al., 2001). These data all indicate a misregulation of electron movement through the photosystems and beyond. The repair rate for PSII reaction centers is severely depressed during cold stress (Allakhverdiev and Murata, 2004; Nath et al., 2013). Moreover *de novo* synthesis of the D1 protein is suppressed (Allakhverdiev and Murata, 2004) and processing the D1 precursor into mature D1 is inhibited (Kanervo et al., 1997) leading to a lack of new PSII reaction center formation during cold stress. The ability to efficiently turnover and repair PSII reaction centers, primarily at the level of the D1 protein, is often the limiting factor in photosynthetic performance (Murata et al., 2007).

The production of reactive oxygen species (ROS) is both beneficial and harmful for cold stressed plants. It has been demonstrated that ROS can act as signaling molecules (Suzuki and Mittler, 2006); however, they can be very damaging to cells, including lipid damage (O'Kane et al., 1996), alteration to protein structure and function (Dietz, 2015, 2016), and DNA alteration leading to strand breakage (Roldan-Arjona and Ariza, 2009). In Arabidopsis the NADPH oxidase AtRbohF (respiratory burst oxidase homologues F) activity is activated by cytosolic calcium, an early indicator of cold stress, and this activity is enhanced by the binding of AtSRC2 (Arabidopsis homologue of soybean gene regulated by cold-2) which accumulates in the cold (Kawarazaki et al., 2013). The resulting burst of ROS is essential for cold tolerance as it primes the system to produce antioxidant related genes to moderate the oxidative damage prolonged cold can induce (Hossain et al., 2015; Wang et al., 2018, 2010).

Alterations in membrane structure and carbohydrate composition have been characterized (Ristic and Ashworth, 1993). In cold, both phospholipase Dδ and diacylglycerol kinase (DAK) are activated to facilitate the conversion of lipids to phosphatidic acid (Li et al., 2004; Vaultier et al., 2006). Phosphatidic acid increases within minutes of cold exposure primarily driven by DAK (Arisz et al., 2013). Increasing levels of phosphatidic acid in plasma membranes stimulate the CBF/DREB regulon, NADPH oxidase activity, and enhance hydrogen peroxide production (Tan et al., 2018). Be-

yond lipid restructuring, protein membrane composition changes as well. Plasma membrane-associated aquaporins and plasma membrane intrinsic proteins (PIPs) are downregulated during cold stress, possibly to prevent desiccation from water loss (Peng et al., 2008).

Exposure to cold results in chloroplast structure change including increased density of stroma, increased number of thylakoids per grana, distorted thylakoids, increased invaginations in the membrane, and the appearance of stromules which are projections from the chloroplast which may contact other organelles (Venzhik et al., 2016). The membrane-associated enzyme SFR2 (sensitive to freezing 2) facilitates stabilization of outer chloroplast membranes (Roston et al., 2014). SFR2 is a galactolipid remodeling enzyme that alters the lipid composition to prevent formation of non-bilayer structures (Moellering et al., 2010). It has been demonstrated that cytosolic acidification and increases in Mg^{2+} are involved in cold sensing by activating SFR2 (Barnes et al., 2016). The inner chloroplast membrane is stabilized by the translocation of COR15a which alters the intrinsic curvature of the membrane to prevent freezing-related damage (Steponkus et al., 1998).

A significant connection has been reported between cold and freezing tolerance with metabolite content (Guy et al., 2008). Polysaccharides play a role in membrane permeability and stability during cold stress (Tarkowski and Van den Ende, 2015). Increases in sugar content, particularly sucrose, have been significantly correlated with increases in freezing tolerance (Hannah et al., 2006; Strand et al., 2003). Sucrose accumulation is driven by the increase in sucrose phosphate synthase (Guy et al., 1992). Sucrose interacts with lipid headgroups in cell membranes decreasing membrane permeability (Strauss and Hauser, 1986). Fructose is transported via vesicle to the plasma membrane where it can be inserted between headgroups to stabilize the membrane (Valluru et al., 2008; Van den Ende, 2013). In the citrus *Poncirus trifoliata*, starch catabolism by the chloroplast-localized β-amylase PtrBAM1 increases soluble sugar levels within the cells during cold stress (Peng et al., 2014). The promoter of *PtRBAM1* contains a CRT/DRE that PtrCBF interacts with during cold

stress. This provides a direct link between sucrose metabolism and the CBF/DREB pathway (Peng et al., 1997). In addition to membrane stabilization, increased sugar level effects include lowering osmotic potential leading to a decreased freezing point inside the cell (O'Neill S, 1983), suppression of ice nucleation formation (MacKenzie, 1977), and reduced inhibition of photosynthesis (Strand et al., 2003).

The accumulation of free proline within cold treated plant cells has been observed repeatedly (Borowski and Michalek, 2014; Chu et al., 1978; Gilmour et al., 2000; Jouve et al., 1993; Xin and Browse, 1998). Overexpression of *CBF/DREB* genes results in proline accumulation even in the absence of cold (Gilmour et al., 2004, 2000). Like sucrose, proline has been demonstrated to lower the osmotic potential inside the cell (Hare and Cress, 1997; Yoshiba et al., 1997) and provide membrane stabilization (Heber et al., 1973). Unlike sucrose, proline is also a nonenzymatic antioxidant, as well as a source of metabolic energy after stress (Hare and Cress, 1997). Proline is an efficient quencher of singlet oxygen radicals (Alia et al., 2001, 1997) and scavenger of hydroxyl radicals (Alia et al., 1997; Kaul et al., 2008; Smirnoff and Cumbes, 1989). Redox potential is balanced by proline metabolism during stress (Giberti et al., 2014; Hare et al., 1998; Sharma et al., 2011) specifically by the oxidation of two NADPH molecules to $NADP^+$ via synthesis of proline from glutamate within the chloroplast (Szkely et al., 2008). The regeneration of $NADP^+$ restores the pool of electron acceptors available to light-dependent photosynthesis. Combining this with the fact that proline can decrease reactive oxygen species within the thylakoid (Alia et al., 1997), it seems likely that proline synthesis is important to prevent photoinhibition during cold periods.

1.3 Soybean Cold Stress Responses

Abiotic stresses, such as cold, are serious issues for agriculture, estimated to cause over 50% of crop losses worldwide (Qin et al., 2011). In the United States, soybean (*Glycine max*) is the second most valuable crop, worth $38.7 billion in 2012 (USDA-

NASS, 2014). Soybean, like tomato, is considered a cold-intolerant species, incapable of any significant response to enable survival during periods of low temperatures (Hume and Jackson, 1981; Littlejohns and Tanner, 1976). Cold stress has a significant impact on survival and yield for soybean, but this impact varies based upon the length and developmental timing of the cold treatment. During reproductive stages, a drop in nighttime temperatures below 17 °C can result in decreases in seed weight and seed yield (Seddigh et al., 1988). Additionally, exposure to 8 °C for 24 hours delays flowering for 7 days, decreases soluble carbohydrates, and partitions biomass towards vegetative shoots instead of flowering and seed set (Wang et al., 1997). Light-dependent photosynthesis is impaired by the cold due to a loss of PSII reaction centers and reduced electron transport through the photosystems (Van Heerden and Kruger, 2000; Van Heerden and Krger, 2002; Van Heerden et al., 2003). Fixation of carbon dioxide by the Calvin cycle is decreased by 87% after one night of 8 °C (Van Heerden and Kruger, 2000).

While not considered cold-tolerant, soybean does possess CBF (GmDREB) homologs. Seven CBF/DREB1 homologs (*GmDREB1A;1, GmDREB1A;2, GmDREB1B;1, GmDREB1B;2, GmDREB1C;1, GmDREB1D;1*, and *GmDREB1D;2*) are spread across 7 chromosomes in the soybean genome (Yamasaki and Randall, 2016). Transcripts of *GmDREB1A;1/2* and *GmDREB1B;1/2* are transiently upregulated during cold stress in a similar expression pattern to that seen in Arabidopsis (Kidokoro et al., 2015; Yamasaki and Randall, 2016), yet downstream target genes are not up-regulated (Yamasaki et al., 2013). When constitutively expressed in Arabidopsis, *GmDREB1A;1, GmDREB1A;2, GmDREB1B;1*, and *GmDREB1B;2* are each sufficient to up-regulate the endogenous Arabidopsis cold responsive genes such as *AtERD14* and *AtRD29a* in the absence of cold (Kidokoro et al., 2015; Yamasaki and Randall, 2016) and to confer cold tolerance (Yamasaki and Randall, 2016). These data suggest that *GmDREB1* genes are either misregulated or otherwise unable to upregulate downstream targets in soybean.

Cultivated tomato (*Solanum lycopersicum*), also has homologs of *CBF1 - 3* despite its cold-intolerant status, but only *SlCBF1* was induced in the cold while *SlCBF2* and *SlCBF3* were not (Zhang et al., 2004). While transformation with *SlCBF1* induced endogenous cold responsive genes and freezing tolerance in Arabidopsis, when *AtCBF3* was transformed into tomato only 4 out of the 8700 genes tested by microarray were affected with no increase in freezing tolerance (Zhang et al., 2004). However, a later study noted that transformation of *AtCBF1* in tomato does relieve photoinhibition caused by low temperature (Zhang et al., 2011). This has led to the hypothesis that *SlCBF* targets no longer have appropriate promoter elements. This may also be the case with soybean, though this has not been tested, as *AtCBF* has not been expressed in soybean to see if cold tolerance is conferred. The soybean dehydrin gene *GmERD14*, as well as other genes, do appear to have potential CRT/DRE sequences (Yamasaki et al., 2013) and thus would be predicted to respond to *AtCBF*s.

Differential regulation of the CBF signaling pathway in soybean compared to Arabidopsis may result in soybean's inadequate response during cold periods. One such difference was noted in the ethylene signaling pathway (Yamasaki, 2013). In early cold treatment of soybean, RNASeq analysis revealed differential regulation of the soybean *EIN3* transcript (Yamasaki, 2013) compared to that of Arabidopsis (Shi et al., 2012). Soybean *EIN3* transcripts are increased by cold temperatures (Yamasaki, 2013) while no change is observed in Arabidopsis **?**. As EIN3 is a negative regulator of the CBF cold pathway in Arabidopsis (Shi et al., 2012), the observed increase in soybean EIN3 levels may play a role in soybeans lack of cold tolerance.

1.4 Ethylene pathway and crosstalk with cold stress

Ethylene is a versatile phytohormone that regulates a wide range of developmental and environmental responses (Street and Schaller, 2016). In the absence of ethylene, CTR1 (constitutive triple response1), phosphorylates EIN2 (ethylene-insensitive 2) so that it remains inactive (Figure 1.2). However, when ethylene binds to the en-

doplasmic reticulum-membrane-bound ethylene receptor ETR1, CTR1 is deactivated (Figure 1.2). This results in proteolytic cleavage of EIN2, a serine/threonine Raf-like kinase, and translocation of the C-terminal fragment to the nucleus where it stabilizes EIN3 so that it is no longer degraded by EBF1/2 SCF ligases (Gallie, 2015; Ju and Chang, 2015). EIN3 is a transcription factor that binds to the consensus sequence ATGYATNY found in the promoters of ethylene responsive genes (Boutrot et al., 2010; Konishi and Yanagisawa, 2008). EIN3 plays a regulatory role in several pathways, including, but not limited to, wounding, sulfur deficiency signaling, iron homeostasis, and cold response (Shi et al., 2012; Song et al., 2014; Wawrzyska and Sirko, 2016; Yang et al., 2014; Zhao and Guo, 2011).

Ethylene regulation has a varied impact on cold stress across, and even within, species. In Arabidopsis, Shi et al. (2012) showed that EIN3 can negatively affect cold tolerance, as *EIN3* over-expression mutants have an increased sensitivity to freezing, while ein3 knockouts have an increased freezing tolerance. It has also been noted that the Arabidopsis ethylene overproducer mutant *eto1-3* has enhanced freezing tolerance (Catal and Salinas, 2015). Ethylene production has been linked to increased cold tolerance in grapevine (Sun et al., 2016) and tomato (Ciardi et al., 1997), while ethylene decreases cold tolerance in *Medicago truncatula* (Zhao et al., 2014), Bermuda grass (Hu et al., 2016), and tobacco (Zhang and Huang, 2010). The wide variety of roles ethylene plays in cold tolerance throughout the plant kingdom requires each species be evaluated.

The perception of ethylene and biosynthesis of ethylene can be chemically modulated. Stimulation of the ethylene signaling pathway is accomplished using 1-aminocyclopropane-1-carboxylic acid (ACC) or ethephon (2-Chloroethylphosphonic acid, $C_2H_6ClO_3P$). ACC is the biological precursor to ethylene in the biosynthetic pathway via the action of ACC oxidase (Wang et al., 2002), while ethephon spontaneously decomposes to ethylene at physiological pH (Zhang and Casida, 2002). Aminoethoxyvinylglycine (AVG), 1-methylcyclopropene (1-MCP), and silver ionic compounds are used to inhibit the ethylene pathway. AVG inhibits ACC synthase,

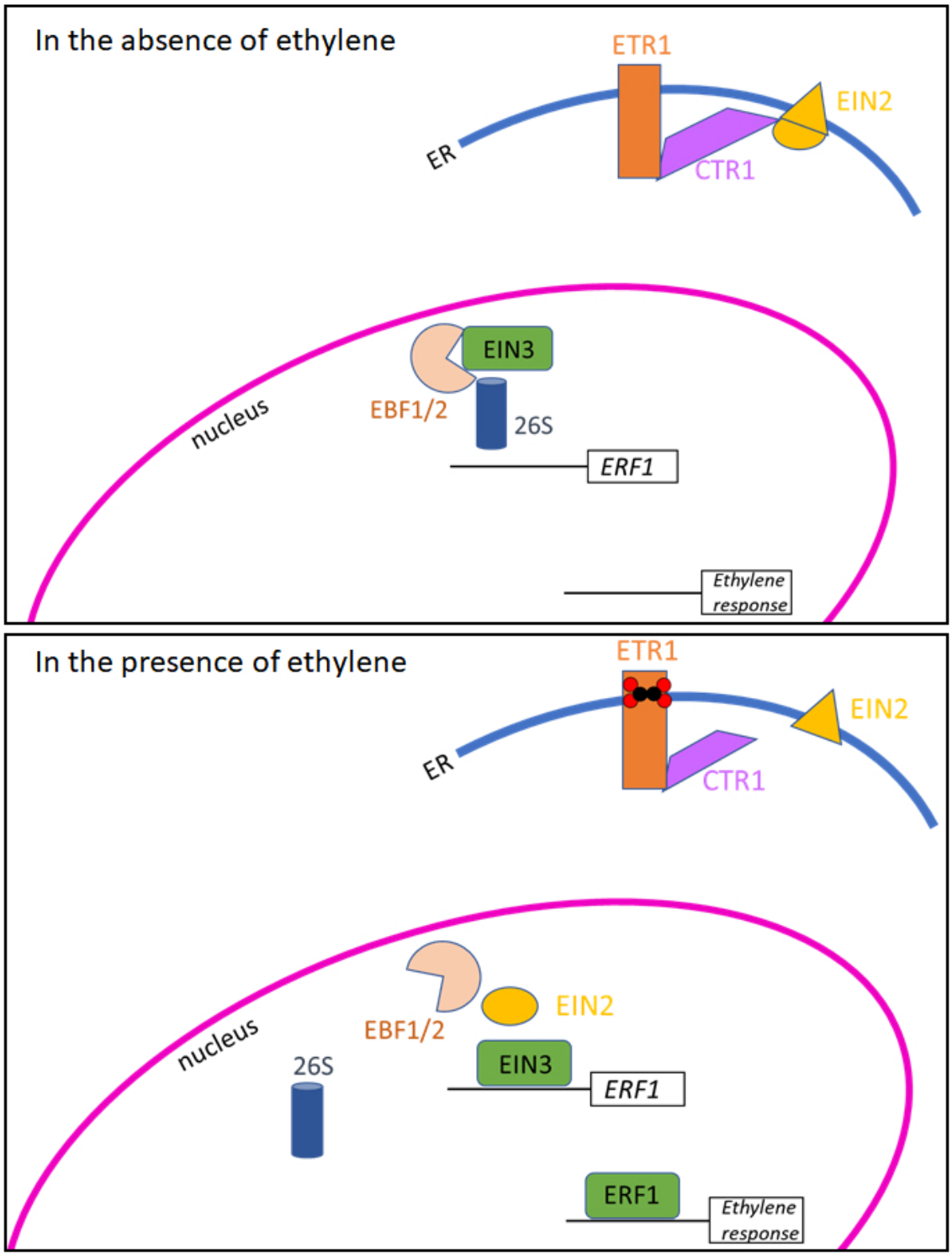

Fig. 1.2. Illustration of the ethylene signaling pathway, in the absence of ethylene (top) and in the presence of ethylene (bottom). See text for full description.

the rate limiting enzyme in the ethylene biosynthesis pathway, which produces ACC (Street and Schaller, 2016). 1-MCP is a competitive inhibitor for ethylene receptors, and silver ions are known to replace the copper ion within the ethylene receptor active site preventing activation even if ethylene is bound (Schaller and Binder, 2017).

The ethylene pathway in soybean has been well characterized at the reproductive stages. During early soybean reproduction (stage R1), inhibition of ethylene signaling with silver thiosulfate (STS), an ethylene perception inhibitor, resulted in a 56% increase in seed yield while stimulation of ethylene by application of ethephon, an ethylene releaser, decreased seed yield by 50% and increased floral abscission rates (Cheng, 2013). Manipulation of ethylene homeostasis has several impacts on other hormonal pathways of reproductive age soybeans. Ethephon and STS treatments have opposite effects on the signaling pathways of auxin, abscisic acid, gibberellic acid, jasmonic acid, and salicylic acid (Cheng et al., 2013). Auxin, abscisic acid, and jasmonic acid signaling were increased with ethephon treatment, while gibberellic acid and salicylic acid signaling were stimulated by STS treatment (Cheng et al., 2013). Exposure to the ethylene perception inhibitor 1-MCP prior to heat stress resulted in increased chlorophyll content, increased photosynthetic efficiency, decreased ROS generation, and membrane damage compared to non-treated soybean (Djanaguiraman and Prasad, 2010). While much is known about ethylene signaling effects in mature reproductive soybean, little information is available for the impact on younger soybean plants or the potential for crosstalk with cold signaling.

1.5 Study Goals

This dissertation examines the responses of soybean to cold stress across different ecotypes to test whether if soybean is indeed completely cold intolerant as indicated by Littlejohns and Tanner (1976). Additionally, this dissertation attempts to identify the molecular mechanisms underlying the limited ability of soybean to cold acclimate,

particularly with respect to the differential expression of ethylene signaling genes in soybean compared to Arabidopsis.

2. MATERIALS AND METHODS

2.1 General Growth Conditions

For seed production, soybean were planted in a mix of equal parts top soil, potting soil, and compost then grown in a greenhouse until seeds were harvested. For experimental samples, soybean seeds were planted in moist potting soil (BX Mycorrhhizae^{TM}, ProMix®) and grown in a controlled environmental chamber (Conviron) with 180 - 200 μmol m^{-2} s^{-1} of light on a 16:8 hour light:dark cycle at 22 °C.

2.1.1 Abiotic Stress

Soybean seedlings were grown for 10 - 12 d prior to sampling. Sampling occurred 4 hours after the light cycle started (Zeitgeber Time + 4 hours (ZT+4)). One unifoliate from each of the four to six individual plants were collected and combined into a single replicate. Cold 0 d plants were collected at the start of the experiment and immediately frozen in liquid nitrogen. Cold 1 d treated plants were placed at 4 °C for 24 hours prior to collection and freezing in liquid nitrogen. Wounding treatments were applied with a 1 cm diameter cork borer to create leaf discs which were then floated in water for either 0 d or 1 d before collection and freezing in liquid nitrogen. Plants to be treated with abscisic acid (ABA) were sprayed until runoff with 1 mM ABA (Sigma A1049) in 0.01% ethanol. Ethanol mock controls for the ABA experiment were sprayed with 0.01% ethanol only. After 1 d, unifoliate leaves were collected, flash frozen in liquid nitrogen and stored at -80 °C until analysis.

For Arabidopsis, seeds were planted in moist soil and cold stratified for 2 d at 4 °C in the dark then grown for a month prior to experimentation. Growth conditions and sampling methods were the same as those described above except that two rosette

leaves from two different individual plants were combined into a single replicate and a 0.5 cm diameter cork borer was used to create leaf discs.

2.1.2 Ethylene Inhibitors and Stimulators

To examine the impact of ethylene on soybeans cold pathways, seedlings were grown 10 - 12 d prior to the start of experimentation. Seedlings were sprayed with 1 mM silver nitrate (Fisher), 100 ppm 1-MCP (AgroFresh), 100 μM AVG (Sigma), 1 mM ACC (Calbiochem), 1.38 mM ethephon (Sigma) or water until run-off at both 24 hours before and immediately prior to the start of cold treatment. All of the solutions listed previously were made with Milli-Q water. Cold treatments were performed at 5 °C for 48 hours. All samples were flash frozen in liquid nitrogen and stored at -80 °C until analysis.

2.2 Establishment and Evaluation of Abiotic Stress Soybean Reporter Lines

2.2.1 Transgenic Soybean Creation

The Arabidopsis *RD29A* promoter region (1,477 bp upstream of the start codon) was analyzed using plantCARE to identify stress responsive motifs (Lescot et al., 2002). This promoter was PCR amplified from Arabidopsis and cloned into pCambia1304 driving mGFP/GUS using Zero Blunt® PCR Cloning Kit (ThermoFisher). This construct (AtRD29Aprom::GFP/GUS) was then digested with EcoR1 and BamHI and ligated into pTF101.1 by Yuji Yamasaki. The plasmid was introduced into Agrobacterium (strain EHA101) and used to transform half-seed explants cv Williams 82. Glufosiante resistance conferred by the bar gene which encodes phosphinothricin acetyltransferase (Thompson et al., 1987) was used for selection (Hu et al., 2013). The transformation and recovery of transgenic soybeans was performed by the Iowa State University Plant Transformation Facility (`http://ptf.agron.iastate.edu`).

2.2.2 Glufosinate Resistance Assay

The bar gene was used to screen plants for the presence of the construct. Herbicide resistance was measured in 2 week old soybean seedlings by placing 0.1% glufosinate (Finale®, Bayer) directly onto the midrib of a single unifoliate leaf (Zhang et al., 1999). Tissue damage was scored as low to marginal damage (no damage to brown spots less than 1 mm in diameter) indicating resistant plants and moderate to high damage (brown spots greater than 1 mm in diameter with yellowing to tissue death) indicating susceptible plants (Figure 2.1).

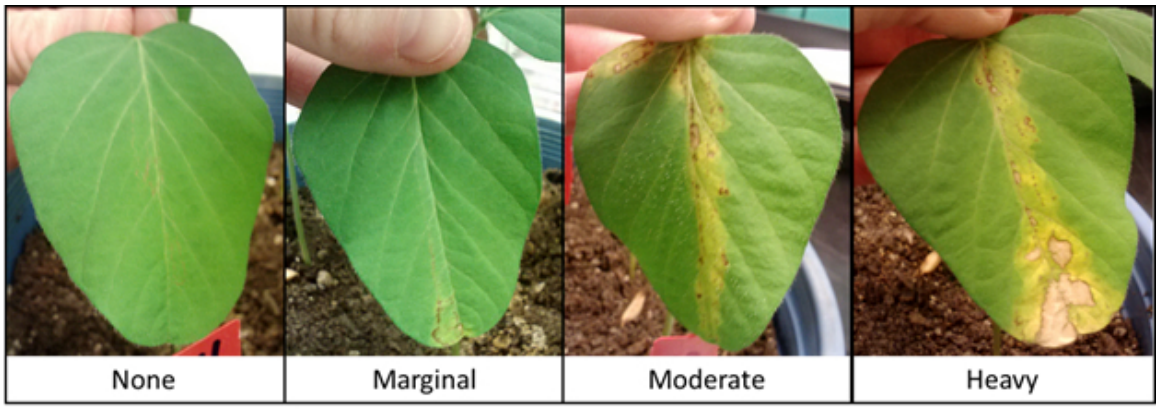

Fig. 2.1. Representative images of glufosinate treated transgenic soybean showing the range from resistant (none and marginal) to susceptible (moderate and heavy).

2.2.3 Screening Transgenic Plants for Identification of Homozygous Lines

Each individual plant's T2 seeds were harvested and stored at 4 °C. T2 seeds were randomly planted in soil containing an equal mixture of top soil, potting soil, and compost then grown in a growth chamber under the general growth conditions described in section 2.1. After 14 d, T2 seedlings were tested for the presence of the transgene via glufosinate resistance assay to identify individuals for T3 seed generation.

Soybeans that showed glufosinate resistance were transferred to the greenhouse during fall 2013 and spring 2014. The resulting T3 seeds from each individual were harvested and stored at 4 °C. T3 seeds were screened to identify homozygote lines via glufosinate evaluation. Initially, eight seeds were planted and scored. If no susceptible plants were identified in the original eight, an additional 30 - 40 seeds were planted and screened to confirm homozygosity of the parent. This screening resulted in the identification of three independently transformed homozygous lines (ST-164-17-9, ST-164-22-23, and ST-164-28-5).

2.2.4 Polymerase Chain Reaction (PCR) Conditions for Genotyping Transgenic Soybean

DNA was isolated from 0.05 g of frozen leaf tissue using Plant DNAzol® Reagent (Invitrogen), following the manufacturer's instructions. GoTaq® (Promega) master mix and polymerase, 200 nM primers (Table 1), and 50 ng of sample DNA were used in each reaction. Reactions were denatured at 94.0 °C for 2 min, then amplified with 22 - 35 cycles (as indicated in Table 2.1) consisting of 94.0 °C for 30 sec, 60 °C for 45 sec and 72.0 °C for 60 sec, followed by final extension at 72.0 °C for 5 min on a thermocycler (GeneAmp PCR System 2400, Perkin Elmer) before storage at -20 °C. Samples were resolved on a 1% Agarose gel stained with ethidium bromide.

Table 2.1.
PCR primers and conditions used for genotyping of ST-164-# lines via PCR.

Target	Primer name	Primer sequence	Product size (bp)	Cycle number
GUS	pCambia1304 + 2134GUS	AATAAACGGTTCAGGCACAGC	964	22
	pCambia1304 + 1170GUS	GGTGATTACCGACGAAAACG		
GmERD14	Gm TC203260 upper	CAATTGAATTCTCCAGAGAGAAGA	1058	35
	Gm TC203260 lower	AAAACAAAGCACACCACAATCAT		

2.3 Fluorometric GUS Assay

The GUS assay procedure is modified from Yoo et al. (2007) and Fior et al. (2009). Leaves were crushed with a metal spatula in liquid nitrogen. From the crushed leaves, 0.1 g was weighed out and ground in liquid nitrogen with a mortar and pestle. The powder was then ground in 1.5 mL microfuge tubes with a motorized pestle for 60 s in 300 μl of lysis buffer (2.5 mM Tris-phosphate (pH 7.8) with 1 mM DTT, 2 mM EDTA, 10% (v/v) glycerol, and 0.1% (v/v) Triton X-100). After centrifugation at 10,000 xg for 10 minutes at 4 °C, the supernatant was removed. Total soluble protein content was determined via Bradford Assay (Bradford, 1976). To assess GUS activity levels, 10 μg of total protein was combined with 100 μl MUG (4-Methylumbelliferyl-β-D-glucuronide dihydrate) substrate (10 mM Tris-HCl (pH 8), 1 mM MUG, and 2 mM $MgCl_2$) in a black bottom 96 well plate. Fluorescence was measured every minute for 1 h at 37 °C on a Spectramax M2 ® (Molecular Devices) with excitation at 360 nm and emission at 460 nm. GUS activity was calculated from the linear slope of the fluorescence readings using the software environment R `https://www.r-project.org/` (R Core Team, 2013). For reference, wild-type soybean leaves have an average GUS activity of -0.97 ± 0.34 with a range of -0.6 to -1.35.

2.4 Generation of cDNA

RNA was extracted from 100 mg powdered leaf tissue with RNeasy ® Plant Mini Kit (Qiagen), treated with DNase (Qiagen), following the manufacturer's instructions. RNA was quantified on a NanoDrop ® spectrophotometer (Thermo Scientific). Complementary DNA was synthesized from 500 ng of RNA with SuperScript ® III First-Strand Synthesis (Invitrogen) following manufacturer's instructions.

2.5 Protein Quantification via Western Blots

After tissue was ground in liquid nitrogen, 50 mg of leaf powder was extracted in 2X hot SSB (80 mM Tris-HCl pH 6.8, 2.0% SDS, 10% glycerol, 0.006% bromphenol blue) plus protease inhibitors (1mM Benzamidine, 1 μg mL^{-1} aprotinin (Sigma), l μM pepstain A (Sigma), and 1 μg mL^{-1} leupeptin (Sigma)) and total protein concentration was determined via amido black (Kaplan and Pedersen, 1985). Ten μg of soluble proteins was separated on 12% acrylamide gels (Laemmli, 1970) prior to electrophoretic transfer to 0.45 μm nitrocellulose membrane (GVS North America). Membranes were blocked with 5% (v/v) milk in PBS prior to probing with primary antibodies (source and dilution as indicated in figure legends) followed by Alexa Fluor® 790 donkey anti-rabbit (1:10,000, Life Technology) secondary antibody. Bands were visualized with the Odyssey ® CLx Imaging System (LI-COR Biosciences) and quantified using Image Studio Lite 5.2 (LI-COR Biosciences).

2.6 Photosynthetic Parameters

Chlorophyll *a* transient curves were measured using a Plant Efficiency Analyzer (Handy-PEA, Hansatech). Fluorescence signal was recorded over 1 s of irradiation with an excitation light of 650 nm at 3600 μmol m^{-1} s^{-1}. Unifoliate leaves were dark adapted for 10 minutes with the provided clips with the Handy-PEA. Clips were placed on the right side of the midrib approximately halfway between the leaf tip and base. Leaves were constrained perpendicular to light to avoid leaf movement conditions that may interfere with photosynthesis measurements. There were nine unifoliate leaves from nine individual plants recorded for each condition.

2.7 Pigment Content

Chlorophyll content was measured using a modification of Warren (2008). Briefly, leaves were ground in liquid nitrogen. Seventy 70 was mixed with 0.7 mL of ice-cold

methanol (Sigma). The tube was vigorously vortexed prior to for 5 minutes incubation with rotation at 4 °C in the dark. Supernatant was collected via centrifugation at 10,000 rpm for 4 min at 4 °C in the dark. The supernatant was saved at -20 °C in the dark while the pellet was re-extracted with methanol. The two supernatants were combined and 200 μL was added to a clear bottom 96 well microplate (Fisher) which was read at 470, 652, and 665 nm on the SpectraMax M2® spectrophotometer with PathCheck^{TM} using a methanol cuvette reference (Molecular Devices). Chlorophyll a and b were calculated using the equations in Warren (2008).

2.8 Proline Content

Proline was measured using the ninhydrin method (Bates et al., 1973). Briefly, leaf tissue (50 mg) previously collected, flash-frozen in liquid nitrogen, and stored at -80 °C was pulverized and then extracted with 15 volumes of ethanol:water (4:6) overnight at 4 °C. The ninhydrin reagent (200 μL) was heated to 95 °C with 100 μL of extract for 20 min. Following cooling and a centrifugal spin to remove particulates, the absorbance of 200 μL aliquot was measured with a microplate reader (SpectraMax M2® spectrophotometer, Molecular Devices) at 520 nm. A standard curve was generated from 0 - 30 nmoles proline. Data was averaged from 3 biological replicates (with each replicate composed of 3 - 4 plants).

2.9 Lipid Peroxidation Measurements

Lipid peroxidation was measured using the 2-thiobarbituric acid-reactive substances assay which measures malondialdehyde (MDA) concentration (Sharmin et al., 2012). Briefly, 50 mg of soybean leaf tissue was homogenized with a motorized pestle in 0.5 mL of 20% trichloroacetic acid, 0.01% butylated hydoxytoluene, and 0.65% 2-thiobarbituiric acid. The samples were boiled at 95 °C for 30 min before incubation on ice for 2 minutes. After centrifugation at 3,000 xg for 10 min, samples were read at 440, 453, and 600 nm on a SpectraMax M2® spectrophotometer using PathCheck^{TM}

with cuvette reference of buffer with no sample added (Molecular Devices). MDA concentration was calculated using the equations of Hodges et al. (1999) to adjust for sucrose interference.

2.10 Soybean Ethylene and CBF/DREB pathway phylogeny

RNASeq was performed as described in Yamasaki and Randall (2016). RNASeq data can be found on NCBI GEO (Accession # GSE117686). A GO analysis (Ashburner et al., 2000; Consortium, 2017) was used to identify ethylene genes regulated by cold treatment. The predicted protein sequences of these genes were retrieved from Soybase ver. 2.1 `https://soybase.org` (Grant et al., 2010) for soybean, and The Arabidopsis Information Resource (TAIR) `https://www.arabidopsis.org` (Lamesch et al., 2012) for Arabidopsis. Clustal Omega (Sievers et al., 2011) was used to compare protein sequence similarity. A phylogenetic tree to visualize the predicted protein sequences of Arabidopsis and soybean genes was generated and annotated with a heatmap by utilizing Interactive Tree of Life, `https://itol.embl.de/` (Letunic and Bork, 2016) visualizing the log2 fold change of transcripts measured in the RNASeq analysis (Yamasaki and Randall, 2016) for soybean and microarray data from Kilian et al. (2007) for Arabidopsis.

2.11 Promoter analysis for *GmDREB1s*

The promoter regions for *GmDREB1A;1, GmDREB1A;2, GmDREB1B;1, GmDREB1B;2* (*Glyma.09g147200, Glyma.16g199000, Glyma.20g155100, Glyma.10g239400* respectively) and Arabidopsis *CBF3* (*At4g25480*) were analyzed to identify potential binding sites for EIN3 and ICE1. All soybean sequences were acquired by copying 1 - 1.5kb upstream of the start codon from Soybase, `https://soybase.org` (Grant et al., 2010) for soybean genes and the Arabidopsis CBF3 sequence was acquired from TAIR, `https://www.arabidopsis.org` (Lamesch et al., 2012). Each promoter region was analyzed for the EIN3 binding sequence $\mathrm{ATG}^{T}/_{C}\mathrm{ATN}^{T}/_{C}$ (Boutrot et al., 2010), and

the ICE1 binding sequence CANNTG (Chinnusamy et al., 2003) using the Sequence Manipulation Suite, `http://www.bioinformatics.org/sms2` (Stothard, 2000).

2.12 Plasmid Extraction

Two hundred mL of *E. coli* culture was collected via centrifugation at 5,000 rpm for 15 minutes at 4 °C with the JA-10 Fixed-Angle Rotor (Beckman Coulter). The pellet was resuspended in 12 mL of GTE (50 mM Glucose, 25 mM Tris, and 10 mM EDTA, pH 8.0) with 5 mg/mL lysozyme. The sample was mixed by inverting three times and incubated for 5 minutes at room temperature. Twelve mL of 0.2 NaOH/1% SDS was added. The sample was mixed by inverting three times and incubated for 5 minutes on ice. To the sample, 7.5 mL of cold 3 M potassium (5M) acetate was added. The sample was mixed by inverting three times and incubated 15 minutes on ice. The pellet and supernatant were separated by centrifugation at 12,000 rpm for 20 minutes at 4 °C with the JA-20 Fixed-Angle Rotor (Beckman Coulter)

The supernatant was carefully removed and measured so that 0.6 volumes of 100% isoproponal could be added. The sample was mixed by inverting three times and incubated 15 minutes at room temperature. The pellet was collected by centrifugation at 12,000 rpm for 15 minutes at 4 °C with the JA-20 Fixed-Angle Rotor. The pellet was rinsed with ice cold 70% ethanol. The pellet was allowed to air-dry 10 minutes. The pellet was resuspended with 1.8 mL TE (25 mM Tris, and 10 mM EDTA, pH 8.0). The sample was split in half (900 μl) and 300 μl 10 M ammonia acetate was added. The samples were mixed by inverting 3 times then incubated on ice for 10 minutes. The supernatant was separated from the pellet by centrifugation at 3,500 rpm for 15 minutes at 4 °C in a microcentrifuge (Eppendorf).

The supernatant was divided into 400 μL aliquots and 800 μL of ice cold 100% ethanol was added. The samples were left on ice for at least 20 minutes; however, the samples can also be left overnight at -20 °C. The pellets were collected by centrifugation at 15,0000 rpm for 5 minutes at 4 °C in a microcentrifuge. The pellets were

washed twice with 500 μL ice cold 70% ethanol. The pellets were allowed to air-dry for 15 minutes. The pellets were combined into a single fraction of 800 μL TE. The samples were divided into two fractions of 400 μL each. The samples were incubated with 10 μg/mL DNase-free RNase A (ThermoFisher) and incubated 15 minutes at 50 °C. To each sample, 400 μL 3 M NaCl and 400 μL 39% PEG-8000 1.5 M NaCl was added. Samples were mixed and incubated for at least 30 minutes on ice or stored overnight at -20 °C.

The pellets were collected by centrifugation at 15,000 rpm for 15 minutes at 4 °C in a microcentrifuge. The supernatants were removed and centrifugation was repeated for 2 minutes. The pellets were resuspended in 1x protinase K buffer with a final concentration of 0.5 mg/mL protinase K (Invitrogen). The samples were incubated for 30 minutes at 37 °C. To each tube, 200 μL 25:24:1 phenol:chloroform:isoamyl alcohol was added. The samples were mixed well prior to centrifugation at 15,000 rpm for 2 minutes at 4 °C in a microcentrifuge. The aqueous (upper) layer was collected. To each tube, 200 μl of nuclease free water was added. The samples were mixed well prior to centrifugation at 15,000 rpm for 2 minutes at 4 °C in a microcentrifuge. The second aqueous (upper) phase was combined with the first aqueous phase. The samples were separated into 350 μL aliquots and 133 μL 10 M ammonium acetate and 933 μl ice cold 100% ethanol was added. The samples were mixed well and incubated at least 1 hour; however, the samples can also be left overnight at -20 °C.

The pellets were collected by centrifugation at 15,000 rpm for 15 minutes at 4 °C in a microcentrifuge. The pellets were washed twice with 200 μl ice cold 70% ethanol. The pellets were allowed to air-dry for 15 minutes. The pellets were combined into 50 μL nuclease free water. DNA concentration was measured with the NanoDrop® spectrophotometer (Thermo Scientific).

2.13 Labeling oligonucleotides with radioactive ^{32}P

The following were added to a microfuge tube in this order: 25 μL nuclease free water, 4 μL 10x PNK buffer, 2 μL of 10 pmol/μL nucleotide, 8 μL γ^{32}ATP (80 μCi), and 1 μL polynucleotide kinase (PNK, Thermo Scientific). The reaction was incubated at 37 °C for 1.5 hours. The reaction was filtered through a Micro Bio-Spin P-30 Tris Chromatography column (BioRad). The column containing the unincorporated radioactive ATP was discarded appropriately. The flow-through was transferred to a fresh tube and 750 μL 95% ethanol, 12.5 μl 10 M sodium acetate and 3 μ PelletPaint® (Novagen) was added. The reaction was stored at -80 °C for at least 1 hour and up to overnight.

The pellet was recovered by centrifugation at 13,000 rpm for 20 minutes at 4 °C in a microcentrifuge. The pellet was washed with 500 μL 70% ethanol. The pellet was resuspended in 20 μL TE and stored at -20 °C. The concentration of radioactive DNA is 100 femtomole/μL.

3. THE COLD ACCLIMATION POTENTIAL OF SOYBEAN

The purpose of this study was to investigate potential differences in cold acclimation within the domesticated *Glycine max* and non-domesticated *Glycine soja* varieties with a goal to determine whether introgression of "wild" species might be advantageous for creating more cold tolerant domestic cultivars. It has been reported that *G. max* is cold intolerant (Littlejohns and Tanner, 1976); however, there was no information regarding *G. soja* in the literature. The following represents the major findings reported in this work which was published in 2017 (Robison et al., 2017) and reprinted in Appendix A.

Cold acclimation was assessed by electrolyte leakage in eight cultivars of *G. max* and six accessions of *G. soja*. After exposure to cold temperatures, all 14 soybean varieties showed a significant improvement in subsequent exposure to freezing demonstrating soybean is capable of cold acclimation and acquiring cold tolerance. This study showed that contrary to previous reports, soybean seedlings have some ability to cold acclimate. Germination rates following cold imbibition were also examined. In *G. soja*, cold imbibition germination rates moderately correlated with cold acclimation potential as measured by electrolyte leakage ($r = 0.7$). This was not the case for *G. max* where no correlation was noted. To determine if there was a link between unsaturated fatty acids and germination after cold imbibition, total fatty acid content was examined in 14 *G. max* cultivars and 6 *G. soja* accessions. Overall *G. max* has a higher percentage of oleic acid (18:1) than *G. soja*, while *G. soja* has a higher percentage of linolenic acid (18:2) in total fatty acid content. There was a significant positive correlation between linoleic acid levels and germination rates after cold imbibition in *G. soja* alone ($r = 0.9$, $p < 0.01$). These results suggest that domestication has not impacted the overall cold tolerance potential of soybean. There

is likely no apparent source of additional cold tolerance within the genome of the non-domesticated soybean *G. soja* (Figure 3.1).

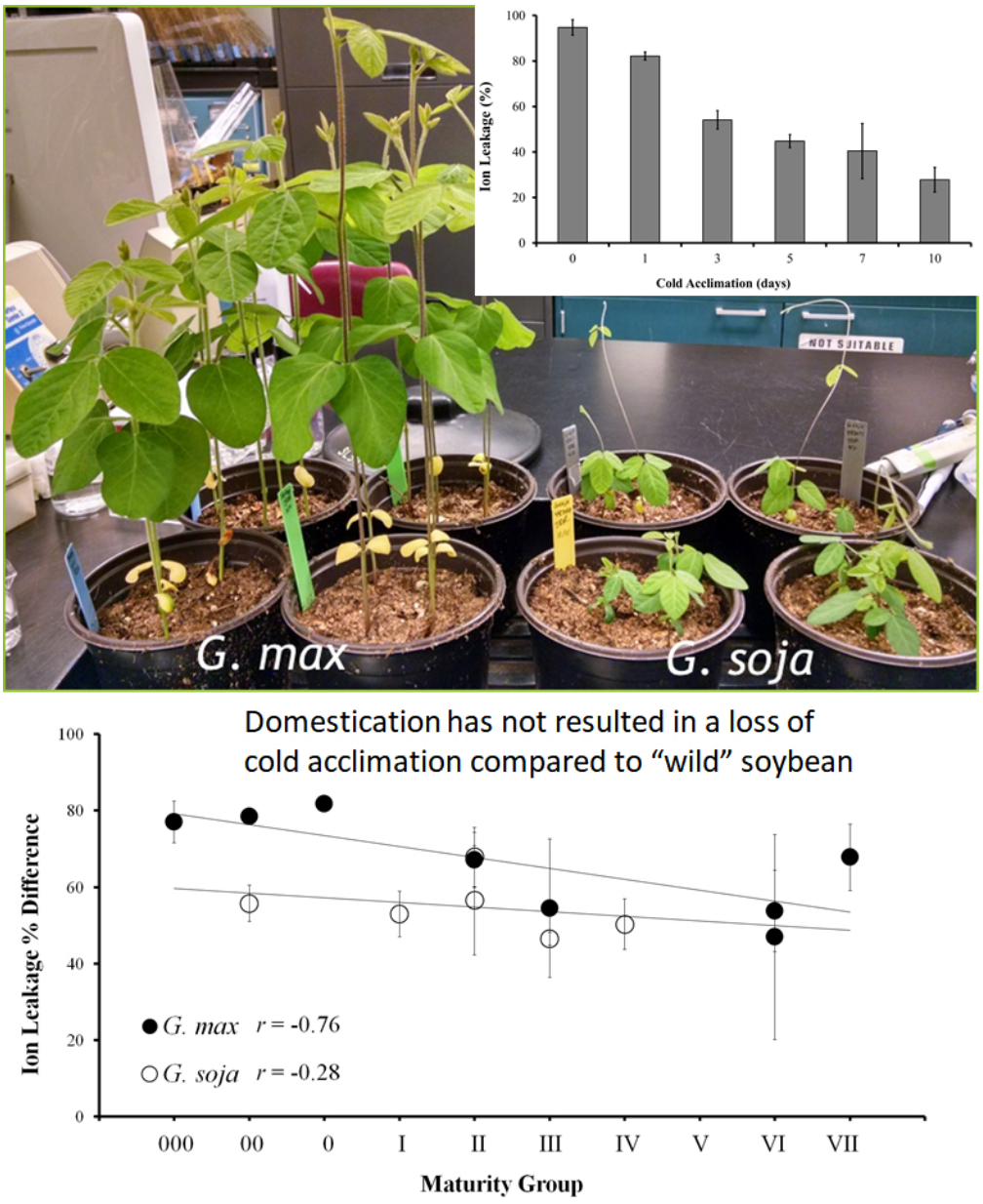

Fig. 3.1. Graphical abstract of cold acclimation potential of *G. max* and *G. soja* from Robison et al. (2017).

Electrolyte leakage assays were performed by myself and M. Saito under my supervision. Seed fatty acid compositions were performed by N. Arora under the supervision of B. Blacklock and S. Randall. Imbibition and germination assays were performed by both N. Arora under S. Randall's supervision and J. Boone under my supervision. Protein content in seeds was established by N. Arora under the supervision of S. Randall. Protein content in cold acclimated and non-cold acclimated leaves was performed by myself.

4. ESTABLISHING AN ABIOTIC STRESS RESPONSIVE STRESS REPORTER SYSTEM IN SOYBEAN

In order to examine cold stress within our species of interest, soybean, it was necessary to create a tool that would allow us to efficiently examine abiotic stress in soybean, and in particular cold stress. Due to soybeans relatively long reproductive time, 3 - 5 months from seed to seed, and the notorious low transformation rate, <1 % (Paz et al., 2004), it is impractical to create a multitude of transgenic soybean lines to investigate every gene. The generation of large datasets, such as transcriptomics or proteomics, requires the investment of significant time and money. To overcome these challenges, we designed an abiotic stress reporter soybean line which can be used to answer many questions surrounding soybean stress responses. The creation of this tool allows us to investigate the impact of various treatments upon abiotic stress responses with a minimal amount of time and money invested. To achieve this, we utilized the highly stress responsive promoter of the Arabidopsis gene *RD29A* (Kasuga et al., 2004).

4.1 Design and Initial Evaluation of Transgenic Soybean

The *AtRD29A* promoter was analyzed with Plant-CARE (Lescot et al., 2002) and shown to possess two CGTCA wounding elements (-1,346, -171 bp), one MBS drought responsive element (-967 bp), three CRT/DRE cold responsive elements (-353, -303, -246 bp), and one ABRE ABA responsive element (-145 bp) within the 1,477 upstream base pair region chosen for use in transgenic soybean (Figure 4.1A). This work was done by J. Robison. The *AtRD29A* promoter was amplified from Arabidopsis and cloned into pCambia1304 to drive mGFP/GUS. The *AtRD29Aprom::GFP/GUS* construct was then cloned into PTF101.1 plasmid for *Agrobacterium* transformation. This work was done by Y. Yamasaki. This construct was subsequently transformed

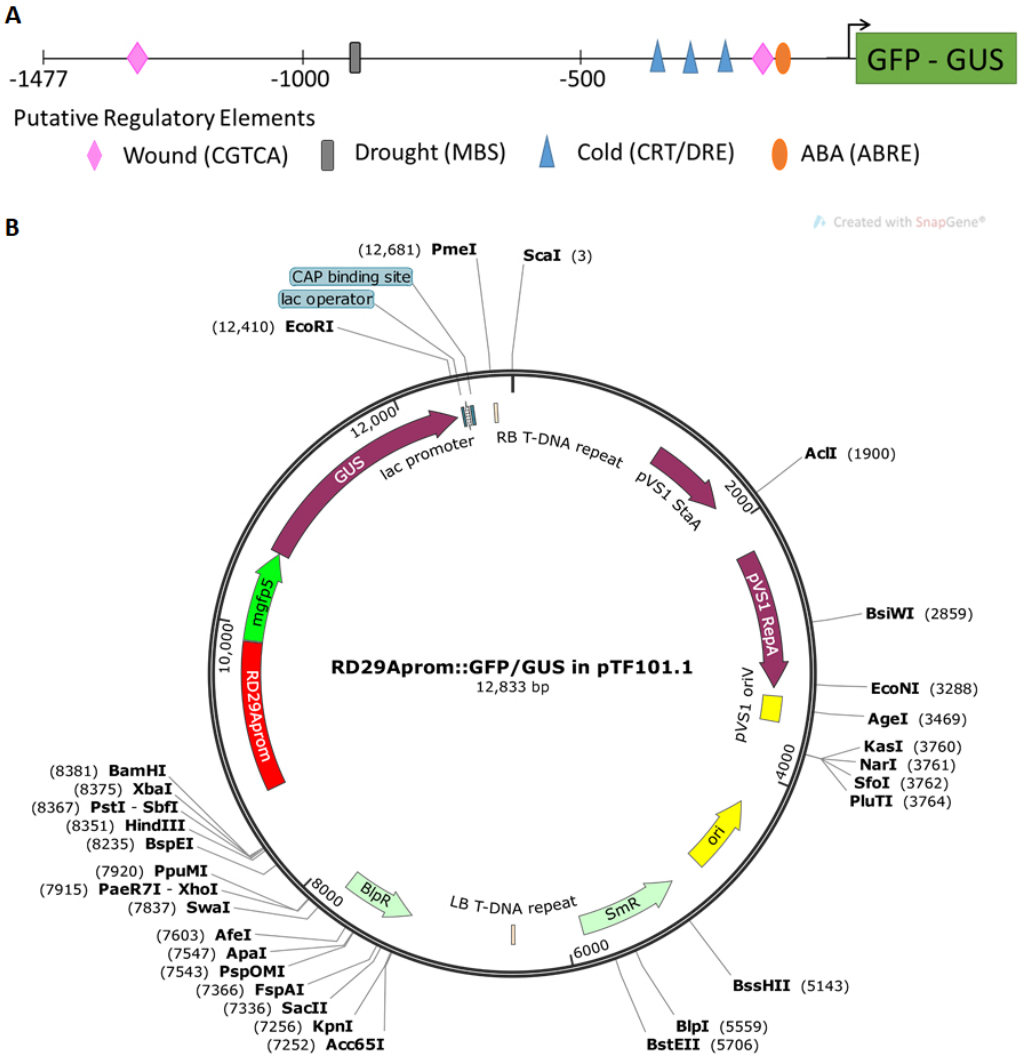

Fig. 4.1. *AtRD29Aprom::GFP/GUS* construct and plasmid utilized for transforming *G. max.* A) J. Robison's promoter analysis using PlantCARE revealed the presence of 3 CRT/DRE, 2 CGTCA, 1 MBS, and 1 ABRE in the AtRD29A promoter. B) Plasmid map of PTF101.1 showing the location of the inserted *RD29Aprom::GFP/GUS* promoter. Construct was created by Y. Yamasaki. Graphic was created by J. Robison [SnapGene software (from GSL Biotech; available at `https://www.snapgene.com`)]

into the soybean cultivar Williams 82. The transformations were performed by the Iowa State Plant Transformation Facility. A low number of seeds (4) from lines -17, -22, -24, and -28 had undergone glufosinate screening at Iowa State Plant Transformation Facility before shipment to IUPUI.

Seeds from seven independent transformants (ST-164-#) were planted in the greenhouse in summer of 2013. After 30 days, the plants were analyzed for the presence of GUS activity in trifoliate leaves via fluorometric analysis (Figure 4.2, methodology in 2.3). This was the first screening performed of these lines after their receipt from the Iowa State Plant Transformation Facility. As seen in Figure 4.2, GUS activity was absent in all individual plants line -6 (only four seeds were obtained from transgenic facility) and all individuals in line -24 (only six individuals). All plants tested from line -5 (five individuals) were positive for GUS expression. There were variable responses in the rest of the lines. Line -17 had three individuals with positive GUS activity levels out of the nine individuals tested. Line -22 had three individuals with positive GUS activity out of the seven individuals tested. Line -28 had nine individuals with positive GUS activity levels out of the eleven individuals tested. Line -39 had nine individuals with positive GUS activity levels out of twelve individuals tested (Figure 4.2).

4.1.1 Genotypic Analysis of T1 Transgenic Soybean

The presence or absence of the *GUS* transgene was used to further verify transformed lines. The *GUS* gene within the construct was amplified by PCR (methodology in chapter 2.2.4) in every individual in line -5, while there was no amplification observed for any individual in line -6 (Figure 4.3A). This was consistent with the GUS fluorometric analysis results (Figure 4.2). In line -17, GUS activity was only detected in three individuals (Figure 4.2); however, the *GUS* gene was present in seven out of nine individuals (Figure 4.3B). In line -22, *GUS* was amplified in six out of seven individuals (Figure 4.3C) of which only three demonstrated basal GUS

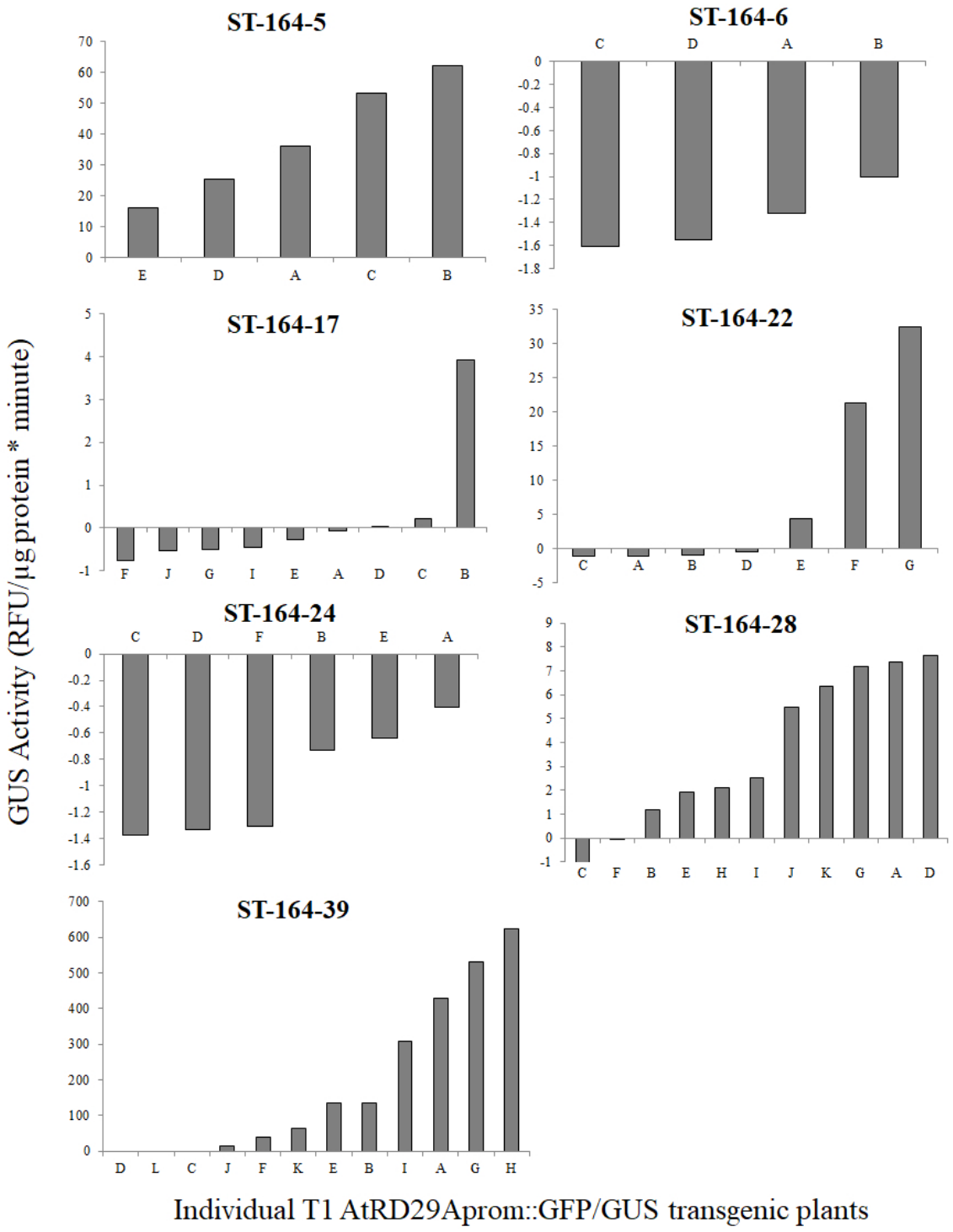

Fig. 4.2. Characterization of basal GUS activity level in a trifoliate from single plants (identified by a letter) in T1 hemizygous *AtRD29Aprom::GFP/GUS* transgenic soybean lines. As each column represents a single individual, there are no standard deviations to express. For reference, wild type soybean leaves have an average GUS activity of -0.97 ± 0.34 with a range of -0.6 to -1.35.

activity (Figure 4.2, 4.3E). Despite no basal GUS activity levels being detected in line -24 (Figure 4.2), the *GUS* gene was detected in all six individuals (Figure 4.3D). In line -28, the *GUS* gene was amplified in all nine individuals that had positive basal GUS activity levels (Figure 4.2) and not found in the two individuals which did not have detectable GUS activity levels (Figure 4.2, 4.3E). In line -39, the *GUS* gene was detected in all twelve samples (Figure 4.3F), but basal GUS activity was detected in only nine individuals (Figure 4.2).

To ensure the lack of detected *GUS* gene was due to the fact that the gene was not present, and not poor DNA quality or contamination, the presence of the endogenous *GmERD14* was confirmed in all *GUS* negative samples (Figure 4.3G). Line ST-164-6 was not examined any further due to the lack of GUS activity, *GUS* gene detection, and low seed numbers. Additionally, lines ST-164-5 and ST-164-24 were not examined further due to low seed stock numbers.

4.1.2 Cold-Induced Reporter Activity in T1 Transgenic Soybean

Cold stress was performed to investigate whether the homogeneity (i.e., that basal levels of expression of GUS activity were similar in all individuals) of T1 transgenic soybeans was sufficient to provide quantitative data. As reported in previous sections, preliminary analysis of the T1 generation showed a wide range of basal GUS activity under greenhouse growth conditions. However, it was unknown if this generation would have a similar high variability under cold conditions. The increase due to cold-induction may be large enough to mask the basal differences. It was thought worthwhile to test if the variability would be within acceptable ranges so that experiments could be initiated immediately and not wait for months to years to obtain stable homozygous lines.

Cold induction of GUS expression was examined in T1 plants for three of the *AtRD29Aprom::GFP/GUS* transgenic soybean lines (ST-164-22, -28, -39) which possessed basal, GUS level and had a high seed stock. Since this is the first generation

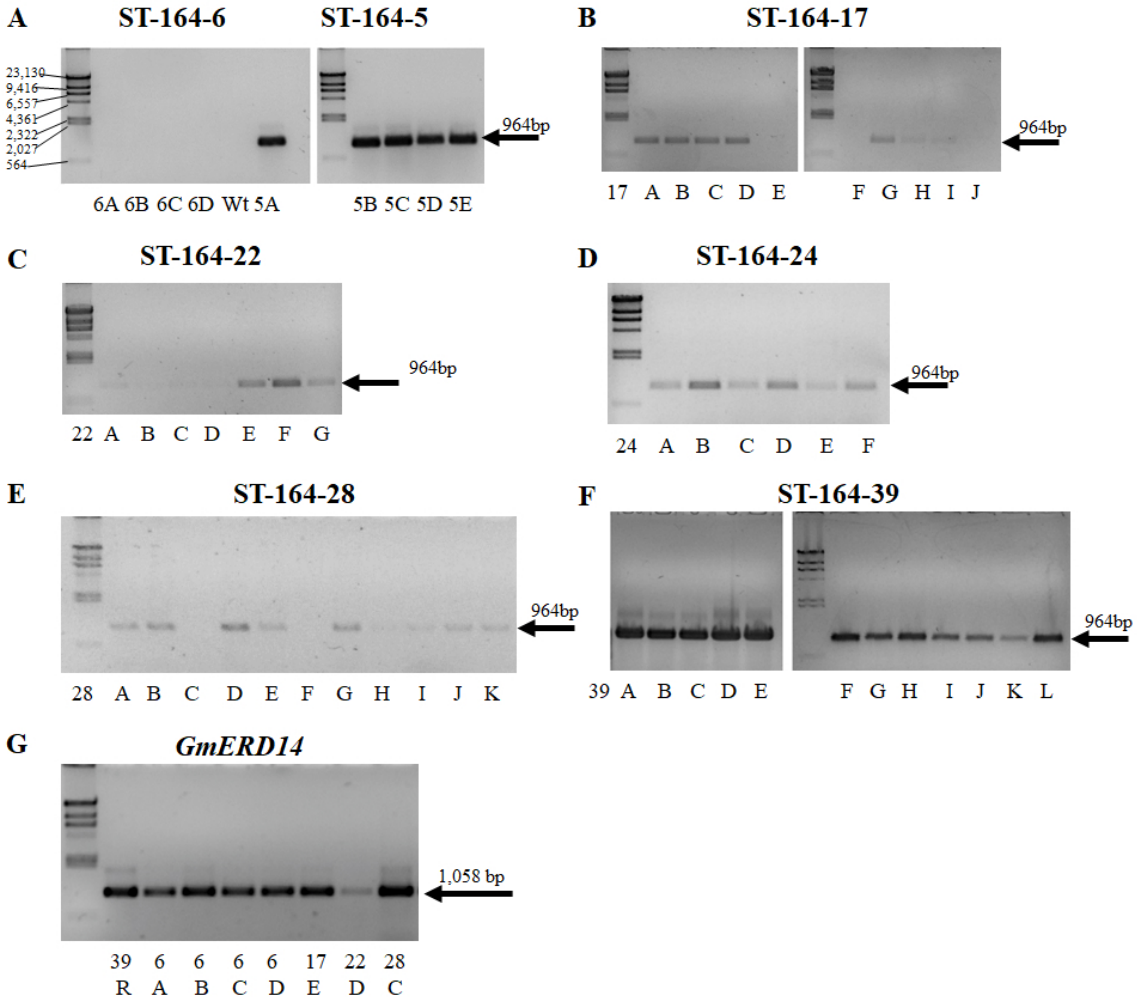

Fig. 4.3. A-F) Presence of *GUS* gene as measured via PCR from a trifoliate of a single plant (identified by letters) in each T1 *AtRD29Aprom::GFP/GUS* transgenic soybean. These are the same individuals as those named in Figure 4.2. The *GUS* fragment was predicted to be 964 bp (arrows indicate predicted size). G) Amplification of endogenous *GmERD14* via PCR to confirm negative *GUS* amplifications in A - F were due to lack of transgene and not poor DNA quality. The *GmERD14* fragment was predicted to be 1,058 bp.

after transformation each plant should be hemizygous individuals, containing only one transgenic allele or contain multiple insertions of single transgenic alleles across the genome. Overall, cold treatment induced GUS activity in 52% of individuals tested (Figure 4.4). Some individuals in lines -22, -28, and -39 had a cold-induced increase in GUS activity while some had cold-induced decreases (Figure 4.4). Even in the absence of cold some individuals from each line had increased GUS activity while some had decreased GUS activity after 24 hours. The presence or absence of the *GUS* gene in the T1 transgenic plants utilized for the cold experiments were determined via PCR (Figure 4.5). The transgene was present in all of the individuals, except for three individuals in line -22 (Figure 4.5A) and 1 in line -39 (Figure 4.5C).

Over the course of cold treatment, trifoliates were removed from the plant until all three trifoliates had been collected. Thus, the first trifoliate was removed at 0 hour as the control and the next two removed at 1 and 24 hours respectively (Figure 4.4. Due to the presence of two wounding motifs in the promoter construct (Figure 4.1A) it was possible that wounding was driving GUS activity. To account for this, cold treatment was done on leaf discs to ensure wounding would be uniform in all samples. All plants were from line -28. Basal GUS activity was low or undetectable in all eleven individuals tested (Figure 4.6). In top graph in Figure 4.6A, four out of the six leaf disc sets had significant cold induction of GUS activity level compared to pre-cold exposure (0 hour). In the bottom graph of Figure 4.6A, four out of five leaf disc sets had significant cold induction of GUS activity level compared to pre-cold exposure (0 hour). When a chilling condition (10 °C) was added, GUS activity was induced in four out of five leaf disc sets (Figure 4.6A, lower). In two sets, chilling treatment resulted in higher GUS activity versus cold stress. Overall, eight of the eleven T1 plants had increased GUS activity under cold conditions; however five plants also had increased GUS activity under control conditions (22 °C). The presence of the *GUS* transgene was confirmed in all eleven T1 line -28 individuals utilized in the leaf disc experiment (Figure 4.6B).

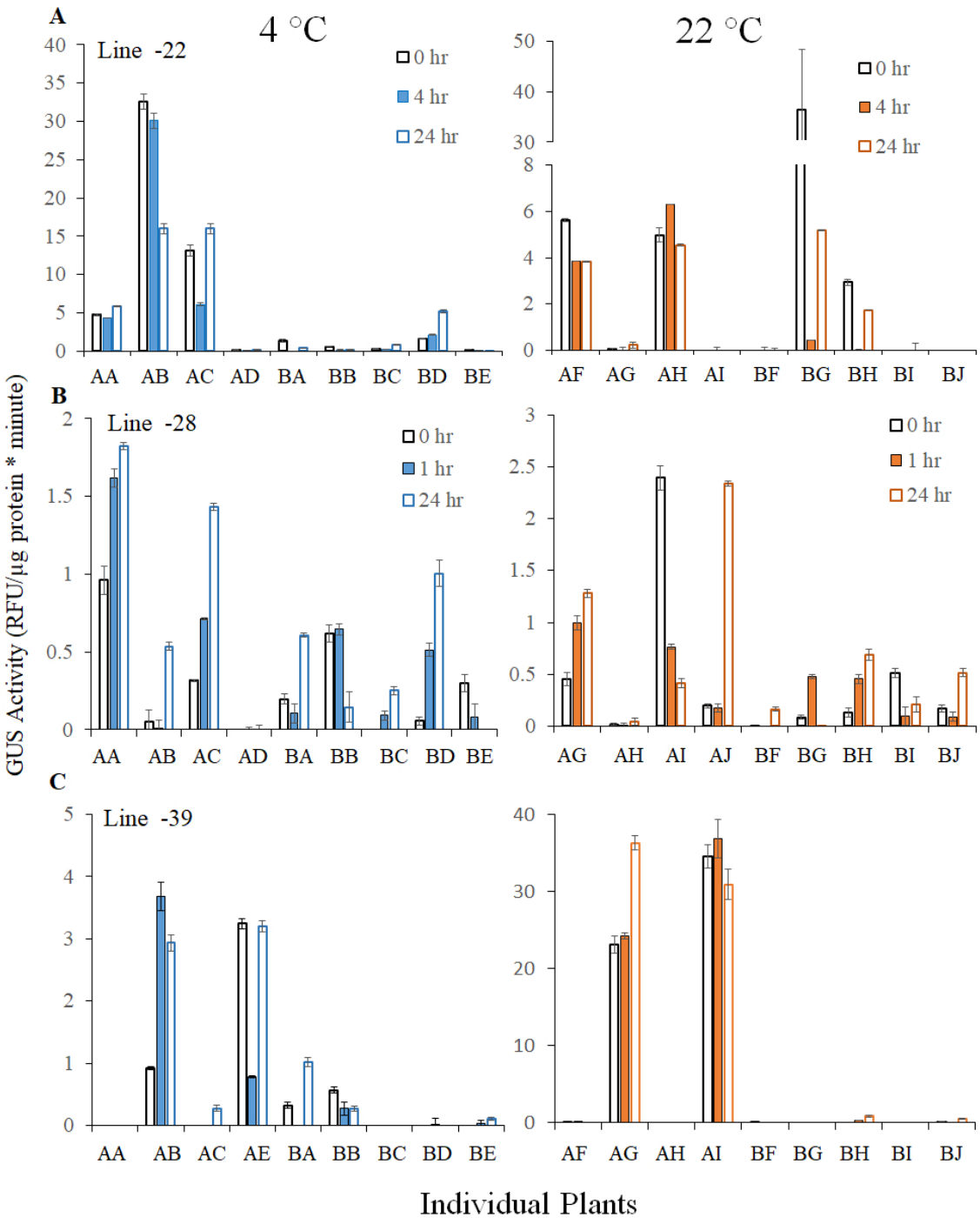

Fig. 4.4. Cold treatment of transgenic T1 ST-164-# *AtRD29Aprom::GFP/GUS* soybean trifoliate leaves. All plants were treated at either 4 or 22 °C for 0, 4, 24 hours. Individual plants are represented with two letters to distinguish them from the individuals presented in Figure 4.2 and 4.3. Error bars represent standard deviation of 3 technical replicates within the GUS assay as each bar represents a single biological individual. A) Line -22 plants. B) Line -28 plants. C) Line -39 plants. For reference, wild type soybean leaves havr an average GUS activity of -0.97 ± 0.34 with a range of -0.6 to -1.35.

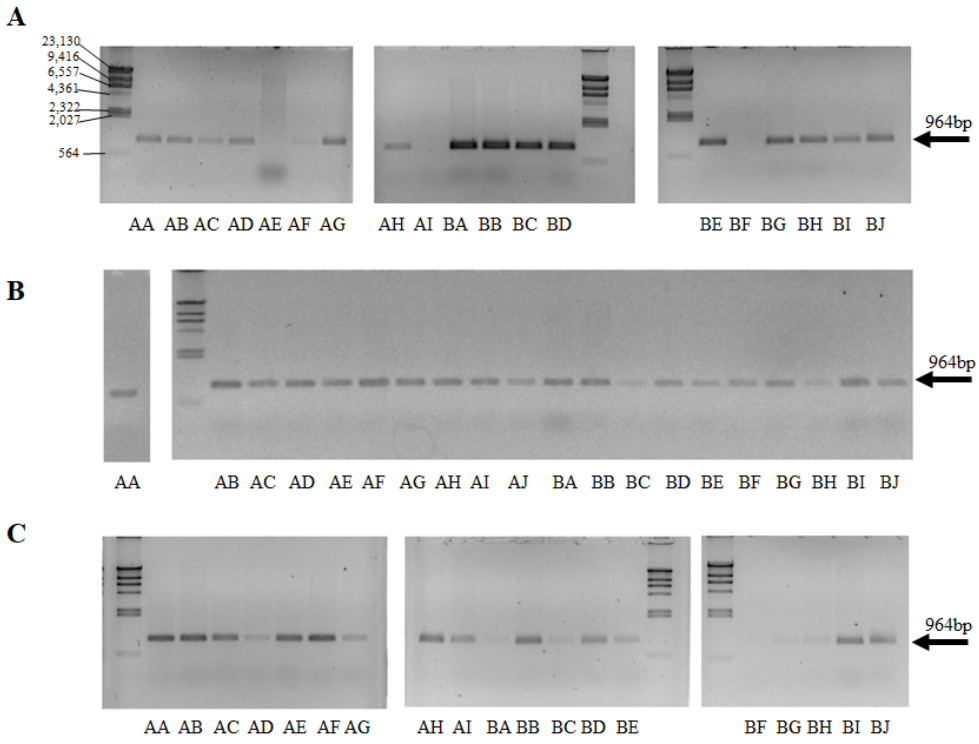

Fig. 4.5. Genetic screening for the presence of the *GUS* transgene in cold treated ST-164-# T1 transgenic *AtRD29Aprom::GFP/GUS* soybean via PCR. A) Line -22, B) Line -28, C) Line -39. These are the same individuals from Figure 4.4. The GUS fragment was predicted to be 964 bp.

Based on these data, we concluded that the utility of T1 lines were marginal at best. The high variability in GUS activity in the examined T1 plants (Figure 4.3, 4.5) could be due to variation in gene copy number with individuals, possessing one, two, or more insertions of the transgene within the genome (Gelvin, 2003). To eliminate this variable, single-insert homozygous lines must be established prior to future cold-induction experiments. Of 31 individuals screened in line -39 (Figure 4.3F, 4.5C), only one did not possess the *AtRD29Aprom::GFP/GUS* transgene suggesting that the *Agrobacterium* transformation of line -39 resulted in multiple insertions. This line was therefore not carried forward. As we wished to have three independent transformations, line -17 was chosen to replace line -39. Line -17 was a good candidate due

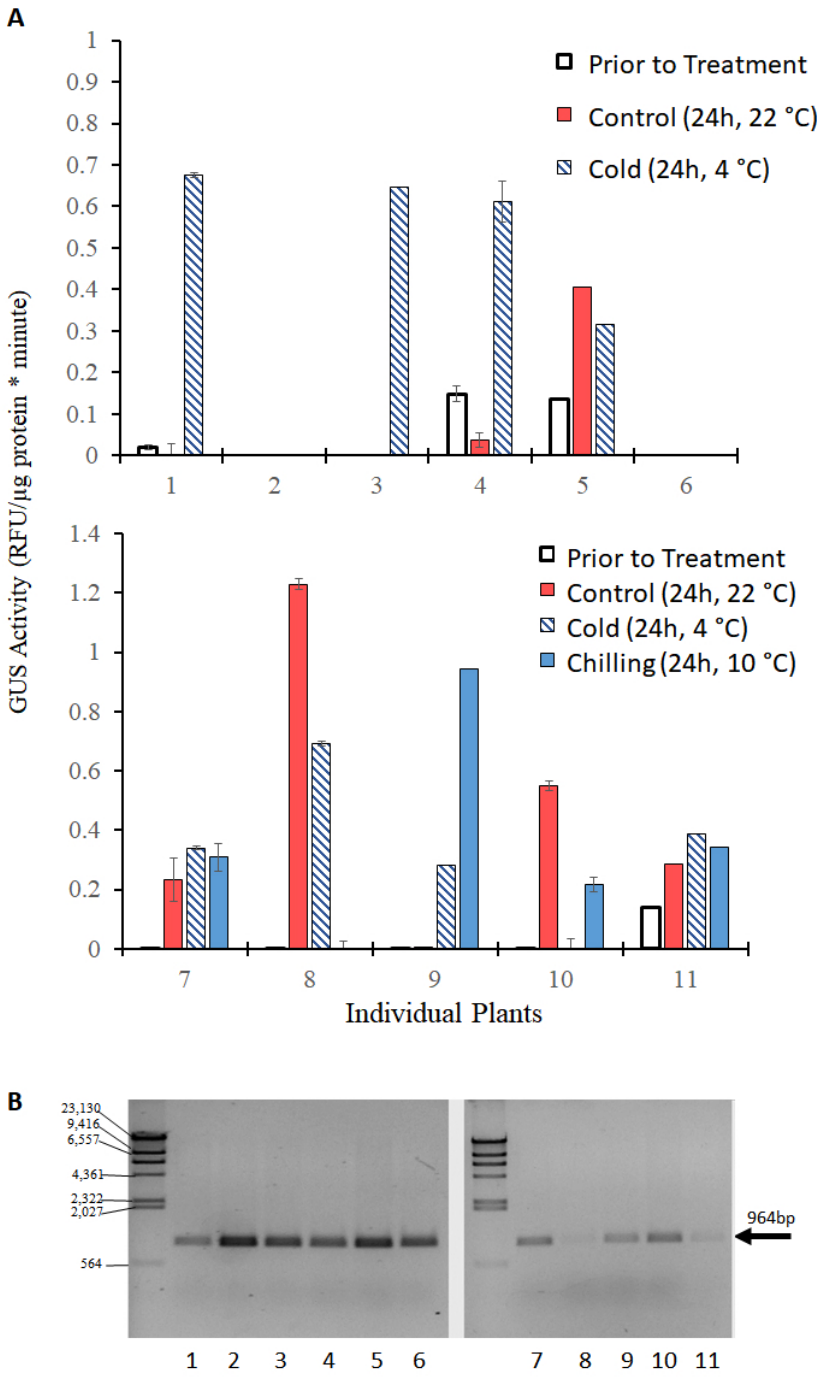

Fig. 4.6. Cold and chilling treatment of leaf discs made from trifoliate leaves from ST-164-28 T1 *AtRD29Aprom::GFP/GUS* transgenic soybean. A) GUS activity in first experiment (top) and second experiment (bottom) performed on different days. B) PCR amplification of the *GUS* transgene was positive in all individuals. The *GUS* fragment was predicted (arrows) to be 964 bp.

to high seed count (about 400) and initial screens indicated that 30% of individuals did not possess the transgene providing a higher likelihood of single insertion event.

4.2 Establishment of Homozygous Transgenic Lines

The T1 generation had a great deal of variability in presence and expression of the *AtRD29Aprom::GFP/GUS* transgene, it was necessary to establish homozygous lines. These lines will have 2 copies of the transgene in the same location of the genome which should remove the genetic variability that was noticed in the T1 generation. To achieve homozygous plants, the T1 generation were selfed to produce the T2 generation. If the transgene was a singular insertion, the inheritance patterns for *AtRD29Aprom::GFP/GUS* should follow Mendelian sorting. Plants from the T2 generation of lines -17, -22, and -28 were examined via glufosinate resistance assay (methodology presented in chapter 2.2). Forty to fifty plants from each line were categorized based on visual examination to be resistant or susceptible to glufosinate (Figure 4.7A). A single insertion of the glufosinate resistance gene (which is linked to the *AtRD29Aprom::GFP/GUS* transgene) was confirmed based on the 3:1 Mendelian sorting of T2 offspring verified by Chi Squared analysis (Figure 4.7B).

To screen T3 plants for homozygous individuals, the glufosinate resistance assay was used again. Initially, eight seeds were planted and evaluated for resistance. If any seedling showed susceptibility to glufosinate, this T3 line was rejected. If all eight seedlings were resistant, another 30 —50 seeds were planted and evaluated for glufosinate resistance. As demonstrated by the 100% glufosinate resistance lines ST-164-17-9 (45 resistant individuals), ST-164-22-23 (38 resistant individuals), and ST-164-28-5 (39 resistant individuals) were identified as independently transformed single-insertions homozygous transgenic lines (Table 4.1). No segregation has been observed in any of the subsequent experiments suggesting this criteria and methodology were adequate. Hereafter these lines will be identified as 17-9, 22-23, and 28-5.

A

Resistant Susceptible

B

Line	Result	Observed	Expected	Chi^2
17	Resistant	36	36.75	$p < 0.01$
	Susceptible	13	12.25	
22	Resistant	37	34.5	$p < 0.01$
	Susceptible	9	11.5	
28	Resistant	34	36.75	$p < 0.01$
	Susceptible	15	12.25	

Fig. 4.7. Analysis of T2 populations of *AtRD29Aprom::GFP/GUS* transgenic soybean lines ST-164-17, ST-164-22, and ST-164-28. A) Representative resistant or susceptible unifoliate leaves 24 hours after glufosinate treatment. B) Population analysis for lines -17, -22, and -28 confirmed 3:1 Mendelian inheritance.

4.3 Characterization of Homozygous Transgenic Lines

Lines 17-9 and 28-5 were initially examined for abiotic stress responsiveness of plants homozygous for the transgene. Line 22-23 was not examined in initial experiments as it took an additional year to isolate the homozygous line. Additionally, a transgenic homozygous Arabidopsis line (H.6.B) containing the same *AtRDA29Aprom::GFP/GUS* construct (Osadczuk, 2013) was examined to compare GUS induction between systems. These lines were tested under cold (4 °C), wounding (leaf disc), and ABA (1 mM) treatment for 24 hours. There was a significant induction of GUS expression in all three transgenic lines under cold and wounding

Table 4.1.
Results of glufosinate treatment (method Chapter 2.2) from individual soybeans from ST-164-# *AtRD29Aprom::GFP/GUS* T3 generation of lines -17, -28, and -22. The three independently transformed homozygous lines established are indicated in bold.

Line – Plant	Resistant	Susceptible
17 – 9	**45 (100%)**	**0 (0%)**
17 – 49	29 (80%)	7 (20%)
28 – 6	25 (75%)	9 (25%)
28 – 9	28 (78%)	8 (22%)
28 – 2	10 (77%)	3 (23%)
28 – 5	**39 (100%)**	**0 (0%)**
28 – 41	12 (92%)	1 (8%)
28 – 44	13 (86%)	2 (13%)
22 – 20	6 (86%)	1 (14%)
22 – 19	8 (62%)	5 (38%)
22 – 33	5 71%)	2 (39%)
22 – 35	9 (90%)	1 (10%)
22 – 10	1 (6%)	15 (94%)
22 – 27	7 (50%)	7 (50%)
22 – 14	8 (67%)	4 (33%)
22 – 3	9 (70%)	5 (30%)
22 – 9	13 (87%)	2 (13%)
22 – 29	6 (75%)	5 (25%)
22 – 23	**38 (100%)**	**0 (0%)**
22 – 11	4 (57%)	3 (43%)

stress, but only soybean line, 17-9, and Arabidopsis line H.6.B significantly increased GUS activity with ABA treatment (Figure 4.8A). Cold induction of GUS activity was significantly increased by 1.5-fold in soybean line 17-9, 2.5-fold in soybean line 28-5, and 3-fold in Arabidopsis line H.6.B (Figure 4.8B). In the transgenic soybean

lines, wounding had the highest induction of GUS activity level, increasing 3.5-fold in soybean line 17-9 and 11-fold in soybean line 28-5 (Figure 4.8B). In Arabidopsis H.6.B wounding increased GUS activity by 5.8-fold. ABA treatment had the highest induction of GUS activity in Arabidopsis with a 16-fold increase (Figure 4.8B). ABA treatment increased GUS activity 1.6-fold in soybean transgenic line 17-9 and 1.3-fold in soybean transgenic line 28-5 (Figure 4.8B). This result was surprising as Yamasaki et al. (2013) showed an ABA response in wild-type soybean cultivar Young and this construct contains the ABRE promoter element associated with this signaling pathway. The previous research used the soybean cultivar Young and the background for the transgenic soybean lines is the Williams 82 cultivar which may underlie the difference as soybean cultivars have been shown to have a wide range in responsiveness to exogenous ABA application (Sloger and Caldwell, 1970).

4.4 Summary

In summary, we have obtained transgenic soybeans expressing *AtRD29Aprom::GFP/GUS* and bred three homozygous lines from distinct single-insertion transformation events. This stress responsive promoter was shown to be responsive under cold stress, wounding, and exogenous ABA application, though to varying levels. When compared with the same construct in Arabidopsis (Osadczuk, 2013), soybean lines were less responsive to cold stress and ABA treatment, but more responsive to wounding. It is known that soybean is to be less cold responsive than Arabidopsis (Yamasaki et al., 2013; Yamasaki and Randall, 2016). Additionally, responses to ABA vary greatly by cultivar (Sloger and Caldwell, 1970) which explains the low ABA response seen in this study using cultivar Williams 82 versus the increased ABA response described in cultivar Young by Yamasaki et al. (2013). These transgenic soybean lines will be valuable tools for further investigations into the abiotic stress responses of domesticated soybean (*Glycine max*).

A

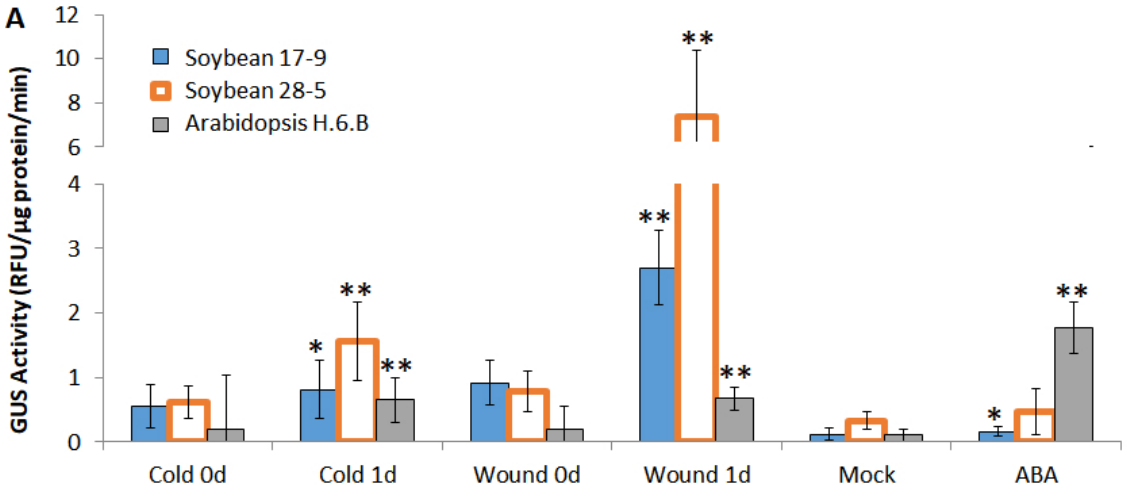

B

Fold Change (24/0hr, Mock/ABA)	Soybean 17-9	Soybean 28-5	Arabidopsis (H.6.B)
Cold	1.5 ± 0.4	2.5 ± 0.7	3.0 ± 2.1
Wound	3.4 ± 1.5	11 ± 4.8	5.8 ± 3.8
ABA	1.6 ± 0.88	1.3 ± 0.95	16 ± 4.4

Fig. 4.8. Abiotic stress responses of *AtRD29Aprom::GFP/GUS*. A) GUS Activity in two homozygous transgenic soybean lines and one homozygous transgenic Arabidopsis line all containing the same *AtRD29Aprom::GFP/GUS* construct. Cold treatment was performed at 4 °C for 24 hours. Wounding was performed by floating cut leaf discs in water for 24 hours. ABA (1 mM) treatment was applied as a foliar spray. Each column represents 9 replicates, containing leaves from 2 plants, except for Arabidopsis Mock/ABA which was only 6 replicates. Error bars represent standard deviation. Significance was determined by Students unpaired T-test, * = $p < 0.05$, ** = $p < 0.01$. B) Fold change of GUS activity level for each transgenic line under examined abiotic condition.

5. CROSSTALK BETWEEN ETHYLENE AND COLD STRESS PATHWAYS IN SOYBEAN

The purpose of this study was to investigate the interaction between the phytohormone ethylene signaling pathway and the cold stress pathway in soybean. It has been reported in Arabidopsis that ethylene negatively regulates cold tolerance (Shi et al., 2012). The following represents the major findings of this work which was published in 2019 (Robison et al., 2019) and reprinted in Appendix B.

In soybean, the ethylene pathway is upregulated in response to cold, mediated by the sustained accumulation of transcripts encoding the transcription factors *GmEIN3*, the increase in ethylene receptors *GmETR*s, and the transient loss of transcripts encoding the negative regulatory F-box binding proteins *GmEBF1*s (Yamasaki and Randall, 2016). In this study it was demonstrated that inhibition of the ethylene signaling pathway resulted in a significant increase in *GmDREB1A;1* and *GmDREB1A;2* transcripts, while stimulation led to decreased *GmDREB1A;1* and *GmDREB1B;1* transcripts. A cold responsive reporter construct (*AtRD29Aprom::GFP/GUS*, Chapter 4), as well as predicted downstream targets of soybean CBF/DREB1 [*Glyma.12g015100* (alcohol dehydrogenase), *Glyma.14g212200* (ubiquitin ligase), *Glyma.05g186700* (AP2-containing protein), and *Glyma.19g014600* (Cytochrome P450)] were impacted by the modulation of the ethylene signaling pathway. Photosynthetic parameters were affected by ethylene pathway stimulation, but only at control temperatures. Freezing tolerance (as measured by electrolyte leakage), free proline, and MDA; in both acclimated and non-acclimated plants were increased by silver nitrate but not by other ethylene pathway inhibitors. This suggests that pre-treatment with silver nitrate increases cold tolerance, though likely through a non-ethylene related pathway.

This work demonstrated a clear impact of the ethylene pathway on the transcription of *GmDREB1s* and on their downstream targets. We suggest that during cold

stress, GmEIN3A;1 negatively regulates *GmDREB1A;1* by interaction with the EIN3 binding motif found in the *GmDREB1A;1* promoter. While ethylene pathway inhibition resulted in an increase in *GmDREB1A;1* transcript levels, there was no general increase in measured cold tolerance parameters (Figure 5.1. This suggests that the initial portions of the CBF/DREB1 pathway (from cold reception to the accumulation of DREB1 transcripts) are not limiting the cold responsive pathway in soybean.

All ethylene pathway manipulation and cold stress experiments were designed and completed by myself. Proline content was measured by S. Randall. RNA-Seq analysis was completed by Y. Yamasaki.

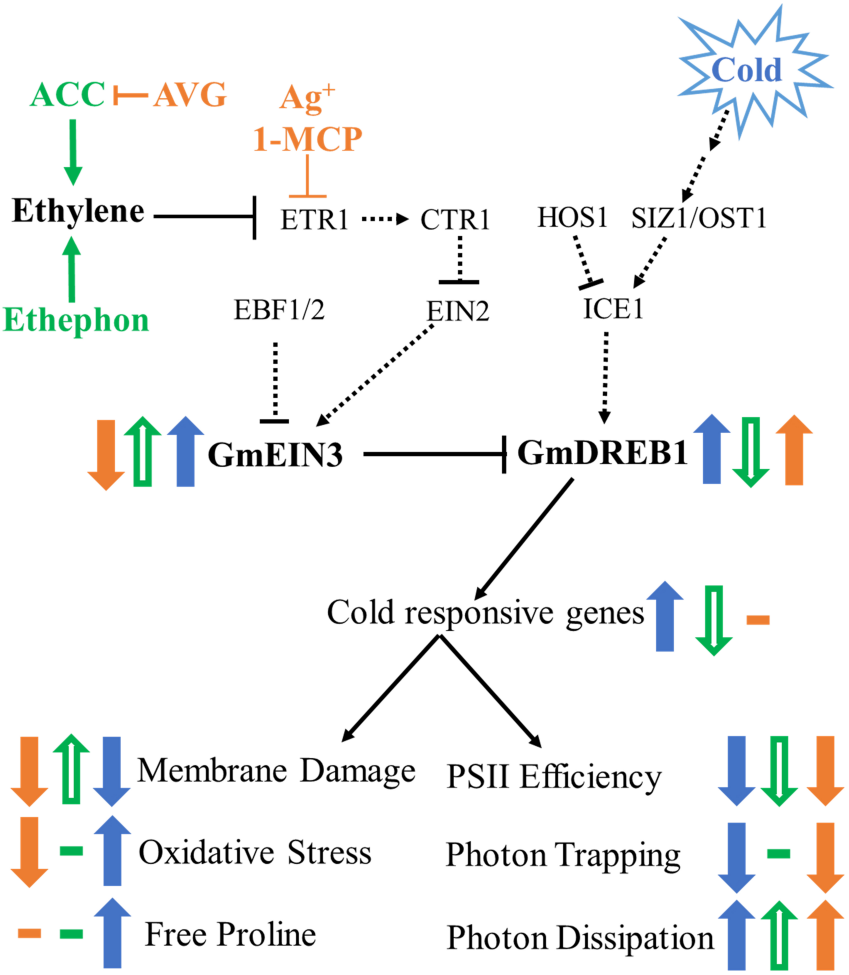

Fig. 5.1. Graphical summary of Robison et al. (2019).

6. EFFECTS OF COLD STRESS AND ETHYLENE PATHWAY MANIPULATION ON SOYBEAN PHOTOSYNTHESIS

Photosynthesis is a critical metabolic function in most plants. Cold stress decreases overall photosynthetic efficiency in soybean seedlings (Robison et al., 2019), as well as in late vegetative and reproductive soybean (Manafi et al., 2015; Tambussi et al., 2004; Van Heerden and Kruger, 2000; Van Heerden et al., 2003). In all of these studies, the effect of cold stress on photosynthesis was measured after at least 2 days of cold exposure. In searching the literature, no time courses were found that examined how and when photosynthesis decreases in the cold. This chapter examines both short and long term effects of cold stress on soybean photosynthesis as well as the effects of ethylene treatments with and without cold treatment using chlorophyll *a* fluorescence as a measurement of photosynthetic efficiency and yield.

Chlorophyll *a* fluorescence is a commonly used method for non-invasive, *in vivo* measurement of photosynthesis (Baker, 2008; Butler, 1972; Gentry et al., 1989; Krause and Weis, 1991; Strasser and Srivastava, 1995). Excitation energy from photon absorbance can be used in photochemistry, dissipated by nonphotochemical quenching (NPQ), or emitted as longer-wavelength light, i.e., red fluorescence. These three pathways compete for photon energy and changes in fluorescence emission are used to calculate the efficiency and production of photochemistry, as well as the amount of energy being shuttled away from photochemistry via NPQ (Butler, 1972). In the dark, PSII reaction centers are open, meaning that the primary quinone (Q_A) electron acceptor is fully oxidized and will provide minimum fluorescence (F_o). When light excites a PSII reaction center, an electron is passed to Q_A which closes the reaction center. Once Q_A has accepted an electron it cannot accept another until the electron is passed to the secondary quinone, Q_B. The closure of reaction centers creates an

increase in fluorescence until the maximum fluorescence (F_m) value is reached. The difference in relative fluorescence values between open and closed reaction centers is used to calculate the maximum quantum yield, which is a measure of the efficiency of photon capture by photosynthesis and energy flow around PSII (Gunderson and Taylor, 1991; Strasser and Srivastava, 1995; Taylor and Gunderson, 1986).

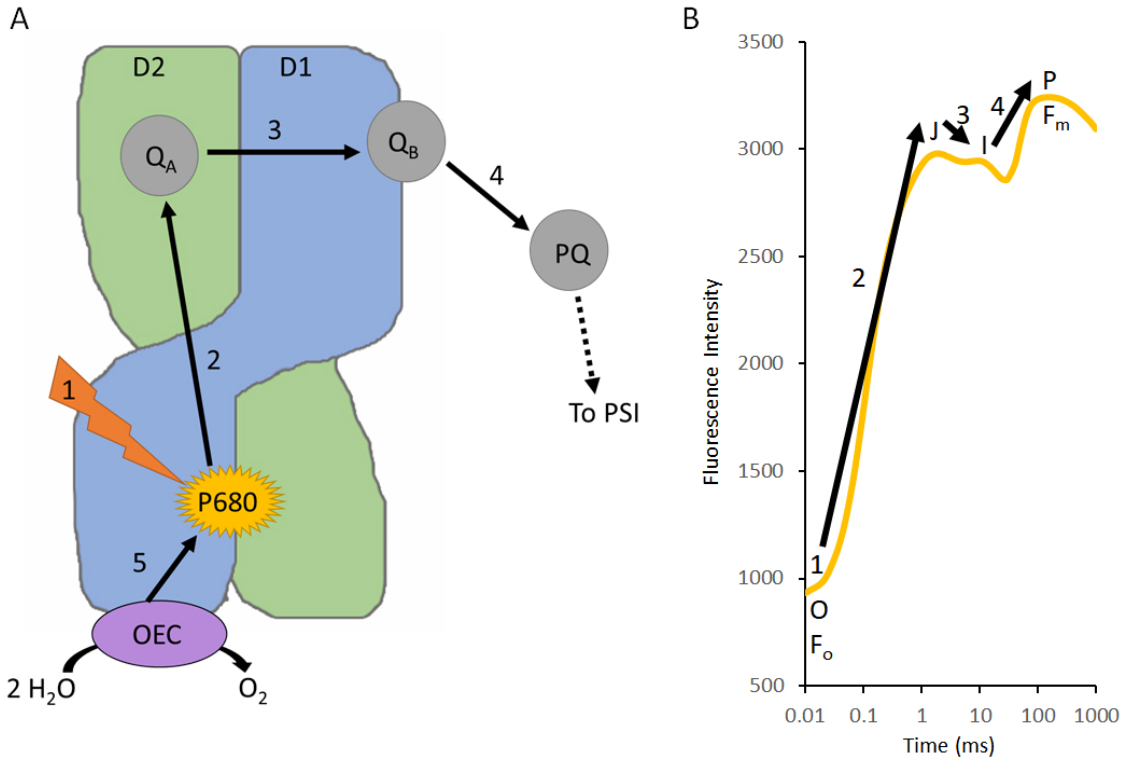

Fig. 6.1. PSII photochemistry and chlorophyll *a* transient fluorescence curves. A) Diagram of electron flow through the PSII reaction center. 1 - light hits the P680 chlorophyll *a* molecule and excites an electron, 2 - electron reduces Q_A, 3 - electron reduces Q_B, 4 - electron is shuttled to the PQ pool and on to PSI, 5 - splitting of water replaces the electron in the P680 chlorophyll *a* molecule. B) Example chlorophyll *a* transient fluorescence curve annotated with O-J-I-P steps. Numbered arrows indicate which step of electron flow (from A) is measured by each point in the curve.

Time resolved transient chlorophyll *a* fluorescence curves (O-J-I-P) between the minimum and maximum fluorescence are utilized to dissect electron flow through the photosystems as each point has been correlated with a physiological state (Figure 6.1 (Strasser and Srivastava, 1995). Briefly, O-J relates to the reduction of Q_A to Q_A^-, J-I the reduction of Q_B to Q_B^{2-}, and I-P the reduction of the plastoquinone (PQ) pool and electron flow into PSI (Boisvert et al., 2006; Zhu et al., 2005). A description of relevant parameters and their physiological function is presented in Table 6.1. Chlorophyll fluorescence methodology is presented in chapter 2.6.

6.1 Long Term Effects of Cold Stress Results

It was earlier demonstrated that soybean requires 5.2 ± 0.6 days to acquire a 50% improvement in cold acclimation (Chapter 3). To evaluate how photosynthesis is impacted during cold-treatment in relationship to maximal cold acclimation, photosynthesis parameters were measured daily for one week of cold or control conditions. The maximum efficiency of PSII (F_v/F_m) did not change significantly over seven days at control temperatures (22 °C, Figure 6.2A). Two days of cold exposure were required before a significant decrease in F_v/F_m was noted (Figure 6.2A). Additionally, the probability that a PSII chlorophyll molecule was acting as a reaction center (γRC) significantly decreased after 2 days and did not recover (Figure 6.2B). To gain a more detailed understanding of the changes occurring in PSII, the full chlorophyll *a* fluorescence transient curve was examined.

The chlorophyll *a* transient fluorescence curve significantly decreased at all steps (O-J-I-P) from day 2 onward (Figure 6.2C). The flattening of the curve, as indicated by the J and P peak reaching the same value in the cold suggested disruption of electron transport from Q_A to Q_B and beyond. The redox state of the PQ pool was evaluated by calculating the area between maximal fluorescence (P) to minimal fluorescence (O) above the OJIP curve. After 2 days, this area was significantly

Table 6.1.
Photosynthetic parameters measured via chlorophyll *a* fluorescence and their physiological references. Based upon Strasser and Srivastava (1995) and Baker (2008).

Parameter	Definition	Physiological Relevance
F_O, F_O'	Minimal fluorescence from dark or light adapted leaf, respectively	PSII reaction centers are open
F_M, F_M'	Maximal fluorescence from dark or light adapted leaf, respectively	PSII reaction centers are closed
F_V, F_V'	Variable fluorescence from dark or light adapted leaf, respectively, F_M - F_O	Ability of PSII to reduce Q_A
F_q'	Difference between maximal and steady state fluorescence emission	Photochemical quenching from open PSII reaction centers
F_V/F_M, F_V'/F_M'	Maximum efficiency of PSII photochemistry in the dark and in the light, respectively	Maximum quantum efficiency at which PSII can use light to reduce Q_A
F_q'/F_M'	PSII operating efficiency in the light	Estimation of the efficiency at which PSII can use light to reduce Q_A at a specific light intensity
OJIP	Transient chlorophyll *a* fluorescence curve	O is equivalent to F_O and P is equivalent to F_M
Area	Area above the transient chlorophyll *a* fluorescent curve between O and P	Redox status of the PQ pool
PI_{ABS}	Performance index	Overall efficiency and capacity of photosynthesis
ABS/CS	Absorbance per cross-section	Photon flux absorbed over the leaf cross-section
DI_O/CS	Dissipation per cross-section	Photon dissipation away from PSII across the leaf cross-section
ET_O/CS	Electron transport per cross-section	Electron transport across the leaf cross-section
TR_O/CS	Trapping per cross-section	Photon trapping by PSII across the leaf cross-section
ETR	Electron transport rate, F_q'/F_M' * 0.84 * 0.5	Electron transport rate at current light levels
γRC	gamma reaction center	Probability that a chlorophyll molecule is acting as a PSII reaction center
RC/CS	(ABS/CS)/(ABS/RC)	Percent active reaction centers per cross-section

decreased, indicating that either PQ molecules were unable to pass electrons through to PSI or there were fewer PQ molecules (Figure 6.2D).

The photon energy flux around PSII was measured daily to evaluate photon usage. Photon absorbance (ABS/RC) was unchanged by cold during the measurement period (Figure 6.3A). However, photon dissipation (DI_o/RC) away from PSII was significantly increased (Figure 6.3B) while photon trapping (TR_o/RC) by PSII was significantly decreased after 2 days of cold exposure (Figure 6.3C). Not surprisingly, overall electron transport (ET_o/RC) through PSII was significantly decreased 3 days post cold exposure (Figure 6.3D). These data demonstrate that while the same quantity of photons was absorbed in the cold, fewer photons were utilized for photochemistry and instead were dissipated away. This dissipation is likely occurring through nonphotochemical quenching (NPQ).

NPQ is the sum of 3 components: qE, high energy quenching; qT, state transitions; and qI, photoinhibition. qE is the main component of thermal dissipation and thus is often referred to simply as NPQ in the literature. NPQ responds and relaxes within seconds to minutes of changing light conditions. An accumulation of protons in the chloroplast lumen results in a decrease in pH which causes protonation of LHCII major and minor proteins resulting in conformational changes. The first quenching site, qE, is the detachment from the PSII-LHCII supercomplex and aggregation of LHCII which releases heat. The second quenching site, qT, occurs by deepoxidation of violaxanthin to zeaxanthin, in the VAZ cycle, within the minor LHCII proteins CP24, CP29, and CP26. Quenching site 1 occurs within seconds, while the second site requires several minutes (Goss and Lepetit, 2015; Ruban et al., 2012). qI is the breakdown of PSII reaction centers and requires hours to days to occur and repair (Goh et al., 2011). Due to the highly oxidative process of passing high energy electrons within the active site, the core photosystem II protein D1 is regularly damaged requiring frequent repair of PSII reaction centers. The PSII repair cycle consists of partial PSII disassembly to allow D1 proteolysis and the insertion of a nascent D1 before the reassembly of PSII subunits (Jrvi et al., 2015).

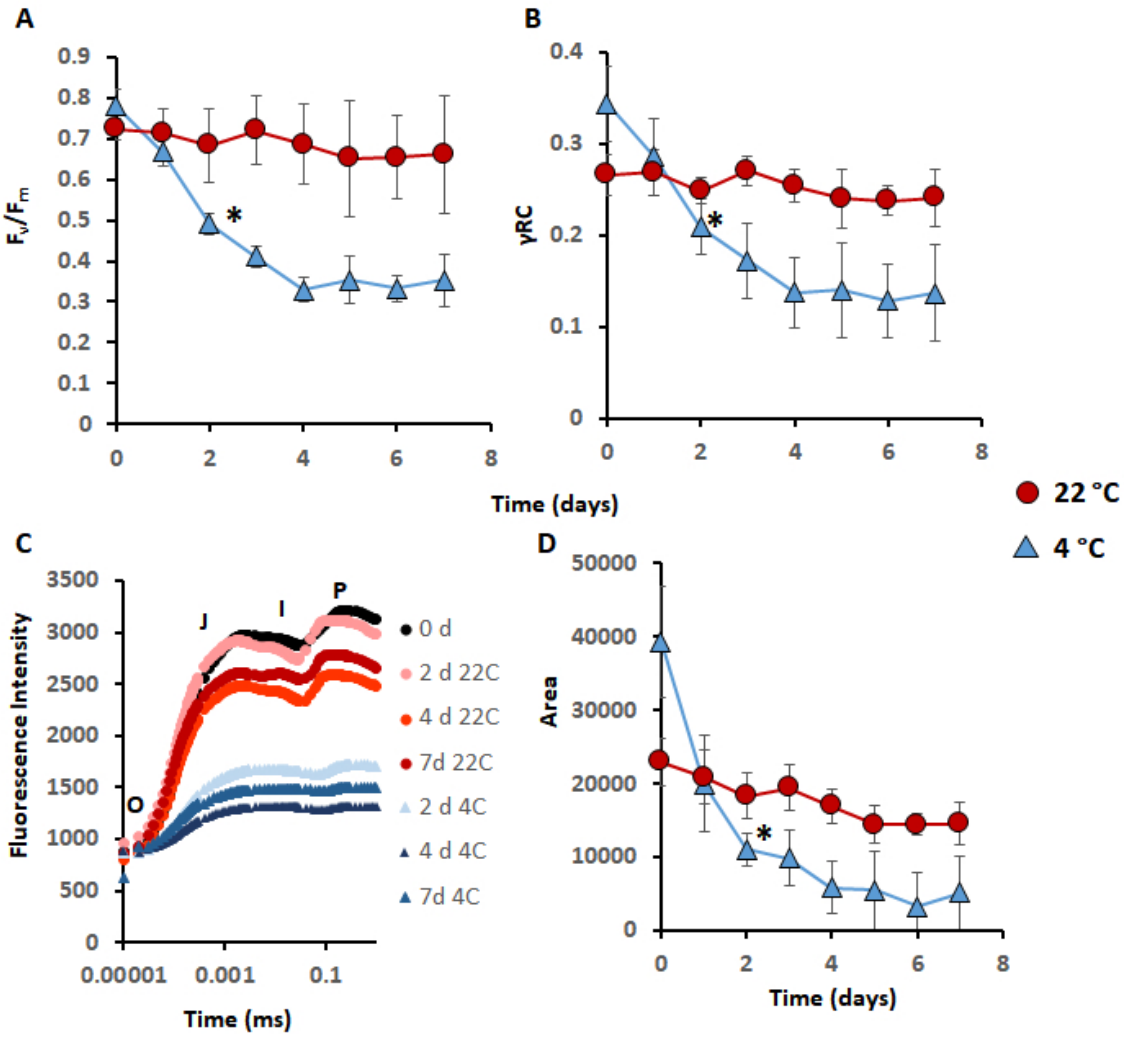

Fig. 6.2. Mean (± SD) daily chlorophyll *a* fluorescence measurements on 2 week old soybean seedlings which were grown with 200 μmol photons per m^{-2} s^{-2} of light on an 16:8 hour light:dark cycle. A) Maximum efficiency of PSII (F_v/F_m) measured daily at both 22 (red circles) and 4 (blue triangles) °C. B) Probability that a chlorophyll was a PSII reaction center molecule (γRC) measured daily at both 22 (red circles) and 4 (blue triangles) °C. C) Transient chlorophyll *a* fluorescence (Kautsky curve) plotted on a logarithmic time axis at the time points indicated. Red indicates 22 and blue indicates 4 °C. For clarity, averages are presented without error bars. D) The size of the PQ pool (Area) measured daily at both 22 (red circles) and 4 (blue triangles) °C. Error bars that are not visible are smaller than symbols. Two-way ANOVA indicated significant interaction of time and temperature for A, B, and D. * indicates $p < 0.01$ compared to 0 d at 4 °C and continuing from that time point onward with Tukey-HSD post-hoc analysis. $n = 9$.

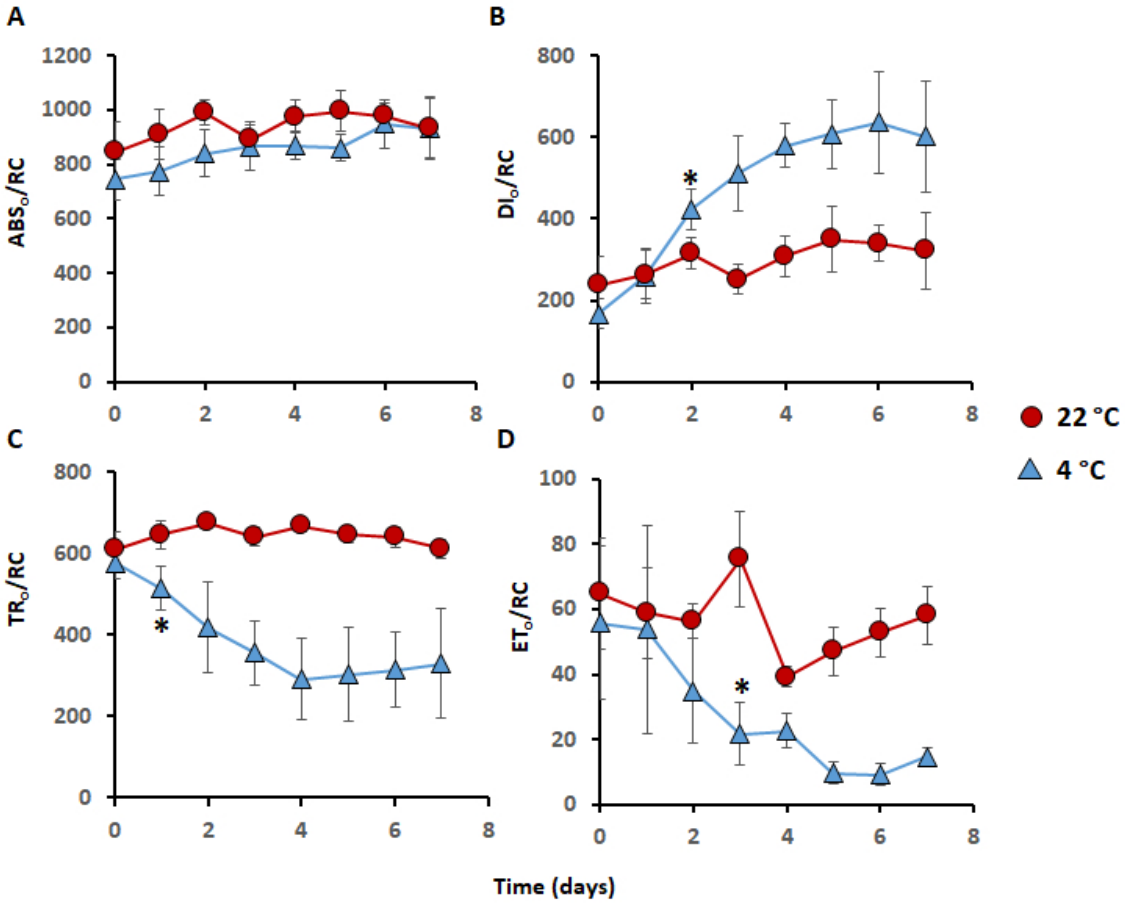

Fig. 6.3. Mean (± SD) daily effects of cold stress on PSII parameters on two week old soybean seedlings which were grown at 200 μmol photons per m^{-2} s^{-2} of light on an 16:8 hour light:dark cycle. A) Photon absorbance per PSII reaction center (ABS/RC), B) Dissipation of photons per PSII reaction center (DI_o/RC), C) Photon trapping per PSII reaction center (TR_o/RC), D) Electron trapping per PSII reaction center measured daily at both 22 (red circles) and 4 (blue triangles) °C. Error bars that are not visible are smaller than symbols. Two-way ANOVA indicated significant interactions of time and temperature for B, C, and D. * indicates $p < 0.01$ compared to 0 d at 4 °C and continuing from that time point onward in post-hoc Tukey-HSD analysis. n = 9.

Given the timing and severity of the damage to PSII, as indicated by the decrease in photochemical efficiency and loss of transient peaks in the chlorophyll *a* fluorescence curve, photoinhibition is likely occurring. Cold temperature can inhibit D1 synthesis thus preventing replacement of the damaged D1 protein (Allakhverdiev and Murata, 2004). The loss of D1 biosynthesis is consistent with the chlorophyll *a* fluorescence parameters measured; however, to be certain, D1 protein levels would need to be directly quantified via Western blot.

6.2 Short Term Effects of Cold Stress

The Randall lab observed that soybean seedling leaves exhibit nastic movement resembling nyctinasty (decreasing leaf angle, often occurring as sleep movements) in early cold stress in the light and do not recover. This observation led to questions about the timing of the effect after cold onset and what may be driving the physiological effect, which we refer to as cryonasty. Studies by undergraduate Jacob Hamilton indicated that this cold response begins within 5 to 50 minutes in a light-dependent manner (leaf angle decreases faster at lower light levels, Figure 6.4). Additionally, leaf movement have been associated with optimizing photosynthetic rates (Zhu et al., 2015). Since leaf movement begins shortly after cold on-set, photosynthetic parameters were measured via chlorophyll *a* fluorescence every 5 minutes for the first hour of cold exposure to determine when photosynthesis is initially impacted and if it was correlated with observed leaf movement. To avoid damage to the leaves a platform was created to hold the leaf clips of the Handy-PEA. When leaves were not being measured they remained horizontal on the platform to reduce shading and changes in light intensity due to cryonasty movements.

6.2.1 Analysis of Photosynthesis in Light Adapted Soybeans

Chlorophyll *a* fluorescence was measured in soybean seedlings under steady state illumination allowing the measurement of operational photosynthesis. Because the

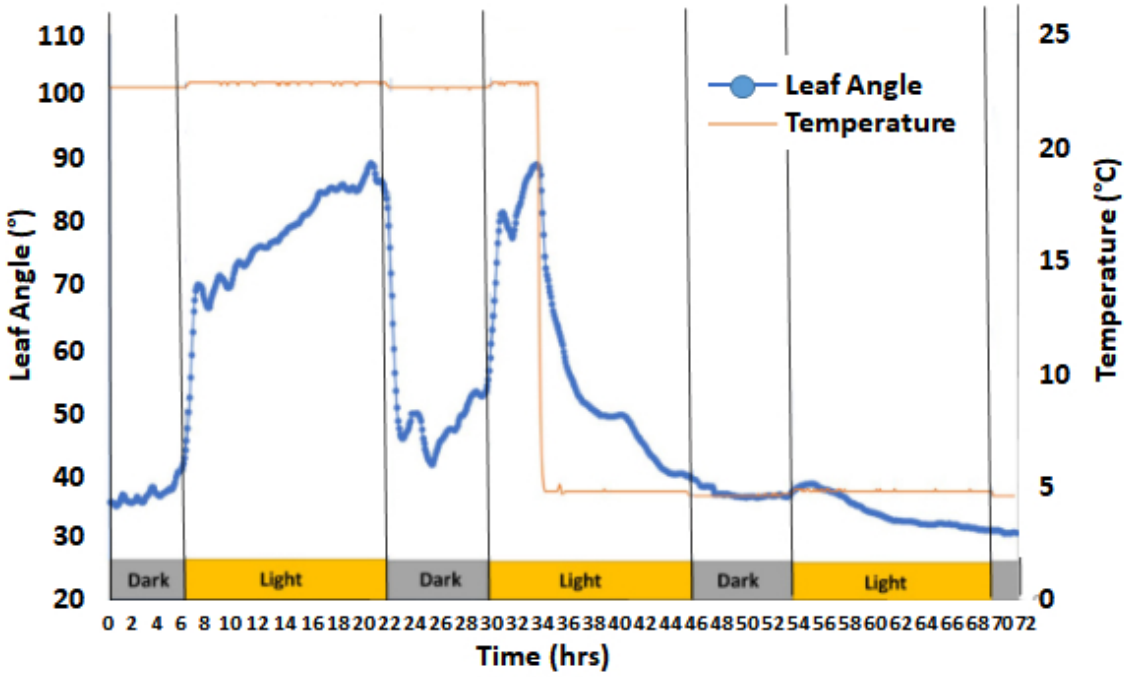

Fig. 6.4. Cryonasty movements as measured by angle between the leaf and the stem. Leaf angle measurements (blue line) were calculated from time-lapse photography taken every 5 minutes over 3 days. Temperature was measured every 5 minutes via temperature logger (orange line). Leaves lift rapidly in the light and fall rapidly in the dark. Four hours into day 2 temperature was shifted to 4 °C. Leaf angle rapidly decreased and did not recover (Hamilton and Randall, unpublished).

samples were not dark adapted, each PSII reaction center was in a different redox state, depressing the maximal fluorescence compared to what would be detected in dark-adapted leaves (Strasser et al., 2000). The maximum efficiency of PSII (F'_v/F'_m) estimates the maximum efficiency if all PSII reaction centers were open, that is available to accept electrons to reduce Q_A. The PSII operating efficiency (F'_v/F'_q) is the efficiency of light absorption being utilized to reduce Q_A under current lighting conditions. F'_v/F'_q is mathematically equal to photochemical quenching and is strongly correlated with carbon dioxide fixation (Baker, 2008). Although NPQ cannot be directly measured without dark adaptation, the differences in F'_v/F'_m (maximum po-

tential) and F'_v/F'_q (operational status) can reflect the contribution of NPQ (Murchie and Lawson, 2013).

PSII maximum efficiency (F'_v/F'_m) began to decrease after 15 minutes and was significantly different after 25 minutes (Figure 6.5A). PSII operating efficiency (F'_q/F'_m) and ETR also decreased after 15 minutes and were significantly different after 25 minutes (Figure 6.5B,C). At all times F'_v/F'_q was lower than F'_v/F'_m, indicating that NPQ was occurring, and as cold treatment continued, the disparity grew, suggesting that NPQ increased with cold treatment. Considering the timing, this was likely due to qE and/or qT, though more research is necessary to establish this. The chlorophyll *a* fluorescence transient curve indicated that electron flow through photosystem II began to slow after 15 minutes as indicated by decreased fluorescence at point J and beyond, further demonstrating that electron transport through PSII was depressed (Figure 6.5D).

Photosynthetic performance index (PI_{ABS}) is a structural and functional measure that relates to the energy conserved from initial light absorption to the reduction of the final PSI acceptors. PI_{ABS} is a calculated value that consists of the products of effective antenna size, maximum quantum yield of PSII, the fraction of active reaction centers of PSII, and the probability that an electron will move into PSI (Strasser et al., 2000). During cold treatment, PI_{ABS} significantly decreased at 105 minutes and remained depressed (Figure 6.6A). Prior to 105 minutes, there was a great deal of variation in PI_{ABS}, though this was not unexpected since the parameter relies on many different measurements (Kalaji et al., 2014). To understand what physiological changes were driving the variability in PI_{ABS}, the parameters underlying it were examined.

The leaf cross-section area is a set value due to the fixed size of the probe, but the number of reaction centers within that cross-section can change. The ratio of reaction centers per cross-section is calculated using the absorbance for each such that RC/CS is equal to (ABS/CS)/(ABS/RC). A significant decrease in reaction center per cross-section started at 25 minutes and remained low for the rest of the experiment (Figure

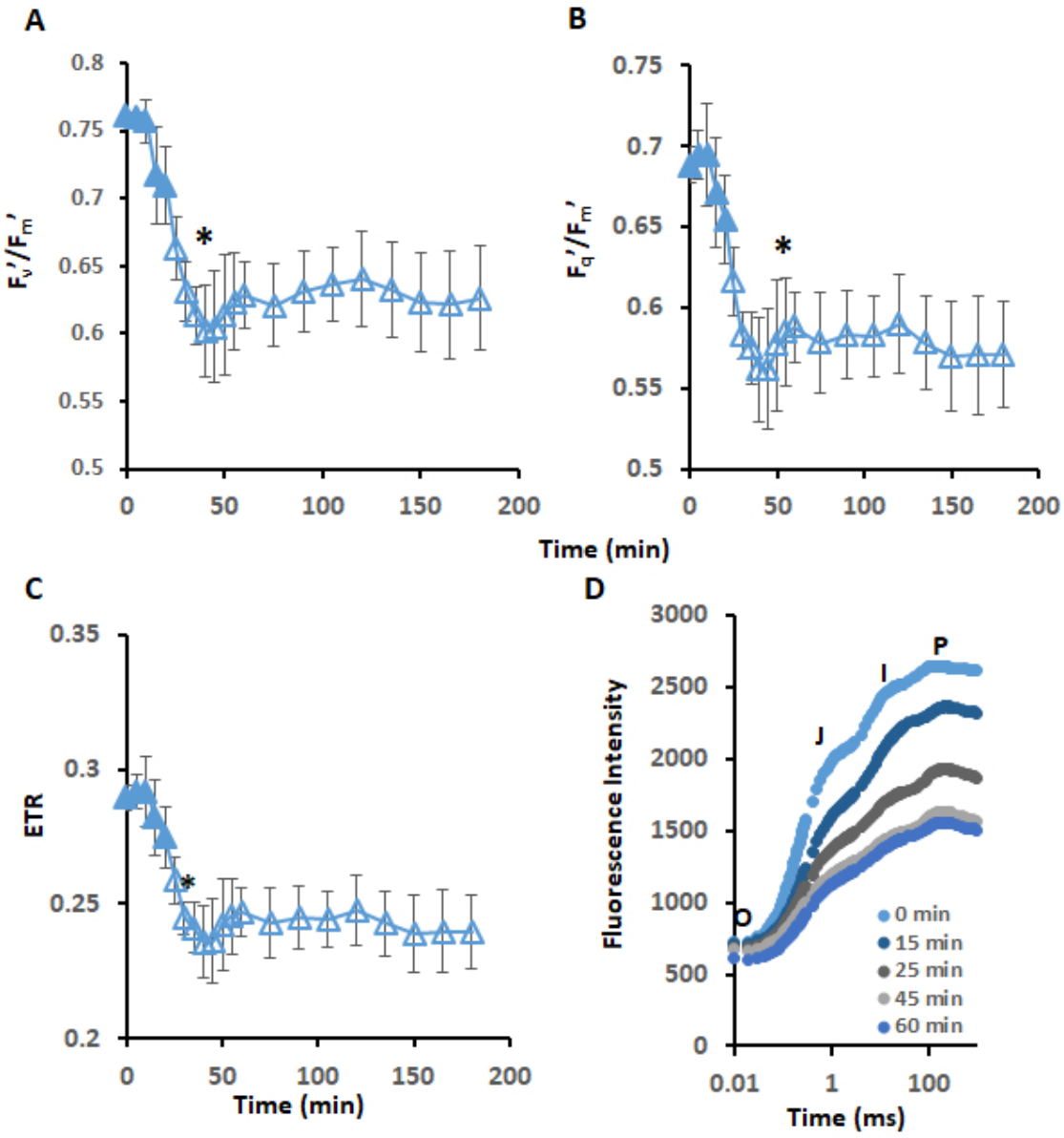

Fig. 6.5. Mean (± SD) short-term cold effects on light-dependent photosynthesis under steady state illumination on 2 week old soybean seedlings which were grown with 200 μmol photons per m^{-2} s^{-2} of light on an 16:8 hour light:dark cycle. A) Maximum efficiency of PSII (F_v'/F_m'), B) PSII operating efficiency (F_v'/F_q'), and C) ETR measured over the first 180 minutes of cold-exposure. Error bars that are not visible are smaller than symbols. One-way ANOVA were significant for all parameters. Post-hoc Tukey-HSD tests were performed to compare each time point to 0 minutes, * and open symbols indicate p <0.01. D) Transient chlorophyll *a* fluorescence (Kautsky curve) plotted on a logarithmic time axis at the time points indicated. Averages are represented without error bars for clarity. n = 9.

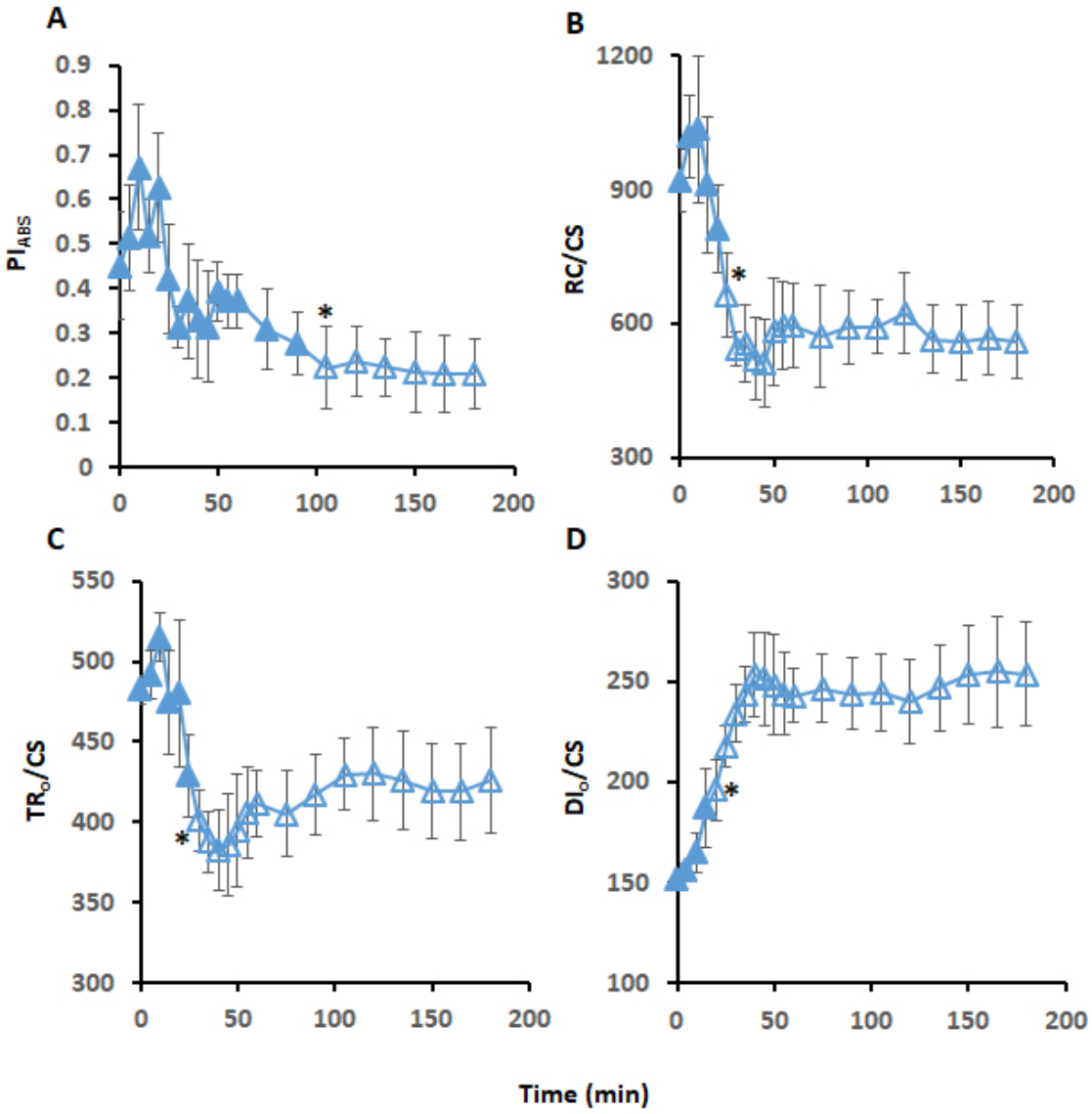

Fig. 6.6. Mean (± SD) short-term cold stress effects on energy flux in PSII under stead-state illumination on 2 week old soybean seedlings which were grown with 200 μmol photons per m^{-2} s^{-2} of light on an 16:8 hour light:dark cycle. A) Photosynthetic performance index (PI_{ABS}), B) reaction centers per cross-section (RC/CS), C) photon trapping per cross-section (TR_O/CS), and D) photon dissipation per cross-section (DI_O/CS) measured over the first 180 minutes of cold-exposure. Error bars that are not visible are smaller than symbols. One-way ANOVA were significant for all parameters. Post-hoc tests using Tukey-HSD were performed to compare each time point to 0 minutes with * and open symbols indicate $p < 0.01$. $n = 9$.

6.6B). This matches the timing of decreasing F'_v/F'_m and F'_v/F'_q. In light-adapted conditions, decreases in RC/CS and F'_v/F'_m have been correlated with increasing photoinhibition (Goh et al., 2011). Since the number of reaction centers decreased significantly, energy flux was examined in relation to the cross-section, which remained stable. Trapping of photons (TR_o/CS) by PSII significantly decreased during cold stress in a similar pattern to RC/CS (Figure 6.6C). The decrease at 30 minutes was significant compared to the start of the experiment and remained significantly lower for the rest of the experiment. Dissipation of photons (DI_o/CS) away from PSII significantly increased during cold stress beginning at 20 minutes (Figure 6.6D).

Taken together all of these data indicate that during early cold stress PSII reaction centers are disabled leading to a decrease in light being trapped by PSII and an increase in the dissipation of light away from PSII. The loss of photon trapping resulted in less photon energy available, driving a decrease in electron transport through PSII and an overall decrease in photosynthetic efficiency. The initial damage occurred at around 15 minutes and was significantly impacted after 25 minutes with stabilization occurring by 105 minutes for most parameters under steady illumination. This represents the current working status of photosynthesis; however, it does not provide information on the maximum working status of photosynthesis (Strasser and Srivastava, 1995; Strasser et al., 2000). To examine maximum photosynthesis requires the dark adaption of the plant so that all reaction centers are open at the start of measurements (Strasser and Srivastava, 1995).

6.2.2 Analysis of Photosynthesis in Dark Adapted Soybeans

Soybean seedlings were dark adapted and photosynthesis was measured over the course of 7 hours (420 min). The maximum efficiency of PSII (F_v/F_m) was not significantly impacted by cold until 360 minutes post exposure (Figure 6.7A). The number of reaction centers per cross-section were not significantly impacted until 420 minutes (Figure 6.7B). Photon dissipation and trapping per cross-section was not significantly

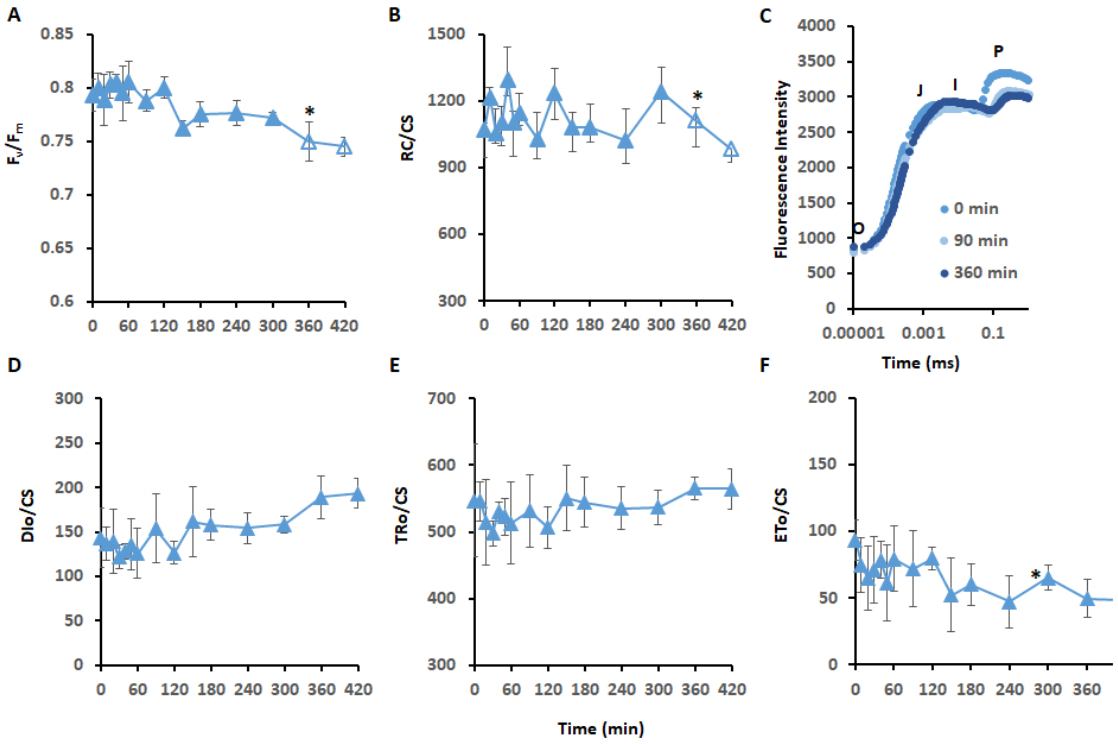

Fig. 6.7. Mean (± SD) effects of cold stress on maximal photosynthesis parameters on 2 week old soybean seedlings which were grown with 200 μmol photons per m^{-2} s^{-2} of light on an 16:8 hour light:dark cycle. A) Maximum efficiency of PSII (F_v/F_m) and B) reaction centers per cross-section (RC/CS) measured over 420 minutes of cold-exposure. One-way ANOVA were significant for all parameters. Post-hoc tests using Tukey-HSD was performed compared to 0 minutes, * and open symbols indicate $p < 0.01$. C) Transient chlorophyll *a* fluorescence (Kautsky curve) plotted on a logarithmic time axis at the time points indicated. Averages are represented without error bars for clarity. D) Photon dissipation per cross-section (DI_O/CS), E) photon trapping per cross-section (TR_O/CS), and F) electron transport per cross-section (ET_O/CS) measured over the 4200 minutes of cold-exposure. Error bars that are not visible are smaller than symbols. One-way ANOVAs were significant for all parameters. Post-hoc tests using Tukey-HSD were performed to compare each time point to 0 minutes, * and open symbols indicate $p < 0.01$. $n = 9$.

impacted over the measurment period (Figure 6.7C,D). Electron transport was not significantly impacted until 420 minutes (Figure 6.7E). The chlorophyll *a* transient

curve indicated a slight decrease between I and P steps however this was not significant (Figure 6.7F). There was no lasting, significant impact on photochemistry until 360 minutes or more. When combined with the steady state illuminated results, these data indicate that the photodamage noted in operational photosynthesis is transient and can be alleviated until at least 6 hours have passed.

Photosynthesis is linked with stomatal conductance, which drives transpiration and internal water potential (Lawson and Vialet-Chabrand, 2019) and can lead to leaf movement and wilting. Leaf movement began, in steady state illumination, between 5 and 50 minutes post cold exposure, which aligned well with the steady-state photosynthesis rates that began to decrease immediately but were not significant until 25 minutes post cold exposure. Cryonasty leaf movement does not recover over-night. When cyronasty was being examined darkness began 12 hours post-cold initiation and lasted for 8 hours. Since dark-adapted photosynthesis showed no permanent damage before 6 hours of cold treatment, the lack of cyronasty recovery overnight is consistent with the timing of permanent PSII damage. Based on the daily measurements of photosynthesis this damage continues for 3 - 4 days of cold exposure until a steady state was reached. Interestingly, while investigating the link between the phytohormone ethylene and cold acclimation in soybean (Chapter 5), it was noted that silver nitrate treatment protected against cold-induced wilting (Figure 6.8). This led us to investigate how ethylene pathway manipulation impacts photosynthesis in both the presence and absence of cold.

6.3 Impact of Ethylene Signaling Pathway Inhibition and Stimulation on Photosynthesis

Chlorophyll *a* fluorescence was used to monitor photosynthesis during stimulation (1 mM ACC and 1.38 mM ethephon, pink bars/symbols in graphs) and inhibition (1 μM AVG, 100 ppm 1-MCP and $AgNO_3$, blue bars/symbols in graphs) of the ethylene signaling pathway both in the presence and absence of cold. Ethylene pathway ma-

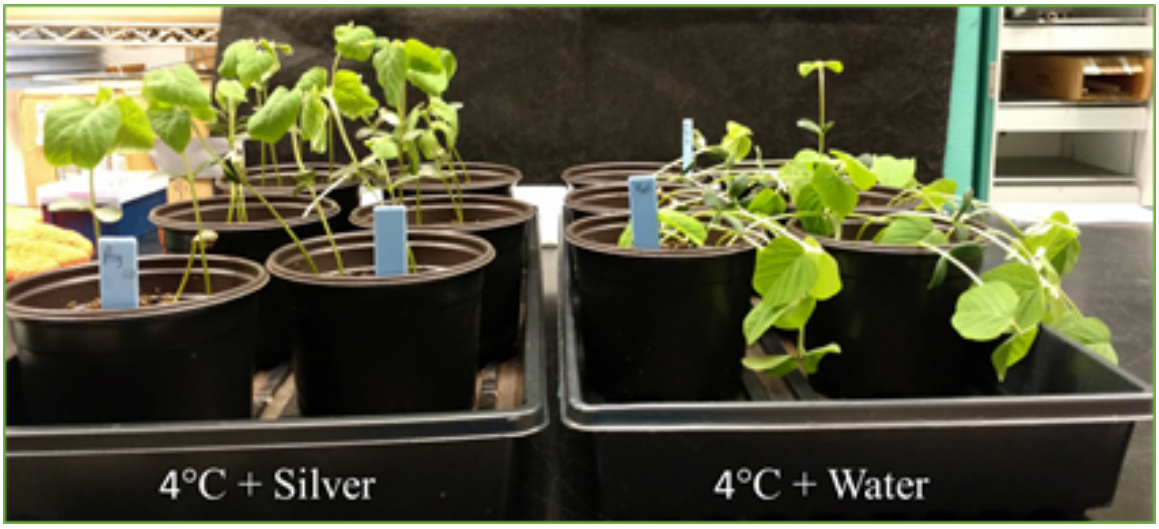

Fig. 6.8. Seedlings post 48 hour cold exposure under 100 μmol photons/m^{-2}*s^{-2} in the presence (left) and absence (right) of 1 mM silver nitrate.

nipulation, growth conditions, and treatment methodology were presented in chapter 2.1. In the absence of cold, photosynthetic efficiency of PSII (F_v/F_m) was increased by inhibition of the ethylene signaling pathway and decreased by stimulation of the ethylene signaling pathway (Figure 6.9A). The performance index of photochemistry (PI_{ABS}) was increased by all ethylene pathway inhibitors and generally decreased by stimulation (Figure 6.9B). The transient chlorophyll *a* fluorescence curve was only impacted by silver nitrate treatment, which decreased the J and I peaks indicating electron transfer between Q_A to Q_B was decreased (Figure 6.9D). Ethylene pathway inhibition significantly increased, while stimulation decreased, the probability that a PSII chlorophyll molecule was acting as a reaction center (γRC, Figure 6.9C).

Ethylene pathway manipulation changed energy capture and utilization per PSII reaction center with inhibition of the ethylene signaling pathway having a photoprotective effect. Photon absorbance per PSII reaction center (ABS/RC) and dissipation energy per reaction center (DI_o/RC) were increased by ethylene pathway stimulation and decreased by inhibition, while photon trapping per reaction center (TR_o/RC)

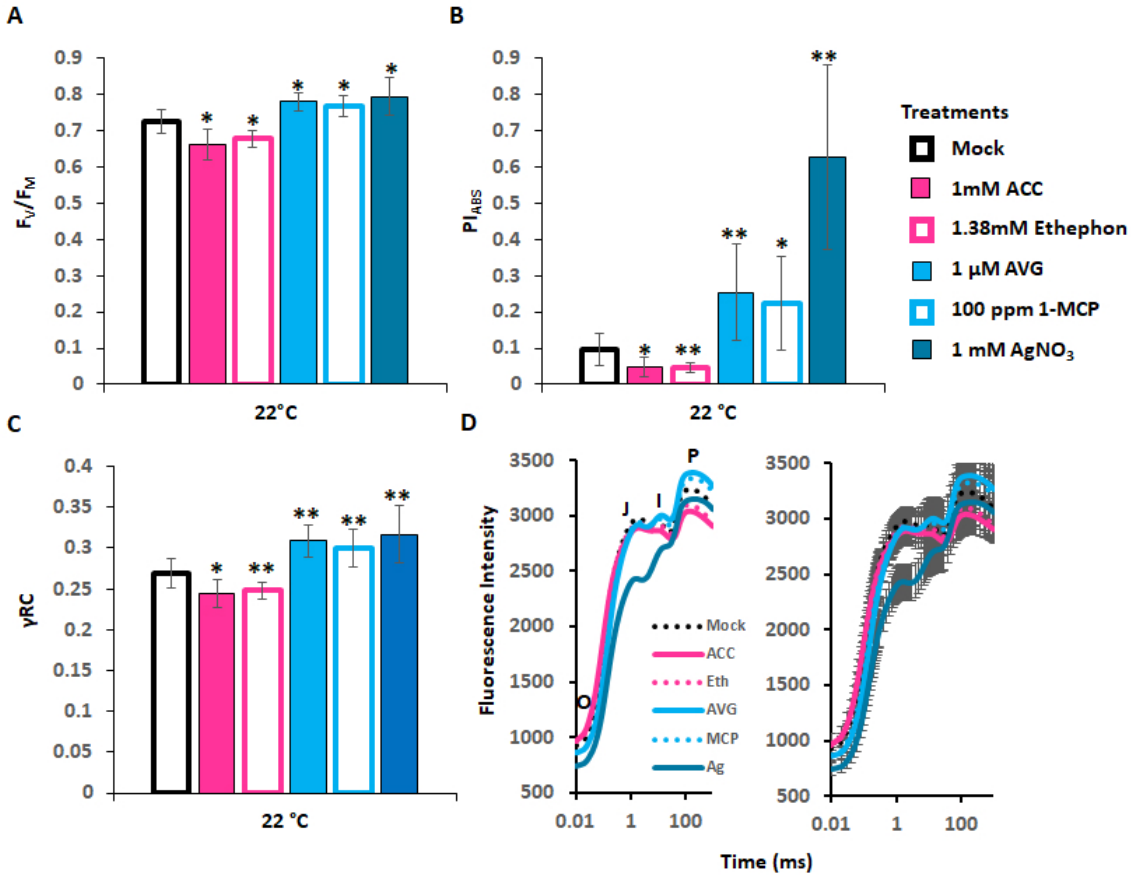

Fig. 6.9. Mean (± SD) effects of ethylene signaling pathway manipulation on photosynthesis after 2 days of control (22 °C) temperatures. Soybean seedlings were were grown with 200 μmol photons per m^{-2} s^{-2} of light on an 16:8 hour light:dark cycle for 2 weeks prior to treatments. A) Quantum yield of photosystem II (F_v/F_m), B) performance index (PI_{ABS}) is a parameter indicating the functionality and capacity of PSII, and C) probability that a chlorophyll is a PSII reaction center (γRC) after 2 days of temperature and foliar spray treatment. Error bars are standard deviations where n = 9. One-way ANOVA were significant for all parameters. Post-hoc analyses using Tukey-HSD were performed to compare treatments with mock, * $p < 0.05$, ** $p < 0.01$. D) Transient chlorophyll *a* fluorescence (Kautsky curve) plotted on a logarithmic time axis. Means are presented on the left without error bars for clarity, and on the right with standard deviation error bars where n = 9.

was decreased by ethylene pathway inhibition (Figure 6.10A-C). Electron transport through PSII was generally decreased by ethylene pathway stimulation and increased by ethylene pathway inhibitions (Figure 6.10D). Additionally, during ethylene pathway inhibition, the energy required to close all PSII reaction centers was decreased (Sm, Figure 6.11A), while the efficiency (ψE_o, Figure 6.11B) and the probability (ϕE_o, Figure 6.10C) of electron transport from Q_A to Q_B were increased, as was the PQ pool so that more PQ molecules were available for reduction to pass electrons through to PSI (Area, Figure 6.11D).

Manipulation of the ethylene pathway under control temperatures resulted in decreases in absorbance per reaction center, electron transport per reaction center, the efficiency and probability that an absorbed photon would be used to send an electron through electron transport, yet photon trapping remained the same and dissipation of photons away from photosystem II was increased. These data are consistent with ethylene treatment increasing NPQ (Chen and Gallie, 2015), since we observed more energy dissipated and less transferred through the entirety of the electron transport chain. More broadly, ethylene treatment results in overall decreases in photosynthetic parameters across species (Ferrante et al., 2012; Gunderson and Taylor, 1991; Khan, 2004; Taylor and Gunderson, 1986, 1988; Tholen et al., 2007, 2008).

When ethylene pathway manipulation was applied in the cold, the results were variable, though generally resulted in lower light-dependent photosynthetic performance regardless of treatment versus cold alone. After 2 days of cold treatment, both positive and negative ethylene signaling pathway manipulation further decreased F_v/F_m (Figure 6.12A). All points along the chlorophyll *a* transient curve (Figure 6.12C) and the probability that a PSII chlorophyll molecule was acting as a reaction center (γRC) decreased compared to cold alone (Figure 6.12D). The performance index of PSII (PI_{ABS}) was only significantly impacted in the cold by silver nitrate treatment, which resulted in a further decrease (Figure 6.12B). Silver nitrate treatment also decreased electron transport (Figure 6.13D), PQ pool size (Figure 6.14A), efficiency (Figure 6.14C) and probability (Figure 6.14D) of electron transfer from Q_A

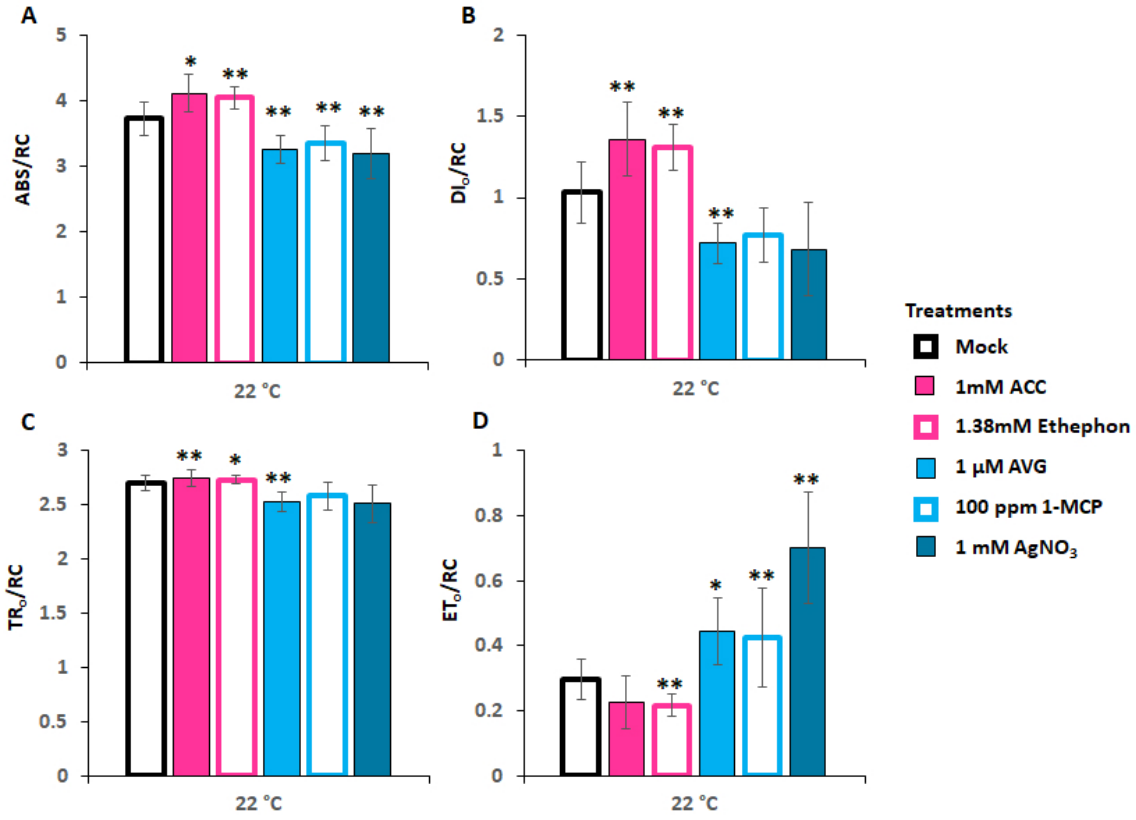

Fig. 6.10. Mean (± SD) effects of ethylene signaling pathway manipulation on energy flux through PSII after 2 days of control (22 °C) temperatures on 2 week old soybean seedlings which were grown with 200 μmol photons per m^{-2} s^{-2} of light on an 16:8 hour light:dark cycle. A) Photon absorbance per reaction center, B) photon dissipation per cross-section (DI_O/CS), C) photon trapping per cross-section (TR_O/CS), and D) electron transport per cross-section (ET_O/CS) after 2 days of temperature and foliar spray. One way ANOVA were significant for all parameters. Post-hoc analyses using Tukey-HSD were performed to compare treatments with mock, * p <0.05, ** p <0.01. n = 9.

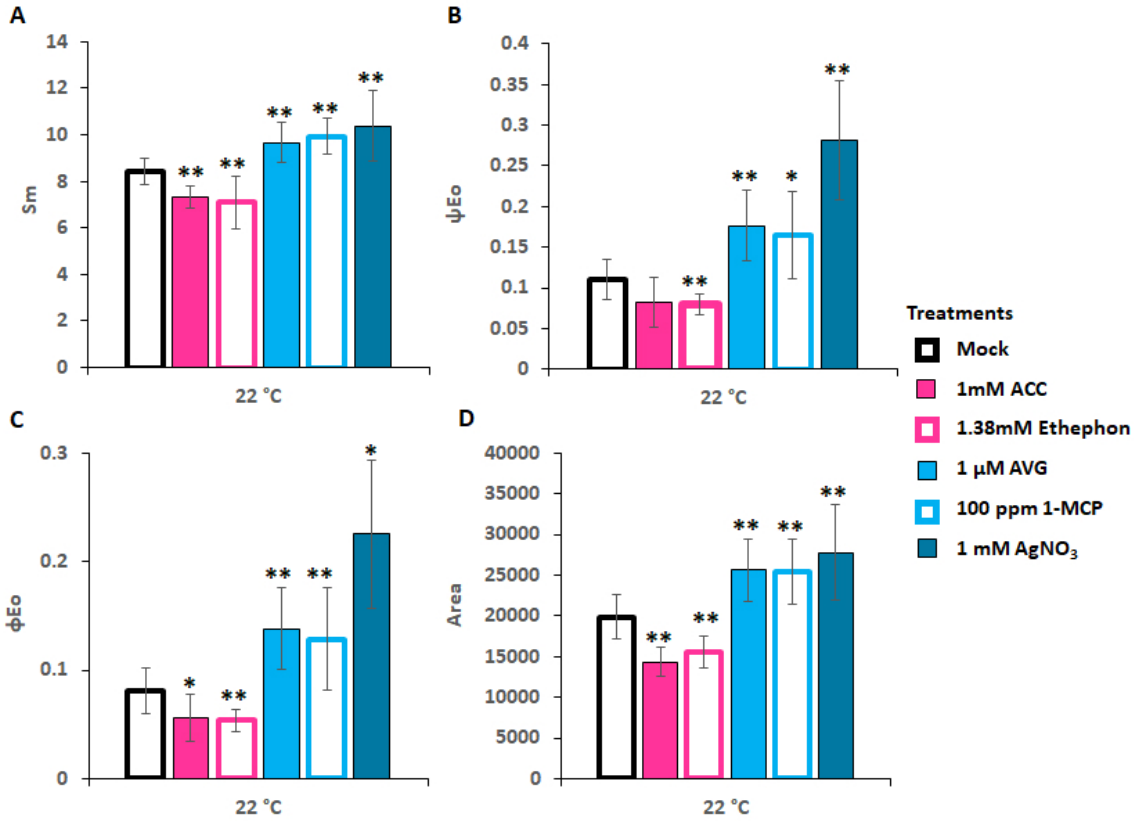

Fig. 6.11. Mean (± SD) effects of ethylene pathway manipulation PSII efficiency and probability of electron transfer occurring after 2 days of control (22 °C) temperatures 2 week old soybean seedlings which were grown with 200 μmol photons per m^{-2} s^{-2} of light on an 16:8 hour light:dark cycle. A) Sm, Area normalized by F_v, is proportional to the energy required to close all PSII reaction centers. B) The probability that an absorbed photon will result in an electron passing through the electron transport chain (ψE_o). C) The efficiency with which an electron is passed into the electron transport chain (ϕE_o). D) Area, measured between F_m and F_o above the curve, is proportional to the size of the PQ pool. One way ANOVAs were significant for all parameters. Post-hoc analyses using Tukey-HSD were performed to compare treatments with mock, * $p < 0.05$, ** $p < 0.01$. n = 9.

to PSI. Ethylene inhibition by AVG and 1-MCP resulted in a significant increase in the energy required to close PSII reaction centers (Sm, Figure 6.14B). Overall, ethylene pathway manipulation in the cold increased absorbance (ABS/RC, Figure 6.13A) and dissipation (DI_o/RC, Figure 6.13B) of photons while decreasing photon trapping (TR_o/RC, Figure 6.13C) and the PQ pool size (Area, Figure 6.14A).

Under cold conditions, all ethylene pathway manipulation resulted in a negative impact on photosynthesis. This is in stark contrast to non-cold treated seedlings where ethylene signaling pathway inhibition has a photoprotective impact. One possible explanation is that since 2 days of cold exposure alone results in severe photoinhibition, any additional disruption results in collapse.

6.4 Summary

In the field, nyctinasty (leaf movement) is associated with dusk and the coming darkness (Nakamura et al., 2010). Dusk also signals for the downregulation of photosynthesis based upon circadian regulation (Dodd et al., 2014). Nyctinasty is controlled by the movement of the pulvinus, a thickened stem connecting the leaf base to the stem. Proteomic analysis of pulvinus tissue in the dark has shown that several light-dependent and light-independent photosynthetic proteins are upregulated in this tissue (Hakme et al., 2014). This suggests that photosynthesis is an important factor in the dropping of leaves at night. Further research would have to be conducted to elucidate which occurs first, leaf movement signaling or the downregulation of photosynthetic performance.

In this study, the timing between the observed cryonasty leaf movement and operational photosynthetic reduction suggests a correlation; however, the nature of that correlation is not fully elaborated based on these data. Since maximal photosynthesis is not significantly impacted until 7 hours of cold exposure, it would first need to be established if cryonasty leaf movement is also reversible within this time frame to strengthen this correlation. Our data on cryonasty leaf movement spans over 48

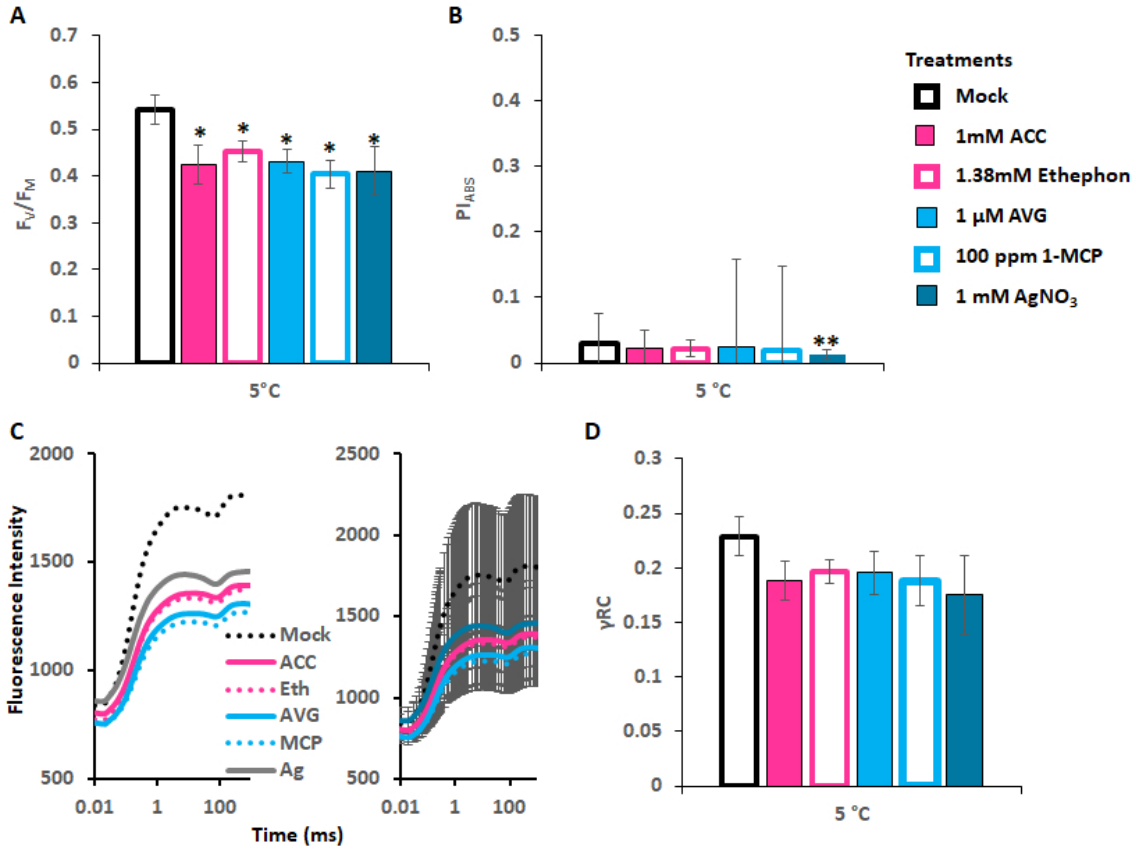

Fig. 6.12. Mean (± SD) effects of ethylene signaling manipulation on photosynthesis after 2 days of cold (5 °C) exposure on 2 week old soybean seedlings which were grown with 200 μmol photons per m^{-2} s^{-2} of light on an 16:8 hour light:dark cycle. A) Quantum yield of photosystem II (F_v/F_m), B) performance index (PI_{ABS}), a parameter indicating the functionality and capacity of PSII, C) Transient chlorophyll *a* fluorescence (Kautsky curve) on a logarithmic time axis. Averages are presented on the left without error bars for clarity, and on the right with standard deviation error bars. D) The Probability that a chlorophyll is a PSII reaction center (γRC) after 2 days of temperature and foliar spray treatment. Error bars represent standard deviation. One-way ANOVA were significant for A, B, and D. Post-hoc analyses using Tukey-HSD were performed to compare treatments with mock, * $p < 0.05$, ** $p < 0.01$. $n = 9$.

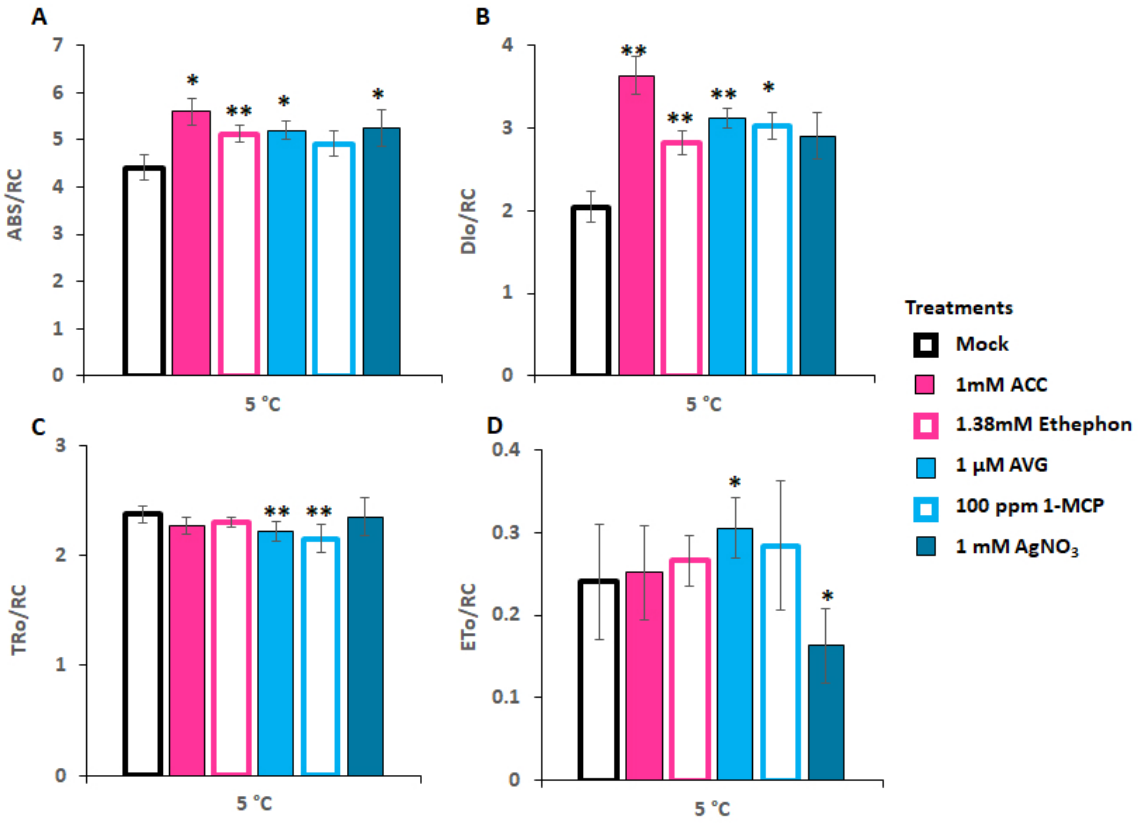

Fig. 6.13. Means (± SD) effects of ethylene signaling pathway manipulation on energy flux through PSII after 2 days of cold (5 °C) exposure 2 week old soybean seedlings which were grown with 200 μmol photons per m^{-2} s^{-2} of light on an 16:8 hour light:dark cycle. A) Photon absorbance per reaction center, B) photon dissipation per cross-section (DI_O/CS), C) photon trapping per cross-section (TR_O/CS), and D) electron transport per cross-section (ET_O/CS) after 2 days of temperature and foliar spray. One-way ANOVA were significant for all parameters. Post-hoc analyses using Tukey-HSD were performed to compare treatments with mock, * $p < 0.05$, ** $p < 0.01$. $n = 9$.

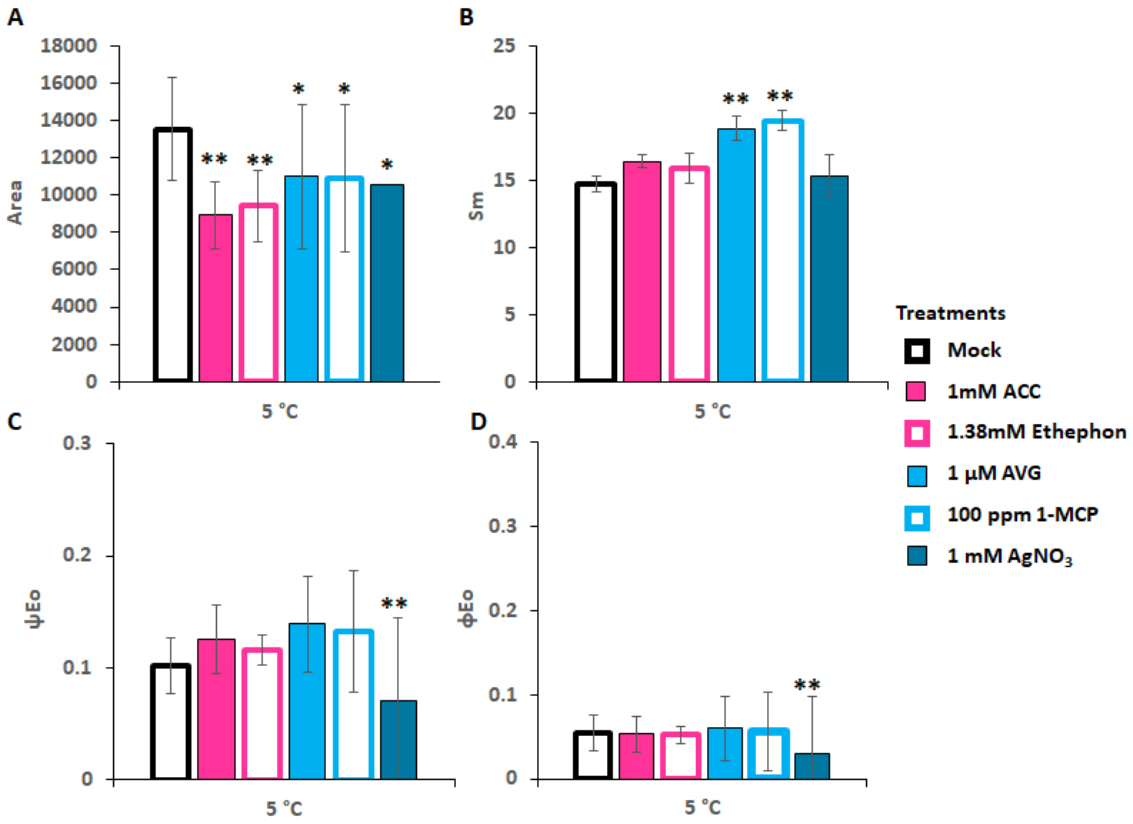

Fig. 6.14. Means (± SD) effects of ethylene pathway manipulation PSII efficiency and probability of electron transfer occurring after 2 days of cold (5 °C) exposure on 2 week old soybean seedlings which were grown with 200 μmol photons per m^{-2} s^{-2} of light on an 16:8 hour light:dark cycle. A) Area, measured between F_m and F_o above the curve, is proportional to the size of the PQ pool. B) Sm (Area normalized by F_v) is proportional to the energy required to close PSII reaction centers. C) The probability that a photon absorbed will result in an electron entering into the electron transport chain (ψE_o). D) The efficiency with which an electron is passed into the electron transport chain (ϕE_o). One-way ANOVA were significant for all parameters. Post-hoc analyses using Tukey-HSD were performed to compare treatments with mock, * $p < 0.05$, ** $p < 0.01$. n = 9.

hours of continuous cold with darkness beginning 12 hours into cold treatment which does not allow for this comparison. Maximal photosynthesis is significantly decreased throughout the 7 day observation period which is similar to the cyronastic leaf movement persisting throughout cold exposure. Additional experiments in Dr. Randall's lab have demonstrated that cyronastic leaf movements recover after 1 - 4 days of cold treatment within 12 hours of warm temperature onset. As this work did not examine recovery of photosynthesis post cold exposure, this is an intriguing avenue for future experiments.

Decreases in light-dependent photosynthetic functionality and efficiency were noted with cold treatment, ethylene signaling pathway stimulation at control temperatures, and ethylene pathway manipulation in the cold regardless of treatment. These decreases were due to an increase in photon dissipation, likely driven by decreased PQ pool size which would limit the electron flow from PSII to PSI. Cold-induced damage to operational photosynthesis began around 25 minutes post exposure while cold-induced damage to maximal photosynthesis required 6 hours of cold exposure. This suggests that NPQ switches from thermal dissipation (qE) to photoinhibition (qI) by 6 hours of cold-exposure. Overall it was evident that cold exposure, even for short periods of time, resulted in severe photodamage leading to the loss of PSII reaction centers and photosynthetic efficiency in soybean seedlings.

7. CLONING, EXPRESSION, AND PARTIAL PURIFICATION OF GmICE1A;1 AND GmEIN3A:1

The CBF/DREB1 cold regulon is transcriptionally regulated by a number of mechanisms (Chapter 1). ICE1 is a positive regulator (Chinnusamy et al., 2003) and EIN3 is a negative regulator (Shi et al., 2012) of CBF/DREB. In Chapter 5, ethylene was reported to be a negative regulator of *GmCBF/DREB1s*. Inhibition of the ethylene signaling pathway decreased the *GmEIN3A;1* transcript levels and increased the transcript levels of *GmDREB1A;1*. Stimulation of the ethylene signaling pathway increased *GmEIN3A;1* transcripts and decreased *GmDREB1A;1* transcripts. The working hypothesis of Chapter 5 was that GmEIN3 bound to the EIN3 motif present in *GmCBF/DREB1* promoters thereby preventing transcriptional activation via GmICE1A.

The promoters of *CBF/GmDREB1* transcription factors were scanned for the putative EIN3 motif (ATGYATNY) (Boutrot et al., 2010; Konishi and Yanagisawa, 2008), as well as the putative MYC binding site (CANNTG) recognized by ICE1 (Chinnusamy et al., 2003). It was shown that the promoters of *GmDREB1A;1* and *GmDREB1B;1* each possessed both motifs (Figure 7.1A). Interestingly, in the promoter of *GmDREB1A;1*, the putative EIN3 motif overlapped by a single nucleotide with the putative ICE1 motif. Currently, it is unknown if soybean EIN3 and ICE1 bind to the DNA sequences correlated with the published motifs from Arabidopsis. In order to test the hypothesis that transcriptional interference occurs between GmEIN3A;1 and GmICE1A on *GmCBF/DREB1* promoters due to their proximity within the *GmDREB1A;1* promoter, appropriate tools need to be created. This chapter describes the steps for cloning, expression, and partial purification of GmICE1A;1 and GmEIN3A;1. These were tested for possible DNA binding activity.

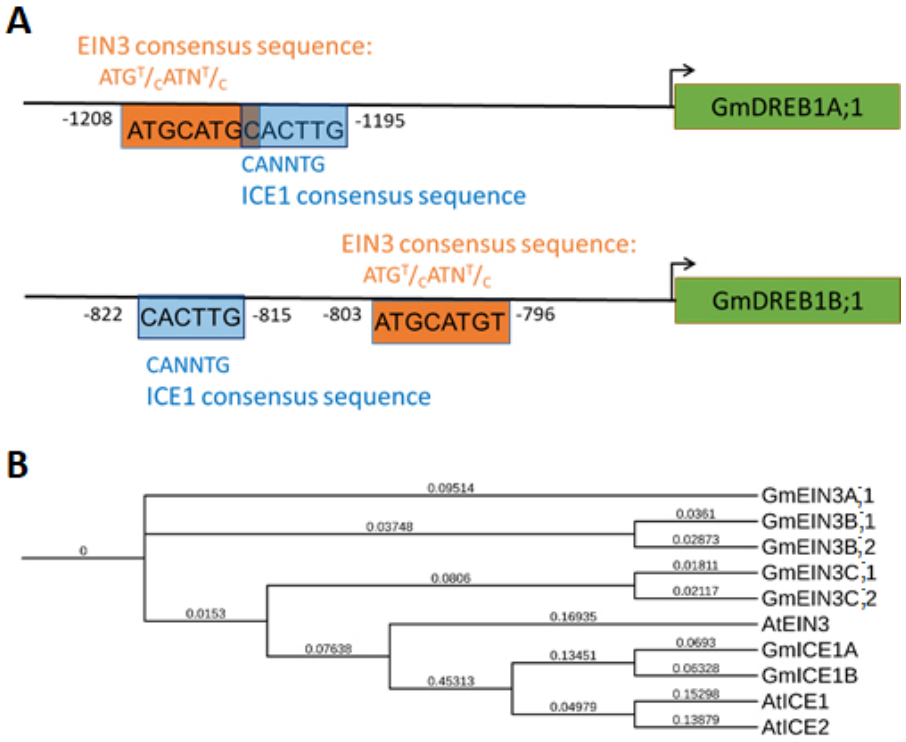

Fig. 7.1. A) *GmDREB1A* promoters containing EIN3 and ICE1 putative binding motifs. The EIN3 motif is in orange and the ICE1 motif is in blue. B) Phylogenetic tree created with iTOL, `https://itol.embl.de/`, (Letunic and Bork, 2016) to align protein sequences of EIN3 and ICE1 from Arabidopsis (Lamesch et al., 2012) and soybean (Severin et al., 2010).

7.1 Gene Selection and Phylogeny

Soybean has undergone two genetic duplication events during its evolution leading to its current tetraploid genomic configuration (Schmutz et al., 2010). Soybean's tetraploid nature results in multiple homologs of Arabidopsis genes. Soybean homologs were identified by comparing Arabidopsis protein sequences with soybean predicted proteins via BLAST on SoyBase (Grant et al., 2010; Severin et al., 2010). Five EIN3 homologs, *GmEIN3A;1, GmEIN3B;1, GmEIN3B;2, GmEIN3C;1, GmEIN3C;2* (Chapter 5) and two ICE1 homologs (*GmICE1A [Glyma.06g165000]* and *GmICE1B*

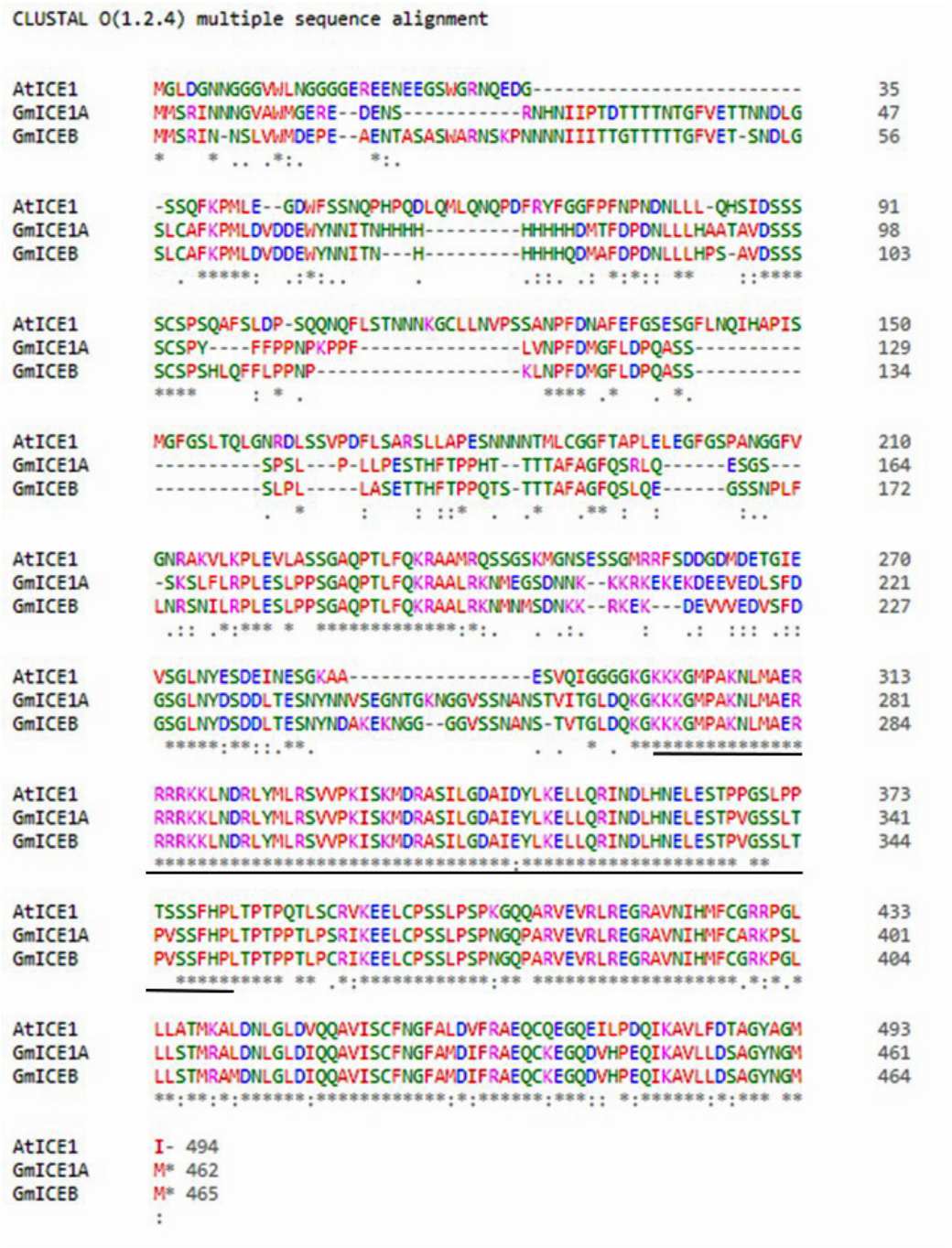

Fig. 7.2. Sequence alignment of Arabidopsis and soybean ICE1 protein homologs. Underlining indicates the basic helix-loop-helix DNA binding region.

[*Glyma.04g200500*]) were identified (Figure 7.1B). The soybean EIN3 homolog *GmEIN3A;1 (Glyma.13g076800)*, was selected for cloning and biochemical analysis based upon the observation that *GmEIN3A;1* transcripts were cold-induced in RNASeq analysis (Yamasaki, 2013) and appeared to be the primary EIN3 gene expressed in soybean (Chapter 5).

To date there is no published information on either GmICE1 homologs. In the RNASeq analysis (Yamasaki, 2013), *GmICE1A* had the highest expression of the potential homologs with 425 counts at 0 h which increased 2.0 fold after 24 hours in the cold. *GmICE1B* expression was 194 counts at 0 hours and increased 1.5 fold at 24 hours. When the predicted protein sequences were aligned with AtICE1, GmICE1A had a 68% sequence identity while GmICE1B was 53% identical (Figure 7.2). Additionally, GmICE1A was 91% identical (Figure 7.2, underlined) to the DNA binding domain present in Arabidopsis ICE1 (Chinnusamy et al., 2003). Based on the homology data, GmICE1A was chosen to be cloned, expressed, and purified.

This chapter describes the protocols for cloning, expression, partial purification, and examining the DNA binding activity of GmEIN3A;1 and GmICE1A.

7.2 Amplification and Ligation of *GmEIN3A;1* into the pET-28b Expression Vector

7.2.1 Materials

1. Chemically competent XL-1 Blue *E. coli* cells (Agilent Technologies)
2. Chemically competent DH5α *E. coli* cells (Courtesy of Dr. A. J. Baucmann)
3. Luria Broth (LB) media (see recipe at the end of the chapter)
4. Super Optimal broth with Catabolite repression (SOC) media (see recipe at the end of the chapter)
5. Kanamycin sulfate, 50 mg/mL

6. LB+Kan plate: LB Agar supplemented with 50 μg/mL kanamycin (see recipe at the end of the chapter)
7. LB+Kan broth: LB supplemented with 50 μg/mL kanamycin(see recipe at the end of the chapter)
8. cDNA from Soybean cv Williams 82
9. PfuUltra High-fidelity DNA Polymerase (Agilent)
10. Primers for GmEIN3A;1 cloning (Table 7.1)
11. Zero Blunt TOPO PCR Cloning Kit (Fisher)
12. Restriction Enzymes: NdeI, NotI, XhoI, NcoI (New England Biolabs)
13. T4 DNA Ligase 2,000U/μL (New England Biolabs)
14. pET-28B plasmid DNA
15. QIAquick Gel Extraction Kit (Qiagen)

7.2.2 Methods

PCR amplification of *GmEIN3A;1*

Soybean (cv Williams 82) cDNA (prepared as in chapter 2.4) was utilized to amplify the entire *GmEIN3A;1* coding sequence which has a length of 1,868 bp. Restriction enzyme sites were introduced during amplification. NdeI site was added to the 3' end by inclusion in the forward primer while NotI site was added to the 5' end, replacing the stop codon, in the reverse primer (Table 7.1). PCR amplification was performed using 100 ng cDNA, PfuUltra High-Fidelity Taq polymerase, and 5 μM primers (Table 7.1). Reactions were started at 95 °C for 2 minutes, followed by 25, 30, or 35 cycles of 95 °C for 30s, 54 °C for 30s and 72 °C for 120s, prior to final extension at 72 °C for 10 minutes. Successful amplification was confirmed by presence

of a band of approximately 1,900 bp following resolution on a 1% agarose gel (Figure 7.3A).

Table 7.1.
Primers utilized for cloning and sequencing *GmEIN3A;1*. Single underline represents the added Nde1 (in the forward primer) and NotI (in the reverse primer) restriction enzyme sites. M13 primers were used to amplify gene insertion region of the TOPO vector. T7 primers were used to amplify gene insertion region of pET-28b vector.

Target	Primer name	Primer sequence	Tm (°C)
GmEIN3A;1	GmEIN3A1 1 Seq For	CATATGATGATGATGTTTGATGAGATGGGGCTT	54
	GmEIN3A1 1 Seq Rev	GCGGCCGCTCACTGGTACCATATTGAAATATCTGGCTG	
M13	M13 Forward	TGTAAAACGACGGCCAGT	
	M13 Reverse	CAGGAAACAGCTATGACC	
GmEIN3A;1 internal sequencing primers	GmEIN3 Seq Mid 3 Rev	GAAGACATTTGGACTGC	
	GmEIN3 Seq Mid 2 For	GCAAAGATTCGCAAGCTTG	
	EIN3 1 Glyma13g03660 Low qPCR	CAGGAAAACTTGGACCCCCA	
T7	T7 Universal Primer	TAATACGACTCACTATAGGG	
	T7 Terminator	GCTAGTTATTGCTCAGCGG	

Ligation of *GmEIN3A;1* into the TOPO vector

The *GmEIN3A;1* amplified through 30 cycles was cloned using Zero Blunt TOPO PCR Cloning Kit. Competent XL-1 Blue *E. coli* cells (25 μL) were thawed on ice. One μL *GmEIN3A;1* PCR product, 0.5 μL salt solution, 1 μL water, and 0.5 μL pCR II-Blunt-TOPO (provided in the Zero Blunt TOPO PCR Cloning Kit) were incubated at room temperature for 15 minutes. One μL was added to the thawed *E. coli*, inverted gently, and incubated on ice for 30 minutes. The cells were heated at 42 °C for 30 seconds then transferred to ice. Room temperature SOC media (125 μL) was added prior to incubation, with shaking at 200 rpm, at 37 °C for one hour. Fifty μL of reaction mixture was spread on LB+Kan agar and incubated overnight at 37 °C.

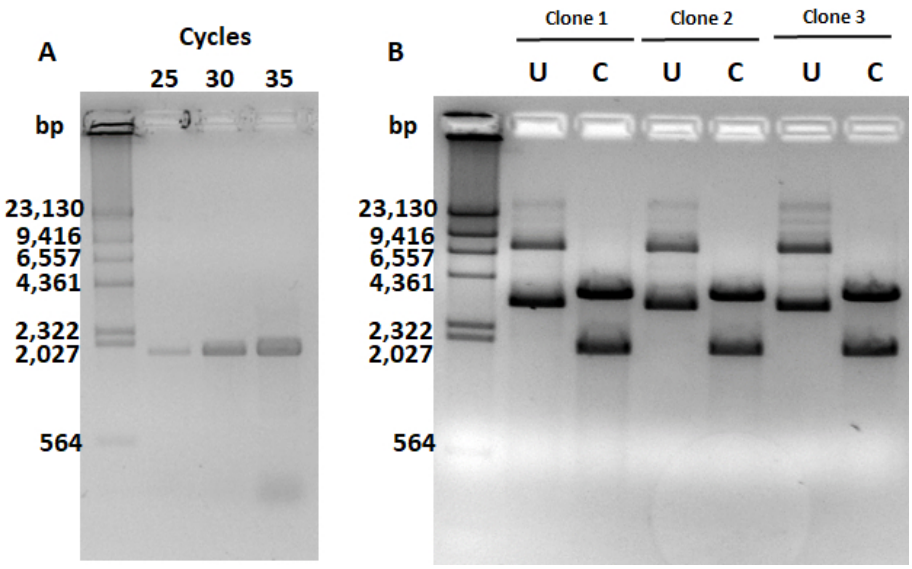

Fig. 7.3. Isolation of *GmEIN3A;1* from soybean cDNA. A) PCR cycle optimization to amplify *GmEIN3A;1* from total soybean cDNA to be cloned into TOPO1. B) Restriction enzyme digestion of multiple clones of TOPO1 containing *GmEIN3A;1* with NdeI and NotI. U signifies undigested plasmid while C signifies digested plasmid. Digested plasmid was expected to generate 5,284 and 1,868 bp fragments.

Confirmation of the presence of *GmEIN3A;1* within the TOPO vector

Plasmids were purified (plasmid purification method in chapter 2.12) from three different colonies (labeled 1 - 3) which had grown overnight in 1 mL LB+Kan media. Plasmids were digested with both restriction enzymes NdeI and NotI following manufacturer's instructions. The predicted fragments from this digest were 1,868 and 5,284 bp. The resulting gel fragments appeared similar to these predicted sizes (Figure 7.3B). Plasmid DNA from colony 3 was sent to the University of Michigan DNA Sequencing Core for sequencing using the M13 Forward and M13 Reverse primers provided by the facility, as well as three internal primers designed specifically for this study (Table 7.1). The resulting sequence fragments were aligned and the cloned *GmEIN3A;1* sequence was identical to the *GmEIN3A;1* coding sequence in Soybase

(Severin et al., 2010), except for a single nucleotide which switched G to A at position 273; however, this change did not result in an amino acid change (data not shown).

Subcloning *GmEIN3A;1* from TOPO vector into pET vector

TOPO-GmEIN3A;1 plasmids isolated from colony 3 were digested with NdeI and NotI overnight at 37 °C. Empty pET-28b vector was digested with NdeI and NotI at 37 °C overnight. The resulting digests were resolved via gel electrophoresis (data not shown). *GmEIN3A;1* and digested pET-28b vector DNA were recovered from the 0.5% agarose gel using the QIAquick Gel Extraction Kit, following the manufacturer's instructions. DNA quantity was measured via Nanodrop (Thermo Scientific). The molarity of 3' and 5' ends was calculated using NEBioCalculator (`http://nebiocalculator.neb.com/#!/dsdnaends`). Ligation of *GmEIN3A;1* and pET-28b vector was performed with 3:1 ratio (moles *GmEIN3A;1:pET-28b vector*) in 1X T4 ligase buffer with 2,000 units of T4 ligase incubated at 16 °C overnight. The ligation reaction was terminated by a 10 minute incubation at 65 °C.

The resulting pET-28b-GmEIN3A;1 plasmid vector (Figure 7.4A) was digested with NcoI, XhoI, and NdeI/NotI restriction enzymes to confirm ligation (Figure 7.4B). The ligate was then transformed into chemically competent DH5α *E. coli*. Fifty μL of DH5α *E. coli* cells were thawed on ice prior to incubation with 4 μL of ligation reaction for 30 minutes. The cells were heated at 42 °C for 30 seconds then transferred to ice for 5 minutes. Room temperature SOC media (450 μL) was added prior to incubation, with shaking at 200 rpm, at 37 °C for one hour. One hundred μL of the reaction mixture was spread on LB+Kan agar and incubated overnight at 37 °C.

Confirmation of the presence of *GmEIN3A;1* in the pET-28b vector

Four colonies from the overnight incubation (3, 6, 8, and 10) were inoculated in 1 mL LB+Kan broth and grown overnight before plasmid purification (plasmid purification method in chapter 2.12). Plasmid DNA isolated from two colonies (3

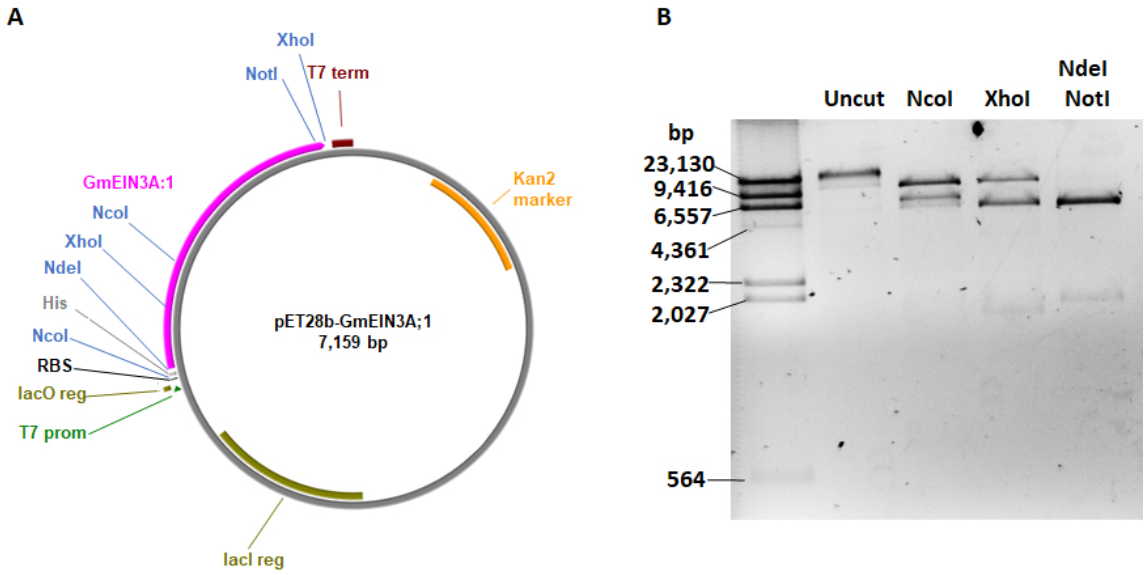

Fig. 7.4. A) pET28b-GmEIN3A;1 plasmid map created with PlasMapper (Dong et al., 2006). B) Restriction enzyme digest of pET28b-GmEIN3A;1. NcoI digest was predicted to result in fragment lengths of 6,564 and 704 (not visible) bp. XhoI digest was predicted to result in fragment lengths of 5,546 and 1,806. Double digest with NdeI and NotI was predicted to result in 5,462 and 1,806 bp.

and 10) were digested with restriction enzymes NcoI, XhoI, and NdeI/NotI overnight at 37 °C. The digested plasmid DNA were separated by gel electrophoresis (Figure 7.4B). The predicted fragment lengths from each digest were: NcoI should result in two fragments (6,564 and 704 bp), XhoI should result in two fragments (5,546 and 1,722 bp), and NdeI/NotI should result in two fragments (5,462 and 1,806 bp). Each digest resulted in fragments that appeared to be correct; however, the two single digests also had a large band which is likely linear plasmid that sustained a single cut instead of a double cut (i.e. partial digest).

The band patterns were similar to the prediction suggesting that *GmEIN3A;1* was present in the pET-28b vector in both colonies (Figure 7.5A). To ensure the ligated *GmEIN3A;1* was in-frame for subsequent translation, the vector junctions from colony 10 were sequenced at the University of Michigan DNA Core (T7 universal

and terminator primers, Table 7.1). The sequence was scanned for open reading frames to confirm the His tag and the gene were in the same reading frame to allow for the proper translation of the GmEIN3A;1 protein when expressed in *E. coli* (Figure 7.5B). The resulting sequence confirmed the presence of in frame *GmEIN3A;1* which should be capable of producing 6xHis-GmEIN3A;1 protein (Figure 7.5C). A glycerol stock of colony 10 was labeled "10" and stored at -80 °C.

The pET-28b containing GmEIN3A;1 plasmid was subcloned into Rosetta 2(DE3) *E. coli* cells for future expression work. Fifty μL of Rosetta 2(DE3) *E. coli* cells were thawed on ice prior to incubation with 1 μL of GmEIN3A;1 in pET-28b plasmid for 30 minutes. The cells were heated at 42 °C for 30 seconds then transferred to ice for 5 minutes. Room temperature SOC media (450 μL) was added prior to incubation, with shaking at 200 rpm, at 37 °C for one hour. One hundred μL of the reaction mixture was spread on LB+Kan agar and incubated overnight at 37 °C. The next morning one colony was inoculated in 1mL LB+Kan and incubated overnight. A glycerol stock labeled "pETEIN in Ros 2" and stored at -80 °C.

7.3 Amplification and Ligation of *GmICE1A* into the pET-28b Expression Vector

7.3.1 Materials

1. cDNA from *GmICE1A*
2. pET-28b vector
3. Restriction enzymes NcoI and XhoI
4. Chemically competent Rosetta (DE3) *E. coli* cells (Novagen)

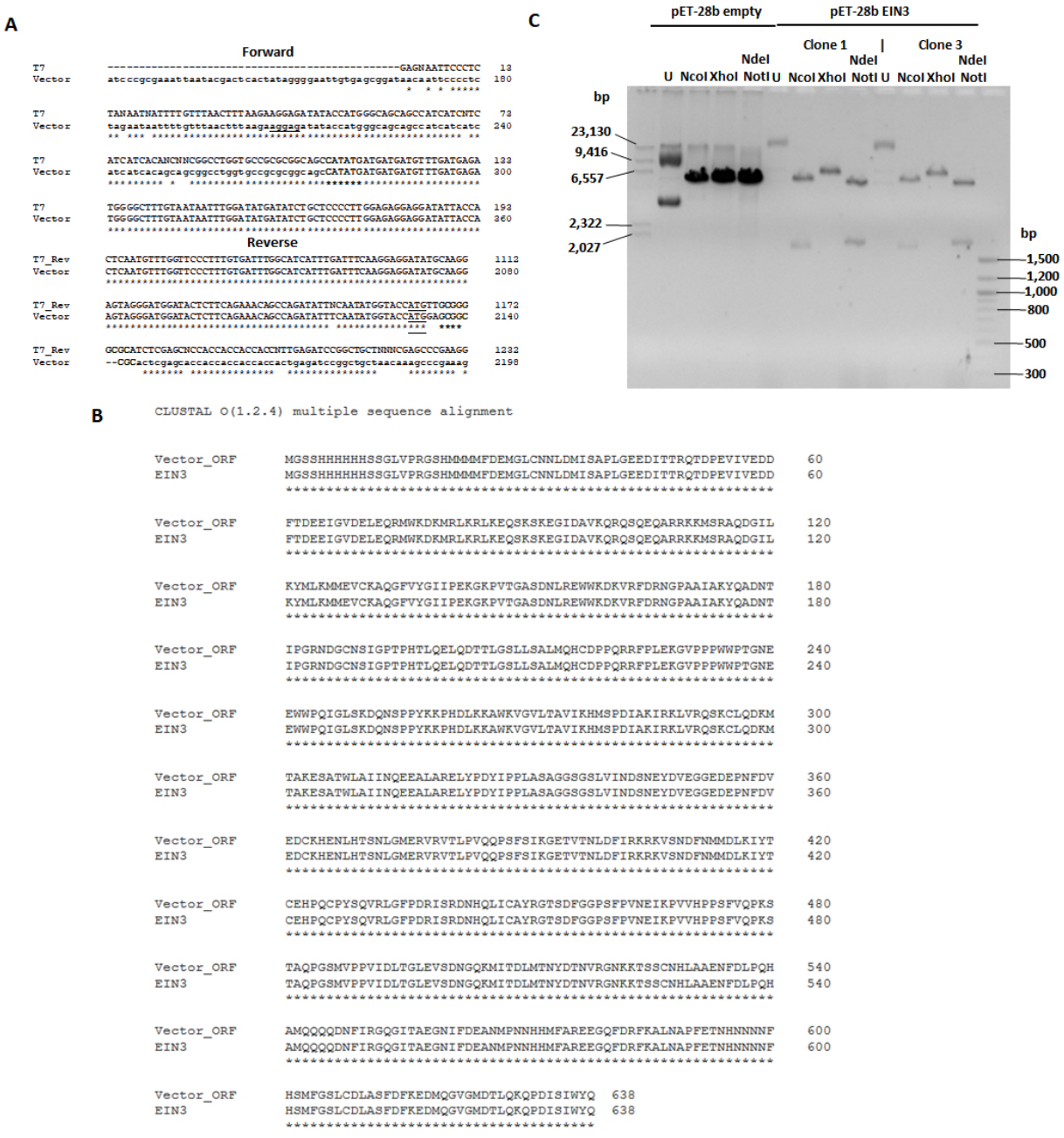

Fig. 7.5. Investigation into the composition of pET-28b vector containing *GmEIN3A;1*. A) Restriction enzyme digest comparing empty vector with two different clones (designated 1 and 3 respectively) containing *GmEIN3A:pET-28b* ligate. B) Sequencing results from the junctions of pET-28b vector and *GmEIN3A;1* ligation from clone 3. Underline region indicates the ribosome binding site, bold letters highlight the restriction enzyme sites used to insert *GmEIN3A;1*. C) An open reading frame search of the DNA sequence of pET-28b containing GmEIN3A;1 predicted a protein that aligns with the predicted GmEIN3A;1 protein sequence in Soybase.

7.3.2 Procedure

One of the soybean ICE1 genes, GmICE1A (Glyma.06g16500) was selected for expression as explained in section 7.1. The gene was chemically synthesized with restriction enzyme sites for NcoI and XhoI and was codon optimized for expression in *E. coli* by GenScript. *GmICE1A;1* was subsequently ligated into the pUC57-KAN vector. *GmICE1A;1* was cut with NcoI and XhoI and ligated into pET-28b (Figure 7.4A, performed by Dr. L. Balakrishnan). The resulting GmICE1A pet-28b vector was transformed into Rosetta^{TM} (DE3) competent *E. coli* cells following manufacturer′s instructions.

7.4 Expression of 6xHis-GmEIN3A;1 in *E. coli*

7.4.1 Materials

1. *GmEIN3A;1* in pET-28b plasmids in Rosetta 2(DE3) *E. coli*
2. Luria Broth (LB) media (see recipe at the end of the chapter)
3. Kanamycin sulfate, 50 mg/mL
4. LB+Kan broth: LB supplemented with 50 μg/mL kanamycin(see recipe at the end of the chapter)
5. Autoinduction media (see recipe at the end of the chapter)
6. YEP media (see recipe at the end of the chapter)
7. Isopropyl-β-D-1-thiogalactopyranoside (IPTG), 1M
8. SDS-PAGE Sample Buffer (SSB), 4X (see recipe at the end of the chapter)
9. anti-His tag monoclonal antibody (Santa Cruz Biotechnology, SC53073)

7.4.2 Procedure

Several induction methods were investigated to identify the most efficient method to induce expression of the 6xHis-GmEIN3A;1 in pET-28b vector. IPTG induction under two different temperatures and an autoinduction method were compared.

IPTG induction of 6xHis-GmEIN3A;1 expression

A 1 mL culture of Rosetta 2(DE3) *E. coli* cells containing *GmEIN3A;1* in pet-28b plasmid were grown overnight in 1 mL LB+Kan media. Two separate 100 mL LB+Kan media were inoculated with 100 μL of the overnight culture. These cultures were shaken at 200 rpm and held at either 37 or 18 °C. The absorbance at 600 nm was measured every few hours until the cultures reached an optical density of 0.4 - 0.6. Once the appropriate optical density was reached, 1 mL of each culture was removed to be saved as the "uninduced" fraction. IPTG was added to reach a final concentration of 1 mM IPTG. The cultures were shaken at 200 rpm for an additional 4 hours at either 37 or 18 °C. After 4 hours, 1 mL of each culture was removed to be saved as the "induced" fraction.

The 1 mL collected fractions were kept on ice until all four had been collected. Cells were pelleted by centrifugation at 17,000 rpm for 15 minutes at 4 °C. The supernatant was removed and the pellets stored at -80 °C. The remaining cultures (approximately 98 mL) were pelleted by centrifugation at 10,000 rpm for 30 minutes at 4 °C. The supernatant was removed and the pellet was washed with 30 mL of distilled water. The pellet was recovered by centrifugation at 3,000 rpm for 20 minutes at 4 °C. The pellets were stored at -80 °C.

Autoinduction of 6xHis-GmEIN3A;1 expression

The autoinduction method utilizes a switch between carbon metabolism over 2 days to induce production of the desired protein. In this method the expression

of the construct is controlled by the lac operon within *E. coli*. Glucose is consumed preferentially until it has been depleted which leads to a secondary lag phase while the bacteria switch to lactose consumption activating the lac operon and transcriptional activation of the target gene (Hellman and Fried, 2007).

Two 1 mL cultures of Rosetta 2(DE3) *E. coli* cells containing *GmEIN3A;1* in pet-28b plasmid were grown overnight in 1 mL LB+Kan media. One culture was added to 100 mL of autoinduction media. The other culture was added to 100 mL of YEP media. Both cultures were grown for 3 days while shaking at 275 rpm at 22 °C (Blommel et al., 2007).

One mL samples were collected from both the autoinduction and the YEP cultures. Cells were pelleted by centrifugation at 8,000 rpm for 15 minutes at 4 °C. The supernatant was removed and the pellets stored at -80 °C. The remaining cultures (approximately 99 mL) were pelleted by centrifugation at 10,000 rpm for 30 minutes at 4 °C. The supernatant was removed and the pellet was washed with 30 mL of distilled water. The pellet was recovered by centrifugation at 3,000 rpm for 20 minutes at 4 °C. The pellets were stored at -80 °C.

Confirmation of 6xHis-GmEIN3A;1 Induction

Cells from 1 mL induced and uninduced samples from the section above were lysed with 1X SDS-PAGE Sample Buffer at 95 ° for 5 minutes. Uninduced cells were lysed with 100 μL. Induced cells were lysed with 200 μL. Proteins were resolved by SDS-PAGE. GmEIN3A;1 is predicted to be 70 kDa. This size closely matches the predicted size of Arabidopsis EIN3; however, when AtEIN3 is resolved by SDS-PAGE it has an apparent molecular weight of 90 kDa (Potuschak et al., 2003). Thus, the 70 - 100 kDa region was examined for potential induction of GmEIN3A;1. While there was no visible Coomassie-stainable induced bands (data not shown); when probed with anti-His tag monoclonal antibody (1:1000 Santa Cruz Biotechnology, SC53073)

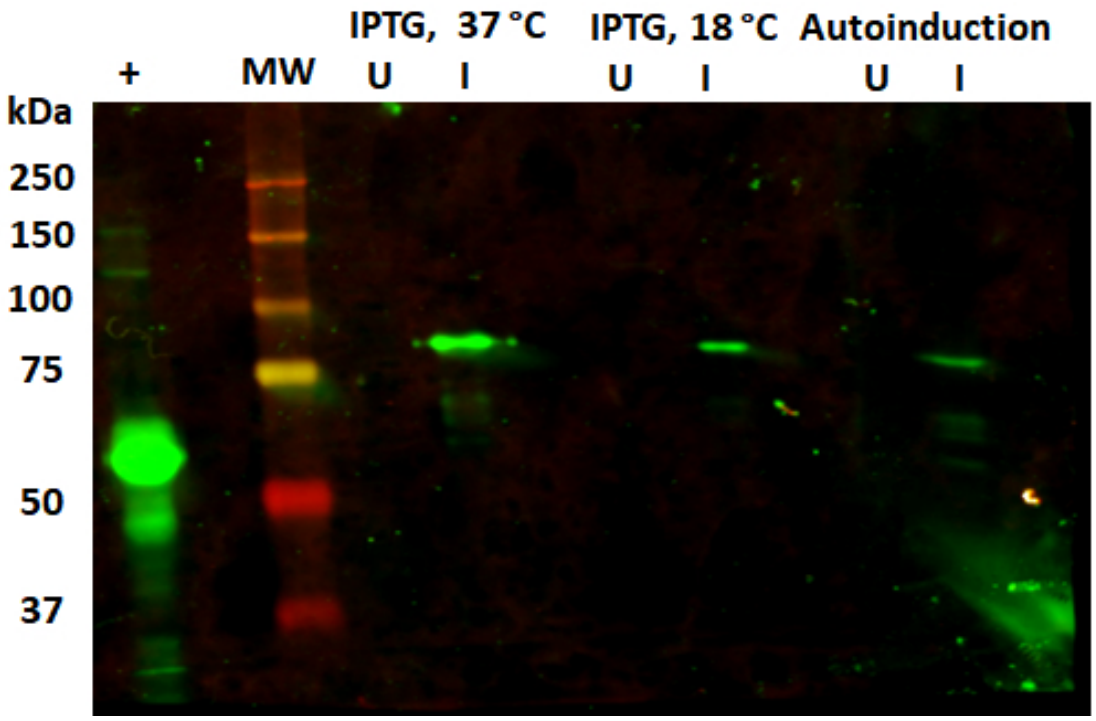

Fig. 7.6. His-tag antibody (mouse monoclonal, 1:1000) used to examine GmEIN3A;1 expression in Rosetta 2(DE3) *E. coli* cells separated on a 10% acrylamide gel. Uninduced (U) and Induced (I) at 37 and 18 °C induced with 1 mM IPTG for 4 hours at the indicated temperatures. Autoinduction at 22 °C for 3 days. Positive (+) His-tagged Arabidopsis glutathione S-transferase (provided by S. Randall).

bands were apparent in all three induced cultures (Figure 7.6) between the 75 and 100 kDa markers.

7.5 Expression of 6xHis-GmICE1A in *E. coli*

7.5.1 Materials

1. *GmICE1A* in pET-28b plasmids in Rosetta (DE3) *E. coli*
2. Luria Broth (LB) media (see recipe at the end of the chapter)

3. Kanamycin sulfate, 50 mg/mL
4. LB+Kan broth: LB supplemented with 50 μg/mL kanamycin(see recipe at the end of the chapter)
5. Autoinduction media (see recipe at the end of the chapter)

7.5.2 Procedure

A cultures of Rosetta (DE3) *E. coli* cells containing *GmICEA1* in pet-28b plasmid was grown overnight in 1 mL LB+Kan media. The culture was added to 100 mL of autoinduction media. The culture was grown for 3 days while shaking at 275 rpm at 22 °C (Blommel et al., 2007). The cells were pelleted by centrifugation, 5,000 rpm for 20 minutes at 4 °C.

7.6 Partial purification of His-tagged GmEIN3A;1 and GmICE1A

7.6.1 Materials

1. A liter of induced Rosetta 2(DE3) *E. coli* expressing 6xHis-GmEIN3A;1 or Rosetta (DE3) *E. coli* cells expressing 6xHis-GmICE1A
2. Ni-NTA Agarose Column Wash Buffer (see recipe at the end of the chapter)
3. Ni-NTA Agarose Column Elution Buffer (see recipe at the end of the chapter)
4. Lysozyme, 10 mg/mL
5. Ni-NTA agarose resin (Bio-Rad)
6. SDS-PAGE Sample Buffer (SSB), 4X (see recipe at the end of the chapter)
7. anti-His tag monoclonal antibody (Santa Cruz Biotechnology, SC53073)

7.6.2 Cell Lysis

One liter of induced *E. coli* cells were pelleted into four even portions by centrifugation at 5,000 rpm for 30 minutes at 4 °C. Cells were kept on ice at all times. Pellets were solubilized with 25 mL of wash buffer and combined into a single container with 10 mg/mL lysozme added for a final concentration of 10 μL/mL. Cells were lysed by sonication. Sonication was performed for 10 minutes with 30 second on/off pulses at an amplitude of 50%. Cell debris was removed by centrifugation at 2,500 rpm for 10 minutes at 4 °C. The supernatant was decanted carefully and saved for purification. The pellet was resuspended in 10 mL of wash buffer and 1 mL saved at -80 °C for later analysis.

7.6.3 Ni-NTA Agarose Column Purification - General Method

Ni-NTA agarose resin was packed into a 5 mL column for use on the NGC^{TM} Chromatography System FPLC (BioRad). The Ni-NTA agarose resin column was equilibrated with 50 mL of wash buffer over the course of 50 minutes. The supernatant from the cell lysis step (input) was loaded onto the column. A 1 mL sample was removed from the flow-through (unbound) for later analysis.

The loaded column was washed with 50 mL of wash buffer. A 1 mL sample was removed from the second flow-through (wash) for later analysis. Elution of the protein was performed with an imidazole gradient. The gradient was applied from 30 - 300 mM of imidizole for GmICEA1 and 10 - 500 mM of imidazole for GmEIN3A;1 with 100 mL flowing at 1 mL per minute. Fractions were collected in 1 mL aliquots. Protein content in the fractions was measured with absorbance (A_{280}). Fractions with high protein content were collected for later analysis.

7.6.4 Results of Fractionation of 6xHis-GmEIN3A;1 with Ni-NTA Agarose Resin

Based upon protein content estimations, the fractions with the highest protein concentrations were 16 - 23 and 57 - 60. Ten μL from input, output, and each fraction were collected. One μL from the pellet was combined with 9 μL of elution buffer. These samples were denatured with 3.3 μL of 4X SSB at 95 °C for five minutes. Proteins were resolved with SDS-PAGE. Coomassie staining of the fractions revealed a large number of bands within the 80 - 100 kDa range indicating probable contamination or degradation (Figure 7.7A).

When probed with anti-His tag antibody, protein was detected in several fractions (Figure 7.7B) at the estimated molecular weight as the induced band from the whole cell lysate from 37 °C induction shown in Figure 7.6. This band had an estimated molecular mass of approximately 91 kDa as determined by relative mobility. The putatitve 6xHis-GmEIN3 band was present in the early fractions 16 - 23 but not in the later fractions 57 - 60. Multiple lower mass bands were detected in fractions 17 - 23. These bands are presumed to be degraded GmEIN3A;1 or perhaps His-rich *E. coli* proteins. A single fraction (16) appeared relatively pure however not enough was recovered to utilize in binding assays.

7.6.5 Results of fractionation of 6xHis-GmICE1A with Ni-NTA Agarose Resin

The fractions with the highest total protein concentrations were 12 - 21. Ten μL from input, output, and each fraction were collected. One μL from the pellet was combined with 9 μL of elution buffer. These samples were denatured with 3.3 μL of 4X SSB at 95 °C for five minutes. GmICE1A purified by Dr. Lata Balakrishnan was utilized as a positive control (+). Proteins were resolved with SDS-PAGE and visualized with Coomassie stain (Figure 7.8). GmICE1A appears to run as a doublet of approximately 70 and 60 kDa which is bigger than the predicted 51 kDa. Frac-

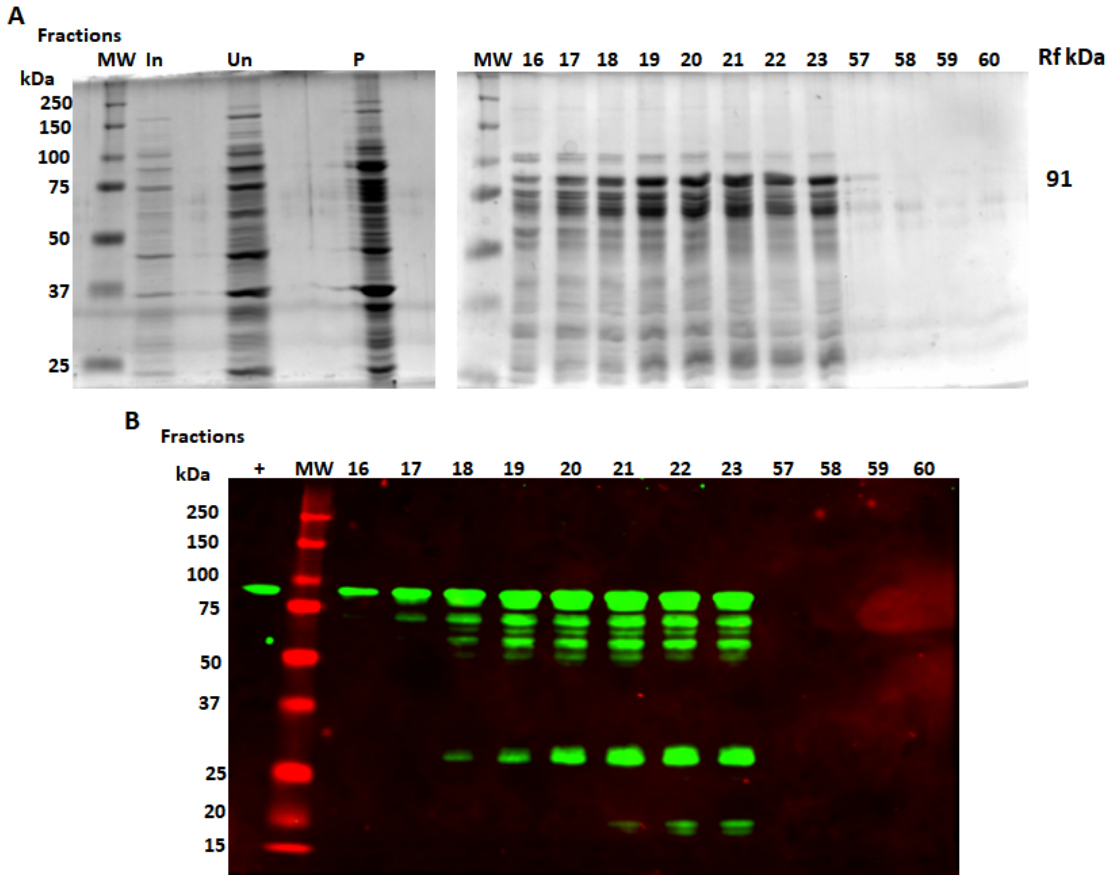

Fig. 7.7. IPTG induction of 6xHis-GmEIN3A;1 in Rosetta 2(DE3) *E. coli* cells. A) Coomassie gels from Ni-NTA agarose resin column purification representing the pellet (P), input (In), unbound (Un) and multiple fractions eluted from the column across a gradient of immidazole. B) His-tag western blot of fractions from column purification in panel A.

tions 14 - 18 were combined. Total protein was measured using the Bradford assay (Bradford, 1976). The combined fractions had a protein concentration of 0.28 μg/μL.

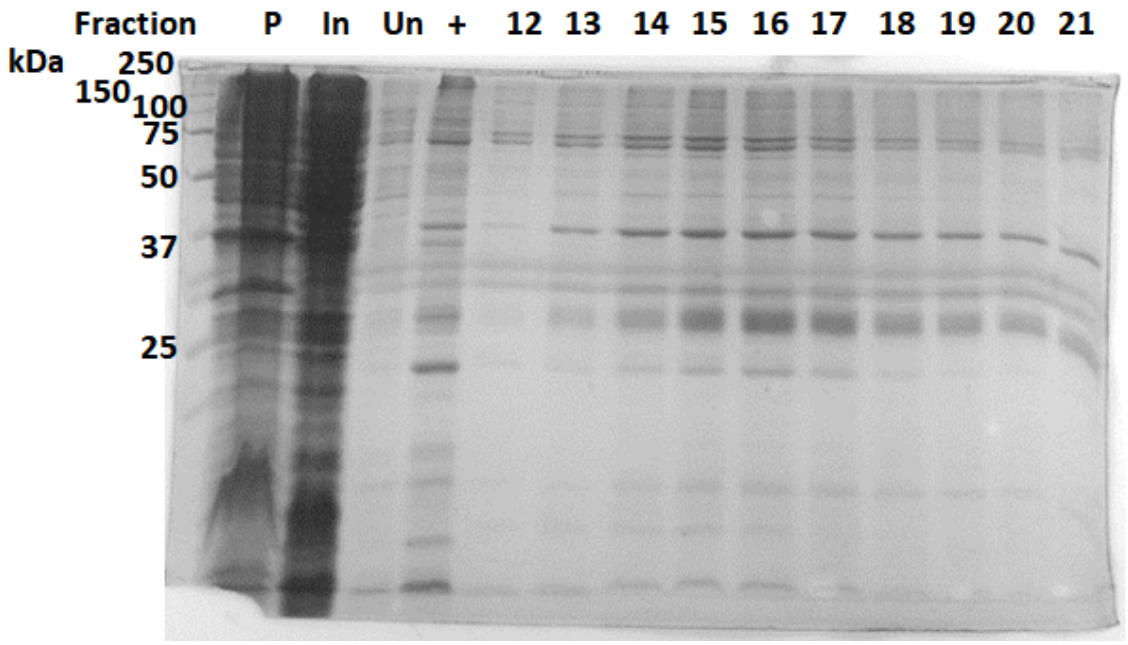

Fig. 7.8. Coomassie gels from Ni-NTA agarose resin column purification representing the pellet (P), input (In), unbound (Un), purified GmICE1A provided by Dr. Lata Balakrishnan (+), and multiple fractions from the column. Note: due to multiple freeze/thaw cycles the + control provided by Dr. Balakrishnan was partially degraded; however, the doublet is still visible.

7.7 Maximization of 6xHis-GmEIN3A;1 Expression, Extraction, and Purification

7.7.1 Materials

1. Electrocompenent Tuner DE3 *E. coli* cells
2. GmEIN3A;1 in pET-28b vector
3. Super Optimal broth with Catabolite repression (SOC) media (see recipe at the end of the chapter)
4. Luria Broth (LB) media (see recipe at the end of the chapter)

5. Kanamycin sulfate, 50 mg/mL
6. LB+Kan broth: LB supplemented with 50 μg/mL kanamycin (see recipe at the end of the chapter)
7. LB+Kan agar: LB supplemented with 50 μg/mL kanamycin (see recipe at the end of the chapter)
8. Isopropyl-β-D-1-thiogalactopyranoside (IPTG), 1M
9. Breaking buffers (see recipes in Table 7.2)
10. Lysozyme, 10 mg/mL
11. Ni-NTA Agarose Column Elution Buffer (see recipe at the end of the chapter)
12. Ni-NTA agarose resin (Bio-Rad)
13. SDS-PAGE Sample Buffer (SSB), 4X (see recipe at the end of the chapter)
14. anti-His tag monoclonal antibody

7.7.2 Procedure

Transformation of Electrocompetent Tuner DE3 *E. coli* cells with pET-28b containing GmEIN3A;1 Plasmids

Electrocompetent Tuner DE3 *E. coli* cells were thawed on ice. GmEIN3A;1 in pET-28b plasmid (500 ng) was added to the cells. Cells were left on ice for 5 minutes. The GenePulser was set to 25 μF, 200 Ω, and 2.5 kV. Cells (200 μL) were placed at the bottom of the GenePulser cuvette. Pulse was applied and then 1 mL of SOC media was added. The cells were transferred to a new tube and incubated at 37 °C with shaking for 1 hour. Fifty μL of reaction mixture was spread on LB+Kan agar and incubated overnight at 37 °C. The next day a single colony was transferred to 1 mL LB+Kan broth

6xHis-GmEIN3A;1 IPTG induction

Ten mL LB+Kan media was inoculated with 100 μL of an overnight culture. The culture was shaken at 200 rpm and held at 37 °C. The absorbance at 600 nm was measured every few hours until the culture reached an optical density of 0.4 - 0.6. Once the appropriate optical density was reached, IPTG was added to reach a final concentration of 1 mM IPTG. The cultures were shaken at 200 rpm for an additional 2 hours at 37 °C. After 2 hours, 4 mL was collected. Cells were pelleted by centrifugation at 17,000 rpm for 15 minutes at 4 °C. The supernatant was removed and the pellets stored at -80 °C.

Cell lysis

To recover the induced protein, cells were lysed by sonication. Pellets were re-suspended in 2 mL wash buffer with 2 μL 10 mg/mL lysozyme. Sonication was performed for a total of 5 minutes with pulsation at 50% amplitude for 20 seconds and 2 minutes rest on ice between pulsation. Lysate was separated via centrifugation at 3,000 rpm for 20 minutes at 4 °C. The supernatant was saved at 4 °C. The pellet was resuspended in 1 mL wash buffer and saved at 4 °C.

Batch Purification

To quickly examine purification conditions it was decided to use a small-scale batch purification method which can be performed in around one hour. Samples were kept cold during this process by holding on ice or in a refrigerator. Fifty μL of Ni-NTA agarose resin was placed in a microfuge tube. The resin was compacted by centrifugation for 2 minutes at 3,000 rpm. The resin was washed three sequential times with 1 mL wash buffer. Washes were applied by adding the buffer, rotating the tube 5 times, centrifugation at 3,000 rpm for 2 minutes, and removal of the wash.

The cell lysate (100 μL) was added to the equilibrated Ni-NTA agarose resin. The reaction mixture was rotated at 4 °C for 15 minutes. The resin and supernatant were separated by centrifugation at 2,000 rpm for 2 minutes. The supernatant was saved and labeled "unbound." The resin was washed two sequential times with 1 mL wash buffer as described above. Each wash was saved and labeled "wash" 1 or 2. The resin was sequentially eluted with 100 μL 100 mM, 300 mM, and 500 mM imidazole elution buffer. Between each elution step, the resin and supernatant were separated by centrifugation at 2,000 rpm for 2 minutes. The supernatants were saved and labeled "100", "300", or "500".

3.3 μL of 95 °C 4X SSB was added to 10 μL of each supernatant and incubated for 5 minutes. Protein was resolved via SDS-PAGE. Anti-His mouse monoclonal antibody was used to identify His-tagged proteins in each fraction. The SDS-PAGE analysis demonstrated a single band of GmEIN3A;1 when eluted with 100 mM imidazole (Figure 7.9). It must be noted that the majority of expressed GmEIN3A;1 protein did not bind to the Ni-NTA agarose resin as indicated by the band present in the unbound fraction.

Identification of optimal cell lysis conditions for GmEIN3A;1 recovery

Tuner DE3 *E. coli* cells were induced as described above in "GmEIN3A;1 IPTG induction". Cell lysis was performed as described above in "Cell lysis" except the "wash buffer" was replaced with Buffers A, B, C, or D from Table 7.2. For each buffer, 100 μL was immediately purified via batch purification. The rest of the lysate was saved at 4 °C for 24 hours prior to batch purification to investigate the degradation rate of GmEIN3A;1 during storage.

Batch purification was performed as described above in "Batch purification" with the following exceptions:

1. 100 μL sample was added to 900 μL of buffer prior to being added to the Ni-NTA agarose resin and rotated for 30 minutes at 4 °C.

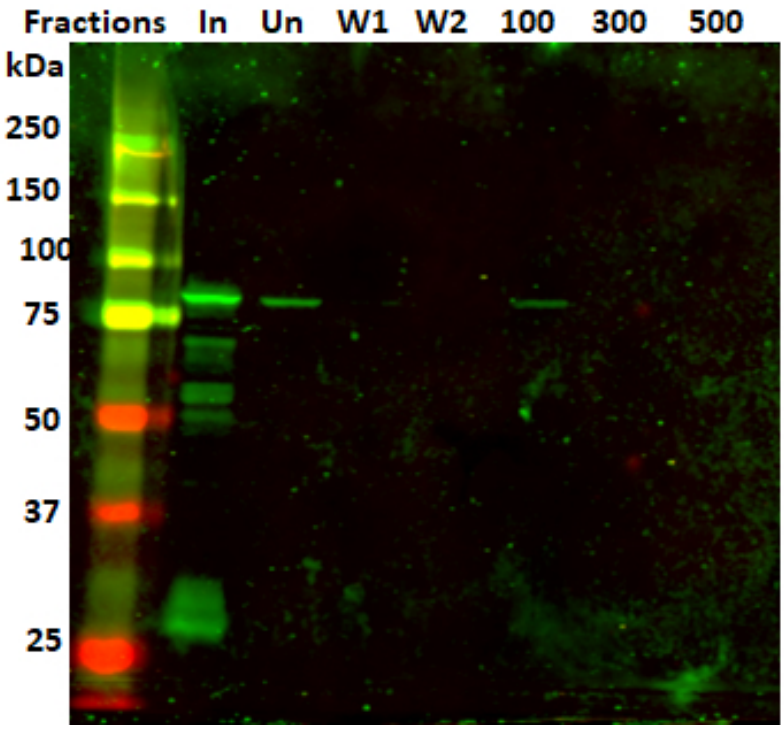

Fig. 7.9. His-tag antibody western blot of batch purification of 6xHis-GmEIN3A;1 from Tuner DE3 E. coli cells. Input (In), unbound (Un), two washes (W) with 10 mM Imidazole, elution with 100, 300, 500 mM Imidazole. 6xHis-GmEIN3A;1 appears to be eluted at 100 mM Imidazole.

2. 50, 100, and 150 mM Imidazole elution buffers were utilized instead of 100, 300, and 500 mM Imidazole elution buffers.

3.3 μL of 95 °C 4X SSB was added to 10 μL of each supernatant and incubated for 5 minutes. Protein was resolved via SDS-PAGE. Anti-His mouse monoclonal antibody was used to identify His-tagged proteins in each fraction for each lysis buffer and condition (Figure 7.10). Examination of the resulting Western blots suggests that buffer C (Table 7.2) had the highest retention amount and the least degradation regardless of lysis storage conditions (Figure 7.10C).

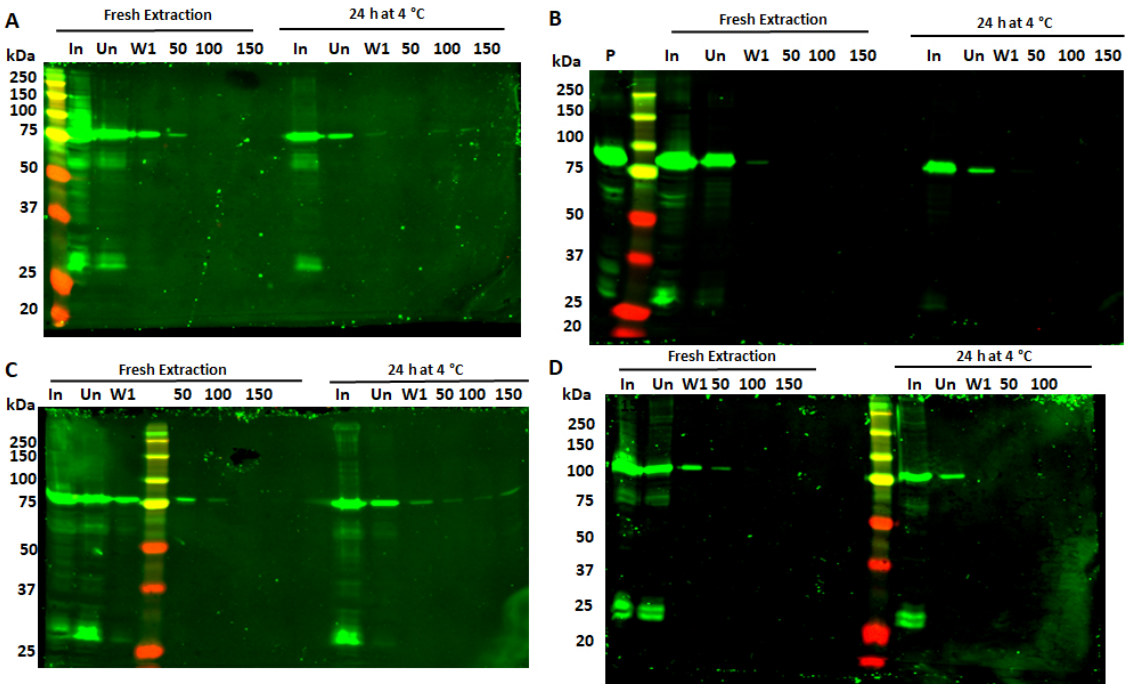

Fig. 7.10. The investigation of optimal breaking conditions for 6xHis-GmEIN3A;1 purification. Panels A - D are His-tag antibody western blots showing batch purification under multiple breaking conditions. Batch purification performed with Ni-NTA agarose resin. Samples were collected from the pellet (P), input (In), unbound (Un), wash (W, 10 mM Imidazole), and eluted with 50, 100, and 150 mM Imidazole. Cell lysis either immediately proceeded batch purification (Fresh Extraction) or were refrigerated for 24 hours prior to batch purification (24 h at 4 °C). Table 7.2 provides the formulation of breaking buffers A - D which corresponds to panels A - D. Images are intentionally overexposed to identify any potential degradation of GmEIN3A;1.

Table 7.2.
Breaking buffers used to determine optimal buffer conditions for isolating GmEIN3A;1. All buffers were adjusted to a pH of 8.0.

Buffer	Contents
A	50 mM sodium phosphate monobasic, 500 mM sodium chloride, 10 mM Imidazole
B	50 mM sodium phosphate monobasic, 500 mM sodium chloride, 10 mM Imidazole, 1 mM EDTA, 0.3 mM pepstatin A, 0.3 µM aprotinin, 10 µM leupeptin, 1 mM PMSF
C	50 mM sodium phosphate monobasic, 500 mM sodium chloride, 10 mM Imidazole, 10 % glycerol, 1 mM EDTA, 0.3 mM pepstatin A, 0.3 µM aprotinin, 10 µM leupeptin, 1 mM PMSF
D	50 mM Tris, 500 mM sodium chloride, 10 mM Imidazole, 1 mM β-mercaptoethanol, 1 mM EDTA, 10 % glycerol, 1x cOmplete™ Protease Inhibitor Cocktail (Roche), 0.3 mM pepstatin A, 0.3 µM aprotinin, 10 µM leupeptin, 1 mM PMSF

7.8 Preliminary DNA binding activity of GmICE1A and GmEIN3A;1

7.8.1 Materials

1. Purified 6xHis-GmEIN3A;1 protein
2. Purified 6xHis-GmICE1A protein
3. Labeled DNA oligonucleotides (method in chapter 2.13, oligonucleotide sequences shown in Figure 7.11A)
4. TE buffer (see recipe at the end of the chapter)
5. Native Acrylamide Gels (see recipe at the end of the chapter)
6. EMSA buffer (see recipe at the end of the chapter)
7. EMSA loading dye (see recipe at the end of the chapter)

8. TBE buffer, 10X (see recipe at the end of the chapter)
9. Filter paper
10. Saran wrap
11. Gel dryer
12. Phosphocassette and phosphoimager

7.8.2 Procedure

To investigate the preliminary binding activity of 6xHis-GmEIN3A;1 and 6xHis-GmICE1A nucleotide sequences had to be designed. The nucleotide sequences used were designed to model the *GmDREB1A;1* promoter, centered around the region of overlap between the EIN3 and ICE1 binding motifs. Two different lengths, 21 and 45 oligonucleotides were created. Additionally, mutations in either ICE1 or EIN3 binding motifs were made to the 21 nucleotide sequence to isolate either ICE1 and EIN3 (Figure 7.11A). Each oligonucleotide was labeled with P^{32} as described in chapter 2.13. To achieve a 10 femtomole/μL "working stock" labeled DNA was diluted 100 fold with TE buffer.

Setting up Reactions

Reaction mixtures were composed of purified protein or additional EMSA buffer, 0.5X EMSA buffer, and 5 femtomole of labeled DNA substrate. The reaction was assembled on ice with the labeled substrate added last. Binding assay reactions were incubated for 10 minutes at room temperature. EMSA loading dye (2 - 3 μL) was added to wells with no protein only. In competition assays, the protein, 0.5X EMSA buffer, and the labeled substrate are incubated for 10 minutes at room temperature prior to the addition of the non-labeled competitor substrate for the desired time.

The wells of the native gel were washed with 1X TBE three or four times before loading reactions. After reactions are loaded into the wells, the gel was run at 250 volts for 90 minutes.

Developing a Native Gel

The gel was transferred to filter paper and covered with saran wrap. The gel was dried at 80 °C for 2 hours. The dried gel was placed in a phosphocasette overnight. The Typhoon FLA 9500 (General Electric) phosphoimager was used to scan the gel and the image was saved as a .tif.

7.8.3 Results

Preliminary binding assays with GmICE1A (0.56 μg per lane) suggest a preference for longer substrate (5 femtomole per lane); however, all substrates examined had some binding activity (Figure 7.11B). After 5 minutes of competition, the binding of ICE+EIN 45-mer substrate was reduced in the presence of unlabeled ICE1 21-mer substrate at 50-fold excess and with the 25-mer substrate when present at 10-fold excess or higher (Figure 7.11C). In a time course, the binding of labeled ICE+EIN 45-mer substrate was also visibly decreased after 5 minutes of competition with 250-fold excess unlabeled ICE+EIN 45-mer substrate (Figure 7.11D).

GmICE1A;1 does not appear to be capable of binding to double stranded 45-mer section of the *GmDREB1A;1* promoter (Figure 7.12). This is significantly different than the reported Arabidopsis binding activity of ICE1 which was shown to bind double stranded DNA (Chinnusamy et al., 2003). Length specificity was not examined by Chinnusamy et al. (2003) as all substrates were 20 bp. The presumed increased affinity for longer DNA sequences demonstrated by soybean GmICE1A cannot be compared with Arabidopsis ICE1 based on current knowledge in the field.

When GmEIN3A;1 binding was examined, there was evidence of substrate degradation when a single-stranded probe was utilized. Due to the degradation of the

A

Oligo name	Sequence
ICE1 EIN3 45-mer	CTAGCATCTGGAACTATGCATGCACTTGGGAATATACCAATAAAG
ICE1 EIN3 45-mer complement	CTTTATTGGTATATTCCCAAGTGCATGCATAGTTCCAGATGCTAG
ICE1 EIN3 21-mer	CTATGCATGCACTTGGGAACC
ICE1 21-mer	GACACTTGTACAACAGTTGTC
EIN3 21-mer	TAGCATCTGGAACTATGCATG
Glyma19g 22-mer	GAGAAGATTGCTAATGGACCCG
25-mer	GTCCACCCGACGCCACCTCCTGCCT

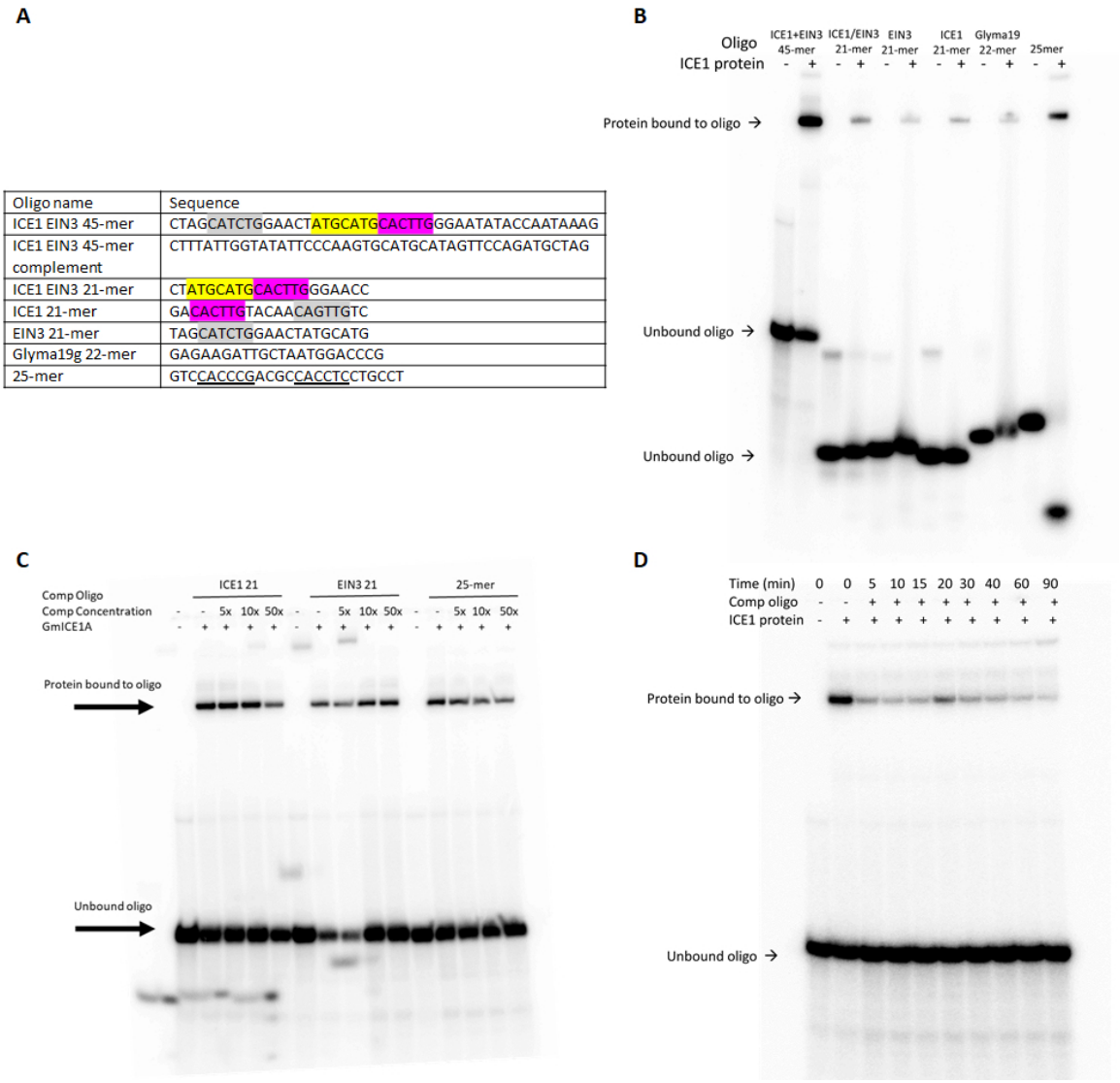

Fig. 7.11. Electrophoretic mobility shift assay (EMSA) demonstrating GmICE1A DNA binding capability. A) DNA substrates used for EMSA. Violet highlighting indicates ICE1 binding motif with the highest observed sequence frequency in soybean *CBF/DREB1* promoters (CACTTG), gray highlighting indicates other possible ICE1 binding motifs, yellow highlighting indicates EIN3 binding motifs. Double underlining present in the 25-mer sequence are similar to the ICE1 consensus sequence except for a single nucleotide. B) Binding ability of GmICE1A for each substrate in Panel A. Representative picture of 3 replicates. C) Five minute competition assay with radioactive phosphorus labeled ICE1-EIN3 45-mer oligonucleotide and non-labeled oligonucleotides as listed. Representative picture of 2 replicates. D) Competition time course with radioactive phosphorus labeled ICE1-EIN3 45-mer and non-labeled ICE1-EIN3 45-mer. Representative picture of 2 replicates.

substrate from an unknown origin, it is not possible to determine if GmEIN3A;1 is capable of binding to single stranded DNA (Figure 7.12). When double stranded probe was utilized, GmEIN3A:1 did bind and shift the probe (Figure 7.12), though a significant amount of unbound probe was still present.

7.9 Conclusions

This chapter describes initial conditions examined for the expression and purification of GmICE1A and GmEIN3A;1 protein for biochemical analysis. Based on Western blot analysis, a significant amount of GmEIN3A;1 protein remains insoluble after extraction. This could be due to the large size of GmEIN3A;1's protein resulting in aggregation or accumulation in exclusion bodies. A mild solubilization of the pellet may improve yield of GmEIN3A;1 as described in Singh et al. (2015). Once pure samples of GmICE1A and GmEIN3A;1 are obtained a positive identification via mass spectrometry should be completed. An important finding is that both these preparations appeared to contain functional DNA-binding activity as described below.

Preliminary analysis of DNA binding capacity suggests that GmEIN3A;1 and GmICE1A have differing binding activity. GmICE1A binds to single stranded probes, but not double stranded probe, which is a finding distinctly different from that found in Arabidopsis ICE1 (Chinnusamy et al., 2003). GmICE1A has a preference for longer nucleotide sequences (45-mer vs 21-mer). At this stage, the only parameter determined for GmEIN3A;1 is that binding was only observed with double stranded DNA probes as there appears to be single-stranded nuclease present in the latter preparation. Further work is required to conclusively demonstrate the binding affinities and potential interactions between GmEIN3A;1 and GmICE1A on the *GmDREB1A;1* promoter. These experiments would be best performed with more highly purified GmICE1A and GmEIN3A;1 protein. Questions remaining to be addressed include:

- What are the optimal binding conditions for GmEIN3A:1 and GmICE1A?

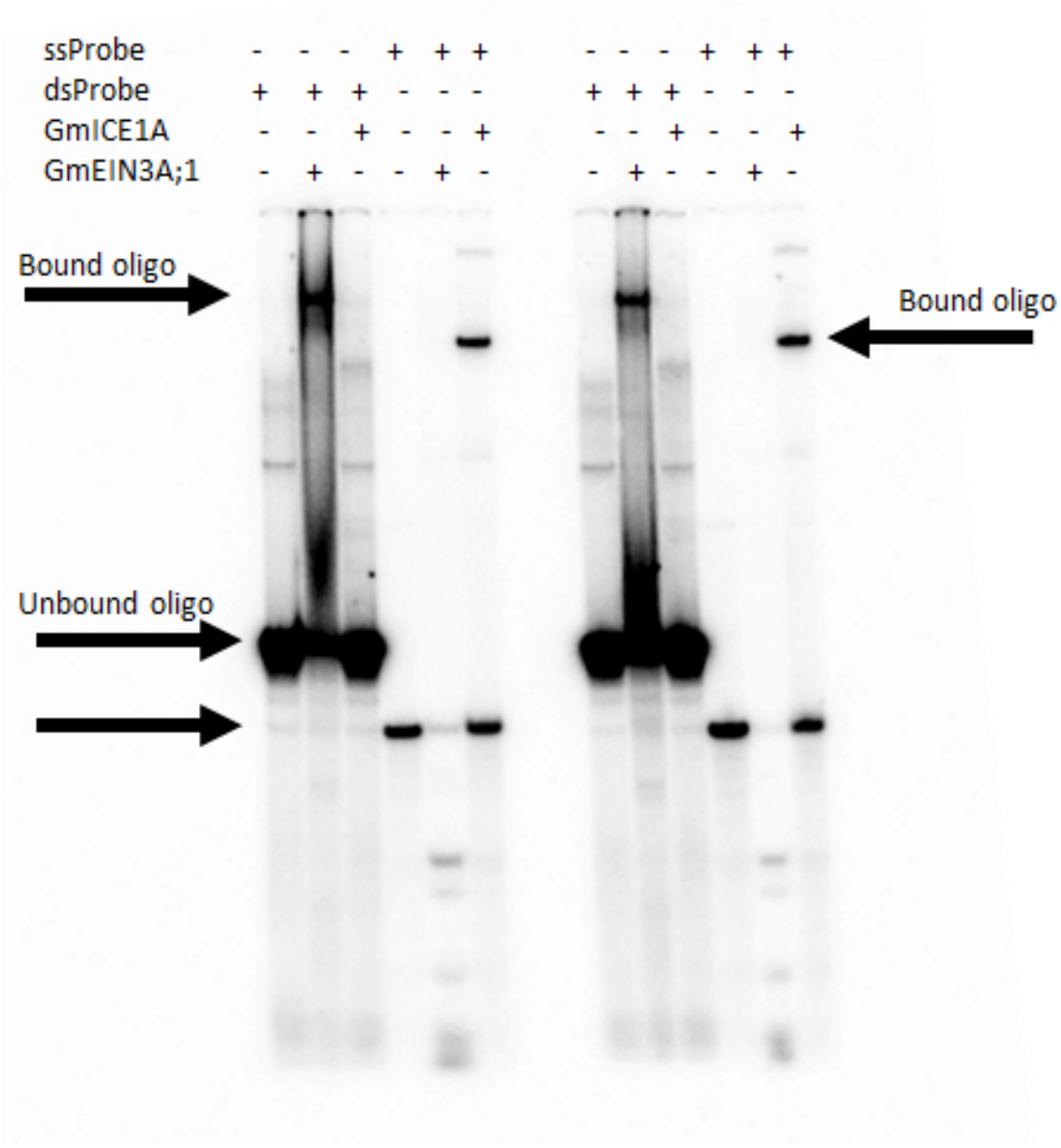

Fig. 7.12. Electrophoretic mobility shift assay (EMSA) demonstrating GmICE1A and GmEIN3A;1 DNA binding capability. 200 femtomole of labeled probe, ICE1-EIN3 45-mer, were mixed and incubated at 22 °C along with 0.28 μg GmICE1A and 0.23 μg GmEIN3A;1 for twenty minutes before loading onto the gel. Single stranded (ssProbe) and double stranded (dsProbe) were examined as indicated. Two separate reactions are shown on this gel. A third gel was run with similar results but is not presented here.

- What are the binding kinetics of GmEIN3A;1 and GmICE1A under optimal conditions?
- How does cold impact these kinetics?
- Which transcription factor has a higher affinity, and thus more likely to bind to, the *GmDREB1A;1* promoter?

Answers to these questions will tease apart the interactions of these two important transcription factors and the potential impacts to the GmCBF/DREB1 cold responsive pathway.

7.10 Recipes

All chemicals were sourced from Sigma or ThermoFisher Scientific unless otherwise noted.

7.10.1 LB Broth

- 2 grams of LB powder (Dot Scientific) per 100 mL of distilled water

Autoclave prior to use
Store at 4 °C

7.10.2 Super Optimal broth with Catabolite repression (SOC) media

- 3.1 gram of SOC powder (Dot Scientific) per 100 mL of distilled water

Autoclave prior to use
Store at -20 °C

7.10.3 LB+Kan Broth

- 2 grams of LB powder (Dot Scientific) per 100 mL of distilled water

Autoclave

Allow solution to cool prior to adding 100 μL of 50 mg/mL kanamycin sulfate

Store at room temperature

7.10.4 LB+Kan Agar

- 4 grams of LB powder (Dot Scientific) per 200 mL of distilled water
- 1.6 grams agar

Autoclave

Allow solution to cool prior to adding 200 μL of 50 mg/mL kanamycin sulfate

Pour approximately 20 mL per undivided 100mm x 15mm Petri plate

Allow to solidify and store at 4 °C

7.10.5 Autoinduction Media

Final concentration: 1.2% peptone, 2.4% yeast extract, 90 mM potassium phosphate pH 7.0, 0.1% glucose, 0.2% lactose, 0.5% glycerol, 50 mg/L Kanamycin

- 700 mL Yeast-Peptone base
- 90 mL 1 M Potassium phosphate buffer
- 100 mL 10 g/L Glucose
- 100 mL 20 g/L Lactose
- 1 mL 50% Glycerol

Keep all material sterile

Add solutions in the order listed to Yeast-Peptone base

Add 1 mL of 50 mg/mL Kanamycin sulfate before use

Yeast-Peptone base

- 12 g Peptone
- 24 g Yeast Extract
- bring to 700 mL with distilled water

Autoclave

Store at 4 °C

1 M Potassium phosphate (KPi) buffer, 500 mL

- 52.25 g K_2HPO_4
- 27.2 g KH_2HPO_4
- pH to 7.0 with KOH
- bring to 500 mL with distilled water

Separate into 90 mL aliquots

Autoclave

Store at room temperature

10 g/L Glucose, 500 mL

- 5 g glucose
- 500 mL distilled water

Separate into 100 mL aliquots

Autoclave

Store at room temperature

20 g/L Lactose, 500 mL

- 10 g lactose

- 500 mL distilled water

Separate into 90 mL aliquots

Autoclave

Store at room temperature

50% Glycerol, 50 mL

- 25 mL Glycerol (Fisher Scientific)
- 25 mL distilled water

Autoclave

Store at room temperature

7.10.6 YEP Media

Final concentration: 1.2% peptone, 2.4% yeast extract, 50 mg/L Kanamycin

- 12 g Peptone
- 24 g Yeast Extract
- 1 L distilled water

Autoclave

Store at room temperature

Add 1 mL of 50 mg/mL Kanamycin sulfate immediately before use

7.10.7 SDS-PAGE Sample Buffer (SSB)

4X stock, 10 mL final concentration: 240 mM Tris-HCl pH 6.8, 8% SDS, 0.04% bromphenol blue, 40% glycerol

- 2 mL 1 M Tris-HCl pH 6.8
- 0.8 g SDS (sodium dodecyl sulfate)

- 0.8 mL 0.1% Bromphenol blue
- 4 mL Glycerol

Combine materials
Heat to 95 °C for 5 minutes Cool to room temperature, then store at -20 °C

7.10.8 Ni-NTA Agarose Column Wash Buffer

1 L final concentration: 50 mM monobasic sodium phosphate (NaH_2PO_4), 300 mM sodium chloride (NaCl) and 10 μM Imidazole

- 6.9 g NaH_2PO_4
- 17.5 g NaCl
- 0.68 g Imidazole
- pH to 8.0 with sodium hydroxide (NaOH)

Combine materials
Add 1 mL of 1M PMSF immediately before use

7.10.9 Ni-NTA Agarose Column Elution Buffer

1 L final concentration: 50 mM monobasic sodium phosphate (NaH_2PO_4), 300 mM sodium chloride (NaCl) and 500 mM Imidazole

- 6.9 g NaH_2PO_4
- 17.5 g NaCl
- 34 g Imidazole
- pH to 8.0 with sodium hydroxide (NaOH)

Combine materials

Add 1 mL of 1M PMSF immediately before use

Note: Several concentrations of Imidazole were utilized in elution buffers throughout this chapter. The correct final concentrations must be calculated. Imadazole has a molecular weight of 68.077 g/mol.

7.10.10 TE buffer

For 100 mL final concentrations 10 mM Tris-HCl and 1 mM EDTA, pH 8.0

- 1 mL of 1 M Tris-HCl, pH 8.0
- 0.2 mL of 0.5 M EDTA

Bring to 100 mL with distilled water

Store at room temperature

7.10.11 Native Acrylamide Gels

To pour 2 4% 50 mL gels:

- 70 mL water
- 10 mL 10X TBE buffer
- 20 mL Accugel (19:1 acrylamide:bisacrylamide)
- 550 μL 10% APS
- 55 μL TEMED

Mix and pour between plates

Allow to polymerize for at least 30 minutes

Use immediately

7.10.12 EMSA buffer

5mL of 1X EMSA buffer Final concentrations 50 mM Tris-HCl pH 8.0, 30 mM NaCl, 0.25 mg/mL BSA, 2 mM DTT, 5% glycerol

- 1 mL 5x Dna2p Buffer (see below)
- 0.5 mL 50% glycerol
- 3.5 mL distilled water

Combine material

Store at -20 °C

5x Dna2p Buffer Final concentration: 250 mM Tris-HCl pH 8.0, 150 mM NaCl, 1.25 mg/mL BSA, 10 mM DTT

- 250 μL 1 M Tris-HCl pH 8.0
- 250 μL 600 mM NaCl
- 10 μL 50 mg/mL BSA
- 10 μL 1 M DTT

Combine material

Store at -20 °C

7.10.13 EMSA loading dye

- 100 μL 1x EMSA buffer
- 20 μL 6X Gel Loading Dye

Combine material

Store at room temperature

7.10.14 TBE buffer, 10X

1 liter final concentration: 1 M Tris, 1 M Boric acid, 0.02 M EDTA

- 10g Tris
- 55 g Boric acid
- 7.5 g EDTA

Combine material

Store at room temperature

8. SUMMARY AND FUTURE DIRECTIONS

Cold stress impacts the growth, reproduction, and distribution of plants around the world (Zhen et al., 2011). Understanding how cold stress affects crop species is of significant interest to feed the growing worldwide population. Soybean is a major crop in global agriculture (Pagano and Miransari, 2016) thus research into how soybean responds to abiotic stress is of particular importance to establishing growth ranges. Soybean is capable of limited cold tolerance, with an average of 5.2 ± 0.6 days of cold acclimation at 4 °C required for 50% survival (LT50) at -2.5 °C (Chapter 3). Based on electrolyte leakage data, there was a weak correlation between maturity group and cold acclimated freezing tolerance in both domestic and non-domestic soybean, with northern maturity groups having a greater acclimation potential than southern maturity groups. It was disappointing to find that the "wild" (undomesticated) soybean *G. soja* varieties had no significantly improved cold tolerance over domestic varieties. This suggests little advantage to utilizing these genotypes to introgress these traits into domestic varieties.

Seed fatty acid composition varied between the species, with undomesticated soybean (*Glycine soja*) accessions containing about 2-times more linolenic acid (18:3) than *G. max*. Furthermore, increases in linoleic acid (18:2) in seeds were positively correlated with germination rates following cold imbibition in *G. soja* only. This suggests that domestication has not impacted the overall ability of soybean to cold acclimate at the seedling stage and that there is some variation within the domesticated species for ability to cold acclimate. To increase cold germination ability, soybean could be bred to contain more linoleic acid within the seeds. Soybeans cold acclimation is still modest compared to Arabidopsis which after a week of cold acclimation at 4 °C has an LT50 of -8 to -10 °C (Gilmour et al., 1988). When photosynthesis was examined during cold stress, the efficiency and yield of photosynthesis

was significantly decreased by the cold within 25 minutes of cold-exposure reaching a steady-state between 2 and 4 days (Chapter 6).

Three independent homozygous transgenic soybean lines were generated containing the promoter of the stress responsive Arabidopsis *RD29A* gene driving GFP/GUS (Chapter 4). The promoter *RD29A* contains one stress hormone ABA (ABRE) responsive element, two wound (CGTCA) responsive elements, one drought (MYB) responsive element, and three cold responsive elements (CRT/DRE). These transgenic lines could allow for rapid and efficient screening of compounds to investigate their impact on a variety of abiotic stresses, as well as the interplay of these stresses.

Using these transgenic soybean it was demonstrated that blocking the ethylene pathway with silver ions prior to cold exposure resulted in a significant cold-dependent increase in GUS activity with a corresponding increase in *GmDREB1A;1* transcript levels (Chapter 5). Likewise, when transgenic soybeans were treated with aminoethoxyvinylglycine (AVG), an inhibitor of ethylene biosynthesis, GUS activity levels significantly increased in the cold compared to vehicle controls. Additionally, manipulation of the ethylene pathway resulted in a negative correlation of *GmDREB1A:1* and *GmEIN3A;1* transcript levels. Ethylene pathway stimulation results in decreased *GmDREB1A;1* transcript levels and decreased transcript levels of several CRT/DRE containing genes. However, while ethylene pathway inhibition resulted in an increase in *GmDREB1A;1* transcript levels, there was no increase in cold tolerance parameters that were examined. Overall this work provides evidence that the ethylene pathway transcriptionally inhibits the CBF/DREB1 pathway in soybean though this interaction may not prove to be field relevant.

Based on the information described in this dissertation, combined with knowledge generated by Yuji Yamasaki (2013), it seems unlikely that improvement to transcript abundance of *CBF/DREB1* transcription factors will improve soybean cold acclimation. To improve soybean cold acclimation targets downstream of *CBF/DREB1* transcription should be examined (suggested targets in Figure 8.1). These targets may include CBF/DREB1 translation, post-translational modification of CBF/DREB1, or

recruitment of CBF/DREB1 to CRT/DRE containing promoters. In Arabidopsis, the 26S proteasome-mediated degradation of CBF1/3 protein is promoted by phosphorylated 14-3-3 (Liu et al., 2017). As 14-3-3 requires post-translational modification to interact with CBF, this interaction would not have been detected in the cold-responsive soybean transcriptome (Yamasaki, 2013). It is conceivable that in soybean, 14-3-3 homologs could be overly activated or that soybean CBF/DREB1A are more susceptible to proteolysis, thus explaining why upregulation of *GmCBF/DREB1* transcripts does not result in the upregulation of target genes. Conversely, it has been shown that OST1 phosphorylates BTF3/3L and facilitates the stabilization of CBF1-3 (Ding et al., 2018). BTF3/3L are two β-subunits of a nascent polypeptide-associated complex. In Arabidopsis OST1 phosphorylated BTF3L directly interacts with the CBF protein significantly increasing turnover time (Ding et al., 2018). These possibilities emphasize the necessity to obtain tools to examine CBF protein levels in the cold.

For successful target gene transcription the entire transcriptional complex must be assembled. The mediator subunit MED16 has been shown to play a crucial role in the regulation of CRT/DRE motif cold responsive genes in Arabidopsis and rice (Hemsley et al., 2014; Knight et al., 2009, 1999; Wathugala et al., 2011). Mutations in the *MED16* gene result in significantly decreased expression of CRT/DRE cold responsive regulated genes during cold stress, while non CRT/DRE genes seem to be regulated normally (Knight et al., 1999). In Arabidopsis, even overexpression of CBF1 and CBF2 in *med16* mutants does not result in the expression of downstream CRT/DRE targets (Knight et al., 2009). Since soybean seems to regulate CBF transcripts similarly to Arabidopsis, yet downstream targets are not upregulated, the soybean GmMED16 is a target worthy of investigation to increase cold tolerance.

Understanding the molecular reason for the limited cold tolerance of soybean may increase the growth region of soybean. This dissertation has established the current limitations on soybeans cold tolerance, created a powerful tool of transgenic soybean lines to screen compounds that may improve this cold tolerance, and identified that the critical area of improvement is post-transcriptional of CBF/DREB1. This

work provides a crucial stepping stone in the molecular dissection of soybeans cold tolerance.

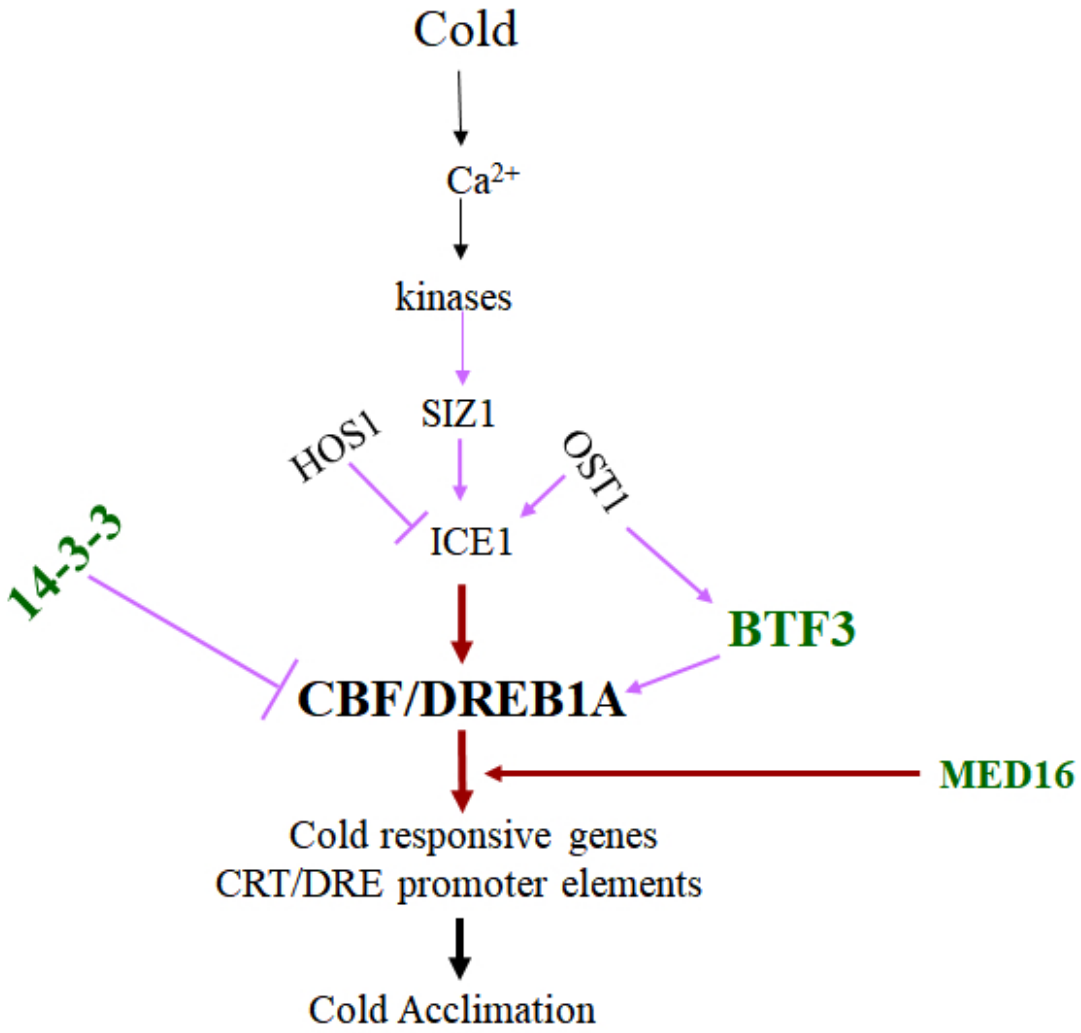

Fig. 8.1. CBF cold responsive pathway with potential targets to investigate to increase soybean cold tolerance shown in green. Purple arrows indicate post-translational regulation, red arrows indicate transcriptional regulation. See text for full description.

Bibliography

Achard, P., Gong, F., Cheminant, S., Alioua, M., Hedden, P., and Genschik, P. (2008). The cold-inducible cbf1 factor-dependent signaling pathway modulates the accumulation of the growth-repressing della proteins via its effect on gibberellin metabolism. *Plant Cell*, 20(8):2117–29.

Alia, Mohanty, P., and Matysik, J. (2001). Effect of proline on the production of singlet oxygen. *Amino Acids*, 21(2):195–200.

Alia, Pardha Saradhi, P., and Mohanty, P. (1997). Involvement of proline in protecting thylakoid membranes against free radical-induced photodamage. *Journal of Photochemistry and Photobiology B: Biology*, 38(2):253–257.

Allakhverdiev, S. I. and Murata, N. (2004). Environmental stress inhibits the synthesis *de novo* of proteins involved in the photodamagerepair cycle of photosystem ii in *Synechocystis* sp. pcc 6803. *Biochimica et Biophysica Acta (BBA) - Bioenergetics*, 1657(1):23–32.

Alsheikh, M., Heyen, B. J., and Randall, S. K. (2003). Ion binding properties of the dehydrin erd14 are dependent upon phosphorylation. *Journal of Biological Chemistry*, 42:40882–40889.

Alsheikh, M., Svensson, J., and Randall, S. K. (2005). Phosphorylation regulated ion-binding is a property shared by the acidic subclass dehydrins. *Plant, Cell & Environment*, 28(9):1114–1122.

Arisz, S. A., van Wijk, R., Roels, W., Zhu, J.-K., Haring, M. A., and Munnik, T. (2013). Rapid phosphatidic acid accumulation in response to low temperature

stress in arabidopsis is generated through diacylglycerol kinase. *Frontiers in plant science*, 4:1–1.

Ashburner, M., Ball, C. A., Blake, J. A., Botstein, D., Butler, H., Cherry, J. M., Davis, A. P., Dolinski, K., Dwight, S. S., Eppig, J. T., Harris, M. A., Hill, D. P., Issel-Tarver, L., Kasarskis, A., Lewis, S., Matese, J. C., Richardson, J. E., Ringwald, M., Rubin, G. M., and Sherlock, G. (2000). Gene ontology: tool for the unification of biology. the gene ontology consortium. *Nature Genetics*, 25(1):25–9.

Baker, N. R. (2008). Chlorophyll fluorescence: a probe of photosynthesis *in vivo*. *Annual Review of Plant Biology*, 59:89–113.

Barnes, A. C., Benning, C., and Roston, R. L. (2016). Chloroplast membrane remodeling during freezing stress is accompanied by cytoplasmic acidification activating sensitive to freezing2. *Plant Physiology*, 171(3):2140–2149.

Bates, L. S., Waldren, R. P., and Teare, I. D. (1973). Rapid determination of free proline for water-stress studies. *Plant and Soil*, 39(1):205–207.

Blommel, P. G., Becker, K. J., Duvnjak, P., and Fox, B. G. (2007). Enhanced bacterial protein expression during auto-induction obtained by alteration of lac repressor dosage and medium composition. *Biotechnology Progress*, 23(3):585–598.

Boisvert, S., Joly, D., and Carpentier, R. (2006). Quantitative analysis of the experimental o-j-i-p chlorophyll fluorescence induction kinetics. apparent activation energy and origin of each kinetic step. *FEBS Journal*, 273(20):4770–7.

Borowski, E. and Michalek, S. (2014). The effect of chilling temperature on germination and early growth of domestic and canadian soybean (*Glycine max* (l.) merr.) cultivars. *Acta Scientiarum Polonorum Hortorum Cultus*, 13(2):31–43.

Boutrot, F., Segonzac, C., Chang, K. N., Qiao, H., Ecker, J. R., Zipfel, C., and Rathjen, J. P. (2010). Direct transcriptional control of the arabidopsis immune receptor

fls2 by the ethylene-dependent transcription factors ein3 and eil1. *Proceedings of the National Academy of Sciences*, 107(32):14502–14507.

Bradford, M. M. (1976). A rapid and sensitive method for the quantitation of microgram quantities of protein utilizing the principle of protein-dye binding. *Analytical Biochemistry*, 72:248–254.

Butler, W. L. (1972). On the primary nature of fluorescence yield changes associated with photosynthesis. *Proceedings of the National Academy of Sciences of the United States of America*, 69(11):3420–3422.

Catal, R. and Salinas, J. (2015). The arabidopsis ethylene overproducer mutant *eto1-3* displays enhanced freezing tolerance. *Plant Signaling and Behavior*, 10(3):e989768.

Chacha, A. R. (2014). *Functional Dissection of ERD14 Phosphorylation-dependent calcium binding activity*. Masters.

Chen, Z. and Gallie, D. R. (2015). Ethylene regulates energy-dependent nonphotochemical quenching in arabidopsis through repression of the xanthophyll cycle. *PLoS ONE*, 10(12):e0144209.

Cheng, F., Lu, J., Gao, M., Shi, K., Kong, Q., Huang, Y., and Bie, Z. (2016). Redox signaling and cbf-responsive pathway are involved in salicylic acid-improved photosynthesis and growth under chilling stress in watermelon. *Frontiers in Plant Science*, 7:1519.

Cheng, Y.-Q. (2013). Rna-seq analysis reveals ethylene-mediated reproductive organ development and abscission in soybean (*Glycine max* l. merr.). *Plant Molecular Biology Report*, 31(3):607–619.

Cheng, Y.-Q., Liu, J., Yang, X., Ma, R., Liu, Q., and Liu, C. (2013). Construction of ethylene regulatory network based on the phytohormones related gene transcriptome profiling and prediction of transcription factor activities in soybean. *Acta Physiology Plant*, 35:1303–1317.

Chinnusamy, V., Ohta, M., Kanrar, S., Lee, B., Hong, X., Agarwal, M., and Zhu, J. (2003). Ice1: a regulator of cold-induced transcriptome and freezing tolerance in arabidopsis. *Genes and Development*, 17(8):1043–1054.

Chu, T. M., JUSAITIS, M., ASPINALL, D., and PALEG, L. G. (1978). Accumulation of free proline at low temperatures. *Physiologia Plantarum*, 43(3):254–260.

Ciardi, J. A., Deikman, J., and Orzolek, M. D. (1997). Increased ethylene synthesis enhances chilling tolerance in tomato. *Physiologia Plantarum*, 101(2):333–340.

Close, T. J. (1996). Dehydrins: Emergence of a biochemical role of a family of plant dehydration proteins. *Physiologia Planatrum*, 97(4):795–803.

Consortium, T. G. O. (2017). Expansion of the gene ontology knowledgebase and resources. *Nucleic Acids Research*, 45(D1):D331–d338.

Dietz, K. J. (2015). Efficient high light acclimation involves rapid processes at multiple mechanistic levels. *J Exp Bot*, 66(9):2401–14.

Dietz, K. J. (2016). Thiol-based peroxidases and ascorbate peroxidases: Why plants rely on multiple peroxidase systems in the photosynthesizing chloroplast? *Molecular Cells*, 39(1):20–5.

Ding, Y., Jia, Y., Shi, Y., Zhang, X., Song, C., Gong, Z., and Yang, S. (2018). Ost1-mediated btf3l phosphorylation positively regulates cbfs during plant cold responses. *The EMBO Journal*, 37(8):e98228.

Ding, Y., Li, H., Zhang, X., Xie, Q., Gong, Z., and Yang, S. (2015). Ost1 kinase modulates freezing tolerance by enhancing ice1 stability in arabidopsis. *Developmental Cell*, 32(3):278–289.

Ding, Y., Zhao, J., Nie, Y., Fan, B., Wu, S., Zhang, Y., Sheng, J., Shen, L., Zhao, R., and Tang, X. (2016). Salicylic-acid induced chilling- and oxidative-stress tolerance

in relation to giberellin homeostasis, c-repeat/dehydration responsive element binding factor pathway, and antioxidant enzyme systems in cold-stored tomato fruit. *Journal of Agriculture and Food Chemistry*, 64(43):8200–8206.

Djanaguiraman, M. and Prasad, P. V. V. (2010). Ethylene production under high temperature stress causes premature leaf senescence in soybean. *Functional Plant Biology*, 37:1071–1084.

Dodd, A. N., Kusakina, J., Hall, A., Gould, P. D., and Hanaoka, M. (2014). The circadian regulation of photosynthesis. *Photosynthesis Research*, 119(1):181–190.

Doherty, C. J., Van Buskirk, H. A., Myers, S. J., and Thomashow, M. F. (2009). Roles for arabidopsis camta transcription factors in cold-regulated gene expression and freezing tolerance. *Plant Cell*, 21(3):972–984.

Dong, C., Agarwal, M., Chang, Y., Xie, Q., and Zhu, J. K. (2006). The negative regulator of plant cold responses, hos1, is a ring e3 ligase that mediates the ubiquitination and degradation of ice1. *Proceedings of the National Academy of Sciences*, 103(21):8281–8286.

Eremina, M., Unterholznera, S. J., Rathnayakea, A. I., Castellanosb, M., Khana, M., Kuglerc, K. G., Mayb, S. T., Mayer, K. F. X., Rozhona, W., and Poppenberger, B. (2016). Brassinosteroids participate in the control of basal and acquired freezing tolerance of plants. *Proceedings of the National Academy of Sciences*, 113(40):E5982–E5991.

Ferrante, A., Trivellini, A., Borghesi, E., and Vernieri, P. (2012). Chlorophyll *a* fluorescence as a tool in evaluating the effects of aba content and ethylene inhibitors on quality of flowering potted bougainvillea. *ScientificWorldJournal*, 2012:684747.

Fior, S., Vianelli, A., and Gerola, P. D. (2009). A novel method for fluorometric continuous measurement of β-glucuronidase (gus) activity using 4-methyl-umbelliferyl-β-d-glucuronide (mug) as substrate. *Plant Science*, 176:130–135.

Fowler, S., Cook, D., and Thomashow, M. F. (2005). Low temperature induction of arabidopsis cbf1, 2, and 3 is gated by the circadian clock. *Plant Physiology*, 137:961–968.

Fowler, S. and Thomashow, M. F. (2002). Arabidopsis transcriptome profiling indicates that multiple regulatory pathways are activated during cold acclimation in addition to the cbf cold response pathway. *The Plant Cell*, 14:1675–1690.

Furuya, T., Matsuoka, D., and Nanmori, T. (2013). Phosphorylation of *Arabidopsis thaliana* mekk1 via ca2+ signaling as a part of the cold stress response. *Journal of Plant Research*, 126(6):833–40.

Gallie, D. R. (2015). Ethylene receptors in plants - why so much complexity? *F100Prime Reports*, 7:39.

Gelvin, S. B. (2003). Agrobacterium-mediated plant transformation: The biology behind the "gene-jockeying" tool. *Microbiology and Molecular Biology Reviews*, 67(1):16–37.

Gentry, B., Briantais, J.-M., and Baker, N. R. (1989). The relationship between the quantum yield of photosynthetic electron transport and quenching of chlorophyll fluorescence. *Biochimica et Biophysica Acta*, 990:87–92.

Giberti, S., Funck, D., and Forlani, G. (2014). δ1-pyrroline-5-carboxylate reductase from *Arabidopsis thaliana*: stimulation or inhibition by chloride ions and feedback regulation by proline depend on whether nadph or nadh acts as co-substrate. *New Phytologist*, 202(3):911–919.

Gilmour, S. J., Fowler, S., and Thomashow, M. F. (2004). Arabidopsis transcriptional activators cbf1, cbf2, and cbf3 have matching functional activities. *Plant Molecular Biology*, 54:761–781.

Gilmour, S. J., Hajela, R. K., and Thomashow, M. F. (1988). Cold acclimation in *Arabidopsis thaliana*. *Plant Physiology*, 87(3):745–50.

Gilmour, S. J., Sebolt, A. M., Salazar, M. P., Everard, J. D., and Thomashow, M. F. (2000). Overexpression of the arabidopsis cbf3 transcriptional activator mimics multiple biochemical changes associated with cold acclimation. *Plant Physiology*, 124(4):1854–1865.

Gilmour, S. J., Zarka, D. G., Stockinger, E. J., Salazar, M. P., Houghton, J. M., and Thomashow, M. F. (1998). Low temperature regulation of the arabidopsis cbf family of ap2 transcriptional activators as an early step in cold induced cor gene expression. *The Plant Journal*, 16(4):443–442.

Goh, C.-H., Ko, S.-M., Koh, S., Kim, Y.-J., and Bae, H.-J. (2011). Photosynthesis and environments: Photoinhibition and repair mechanisms in plants. *Journal of Plant Biology*, 55(2):93–101.

Goss, R. and Lepetit, B. (2015). Biodiversity of npq. *Journal of Plant Physiology*, 172:13–32.

Grant, D., Nelson, R. T., Cannon, S. B., and Shoemaker, R. C. (2010). Soybase, the usda-ars soybean genetics and genomics database. *Nucleic Acids Research*, 38(S1):D843–D846.

Gunderson, C. A. and Taylor, G. E. (1991). Ethylene directly inhibits foliar gas exchange in *Glycine max*. *Plant Physiology*, 95(1):337–339.

Guy, C., Kaplan, F., Kopka, J., Selbig, J., and Hincha, D. K. (2008). Metabolomics of temperature stress. *Physiology Plantarum*, 132(2):220–35.

Guy, C. L., Huber, J. L. A., and Huber, S. C. (1992). Sucrose phosphate synthase and sucrose accumulation at low temperature. *Plant Physiology*, 100(1):502–508.

Haake, V., Cook, D., Riechmann, J. L., Pineda, O., Thomashow, M. F., and Zhang, J. (2002). Transcription factor cbf4 is a regulator of drought adaptation in arabidopsis. *Plant Physiology*, 130:639–648.

Hakme, L., Garrett, W. M., Sullivan, J., Forseth, I., and Natarajan, S. S. (2014). Proteomic analysis of the pulvinus, a heliotropic tissue, in *Glycine max*. *International Journal of Plant Biology*, 5(1):8–12.

Hannah, M. A., Wiese, D., Freund, S., Fiehn, O., Heyer, A. G., and Hincha, D. K. (2006). Natural genetic variation of freezing tolerance in arabidopsis. *Plant Physiology*, 142(1):98–112.

Hare, P. and Cress, W. (1997). Metabolic implications of stress-induced proline accumulation in plants. *Plant Growth Regulation*, 21(2):79–102.

Hare, P. D., Cress, W. A., and Van Staden, J. (1998). Dissecting the roles of osmolyte accumulation during stress. *Plant, Cell & Environment*, 21(6):535–553.

Heber, U., Tyankova, L., and Santarius, K. A. (1973). Effects of freezing on biological membranes *in vivo* and *in vitro*. *Biochimica et Biophysica Acta (BBA) - Biomembranes*, 291(1):23–37.

Hellman, L. C. and Fried, M. G. (2007). Electrophoretic mobility shift assay (emsa) for detecting protein-nucleic acid interactions. *Nature Protocols*, 2(8):1849–1861.

Hemsley, P. A., Hurst, C. H., Kaliyadasa, E., Lamb, R., Knight, M. R., De Cothi, E. A., Steele, J. F., and Knight, H. (2014). The arabidopsis mediator complex subunits med16, med14, and med2 regulate mediator and rna polymerase ii recruitment to cbf-responsive cold-regulated genes. *Plant Cell*, 26(1):465–84.

Hodges, D. M., DeLong, J. M., Forney, C. F., and Prange, R. K. (1999). Improving the thiobarbituric acid-reactive-substances assay for estimating lipid peroxidation in plant tissues containing anthocyanin and other interfering compounds. *Planta*, 207:604–611.

Hossain, M. A., Bhattacharjee, S., Armin, S. M., Qian, P., Xin, W., Li, H. Y., Burritt, D. J., Fujita, M., and Tran, L. S. (2015). Hydrogen peroxide priming modulates

abiotic oxidative stress tolerance: insights from ros detoxification and scavenging. *Front Plant Sci*, 6:420.

Hu, Y., Jiang, L., Wang, F., and Yu, D. (2013). Jasmonate regulates the inducer of cbf expressionc-repeat binding factor/dre binding factor1 cascade and freezing tolerance in arabidopsis. *The Plant Cell*, 25(8):2907–2924.

Hu, Z., Fan, J., Chen, K., Amombo, E., Chen, L., and Fu, J. (2016). Effects of ethylene on photosystem ii and antioxidant enzyme activity in bermuda grass under low temperature. *Photosynthesis Research*, 128(1):59–72.

Hume, D. J. and Jackson, A. K. H. (1981). Frost tolerance in soybean. *Crop Science*, 21(5):689–692.

Jaglo-Ottosen, K. R., Gilmour, S. J., Zarka, D. G., Schabenberger, O., and Thomashow, M. F. (1998). Arabidopsis cbf1 overexpression induces cor genes and enhances freezing tolerance. *Science*, 280(5360):104–106.

Jia, Y., Ding, Y., Shi, Y., Zhang, X., Gong, Z., and Yang, S. (2016). The *cbfs* triple mutants reveal the essential functions of cbfs in cold acclimation and allow the definition of cbf regulons in arabidopsis. *New Phytologist*, 212(2):345–53.

Jiang, B., Shi, Y., Zhang, X., Xin, X., Qi, L., Guo, H., Li, J., and Yang, S. (2017). Pif3 is a negative regulator of the cbf pathway and freezing tolerance in arabidopsis. *Proceedings of the National Academy of Sciences*, 114(32):E6695–E6702.

Jouve, L., Engelmann, F., Noirot, M., and Charrier, A. (1993). Evaluation of biochemical markers (sugar, proline, malonedialdehyde and ethylene) for cold sensitivity in microcuttings of two coffee species. *Plant Science*, 91(1):109–116.

Ju, C. and Chang, C. (2015). Mechanistic insights in ethylene perception and signal transduction. *Plant Physiology*, 169(1):85–95.

Jung, J.-H., Domijan, M., Klose, C., Biswas, S., Ezer, D., Gao, M., Khattak, A. K., Box, M. S., Charoensawan, V., Cortijo, S., Kumar, M., Grant, A., Locke, J. C. W.,

Schfer, E., Jaeger, K. E., and Wigge, P. A. (2016). Phytochromes function as thermosensors in arabidopsis. *Science*, 354(14):886–889.

Jrvi, S., Suorsa, M., and Aro, E.-M. (2015). Photosystem ii repair in plant chloroplasts - regulation, assisting proteins and shared components with photosystem ii biogenesis. *Biochimica et Biophysics Acta*, 1847:900–909.

Kalaji, H. M., Schansker, G., Ladle, R. J., Goltsev, V., Bosa, K., Allakhverdiev, S. I., Brestic, M., Bussotti, F., Calatayud, A., Dbrowski, P., Elsheery, N. I., Ferroni, L., Guidi, L., Hogewoning, S. W., Jajoo, A., Misra, A. N., Nebauer, S. G., Pancaldi, S., Penella, C., Poli, D., Pollastrini, M., Romanowska-Duda, Z. B., Rutkowska, B., Serdio, J., Suresh, K., Szulc, W., Tambussi, E., Yanniccari, M., and Zivcak, M. (2014). Frequently asked questions about *in vivo* chlorophyll fluorescence: practical issues. *Photosynthesis Research*, 122(2):121–158.

Kanervo, E., Tasaka, Y., Murata, N., and Aro, E. M. (1997). Membrane lipid unsaturation modulates processing of the photosystem ii reaction-center protein d1 at low temperatures. *Plant Physiology*, 114(3):841–849.

Kaplan, R. S. and Pedersen, P. L. (1985). Determination of microgram quantities of protein in the presence of milligram levels of lipids with amido black 10b. *Analytical Biochemistry*, 150(1):97–104.

Kasuga, M., Miura, S., Shinozaki, K., and Yamaguchi-Shinozaki, K. (2004). A combination of the arabidopsis dreb1a gene and stress-inducible rd29a promotor improved drought- and low-temperature stress tolerance in tobacco by gene transfer. *Plant Cell and Physiology*, 45(3):346–350.

Kaul, S., Sharma, S. S., and Mehta, I. K. (2008). Free radical scavenging potential of l-proline: evidence from *in vitro* assays. *Amino Acids*, 34(2):315–320.

Kawarazaki, T., Kimura, S., Iizuka, A., Hanamata, S., Nibori, H., Michikawa, M., Imai, A., Abe, M., Kaya, H., and Kuchitsu, K. (2013). A low temperature-inducible

protein atsrc2 enhances the ros-producing activity of nadph oxidase atrbohf. *Biochimica et Biophysica Acta (BBA) - Molecular Cell Research*, 1833(12):2775–2780.

Khan, N. (2004). An evaluation of the effects of exogenous ethephon, an ethylene releasing compound, on photosynthesis of mustard (*Brassica juncea*) cultivars that differ in photosynthetic capacity. *BMC Plant Biology*, 4(1):21.

Kidokoro, S., Watanabe, K., Ohori, T., Moriwaki, T., Maruyama, K., Mizoi, J., Myint, N., Htwe, P. S., Fujita, Y., Sekita, S., Shinozaki, K., and Yamaguchi-Shinozaki, K. (2015). Soybean dreb1/cbf-type transcription factors function in heat and drought as well as cold stress-responsive gene expression. *The Plant Journal*, 81:505–518.

Kilian, J., Whitehead, D., Horak, J., Wanke, D., Weinl, S., Batistic, O., D'Angelo, C., Bornberg-Bauer, E., Kudla, J., and Harter, K. (2007). The atgenexpress global stress expression data set: protocols, evaluation and model data analysis of uv-b light, drought and cold stress responses. *Plant J*, 50(2):347–63.

Kim, Y. S., Lee, M., Lee, J.-H., Lee, H.-J., and Park, C.-M. (2015). The unified icecbf pathway provides a transcriptional feedback control of freezing tolerance during cold acclimation in arabidopsis. *Plant Molecular Biology*, 89(1):187–201.

Knight, H., Mugford, S. G., Ulker, B., Gao, D., Thorlby, G., and Knight, M. R. (2009). Identification of sfr6, a key component in cold acclimation acting post-translationally on cbf function. *Plant J*, 58(1):97–108.

Knight, H., Veale, E. L., Warren, G. J., and Knight, M. R. (1999). The sfr6 mutation in arabidopsis suppresses low-temperature induction of genes dependent on the crt/dre sequence motif. *Plant Cell*, 11(5):875–86.

Knight, M. R., Campbell, A. K., Smith, S. M., and Trewavas, A. J. (1991). Transgenic plant aequorin reports the effects of touch and cold-shock and elicitors on cytoplasmic calcium. *Nature*, 352(6335):524–526.

Koehler, G., Weisel, T. J., and Randall, S. K. (2007). Transcript expression analysis indicates distinct roles for dehydrin subclasses. *Current Topics in Phytochemistry*, 8:73–83.

Konishi, M. and Yanagisawa, S. (2008). Ethylene signaling in arabdiopsis involves feedback regulation via the elaborate control of ebf2 expression by ein3. *The Plant Journal*, 55(5):821–831.

Kovacs, D., Kalmar, E., Torok, Z., and Tompa, P. (2008). Chaperone activity of erd10 and erd14, two disordered stress-related plant proteins. *Plant Physiology*, 147(1):381–390.

Krause, G. H. and Weis, E. (1991). Chlorophyll fluorescence and photosynthesis: the basics. *Annual Reviews of Plant Physiology and Plant Molecular Biology*, 42:313–349.

Kurepin, L. V., Dahal, K. P., Savitch, L. V., Singh, J., Bode, R., Ivanov, A. G., Hurry, V., and Hner, N. P. A. (2013). Role of cbfs as integrators of chloroplast redox, phytochrome and plant hormone signaling during cold acclimation. *International Journal of Molecular Sciences*, 14:12729–12763.

Laemmli, U. K. (1970). Cleavage of structural proteins during the assembly of the head of bacteriophage t4. *Nature*, 227(5259):680–685.

Lamesch, P., Berardini, T. Z., Li, D., Swarbreck, D., Wilks, C., Sasidharan, R., Muller, R., Dreher, K., Alexander, D. L., Garcia-Hernandez, M., Karthikeyan, A. S., Lee, C. H., Nelson, W. D., Ploetz, L., Singh, S., Wensel, A., and Huala, E. (2012). The arabidopsis information resource (tair): improved gene annotation and new tools. *Nucleic Acids Research*, 40(Database issue):D1202–D1210.

Lawson, T. and Vialet-Chabrand, S. (2019). Speedy stomata, photosynthesis and plant water use efficiency. *New Phytologist*, 221(1):93–98.

Lee, C.-M. and Thomashow, M. F. (2012). Photoperiodic regulation of the c-repeat binding factor (cbf) cold acclimation pathway and freezing tolerance in *Arabidopsis thaliana*. *Proceedings of the National Academy of Sciences*, 109(37):15054–15059.

Lee, S., Cheng, H., King, K. E., Wang, W., He, Y., Hussain, A., Lo, J., Harberd, N. P., and Peng, J. (2002). Gibberellin regulates arabidopsis seed germination via rgl2, a gai/rga-like gene whose expression is up-regulated following imbibition. *Genes Dev*, 16(5):646–58.

Legris, M., Klose, C., Burgie, E. S., Costigliolo, C., Neme, M., Hiltbrunner, A., Wigge, P. A., Schfer, E., Vierstra, R. D., and Casal, J. J. (2016). Phytochrme b integrates light and temperature signals in arabidopsis. *Science*, 354(6314):897–900.

Lescot, M., Dehais, P., Thijs, G., Marchal, K., Moreau, Y., Van de Peer, Y., Rouze, P., and Rombauts, S. (2002). Plantcare, a database of plant cis-acting regulatory elements and a portal to tools for in silico analysis of promoter sequences. *Nucleic Acids Res*, 30(1):325–7.

Letunic, I. and Bork, P. (2016). Interactive tree of life (itol) v3: an online tool for the display and annotation of phylogenetic and other trees. *Nucleic Acids Res*, 44(W1):W242–5.

Li, H., Ye, K., Shi, Y., Cheng, J., Zhang, X., and Yang, S. (2017). Bzr1 positively regulates freezing tolerance via cbf-dependent and cbf-independent pathways in arabidopsis. *Molecular Plant*, 10(4):545–559.

Li, W., Li, M., Zhang, W., Welti, R., and Wang, X. (2004). The plasma membrane-bound phospholipase ddelta enhances freezing tolerance in *Arabidopsis thaliana*. *Nature Biotechnology*, 22(4):427–33.

Littlejohns, D. A. and Tanner, J. W. (1976). Preliminary studies on the cold tolerance of soybean seedlings. *Canadian Journal of Plant Science*, 56:371–375.

Liu, Q., Kasuga, M., Sakuma, Y., Abe, H., Miura, S., Yamaguchi-Shinozaki, K., and Shinozaki, K. (1998). Two transcription factors, dreb1 and dreb2, with an erebp/ap2 dna binding domain separate two cellular signal transduction pathways in drought- and low-temperature-responsive gene expression, respectively, in arabidopsis. *Plant Cell*, 10(8):1391–1406.

Liu, Z., Jia, Y., Ding, Y., Shi, Y., Li, Z., Guo, Y., Gong, Z., and Yang, S. (2017). Plasma membrane crpk1-mediated phosphorylation of 14-3-3 proteins induces their nuclear import to fine-tune cbf signaling during cold response. *Molecular Cell*, 66(1):117–128.e5.

MacKenzie, A. P. (1977). Non-equilibrium freezing behaviour of aqueous systems. *Philos Trans R Soc Lond B Biol Sci*, 278(959):167–89.

Maibam, P., Nawkar, G. M., Park, J. H., Sahi, V. P., Lee, S. Y., and Kang, C. H. (2013). The influence of light quality, circadian rhythm, and photoperiod on the cbf-mediated freezing tolerance. *International Journal of Molecular Sciences*, 14(6):11527–43.

Manafi, E., Modarres Sanavy, S. A. M., Aghaalikhani, M., and Dolatabadian, A. (2015). Exogenous 5-aminolevulenic acid promotes antioxidative defence system, photosynthesis and growth in soybean against cold stress. *Notulae Scientia Biologicae*, 7(4):486–494.

Medina, J., Bargues, M., Terol, J., Prez-Alonso, M., and Salinas, J. (1999). The arabidopsis cbf gene family is composed of three genes encoding ap2 domain-containing proteins whose expression is regulated by low temperature but not by abscisic acid or dehydration. *Plant Physiology*, 199(2):463–470.

Miura, K., Jin, J., Lee, J., Yoo, C., Stirm, V., Miura, T., Ashworth, E., Bressan, R., Yun, D.-J., and Hasegawa, P. (2007). Siz1-mediated sumoylation of ice1 controls cbf3/dreb1a expression and freezing tolerance in arabidopsis. *Plant Cell*, 19(4):1403–1414.

Moellering, E. R., Muthan, B., and Benning, C. (2010). Freezing tolerance in plants requires lipid remodeling at the outer chloroplast membrane. *Science*, 330(6001):226–228.

Mori, K., Renhu, N., Naito, M., Nakamura, A., Shiba, H., Yamamoto, T., Suzaki, T., Iida, H., and Miura, K. (2018). Ca(2+)-permeable mechanosensitive channels mca1 and mca2 mediate cold-induced cytosolic ca(2+) increase and cold tolerance in arabidopsis. *Scientific reports*, 8(1):550–550.

Murata, N., Takahashi, S., Nishiyama, Y., and Allakhverdiev, S. I. (2007). Photoinhibition of photosystem ii under environmental stress. *Biochimica et Biophysica Acta (BBA) - Bioenergetics*, 1767(6):414–421.

Murchie, E. H. and Lawson, T. (2013). Chlorophyll fluorescence analysis: a guide to good practice and understanding some new applications. *J Exp Bot*, 64(13):3983–98.

Nakamura, Y., Manabe, Y., Inomata, S., and Ueda, M. (2010). Recent advances on bioorganic chemistry of plant metabolites controlling nyctinasty. *The Chemical Record*, 10(2):70–79.

Nath, K., Jajoo, A., Poudyal, R. S., Timilsina, R., Park, Y. S., Aro, E.-M., Nam, H. G., and Lee, C. H. (2013). Towards a critical understanding of the photosystem ii repair mechanism and its regulation during stress conditions. *FEBS Letters*, 587(21):3372–3381.

Norn, L., Kindgren, P., Stachula, P., Rhl, M., Eriksson, M. E., Hurry, V., and Strand, . (2016). Circadian and plastid signaling pathways are integrated to ensure correct

expression of the cbf and cor genes during photoperiodic growth. *Plant Physiology*, 171(2):1392–1406.

Novillo, F., Alonso, J. M., Ecker, J. R., and Salinas, J. (2004). Cbf2/dreb1c is a negative regulator of cbf1/dreb1b and cbf3/dreb1a expression and plays a central role in stress tolerance in arabidopsis. *Proceedings of the National Academy of Sciences*, 101(11):3985–3990.

Nylander, M., Svensson, J., Palva, E. T., and Welin, B. V. (2001). Stress-induced accumulation and tissue-specific localization of dehydrins in *Arabidopsis thaliana*. *Plant Molecular Biology*, 45(3):263–279.

O'Kane, D., Gill, V., Boyd, P., and Burdon, R. (1996). Chilling, oxidative stress and antioxidant responses in *Arabidopsis thaliana* callus. *Planta*, 198(3):371–377.

O'Neill S, D. (1983). Osmotic adjustment and the development of freezing resistance in fragaria virginiana. *Plant Physiol*, 72(4):938–44.

Orvar, B. L., Sangwan, V., Omann, F., and Dhindsa, R. S. (2000). Early steps in cold sensing by plant cells: the role of actin cytoskeleton and membrane fluidity. *Plant J*, 23(6):785–94.

Osadczuk, E. A. (2013). *Characterization of a Cold-Responsive Dehydrin Promoter*. Masters.

Pagano, M. C. and Miransari, M. (2016). *1 - The importance of soybean production worldwide*, pages 1–26. Academic Press, San Diego.

Park, S., Lee, C.-M., Doherty, C. J., Gilmour, S. J., Kim, Y., and Thomashow, M. F. (2015). Regulation of the arabidopsis cbf regulon by a complex low-temperature regulatory network. *The Plant Journal*, 82(2):193–207.

Paz, Margie M. Shou, H., Guo, Z., Zhang, Z., Banerjee, A. K., and Wang, K. (2004). Assessment of conditions affecting agrobacterium-mediated soybean transformation using the cotyledonary node explant. *Euphytica*, 136:167–179.

Peng, J., Carol, P., Richards, D. E., King, K. E., Cowling, R. J., Murphy, G. P., and Harberd, N. P. (1997). The arabidopsis gai gene defines a signaling pathway that negatively regulates gibberellin responses. *Genes Dev*, 11(23):3194–205.

Peng, T., Zhu, X., Duan, N., and Liu, J. H. (2014). Ptrbam1, a beta-amylase-coding gene of *Poncirus trifoliata*, is a cbf regulon member with function in cold tolerance by modulating soluble sugar levels. *Plant Cell Environ*, 37(12):2754–67.

Peng, Y., Arora, R., Li, G., Wang, X., and Fessehaie, A. (2008). Rhododendron catawbiense plasma membrane intrinsic proteins are aquaporins, and their over-expression compromises constitutive freezing tolerance and cold acclimation ability of transgenic arabidopsis plants. *Plant, Cell & Environment*, 31(9):1275–1289.

Pirzadah, T. B., Malik, B., Rehman, R. U., Hakeem, K. R., and Qureshi, M. I. (2014). *Signaling in response to cold stress*, book section 10, pages 193–218. Springer, India.

Potuschak, T., Lechner, E., Parmentier, Y., Yanagisawa, S., Grava, S., Koncz, C., and Genschik, P. (2003). Ein3-dependent regulation of plant ethylene hormone signaling by two arabidopsis f box proteins: Ebf1 and ebf2. *Cell*, 115(6):679–89.

Puhakainen, T., Hess, M. W., Mkel, P., Svensson, J., Heino, P., and Palva, E. T. (2004). Overexpression of multiple dehydrin genes enhances tolerance to freezing stress in arabidopsis. *Plant Molecular Biology*, 54(5):743–753.

Qin, F., Shinozaki, K., and Yamaguchi-Shinozaki, K. (2011). Achievements and challenges in understanding plant abiotic stress responses and tolerance. *Plant Cell and Physiology*, 52(9):1569–1582.

R Core Team, R. (2013). http://www.r-project.org date last accessed march 25, 2019.

Ristic, Z. and Ashworth, E. (1993). Changes in leaf ultrastructure and carbohydrates in *Arabidopsis thaliana* l. (heyn) cv. columbia during rapid cold acclimation. *Protoplasma*, 172(2-4):111–123.

Robison, J., Arora, N., Yamasaki, Y., Saito, M., Boone, J., Blacklock, B. J., and Randall, S. K. (2017). *Glycine max* and *Glycine soja* are capable of cold acclimation. *Journal of Agronomy and Crop Science*, 203(6):553–561.

Robison, J. D., Yamasaki, Y., and Randall, S. K. (2019). The ethylene signaling pathway negatively impacts cbf/dreb-regulated cold response in soybean (*Glycine max*). *Frontiers in Plant Science*, 10(121).

Roldan-Arjona, T. and Ariza, R. R. (2009). Repair and tolerance of oxidative dna damage in plants. *Mutat Res*, 681(2-3):169–79.

Roston, R. L., Wang, K., Kuhn, L. A., and Benning, C. (2014). Structural determinants allowing transferase activity in sensitive to freezing 2, classified as a family i glycosyl hydrolase. *J Biol Chem*, 289(38):26089–106.

Roychoudhury, A., Paul, S., and Basu, S. (2013). Cross-talk between abscisic acid-dependent and abscisic acid-independent pathways during abiotic stress. *Plant Cell Reports*, 32:985–1006.

Ruban, A. V., Johnson, M. P., and Duffy, C. D. P. (2012). The photoprotective molecular switch in the photosystem ii antenna. *Biochimica et Biophysics Acta*, 1817(1):167–181.

Sah, S. K., Reddy, K. R., and Li, J. (2016). Abscisic acid and abiotic stress tolerance in crop plants. *Frontiers in Plant Science*, 7:571.

Savitch, L. V., Barker-strom, J., Ivanov, A. G., Hurry, V., quist, G., Huner, N. P., and Gardestrm, P. (2001). Cold acclimation of *Arabidopsis thaliana* results in incomplete recovery of photosynthetic capacity, associated with an increased reduction of the chloroplast stroma. *Planta*, 214(2):295–303.

Schaller, G. E. and Binder, B. M. (2017). *Inhibitors of Ethylene Biosynthesis and Signaling*, book section 15, pages 223–235. Springer Science+Business Media LLC.

Schmutz, J., Cannon, S. B., Schlueter, J., Ma, J., Mitros, T., Nelson, W., Hyten, D. L., Song, Q., Thelen, J. J., Cheng, J., Xu, D., Hellsten, U., May, G. D., Yu, Y., Sakurai, T., Umezawa, T., Bhattacharyya, M. K., Sandhu, D., Valliyodan, B., Lindquist, E., Peto, M., Grant, D., Shu, S., Goodstein, D., Barry, K., Futrell-Griggs, M., Abernathy, B., Du, J., Tian, Z., Zhu, L., Gill, N., Joshi, T., Libault, M., Sethuraman, A., Zhang, X.-C., Shinozaki, K., Nguyen, H. T., Wing, R. A., Cregan, P., Specht, J., Grimwood, J., Rokhsar, D., Stacey, G., Shoemaker, R. C., and Jackson, S. A. (2010). Genome sequence of the palaeopolyploid soybean. *Nature*, 463(463):178–183.

Seddigh, M., Jolliff, G. D., and Orf, J. H. (1988). Field evaulation of early maturing soybean genotypes adaptation to low night temperatures. *Crop Science*, 28:639–643.

Seo, E., Lee, H., Jeon, J., Park, H., Kim, J., Noh, Y. S., and Lee, I. (2009). Crosstalk between cold response and flowering in arabidopsis is mediated through the flowering-time gene soc1 and its upstream negative regulator flc. *Plant Cell*, 21(10):3185–97.

Severin, A. J., Woody, J. L., Bolon, Y.-T., Joseph, B., Diers, B. W., Farmer, A. D., Muehlbauer, G. J., Nelson, R. T., Grant, D., Specht, J. E., Graham, M. A., Cannon, S. B., May, G. D., Vance, C. T., and Schomaker, R. C. (2010). Rna-seq atlas of glyxine max: A guide to the soybean transcriptome. *BMC Plant Biology*, 10(160-177):160.

Sharma, S., Villamor, J. G., and Verslues, P. E. (2011). Essential role of tissue-specific proline synthesis and catabolism in growth and redox balance at low water potential. *Plant Physiology*, 157(1):292–304.

Sharmin, S. A., Alam, I., Kim, K.-H., Kim, Y.-G., Kim, P. J., Bahk, J. D., and Lee, B.-H. (2012). Chromium-induced physiological and proteomic alterations in roots of *Miscanthus sinensis*. *Plant Science*, 187:113–126.

Shi, Y., Tian, S., Hou, L., Huang, X., Zhang, X., Guo, H., and Yang, S. (2012). Ethylene signaling negatively regulates freezing tolerance by repressing expression of cbf and type-a arr genes in arabidopsis. *Plant Cell*, 24(6):2578–95.

Shimosaka, E. and Ozawa, K. (2015). Overexpression of cold-inducible wheat galactinol synthase confers tolerance to chilling stress in transgenic rice. *Breeding science*, 65(5):363–371.

Sievers, F., Wilm, A., Dineen, D., Gibson, T. J., Karplus, K., Li, W., Lopez, R., McWilliam, H., Remmert, M., Sding, J., Thompson, J. D., and Higgins, D. G. (2011). Fast, scalable generation of highquality protein multiple sequence alignments using clustal omega. *Molecular Systems Biology*, 7(1):539.

Silverstone, A. L., Ciampaglio, C. N., and Sun, T. (1998). The arabidopsis rga gene encodes a transcriptional regulator repressing the gibberellin signal transduction pathway. *Plant Cell*, 10(2):155–69.

Singh, A., Upadhyay, V., Upadhyay, A. K., Singh, S. M., and Panda, A. K. (2015). Protein recovery from inclusion bodies of *Escherichia coli* using mild solubilization process. *Microbial cell factories*, 14:41–41.

Sloger, C. and Caldwell, B. E. (1970). Response of cultivars of soybeans to synthetic abscisic acid. *Plant Physiology*, 45:634–635.

Smirnoff, N. and Cumbes, Q. J. (1989). Hydroxyl radical scavenging activity of compatible solutes. *Phytochemistry*, 28(4):1057–1060.

Song, S., Huang, H., Gao, H., Wang, J., Wu, D., Liu, X., Yang, S., Zhai, Q., Li, C., Qi, T., and Xie, D. (2014). Interaction between myc2 and ethylene insensitive3 modulates antagonism between jasmonate and ethylene signaling in arabidopsis. *Plant Cell*, 26(1):263–79.

Steponkus, P. L., Uemura, M., Joseph, R. A., Gilmour, S. J., and Thomashow, M. F. (1998). Mode of action of the cor15a gene on the freezing tolerance of *Arabidopsis thaliana*. *Proceedings of the National Academy of Sciences*, 95(24):14570–14575.

Stockinger, E. J., Gilmour, S. J., and Thomashow, M. F. (1997). *Arabidopsis thaliana* cbf1 encodes an ap2 domain-containing transcriptional activator that binds to the c-repeat/dre, a cis-acting dna regulatory element that stimulates transcription in response to low temperature and water deficit. *Proceedings of the National Academy of Sciences*, 94:1035–1040.

Stothard, P. (2000). The sequence manipulation suite: Javascript programs for analyzing and formatting protein and dna sequences. *Biotechniques*, 28(6):1102–1104.

Strand, A., Foyer, C. H., Gustafsson, P., Gardestrom, P., and Hurry, V. (2003). Altering flux through the sucrose biosynthesis pathway in transgenic *Arabidopsis thaliana* modifies photosynthetic acclimation at low temperatures and the development of freezing tolerance. *Plant, Cell & Environment*, 26(4):523–535.

Strasser, R. J. and Srivastava, A. (1995). Polyphasic chlorophyll a fluorescence transient in plants and cyanobacteria. *Photochemistry and Photobiology*, 61(1):32–42.

Strasser, R. J., Srivastava, A., and Tsimilli, M. (2000). *The fluorescence transient as a tool to characterize and screen photosynthetic samples*, book section 25, pages 445–483. Taylor Francis, London.

Strauss, G. and Hauser, H. (1986). Stabilization of lipid bilayer vesicles by sucrose during freezing. *Proceedings of the National Academy of Sciences*, 83(8):2422–2426.

Street, I. H. and Schaller, G. E. (2016). Ethylene: a gaseous signal in plants and bacteria. *Annual Review of Cell and Developmental Biology*, 16:1–18.

Sun, Z., Zhao, T., Gan, S., Ren, X., Fang, L., Karungo, S. K., Wang, Y., Chen, L., Li, S., and Xin, H. (2016). Ethylene positively regulates cold tolerance in grapevine

by modulating the expression of ethylene response factor 057. *Scientific Reports*, 6:24066.

Suzuki, N. and Mittler, R. (2006). Reactive oxygen species and temperature stresses: A delicate balance between signaling and destruction. *Physiologia Plantarum*, 126(1):45–51.

Szkely, G., brahm, E., Cspl, ., Rig, G., Zsigmond, L., Csiszr, J., Ayaydin, F., Strizhov, N., Jsik, J., Schmelzer, E., Koncz, C., and Szabados, L. (2008). Duplicated p5cs genes of arabidopsis play distinct roles in stress regulation and developmental control of proline biosynthesis. *The Plant Journal*, 53(1):11–28.

Taji, T., Ohsumi, C., Iuchi, S., Seki, M., Kasuga, M., Kobayashi, M., Yamaguchi-Shinozaki, K., and Shinozaki, K. (2002). Important roles of drought- and cold-inducible genes for galactinol synthase in stress tolerance in arabidopsis thaliana. *Plant J*, 29(4):417–26.

Tambussi, E. A., Bartoli, C. G., Guiamet, J. J., Beltrano, J., and Araus, J. L. (2004). Oxidative stress and photodamage at low temperatures in soybean (*Glycine max* l. merr.) leaves. *Plant Science*, 167:19–26.

Tan, W.-J., Yang, Y.-C., Zhou, Y., Huang, L.-P., Xu, L., Chen, Q.-F., Yu, L.-J., and Xiao, S. (2018). Diacylglycerol acyltransferase and diacylglycerol kinase modulate triacylglycerol and phosphatidic acid production in the plant response to freezing stress. *Plant Physiology*, 177(3):1303–1318.

Tarkowski, . P. and Van den Ende, W. (2015). Cold tolerance triggered by soluble sugars: a multifaceted countermeasure. *Frontiers in plant science*, 6:203–203.

Taylor, G. E. and Gunderson, C. A. (1986). The response of foliar gas exchange to exogenously applied ethylene. *Plant Physiology*, 82(3):653–657.

Taylor, G. E. and Gunderson, C. A. (1988). Physiological site of ethylene effects on carbon dioxide assimilation in *Glycine max* l. merr. *Plant Physiology*, 86(1):85–92.

Teige, M., Scheikl, E., Eulgem, T., Dczi, R., Ichimura, K., Shinozaki, K., Dangl, J. L., and Hir, H. (2004). The mkk2 pathway mediates cold and salt stress signaling in arabidopsis. *Molecular Cell*, 15(1):141–152.

Tholen, D., Pons, T. L., Voesenek, L. A., and Poorter, H. (2007). Ethylene insensitivity results in down-regulation of rubisco expression and photosynthetic capacity in tobacco. *Plant Physiology*, 144(3):1305–15.

Tholen, D., Pons, T. L., Voesenek, L. A., and Poorter, H. (2008). The role of ethylene perception in the control of photosynthesis. *Plant Signal Behavior*, 3(2):108–9.

Thomashow, M. F. (1999). Plant cold acclimation: freezing tolerance genes and regulatory mechanisms. *Annual Review of Plant Physiology and Plant Molecular Biology*, 50:571–599.

Thompson, C. J., Movva, N. R., Tizard, R., Crameri, R., Davies, J. E., Lauwereys, M., and Botterman, J. (1987). Characterization of the herbicide-resistance gene bar from streptomyces hygroscopicus. *Embo j*, 6(9):2519–23.

Tuteja, N. (2007). Abscisic acid and abiotic stress signaling. *Plant Signaling & Behavior*, 2(3):135–138.

USDA-NASS, U. (2014). 2012 census of agriculture highlights, may 2014.

Valluru, R., Lammens, W., Claupein, W., and Van den Ende, W. (2008). Freezing tolerance by vesicle-mediated fructan transport. *Trends Plant Sci*, 13(8):409–14.

Van den Ende, W. (2013). Multifunctional fructans and raffinose family oligosaccharides. *Frontiers in plant science*, 4:247–247.

Van Heerden, P. D., Tsimilli-Michael, M., Kruger, G. H., and Strasser, R. J. (2003). Dark chilling effects on soybean genotypes during vegetative development: parallel studies of co2 assimilation, chlorophyll a fluorescence kinetics o-j-i-p and nitrogen fixation. *Physiologia Plantarum*, 117(4):476–491.

Van Heerden, P. D. R. and Kruger, G. H. (2000). Photosynthetic limitation in soybean during cold stress. *South African Journal of Science*, 96:201–206.

Van Heerden, P. D. R. and Krger, G. H. J. (2002). Separately and simultaneously induced dark chilling and drought stress effects on photosynthesis, proline accumulation and antioxidant metabolism in soybean. *Journal of Plant Physiology*, 159:1077–1086.

Vaultier, M.-N., Cantrel, C., Vergnolle, C., Justin, A.-M., Demandre, C., Benhassaine-Kesri, G., iek, D., Zachowski, A., and Ruelland, E. (2006). Desaturase mutants reveal that membrane rigidification acts as a cold perception mechanism upstream of the diacylglycerol kinase pathway in arabidopsis cells. *FEBS Letters*, 580(17):4218–4223.

Venzhik, Y., Talanova, V., and Titov, A. (2016). The effect of abscisic acid on cold tolerance and chloroplast ultrastructure in wheat under optimal and cold stress conditions. *Acta Physiologiae Plantarum*, 38(3):63.

Vogel, J. T., Zarka, D. G., Van Buskirk, H. A., Fowler, S., and Thomashow, M. F. (2005). Roles of the cbf2 and zat12 transcription factors in configuring the low temperature transcriptome of arabidopsis. *The Plant Journal*, 41(2):195–211.

Wang, K. L.-C., Li, H., and Ecker, J. R. (2002). Ethylene biosynthesis and signaling networks. *Plant Cell*, 14 Suppl(Suppl):s131–s151.

Wang, W., Chen, D., Zhang, X., Liu, D., Cheng, Y., and Shen, F. (2018). Role of plant respiratory burst oxidase homologs in stress responses. *Free Radical Research*, 52(8):826–839.

Wang, Y., Li, J., Wang, J., and Li, Z. (2010). Exogenous h2o2 improves the chilling tolerance of manilagrass and mascarenegrass by activating the antioxidative system. *Plant Growth Regulation*, 61(2):195–204.

Wang, Z., Reddy, K. J., and Quebedeaux, B. (1997). Growth and photosynthetic responses of soybean to short-term cold temperature. *Environmental and Experimental Botany*, 37:13–24.

Warren, C. R. (2008). Rapid measurement of chlorophylls with a microplate reader. *Journal of Plant Nutrition*, 31:1321–1332.

Wathugala, D. L., Richards, S. A., Knight, H., and Knight, M. R. (2011). Ossfr6 is a functional rice orthologue of sensitive to freezing-6 and can act as a regulator of cor gene expression, osmotic stress and freezing tolerance in arabidopsis. *New Phytol*, 191(4):984–95.

Wawrzyska, A. and Sirko, A. (2016). Ein3 interferes with the sulfur deficiency signaling in *Arabidopsis thaliana* through direct interaction with the slim1 transcription factor. *Plant Science*, 253:50–57.

Xin, Z. and Browse, J. (1998). eskimo1 mutants of arabidopsis are constitutively freezing-tolerant. *Proceedings of the National Academy of Sciences*, 95(13):7799–7804.

Yamasaki, Y. (2013). *Responses of soybean to cold temperature dehydrins in Arabidopsis and soybean*. Phd.

Yamasaki, Y., Koehler, G., Blacklock, B. J., and Randall, S. K. (2013). Dehydrin expression in soybean. *Plant Physiology and Biochemistry*, 70:213–220.

Yamasaki, Y. and Randall, S. K. (2016). Functionality of soybean cbf/dreb1 transcription factors. *Plant Science*, 246:80–90.

Yang, Y., Ou, B., Zhang, J., Si, W., Gu, H., Qin, G., and Qu, L. J. (2014). The arabidopsis mediator subunit med16 regulates iron homeostasis by associating with ein3/eil1 through subunit med25. *Plant J*, 77(6):838–51.

Yoo, S.-D., Cho, Y.-H., and Sheen, J. (2007). Arabidopsis mesophyll protoplasts: a versatile cell system for transient gene expression analysis. *Nature Protocols*, 2(7):1565–1572.

Yoshiba, Y., Kiyosue, T., Nakashima, K., Yamaguchi-Shinozaki, K., and Shinozaki, K. (1997). Regulation of levels of proline as an osmolyte in plants under water stress. *Plant and Cell Physiology*, 38(10):1095–1102.

Zarka, D. G., Vogel, J. T., Cook, D., and Thomashow, M. F. (2003). Cold induction of arabidopsis cbf genes involves multiple ice (induce of cbf expression) promoter elements and a cold-regulatory circuit that is desensitized by low temperature. *Plant Physiology*, 133(2):910–918.

Zhang, J., Chen, N., Zhang, Z., Pan, L., Chen, M., Wang, M., Wang, T., Chi, X., Yang, Z., Liu, F., Yu, S., and Wan, Y. (2016). Peanut ethylene-responsive element binding factor (aherf6) improves cold and salt tolerance in arabidopsis. *Acta Physiology Plant*, 38(7):185.

Zhang, N. and Casida, J. E. (2002). Novel irreversible butyrylcholinesterase inhibitors: 2-chloro-1-(substituted-phenyl)ethylphosphonic acids. *Bioorganic & medicinal chemistry*, 10(5):1281–1290.

Zhang, X., Fowler, S., Cheng, H., Lou, Y., Rhee, S. Y., Stockinger, E. J., and Thomashow, M. F. (2004). Freezing-sensative tomato has a functional cbf cold response pathway, but a cbf regulon that differs from that of freezing-tolerant arabidopsis. *The Plant Journal*, 39:905–919.

Zhang, Y.-J., Yang, J.-S., Guo, S.-J., Meng, J.-J., Zhang, Y.-L., Wan, S.-B., He, Q.-W., and Li, X.-G. (2011). Over-expression of the arabidopsis cbf1 gene improves resistance of tomato leaves to low temperature under low irradiance. *Plant Biology*, 13(2):362–367.

Zhang, Z. and Huang, R. (2010). Enhanced tolerance to freezing in tobacco and tomato overexpressing transcription factor terf2/leerf2 is modulated by ethylene biosynthesis. *Plant Molecular Biology*, 73(3):241–249.

Zhang, Z., Xing, A., Staswick, P., and Clemente, T. E. (1999). The use of glufosinate as a selective agent in agrobacterium-mediated transformation of soybean. *Plant Cell*, 56:37–46.

Zhao, C., Zhang, Z., Xie, S., Si, T., Li, Y., and Zhu, J.-K. (2016). Mutational evidence for the critical role of cbf in cold acclimation in arabidopsis. *Plant Physiology*, 171(4):2744–59.

Zhao, M., Liu, W., Xia, X., Wang, T., and Zhang, W.-H. (2014). Cold acclimation-induced freezing tolerance of medicago truncatula seedlings is negatively regulated by ethylene. *Physiologia Plantarum*, 152(1):115–129.

Zhao, Q. and Guo, H.-W. (2011). Paradigms and paradox in the ethylene signaling pathway and interaction network. *Molecular Plant*, 4(4):626–634.

Zhen, Y., Dhakal, P., and Ungerer, M. C. (2011). Fitness benefits and costs of cold acclimation in *Arabidopsis thaliana*. *The American Naturalist*, 178(1):44–52.

Zhu, C. G., Chen, Y. N., Li, W. H., Chen, X. L., and He, G. Z. (2015). Heliotropic leaf movement of *Sophora alopecuroides* l.: An efficient strategy to optimise photochemical performance. *Photosynthetica*, 53(2):231–240.

Zhu, J.-Y., Sae-Seaw, J., and Wang, Z.-Y. (2013). Brassinosteroid signalling. *Development (Cambridge, England)*, 140(8):1615–1620.

Zhu, X.-G., Govindjee, Baker, N. R., deSturler, E., Ort, D. R., and Long, S. P. (2005). Chlorophyll a fluorescence induction kinetics in leaves predicted from a model describing each discrete step of excitation energy and electron transfer associated with photosystem ii. *Planta*, 223(1):114–133.

APPENDICES

A. ROBISON ET AL., 2017

Robison, J. D., N. Aurora, Y. Yamasaki, M. Saito, J. Boone, B. Blacklock, S. Randall, 2017. Cold Acclimation Potentials of *Glycine max* and *Glycine soja*. Journal of Agronomy and Crop Science, 203:553-561.

See paper on next page.

Accepted: 5 May 2017
DOI: 10.1111/jac.12219

CHILLING/FREEZING STRESS

WILEY Journal of Agronomy and Crop Science

Glycine max and *Glycine soja* are capable of cold acclimation

J. Robison | N. Arora | Y. Yamasaki | M. Saito | J. Boone | B. Blacklock | S. Randall

Indiana University Purdue University Indianapolis, Indianapolis, IN, USA

Correspondence
S. Randall, Indiana University Purdue University Indianapolis, Indianapolis, Indiana, USA.
Email: srandal@iupui.edu

Funding information
United Soybean Board (USB)

Abstract

Soybean has been considered a cold intolerant species; based largely upon seed germination and soil emergent evaluations. This study reports a distinct acquisition of cold tolerance, in seedlings, following short acclimation periods. Diversity in cold responses was assessed in eight cultivars of *Glycine max* and six accessions of *G. soja*. All varieties of soybean significantly increased in freezing tolerance following acclimation. This study indicates soybean seedlings are indeed capable of sensing cold and acquiring cold tolerance. Germination rates after cold imbibition were negatively correlated with maturity group, but positively correlated with cold acclimation potential in *G. soja*. Seed fatty acid composition was varied between the species, with *Glycine soja* accessions containing about 2-times more linolenic acid (18:3) than *G. max*. Furthermore, high levels of linoleic acid (18:2) in seeds were positively correlated with germination rates following cold imbibition in *G. soja* only. We suggest that domestication has not impacted the overall ability of soybean to cold acclimate at the seedling stage and that there is little variation within the domesticated species for ability to cold acclimate. Thus, this brief comparative study reduces the enthusiasm for the "wild" species as an additional source of genetic diversity for cold tolerance.

KEYWORDS
cold acclimation, cold tolerance, fatty acid composition, germination, ion leakage, soybean

1 | INTRODUCTION

Domesticated soybean, *Glycine max* [L.] Merr., is an important agricultural crop, valued within the United States at $38.7 billion in 2012 (USDA-NASS 2014). *Glycine max* cultivars are grouped into 13 maturity groups, ranging from 000 to X, based primarily on photoperiodism (Zhang et al., 2007). Higher maturity groups (V to X) generally flower in response to shorter days than lower maturity groups (000 – IV). These maturity group designations are also utilised for *Glycine soja* Sieb. & Zucc., which is considered the closest wild progenitor for *G. max* (Broich & Palmer, 1980; Li et al., 2010).

Glycine soja is smaller in both size and yield than *G. max*, possessing hard, long-dormancy seeds and slender vine-like branches (Broich & Palmer, 1980; Saitoh, Nishimura, & Kuroda, 2004). Some cultivars of *G. soja* are less susceptible to salt stress (Luo, Yu, & Liu, 2005) and dehydration stress (Chen, Chen, & de los Reyes, 2006) than their domestic counterparts (*G. max*). Based on sequencing, *G. soja* have a greater genetic diversity and may be a source for expanding the abiotic stress tolerance of *G. max* (Lam et al., 2010; Li et al., 2010).

In freezing survival experiments, *G. max* genotypes were characterised by high death rates following a −3°C cold treatment with no significant differences between cultivars being observed (Hume & Jackson, 1981). The work described here allows for a more quantitative evaluation of cold and freezing tolerance. Although *G. soja*'s cold tolerance has not yet been examined; several soybean cold-accumulated proteins, when transgenically expressed, have been shown to enhance cold tolerance in Arabidopsis (Luo et al., 2012; Yang et al., 2014). We have chosen to closely examine the ability of soybean to cold acclimate and to acquire cold tolerance. Further, we have examined a few selected accessions of *G. soja* to determine whether it is likely the wild varieties are a potential source for variation in cold tolerance. We further examined the variation of cold tolerance (seed

germination) in soybeans and whether there is an association of these abilities with seed lipid composition and/or dehydrin abundance and response.

This study aimed to determine the variation in cold tolerance and the relationship to the maturity group of *Glycine* species (*max* and *soja*) at both germinating seed stage and in young seedlings, and the impact of cold acclimation on freezing plant tolerance.

2 | MATERIALS AND METHODS

2.1 | Ion leakage freezing assay

To obtain seed, plants were all grown (from May to August) under natural lighting in a greenhouse with temperature ranging from 15 to 38°C, except for *G. soja*, several of which were grown with short-day periods (10 h days) at 25°C in a growth chamber (PI 391,587, 483,464 and 483,071). For experimental work, *Glycine max* or *G. soja* (Table 1) seeds were planted in moist potting soil and grown for 2 weeks at 22°C under approximately 150 μmol m^{-2} s^{-1} of light on a 16:8 light:dark cycle. At this point, the plants were at stage VC – V1, with unifoliate leaves completely unfurled and the first trifoliate set expanding. Cold acclimation was 4°C at night and 5°C during the day under the same light cycle as growth conditions. After cold acclimation, ranging from 0 to 10 days, unifoliate leaves from 14 to 16 individual soybean seedlings were removed and 1-cm diameter leaf discs punched, avoiding the midrib. Each replicate (usually six replicates), consisted of 3 to 4 leaf discs in a 16 × 100 mm glass test tube.

Freezing assays were performed in an ethylene glycol bath (Brinkmann Lauda MGW RC 20) with temperatures starting at −1.0°C and lowered by 0.5°C every 2 hrs until −2.5°C was reached (unless otherwise noted) where they were maintained for another 2 hrs prior to removal and recovery overnight at 4°C. To ensure ice nucleation, a 50 μl di water ice pellet was placed against the leaves after the first hour at −1.0°C. After recovery at 4°C, 3 ml of distilled water was added to each replicate, and vigorous shaking was applied for 6 hrs. Electrical conductivity was measured by a portable conductivity metre (Milwaukee Model MW301 EC meter). One hundred per cent electrolyte leakage was determined by rereading conductivity after freezing the same samples at −80°C.

TABLE 1 Varieties of *G. max* and *G. soja* utilised in this study based on maturity group. Refer to figures for specific cultivars usage in individual experiments

Species	Maturity Group	Cultivar name	PI #	Country of origin
G. max	000	Fiskeby V	360955A	Sweden
G. max	000	Traff	470930	Sweden
G. max	000	Maple Presto	548593	Canada
G. max	00	Maple Arrow	548593	Canada
G. max	00	McCall	548582	USA
G. max	0	Shinsei	594279	Japan
G. max	I	Koganejiro	317335	Japan
G. max	I		522189	Russia
G. max	II	Amcor 89	546375	USA
G. max	III	Williams 82	518671	USA
G. max	III	Woodworth	548632	USA
G. max	VI	Harbar	561702	Mexico
G. max	VI	Young	508266	USA
G. max	VII	Bragg	548266	USA
G. soja	00		464866A	China
G. soja	I		447003B	China
G. soja	II		101404A	China
G. soja	II	Ye sheng-tou	391587	China
G. soja	III		483464B	China
G. soja	IV		483071B	China

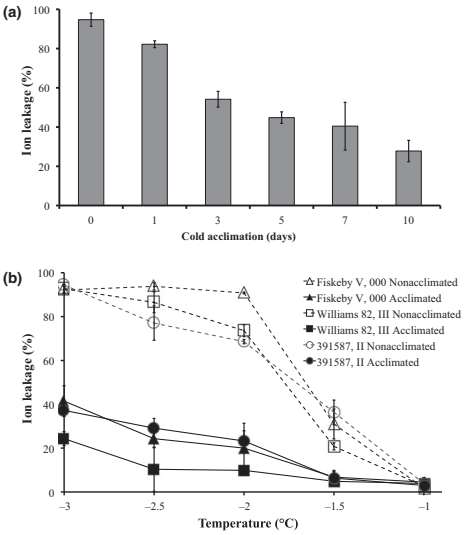

FIGURE 1 Cold acclimation potential in *G. max* and *G. soja*. (a) Ion leakage in 14-day-old *G. max* cv Williams 82 acclimated at 4°C for 0 to 10 days prior to freezing treatment of −2.5°C. All acclimation periods were statistically significant when compared to 0 day (*t* test $p < .01$). (b) Electrolyte leakage in 14-day-old *G. max* cv Williams 82, Fiskeby V and *G. soja* PI 391,587 soybean seedlings acclimated for 7 days (solid line, closed symbol) or 0 days (dash lines, open symbol) at 4°C prior to freezing treatment. Error bars are standard deviations. At all temperatures below −1°C, acclimation was statistically significant compared to non-acclimation (*t* test $p < .01$)

2.2 | Germination assay

Seeds from *G. max* and *G. soja* (Table 1) were covered halfway with water for 24 hrs at 4, 8 or 22°C in the dark. Seeds were then placed on moistened paper towels at control temperature (22°C) for 5 days prior to scoring germination. Seeds were considered to have germinated if any visible root extended beyond the seed coat. Each condition consisted of 15 seeds and the experiment was repeated 4 times for a total of 60 seeds for each soybean variety.

2.3 | Fatty acid determination

Seeds from *G. max* and *G. soja* varieties (Table 1) were collected from greenhouse grown plants. For each experiment, 20 seeds of each *G. max* cultivar and 40 to 50 seeds of each *G. soja* variety were ground into a powder in liquid nitrogen. Fatty acid methyl esters were prepared from 2 mg seed powder by transesterification of total lipids (2% H_2SO_4/methanol) at 80°C for 1 hr. Fatty acid methyl esters (FAMEs) were extracted into hexanes and analysed by gas chromatography–mass spectrometry with an Agilent Technologies 7890A GC/5975C MS and DB23 column (J&W Scientific). The fatty acid profile was expressed as the total per cent FAMEs.

2.4 | Protein analysis

For both leaf and seed samples, proteins were extracted with 2 × Laemmli SDS-PAGE sample buffer (Laemmli, 1970) containing protease inhibitors (1 mM Benzamidine, 1 μg/ml aprotinin [Sigma], 1 μM pepstain A [Sigma] and 1 μg/ml leupeptin [Sigma]). Total protein concentration was determined via amido black (Kaplan & Pedersen, 1985). Proteins (10 μg) were separated on 12% SDS polyacrylamide gels (Laemmli, 1970). Samples were electrophoretically transferred to nitrocellulose membrane. Membranes were blocked with 5% (w/v) milk in PBS prior to antibody probing. Seed samples were probed with a dehydrin antibody (1:2000 dilution, K-segment specific (Close, Fenton, & Moonan, 1993), while leaf samples were probed with an antibody that recognises GmERD14 (1:2000 dilution, (Yamasaki, Koehler, Blacklock, & Randall, 2013). The secondary antibody was goat anti-rabbit IgG conjugated with horseradish peroxidase (1:4000

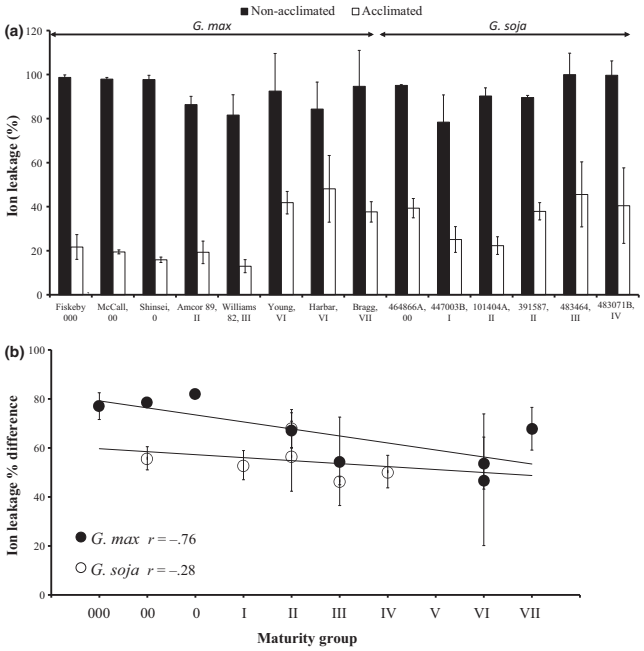

FIGURE 2 Cold acclimation across maturity groups of *G. max* and *G. soja*. (a) Ion leakage in soybean seedlings acclimated for 7 days (open bars) or 0 days (solid bars) at 4°C prior to freezing treatment (−2.5°C). Acclimation was statistically significant compared to non-acclimated samples in every cultivar (*t* test $p < .01$). (b) Correlation of the difference between non-acclimated and acclimated ion leakage versus maturity group in both *G. max* (closed circles) and *G. soja* (open circles). Error bars (standard deviations) not shown are smaller than the symbols. The correlation between *G. max* maturity group and cold acclimation was statistically significant ($p < .05$), while that of *G. soja* was not ($p = .59$)

dilution, Sigma). Peroxidase was visualised with Super Signal Western Dura (Pierce Biotechnology) and imaged on a Bio-Rad Chemi-Doc XRS+ (Bio-Rad Laboratories).

2.5 | Statistical analysis

Student's unpaired *t* tests were calculated using Microsoft Excel (Professional Plus 2013). Pearson's correlation coefficients (*r*) and associated *p* values were calculated with R (R Core Team 2013).

3 | RESULTS

3.1 | Cold acclimation in soybean seedlings

Exposure to a low, but non-freezing temperature (cold acclimation), resulted in acquisition of freezing tolerance as measured by a decrease in ion leakage in *G. max* cv Williams 82 (Figure 1a). The acclimation time required for 50% enhancement of freezing tolerance was 5.2 ± 0.6 days (calculated from the data in Figure 1a and two additional experiments, not shown). Seven days of cold treatment were chosen to compare the *G. max* and *G. soja* genotypes for their ability to cold acclimate. Acclimated and non-acclimated *G. max* cv Fiskeby V (MG 000), Williams 82 (MG III) and *G. soja* PI 391,587 (MG II) were examined for ion leakage across a range of freezing temperatures from −1.0 to −3.0°C (Figure 1b). Following cold acclimation, all three cultivars showed significant ($p < .05$) improvement in freezing tolerance at all temperatures less than −1.0°C. However, the cultivars were not significantly different from each other in sensitivity to freezing temperatures regardless of acclimation status.

To investigate whether maturity group might impact cold tolerance, we surveyed eight cultivars of *G. max* and six varieties of *G. soja* which encompassed a wide range of maturity groups (Figure 2a). After 7 days of cold acclimation, all soybean varieties showed a significant increase (Student's *t* test $p < .05$ compared to 0 days) in freezing tolerance (electrolyte leakage after exposure to −2.5°C). Interestingly, the ability to acclimate was significantly correlated with maturity group in *G. max* ($r = -.76$, $p < .05$), while there was no significant correlation in *G. soja* ($r = -.28$, Figure 2b). This suggests that while all soybean genotypes show an ability to cold

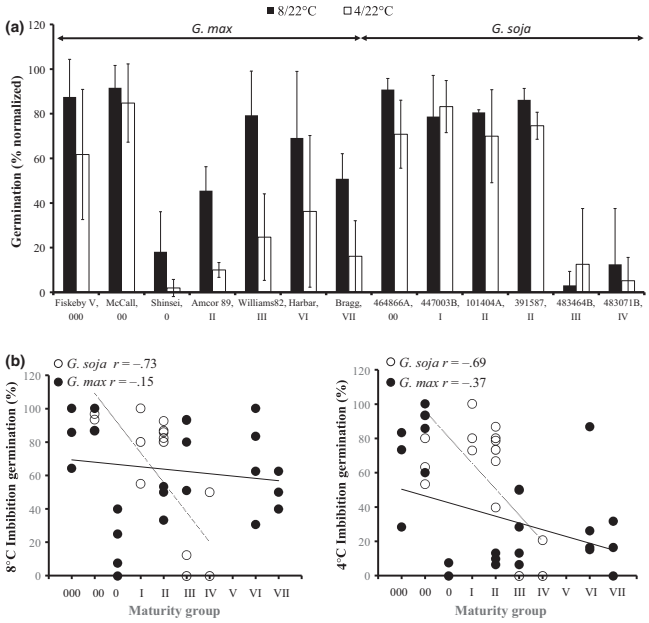

FIGURE 3 Cold imbibed germination rates for *G. max* and *G. soja*. (a) Germination rates at 8°C (closed box) or 4°C (open box) were expressed as a percentage of germination rates at 22°C. Control (22°C imbibition) seeds germinated greater than 90% except for *G. max* cv Shinsei (63%) and *G. soja* PI 483464B (53%) and PI 483071B (15%). (b) Correlation of seed germination rates after cold (4°C) imbibition with maturity group in *G. max* (closed circles) and *G. soja* (open circles) varieties. (c) Correlation of seed germination rates after chilling (8°C) imbibition with maturity group in *G. max* (closed circles) and *G. soja* (open circles) varieties. There was significant correlation between *G. soja* germination at 4°C imbibition and 8°C imbibition ($p < .01$), while there was no significance in *G. max* at either imbibition temperature ($p = .47$, .06, respectively). Control (22°C imbibition) seeds germinated greater than 90% except for *G. max* cv Shinsei (63%) and *G. soja* PI 483464B (53%) and PI 483071B (15%)

acclimate there may be inherent (or baseline) differences in cold tolerance across varieties that may be dictated by maturity group in *G. max* but not in *G. soja*.

3.2 | The impact of cold on seed germination

Seven cultivars of *G. max* and six varieties of *G. soja* across a range of maturity groups were examined for their ability to germinate after being allowed to imbibe water for 24 hrs at various temperatures (Figure 3a). There was no direct correlation between maturity group and the ability to germinate under chilling (8°C) or cold (4°C) imbibition conditions in *G. max* ($r = -.15, -.37$, Figure 3b,c; respectively). Conversely, there was a significant correlation ($r = -.73, -.69$ at 8°C and 4°C; respectively, $p < .01$) in *G. soja* with chilling and cold imbibition negatively impacting germination with increasing maturity group (Figure 3b,c). Within the early maturity groups (0 – II), *G. soja* had substantially higher germination rates than *G. max* of the same maturity group (compare 464866A to Shinsei; 101404A & 391,587 to Amcor 89). Yet in maturity groups above III, *G. max* exhibited greater than 50% germination rate, while *G. soja* germination rates were less than 20%. The 000 and 00 maturity group in *G. max* had very high germination rates following treatments at either 8 or 4°C.

When examining the cold acclimation potential (as measured by per cent difference in electrolyte leakage between acclimated and non-acclimated plants), there was a moderate positive correlation between germination rate when cold imbibed and cold acclimation at both imbibition temperatures (4 and 8°C) in *G. soja* ($r = .66, .73$ respectively, Figure 4a). This trend was absent in *G. max* ($r = .14, -.18$, respectively, Figure 4b).

3.3 | Fatty acid content and the ability to germinate in the cold

In the Fabaceae family, seeds that were resistant to chilling injury during imbibition generally contained higher unsaturated to saturated fatty acids proportions, particularly linolenic acid (18:3) and linoleic acid (18:2) versus oleic acid (18:1) (Dogras, Dilley, & Herner, 1977). To investigate if this could be used as a physiological marker that relates to the observed cold germination patterns, we examined the total fatty acid content of 14 cultivars of *G. max* and six accessions of *G. soja* (Figure 5). Marked differences in *G. max* versus *G. soja* were found in relative amounts of oleic acid (18:1) and linolenic acid (18:3). When comparing the average percentages of all varieties, *G. max* has a higher per cent total fatty acid of oleic acid than *G. soja* (14.8 ± 3.4 vs 7.7 ± 2.1%, respectively), while *G. soja* had significantly more linolenic acid than *G. max* (17.1 ± 2.3 vs 8.7 ± 1.1%, respectively) which is consistent with other reports (Shibata et al., 2008). Within the species, as maturity group increased, the percentage of linoleic acid (18:2) decreased in *G. soja* and increased in *G. max* (Figure 5). In contrast, oleic acid (18:1) and linolenic acid increased in *G. soja* and oleic acid decreased in *G. max* as maturity group increased. No significant differences relative to species or maturity group were observed in the amounts of palmitic acid (16:0) or stearic acid (18:0). Only in the *G. max* cultivar Traff and *G. soja* varieties 447003B and 101404A were 24:0 fatty acids detected at 0.1% total composition (not shown).

The ability to germinate following cold imbibition was compared with seed lipid content (oleic acid, linoleic acid and linolenic acid, Figure 6). There was a moderate negative correlation between germination rates and oleic acid content in *G. soja* seeds after imbibition at 4 and 8°C ($r = -.65, -.61$, respectively). In *G. max*, the moderate negative correlation between germination rates and oleic acid content was only noted after 8°C and not after 4°C imbibition ($r = .32, -.10$, respectively). Interestingly, *G. soja*, linoleic acid levels statistically correlated with elevated germination rates after both 4 and 8°C imbibition ($r = .90, .91$, respectively, $p < .01$), while there was no significant correlation observed in *G. max* after 4°C imbibition, there was a slight, though not significant, positive correlation after 8°C imbibition($r = -.10, .34$, respectively).

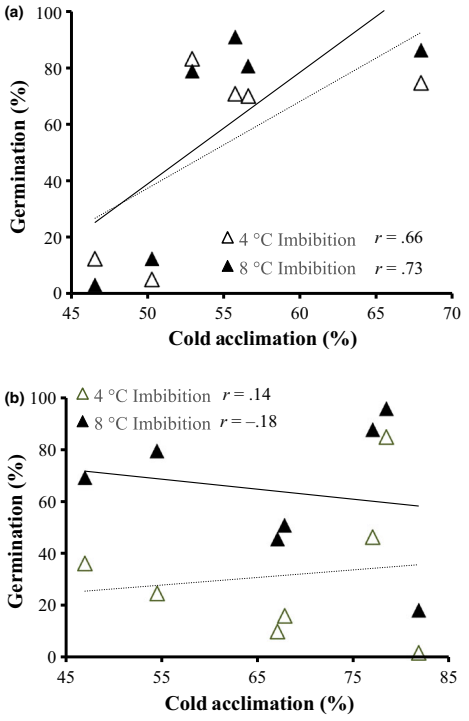

FIGURE 4 Correlation between germination and cold acclimation potential. (a) Cold (4°C, open triangles) and chilling (8°C, closed triangles) imbibition germination percentages versus cold acclimation (difference between % non-acclimated and % acclimated ion leakage) in *G. soja*. (b) Cold (4°C, open triangles) and chilling (8°C, closed triangles) imbibition germination percentages versus cold acclimation in *G. max*

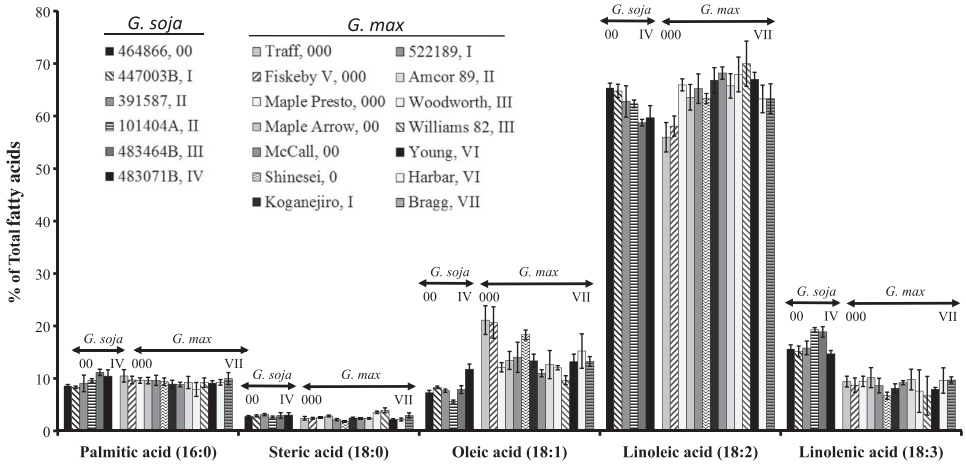

FIGURE 5 Major fatty acid profile of *G. soja* and *G. max* seeds. Fatty acid composition of *G. soja* and *G. max* seeds expressed as per cent of total quantified fatty acids. Fatty acids greater than 20 carbons accounted for less than 1% of the total and are not depicted.

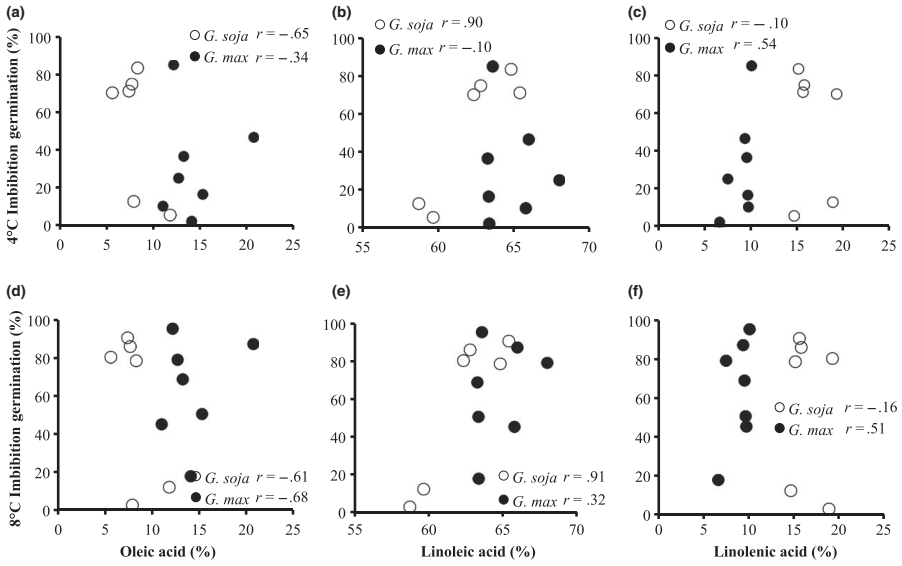

FIGURE 6 Fatty acid composition and cold germination in *G. max* and *G. soja*. Panels *A*, *C*, *E*; germination following cold imbibition at 4°C, Panels *B*, *D*, *F*; germination following cold imbibition at 8°C. Panels *A*, *B*; Oleic acid (18:1), Panels *C*, *D*; Linoleic acid (18:2) and Panels *E*, *F*; Linolenic acid (18:3). Open symbols indicate *G. soja*, and closed symbols indicate *G. max*. Only the correlations between linoleic acid and germination after imbibition at both 8 and 4°C in *G. soja* were statistically significant ($p < .01$)

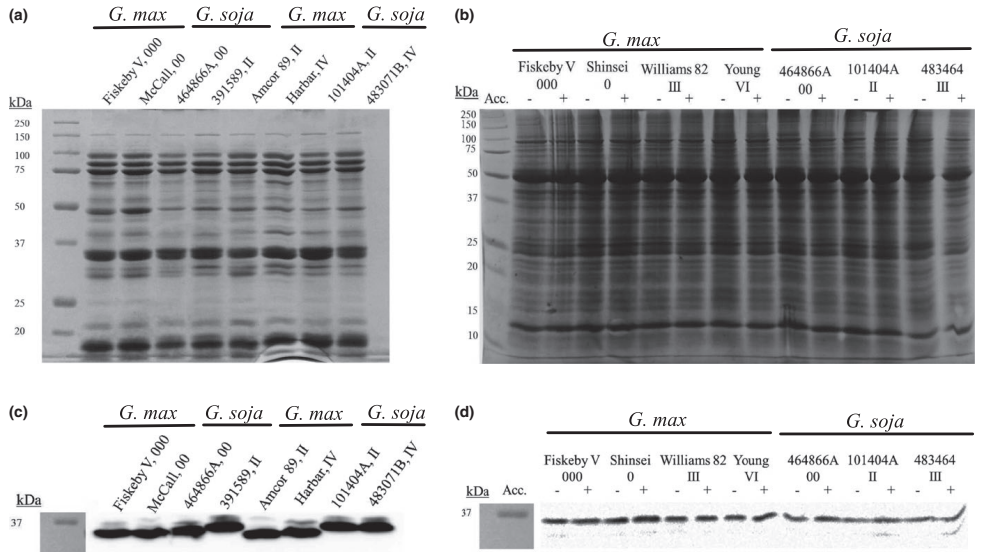

FIGURE 7 Protein content in *G. max* and *G. soja* seeds and leaves. (a) Coomassie stained gel from soybean seeds. (b) Coomassie stained gel from leaves after either a 7-d cold acclimation (+) or no acclimation (–). (c) Western blot probed for K-segment containing dehydrin protein levels in soybean seeds. (d) Western blot probed for GmERD14 protein levels in soybean leaves after either a 7-d cold acclimation or no acclimation. Each image is representative of 3 gels/blots

3.4 | Protein composition and dehydrin content in *G. max* and *G. soja*

Proteins, mainly storage proteins, in the seeds of the *G. max* and *G. soja* cultivars are remarkably similar in quality and quantity (Figure 7a). Additionally, protein quantity and quality in leaves of cold acclimated seedlings were also quite similar both within varieties and between *G. max* and *G. soja* (Figure 7b). Considering the dehydrin family of proteins is known to be important in cold acclimation and cold tolerance of other plant species (Bannerjee & Roychoudhury, 2015; Graether & Boddington, 2014), we examined levels of dehydrins in soybean seeds and leaves. Previous examination of *G. max* cv. Young (Yamasaki et al., 2013) showed minimal changes of dehydrin family members in response to environment stresses. The examination here shows there was no significant difference in seed dehydrin content regardless of maturity group (Figure 7b); nor was there any increase in the acidic dehydrin GmERD14 content compared to non-cold acclimated seedling leaves in *G. soja* or *G. max* (Figure 7d).

4 | DISCUSSION

Glycine max has been previously characterised as a cold intolerant species with little genetic potential for cold acclimation (Hume & Jackson, 1981). In this work, we focused on a more detailed analysis of the cold acclimation process and determination of whether there was any correlation with maturity groups. Further, we compared the ability for seedlings to acclimate and seeds to germinate in the cold with lipid content and the expression of the stress tolerance-related dehydrin proteins. In this study, *G. max* cv Williams 82 seedling leaves demonstrated enhanced freezing tolerance with longer cold acclimation periods. After a single day of acclimation there was measurable improvement in freezing tolerance, which continually improved until day 10. All *G. max* and *G. soja* varieties examined had significantly improved freezing tolerance after 7 days of cold acclimation. These data indicate that soybean clearly does have the ability to cold acclimate as previously suggested (Hume & Jackson, 1981). The argument can be made that *G. max* cold acclimation is weakly correlated with maturity group, with northern maturity groups acclimating better than southern cultivars. Previous reports suggested that overall cold tolerance, as measured by seed germination and emergence (Littlejohns & Tanner, 1976) and plant damage (Hume & Jackson, 1981), did not correlate well with maturity group. This correlation between cold tolerance and maturity group was not apparent in wild genotypes of *G. soja* in the present work; although there were some varieties that performed significantly better than others at low temperatures.

Cold germination ability in soybean is a distinctive measure of cold tolerance as imbibition by the seed is a process extremely

sensitive to cold. For example, cold imbibition has been shown to clearly decrease the survival rate of *G. max* cv Wayne (MG III), after only 30 min (Bramlage, Leopold, & Parrish, 1978). Based on work presented here there is clear genetic potential for enhanced germination rates in the cold, illustrated by the Fiskeby V and McCall *G. max* genotypes and the several *G. soja* (MG 0 to II). Additionally, in *G. soja* the noted correlation between cold imbibition germination rates and cold acclimation suggests that these traits may be linked. The ability to germinate following cold imbibition could be a potential predictor for seedling cold survival.

Lipid (total fatty acid content) analysis of soybean seeds was evaluated to determine whether this parameter might be predictive for the ability of seeds to germinate in the cold and perhaps seedlings to survive freezing damage. Previous studies clearly showed an adaptive change in lipid composition occurs in response to cold acclimation in other members of Fabaceae family (Dogras et al., 1977). Additionally, *Arabidopsis thaliana* ecotypes that originate in cooler, mountainous regions of the world have lower levels of very long-chain fatty acids compared to ecotypes from warmer, lower altitudes (Millar & Kunst, 1999). Recently, it was shown that soybean seeds maturing in warmer climates generally had higher levels of total fatty acid content with a decreased levels of linolenic acid and increased levels of oleic acid which correlated with mean daily temperatures, but not to maturity group (Song et al., 2016). In this study, we examined the lipid composition in seeds which had not been acclimated during maturation (all grown under similar constant and normal growth conditions) to identify any potential markers within fatty acid composition that could be used to predict cold/chilling germination success. It was noted that basal levels in oleic acid negatively correlated with cold imbibition germination rates in both *G. soja* and *G. max*. While basal linoleic acid percentages were positively correlated with cold imbibition germination in only *G. soja*. Additionally, increases in cold germination ability also correlated with increased freezing tolerance in seedlings of *G. soja*. This later trend was not observed in *G. max*. However, as *G. max* consistently had equal or higher linoleic acid percentages as that of *G. soja*, this is unlikely to be an avenue worthy of further pursuit to increase cold imbibition or seedling tolerance.

Another physiological potential for the differences observed in freezing acclimation is the presence of dehydrin proteins. Dehydrins are known to be expressed in seeds, and vegetative tissue of Arabidopsis and dehydrin expression is highly upregulated in vegetative tissues during periods of cold (Nylander, Svensson, Palva, & Welin, 2001) and are important for freezing tolerance (Puhakainen et al., 2004). The observation that none of the genotypes tested showed cold upregulated levels of acidic dehydrins was not unexpected as the lack of cold-induced dehydrin expression was previously reported in the *G. max* cv Young (Yamasaki et al., 2013). This is despite the observation that soybean exhibits apparently normal characteristics of functional cold perception and initial stages in cold responses (Yamasaki & Randall, 2016). We conclude that the lack of dehydrin response in soybean is reflective of a partly deficient cold acclimation response system, relative to most cold tolerant plants.

5 | SUMMARY

Overall, there appears to be a cold tolerance potential in the *Glycine max* and *Glycine soja* genotypes. This is particularly evident in cold seed germination variability among the various genotypes. For example, maturity groups 000 *G. max* and 0 in *G. soja* genotypes clearly confer cold germination phenotypes.

We present evidence here that young soybean seedlings can cold acclimate, although it should be noted that this ability to adjust molecular and physiological components results in a much less overall cold tolerance than that reported for more cold tolerant species (e.g. Arabidopsis, strawberry). As all genotypes tested have similar ability to adjust following cold exposure (acclimate); most of the variation in cold tolerance of seedling is contributed by inherent (under non-acclimating or basal conditions) differences in metabolism and gene expression. This suggests that while all soybean genotypes show similar ability to acclimate, there are inherent (or basal) differences in cold tolerance.

ACKNOWLEDGEMENTS

Funding provided in part by a grant awarded to SKR by the United Soybean Board (USB) Project Grant # 0238. We would like to thank the USDA-ARS National Plant Germplasm system for providing *G. max* or *G. soja* seeds for all varieties, except for *G. max* cv "Young" which was graciously provided by Dr. Tommy Carter (USDA-ARS, North Carolina State University, Raleigh, NC). The authors wish to thank John C Watson for helpful comments on this manuscript and W. A. Robison for general laboratory assistance.

REFERENCES

Bannerjee, A., & Roychoudhury, A. (2016). Group II late embryogenesis abundant (LEA) proteins: Structural and functional aspects in plant abiotic stress. *Plant Growth Regulation*, *79*, 1–17.

Bramlage, W. J., Leopold, A. C., & Parrish, D. J. (1978). Chilling stress to soybeans during imbibition. *Plant Physiology*, *61*, 525–529.

Broich, S. L., & Palmer, R. G. (1980). A cluster analysis of wild and domesticated soybean phenotypes. *Euphytica*, *29*, 23–32.

Chen, Y., Chen, P., & de los Reyes, B. G. (2006). Differential response of the cultivated and wild species of soybean to dehydration stress. *Crop Science*, *46*, 2041–2046.

Close, T., Fenton, R., & Moonan, F. (1993). A view of plant dehydrins using antibodies specific to the carboxy terminal peptide. *Plant Molecular Biology*, *23*, 279–286.

Dogras, C. C., Dilley, D. R., & Herner, R. C. (1977). Phospholipid biosynthesis and fatty acid content in relation to chilling injury during germination of seeds. *Plant Physiology*, *60*, 897–902.

Graether, S. P., & Boddington, K. F. (2014). Disorder and function: A review of the dehydrin protein family. *Frontiers in Plant Science*, *5*, 576.

Hume, D. J., & Jackson, A. K. H. (1981). Frost Tolerance in Soybean. *Crop Science*, *21*, 689–692.

Kaplan, R. S., & Pedersen, P. L. (1985). Determination of microgram quantities of protein in the presence of milligram levels of lipids with Amido Black 10B. *Analytical Biochemistry*, *150*, 97–104.

Laemmli, U. K. (1970). Cleavage of structural proteins during the assembly of the head of bacteriophage T4. *Nature*, *227*, 680–685.

Lam, H.-M., Xu, X., Liu, X., Chen, W., Yang, G., Wong, F.-L., … Zhang, G. (2010). Resequencing of 31 wild and cultivated soybean genomes identifies patterns of genetic diversity and selection. *Nature Genetics*, *42*, 1053–1059.

Li, Y.-H., Li, W., Zhang, C., Yang, L., Chang, R.-Z., Gaut, B. S., & Qiu, L.-J. (2010). Genetic diversity in domesticated soybean (*Glycine max*) and its wild progenitor (*Glycine soja*) for simple sequence repeat and single-nucleotide polymorphism loci. *New Phytologist*, *188*, 242–253.

Littlejohns, D. A., & Tanner, J. W. (1976). Preliminary studies on the cold tolerance of soybean seedlings. *Canadian Journal of Plant Science*, *56*, 371–375.

Luo, X., Bai, X., Zhu, D., Li, Y., Ji, W., Cai, H., … Zhu, Y. (2012). GsZFP1, a new Cys2/His2-type zinc-finger protein, is a positive regulator of plant tolerance to cold and drought stress. *Planta*, *235*, 1141–1155.

Luo, Q., Yu, B., & Liu, Y. (2005). Differential sensitivity to chloride and sodium ions in seedlings of *Glycine max* and *G. soja* under NaCl stress. *Journal of Plant Physiology*, *162*, 1003–1012.

Millar, A. A., & Kunst, L. (1999). The natural genetic variation of the fatty-acyl composition of seed oils in different ecotypes of *Arabidopsis thaliana*. *Phytochemistry*, *52*, 1029–1033.

Nylander, M., Svensson, J., Palva, E. T., & Welin, B. V. (2001). Stress-induced accumulation and tissue-specific localization of dehydrins in *Arabidopsis thaliana*. *Plant Molecular Biology*, *45*, 263–279.

Puhakainen, T., Hess, M. W., Mäkelä, P., Svensson, J., Heino, P., & Palva, E. T. (2004). Overexpression of multiple dehydrin genes enhances tolerance to freezing stress in Arabidopsis. *Plant Molecular Biology*, *54*, 743–753.

R Core Team (2013). *R: A language and environment for statistical computing*. Vienna, Austria: R Foundation for Statistical Computing. http://www.R-project.org/

Saitoh, K., Nishimura, K., & Kuroda, T. (2004). Characteristics of flowering and pod set in wild and cultivated types of soybean. *Plant Production Science*, *7*, 172–177.

Shibata, M., Takayama, K., Ujiie, A., Yamada, T., Abe, J., & Kitamura, K. (2008). Genetic relationship between lipid content and linolenic acid concentration in soybean seeds. *Breeding Science*, *58*, 361–366.

Song, W., Yang, R., Wu, T., Wu, C., Sun, S., Zhang, S., … Han, T. (2016). Analyzing the effects of climate factors on soybean protein, oil contents, and composition by extensive and high-density sampling in China. *Journal of Agricultural and Food Chemistry*, *64*, 4121–4130.

USDA-NASS (2014). 2012 Census of Agriculture Highlights, May 2014. USDA, www.agcensus.usda.gov

Yamasaki, Y., Koehler, G., Blacklock, B. J., & Randall, S. K. (2013). Dehydrin expression in soybean. *Plant Physiology and Biochemistry*, *70*, 213–220.

Yamasaki, Y., & Randall, S. K. (2016). Functionality of soybean CBF/DREB1 transcription factors. *Plant Science*, *246*, 80–90.

Yang, L., Wu, K., Gao, P., Liu, X., Li, G., & Wu, Z. (2014). GsLRPK, a novel cold-activated leucine-rich repeat receptor-like protein kinase from *Glycine soja*, is a positive regulator to cold stress tolerance. *Plant Science*, *215–216*, 19–28.

Zhang, L. X., Kyei-Boahen, S., Zhang, J., Zhang, M. H., Freelad, T. B., Watson, C. E., & Liu, X. (2007). Modifications of optimum adaptation zones for soybean maturity groups in the USA. *Online. Crop Management*, doi:10.1094/CM-2007-0927-01-RS.

How to cite this article: Robison J, Arora N, Yamasaki Y, et al. *Glycine max* and *Glycine soja* are capable of cold acclimation. *J Agro Crop Sci*. 2017;00:1–9. https://doi.org/10.1111/jac.12219

B. ROBISON ET AL., 2019

Robison, J. D., Y. Yamasaki, S. Randall, 2019. The ethylene signaling pathway negatively impacts CBF/DREB-regulated cold response in soybean *Glycine max*. Frontiers in Plant Science, 10:121.

See paper on next page.

frontiers in Plant Science

ORIGINAL RESEARCH
published: 12 February 2019
doi: 10.3389/fpls.2019.00121

The Ethylene Signaling Pathway Negatively Impacts CBF/DREB-Regulated Cold Response in Soybean (*Glycine max*)

*Jennifer D. Robison†, Yuji Yamasaki† and Stephen K. Randall**

Department of Biology, Indiana University–Purdue University Indianapolis, Indianapolis, IN, United States

OPEN ACCESS

Edited by:
Rudy Dolferus, Commonwealth Scientific and Industrial Research Organisation (CSIRO), Australia

Reviewed by:
Haitao Shi, Hainan University, China
Colleen J. Doherty, North Carolina State University, United States
Gabor Galiba, Centre for Agricultural Research (MTA), Hungary

***Correspondence:**
Stephen K. Randall
srandal@iupui.edu

†Present address:
Jennifer D. Robison, Niswander Department of Biology, Manchester University, North Manchester, IN, United States
Yuji Yamasaki, Arid Land Research Center, Tottori University, Tottori, Japan

Specialty section:
This article was submitted to Plant Abiotic Stress, a section of the journal Frontiers in Plant Science

Received: *15 October 2018*
Accepted: *24 January 2019*
Published: *12 February 2019*

Citation:
Robison JD, Yamasaki Y and Randall SK (2019) The Ethylene Signaling Pathway Negatively Impacts CBF/DREB-Regulated Cold Response in Soybean (Glycine max). Front. Plant Sci. 10:121. doi: 10.3389/fpls.2019.00121

During cold stress, soybean CBF/DREB1 transcript levels increase rapidly; however, expected downstream targets appear unresponsive. Here, we asked whether the ethylene signaling pathway, which is enhanced in the cold can negatively regulate the soybean CBF/DREB1 cold responsive pathway; thus contributing to the relatively poor cold tolerance of soybean. Inhibition of the ethylene signaling pathway resulted in a significant increase in *GmDREB1A;1* and *GmDREB1A;2* transcripts, while stimulation led to decreased *GmDREB1A;1* and *GmDREB1B;1* transcripts. A cold responsive reporter construct (*AtRD29A*$_{prom}$*::GFP/GUS*), as well as predicted downstream targets of soybean CBF/DREB1 [*Glyma.12g015100* (ADH), *Glyma.14g212200* (ubiquitin ligase), *Glyma.05g186700* (AP2), and *Glyma.19g014600* (CYP)] were impacted by the modulation of the ethylene signaling pathway. Photosynthetic parameters were affected by ethylene pathway stimulation, but only at control temperatures. Freezing tolerance (as measured by electrolyte leakage), free proline, and MDA; in both acclimated and non-acclimated plants were increased by silver nitrate but not by other ethylene pathway inhibitors. This work provides evidence that the ethylene signaling pathway, possibly through the action of EIN3, transcriptionally inhibits the CBF/DREB1 pathway in soybean.

Keywords: soybean, cold temperature, ethylene, proline, electrolytes, transcription factor, transcriptome, CBF/DREB

INTRODUCTION

Low temperature can be a limiting factor for plant growth and reproduction. Cold tolerant plants are able to modify gene expression resulting in higher survival rates during periods of low temperature (Gilmour et al., 1998; Thomashow, 1999). The most comprehensively studied cold responsive pathway is that regulated by the CBF/DREB1 (*C*-repeat responsive element *b*inding *f*actor/*d*ehydration-*r*esponsive *e*lement *b*inding factor) family of transcription factors (Liu et al., 1998; Thomashow, 1999; Park et al., 2015). These transcription factors contain an AP2-domain and bind the CRT/DRE (*C*-*r*epeat/*d*ehydration-*r*esponsive *e*lement) which has the core nucleotide sequence of CCGAC (Stockinger et al., 1997; Liu et al., 1998; Medina et al., 1999). Cold induction of CBF/DREB1 relies on the stabilization of the transcription factor ICE1 (*i*nducer of CBF *e*xpression 1) which activates CBF/DREB1 (Zarka et al., 2003). During normal temperatures, ICE1

is ubiquitinated by HOS1 (*h*igh expression of *os*motically responsive genes) and degraded by the 26S proteasome (Dong et al., 2006); however, in the cold ICE1 is sumoylated by the SUMO E3 ligase SIZ1 and phosphorylated by OST1 (*o*pen *st*omata 1) resulting in ICE1 stabilization and increased CBF/DREB1 expression (Miura et al., 2007; Ding et al., 2015). Cold stress induces significant upregulation of *AtCBF1*, *AtCBF2*, and *AtCBF3* (also known as *AtDREB1B*, *AtDREB1C*, *AtDREB1A*, respectively) within 15 min with maximal expression between 2 and 4 h (Gilmour et al., 1998). Downstream target transcripts containing CRT/DRE promoter elements significantly increase between 4 and 24 h later (Gilmour et al., 1998). Overexpression of *AtCBF1-3* in Arabidopsis leads to an increase of CRT/DRE containing transcripts and enhanced freezing survival (Jaglo-Ottosen et al., 1998). Conversely, when *CBF1-3* were knocked out via CRISPR/Cas9, Arabidopsis seedlings were hypersensitive to cold stress (Jia et al., 2016). *CBF/DREB1s* control 134 cold responsive genes (Jia et al., 2016), thus this regulon seems to be crucial to cold survival.

The exact mechanism by which the CBF regulon imparts cold tolerance remains incompletely characterized. However, metabolic changes resulting in the alteration of enzymes which combat oxidative damage, production of cryoprotective proteins, and changes in sugar content have all been reported (Steponkus et al., 1998; Cook et al., 2004; Gilmour et al., 2004; Kaplan et al., 2007; Hughes et al., 2013). Cold temperatures induce many physiological changes in plants, several of which are used to identify exposure or response to cold. During a period of cold temperatures, soluble sugars (Ristic and Ashworth, 1993) and free proline (Xin and Browse, 1998) accumulate in cold tolerant plants. Cold induces oxidative damage to lipids (O'Kane et al., 1996), which can be estimated by measuring the accumulation of malondialdehyde (MDA), an end product from the decomposition of lipid peroxidation (Janero, 1990). Photosynthesis is also disrupted by cold temperatures, exhibiting decreased electron transport rates, increased closed photosystem II (PSII) reaction centers, and decreased photosystem I (PSI) activity (Savitch et al., 2001).

Soybean (*Glycine max* [L.] Merr.) is an important agricultural species that is cold sensitive with severe tissue damage occurring near freezing temperatures and loss of vegetative growth below 6–7°C (Littlejohns and Tanner, 1976). Despite soybean's cold sensitivity it does have the capability to cold acclimate, though its response is diminished related to cold-tolerant species (Robison et al., 2017). Within the soybean genome, 7 *CBF/DREB1* homologs have been identified: *GmDREB1A;1, GmDREB1A;2, GmDREB1B;1, GmDREB1B;2, GmDREB1C;1, GmDREB1D;1, GmDREB1D;2* (Kidokoro et al., 2015; Yamasaki and Randall, 2016). During cold stress, transcripts for all seven homologs were significantly upregulated after 1 h and remained elevated at 24 h (Yamasaki and Randall, 2016). However, predicted downstream CRT/DRE containing targets were largely unaffected by cold stress (Yamasaki et al., 2013; Yamasaki and Randall, 2016). When *GmDREB1A;1* and *GmDREB1A;2* were constitutively expressed in Arabidopsis the native CRT/DRE containing genes were upregulated in the absence of cold stress (Yamasaki and Randall, 2016), and enhanced freezing tolerance was imparted; indicating that *GmDREB1* transcription factors are capable of inducing CRT/DRE containing genes.

Ethylene is a versatile phytohormone that regulates a wide range of developmental and environmental responses (Street and Schaller, 2016). In the absence of ethylene, *c*onstitutive *t*riple *r*esponse (CTR1), phosphorylates *e*thylene-*in*sensitive 2 (EIN2) so that it remains inactive. However, when ethylene binds to the endoplasmic reticulum-membrane bound *et*hylene *r*eceptors (ETR1), CTR1 is deactivated. This results in proteolytic cleavage of EIN2, a serine/threonine Raf-like kinase, and translocation of the C-terminal fragment to the nucleus where it stabilizes *e*thylene-*in*sensitive 3 (EIN3) so that it is no longer degraded by *E*IN3 *b*inding *F*actor (EBF1/2) SCF ligases (Gallie, 2015; Ju and Chang, 2015). EIN3 is a transcription factor that binds to the consensus sequence ATGYATNY found in the promoters of ethylene responsive genes (Konishi and Yanagisawa, 2008; Boutrot et al., 2010). Ethylene regulation has a varied impact on cold stress across, and even within species. EIN3 can negatively impact cold tolerance, as *EIN3* over-expression mutants have decreased freezing tolerance while *ein3* knockouts have an increased freezing tolerance (Shi et al., 2012). Conversely, it has also been noted that the ethylene overproducer Arabidopsis mutant *eto1-3* has enhanced freezing tolerance (Catalá and Salinas, 2015). Ethylene production has also been linked to increased cold tolerance in grapevine (Sun et al., 2016) and tomato (Ciardi et al., 1997), while ethylene decreased cold tolerance in *Medicago truncatula* (Zhao et al., 2014), Bermuda grass (Hu et al., 2016), and tobacco (Zhang and Huang, 2010). The wide variety of roles ethylene plays in cold tolerance throughout the plant kingdom requires each species to be evaluated individually.

The perception or biosynthesis of ethylene can be chemically modulated. Stimulation of the ethylene signaling pathway is often accomplished using 1-aminocyclopropane-1-carboxylic acid (ACC) or ethephon (2-Chloroethylphosphonic acid). ACC is the biological precursor to ethylene in the biosynthetic pathway via the action of ACC oxidase, while ethephon is an ethylene producing molecule (Wang et al., 2002). Aminoethoxyvinylglycine (AVG), 1-methylcyclopropene (1-MCP), and silver ionic compounds are commonly utilized to inhibit the ethylene pathway. AVG inhibits ACC synthase, the rate limiting enzyme in the ethylene biosynthesis pathway, which produces ACC (Street and Schaller, 2016). 1-MCP is a competitive inhibitor for ethylene receptors, and silver ions are known to replace the copper ion within the ethylene receptor active site preventing activation even if ethylene is bound (Schaller and Binder, 2017).

The ethylene response in soybean has been well characterized at the reproductive stages. During early soybean reproduction (stage R1), inhibition of ethylene signaling with silver thiosulfate (STS), an ethylene perception inhibitor, resulted in a 55.6% increase in seed yield while ethylene production by application of ethephon, decreased seed yield by 50% and increased floral abscission rates (Cheng, 2013). Manipulation of ethylene homeostasis has several impacts on other hormonal pathways of reproductive age soybeans. Ethephon and STS treatments had opposite effects on the signaling pathways of auxin, abscisic acid,

gibberellic acid, jasmonic acid, and salicylic acid (Cheng et al., 2013). Auxin, abscisic acid, and jasmonic acid signaling were increased with ethephon treatment, while gibberellic acid and salicylic acid signaling were stimulated by STS treatment (Cheng et al., 2013). Exposure to 1-MCP, an ethylene perception inhibitor, prior to heat stress resulted in increased chlorophyll content, photosynthetic efficiency, and decreased reactive oxygen species generation, and membrane damage compared to non-treated soybean (Djanaguiraman and Prasad, 2010). While much is known about ethylene signaling impacts in mature reproductive soybean, little information is available for the impact on younger soybean plants.

This study examines the role of ethylene regulation on the CBF/DREB1 cold stress pathway in soybean seedlings. First the physiological impact of ethylene signaling inhibitors in soybean seedlings was demonstrated and then the impact of manipulation of the ethylene pathway during cold treatment is examined.

MATERIALS AND METHODS

Plant Materials and Growth Conditions

Glycine max, c.v Williams 82 was used in all experiments. Plants were grown in soil (BX Mycorrhizae^{TM}, ProMix®) at 22°C under a long-day light cycle (16:8 light dark) with 180–200 μmol photon m^{-1} s^{-1}. Initiation of treatments in all experiments took place 4 h after the lights came on (Zeitgeber+4) with 10–12 day old seedlings that had fully unrolled unifoliate leaves, stage VC (Hanway and Thompson, 1967). Unifoliate leaves were utilized in all experiments.

Construction and Screening of Transgenic Plants Expressing $RD29A_{prom}$::GFP/GUS

The Arabidopsis *RD29A* promoter (1,477 bp upstream of the start codon) was analyzed with plantCARE to identify stress responsive motifs present (Lescot et al., 2002). The *AtRD29A* promoter was amplified from Arabidopsis and cloned into pCambia1304 driving mGFP/GUS using Zero Blunt® PCR Cloning Kit (ThermoFisher). The *AtRD29A*$_{prom}$::*GFP/GUS* was ligated into pTF101.1 using EcoR1 and BamHI sites and then was introduced into *Agrobacterium* (strain EHA101) and used to transform half-seed explants cv Williams 82 using the bar gene for selection (Paz et al., 2004). The transformation and recovery of transgenic soybeans was performed by the Iowa State University Plant Transformation Facility[1]. Three independently transformed lines were selfed in a greenhouse to achieve homozygous lines, which were identified by herbicide resistance using 0.1% glufosinate (Finale®, Bayer) application to the midrib (**Supplementary Figure S2**).

Soybean Ethylene Pathway Genes Homology and Expression

RNA-Seq data initially described in Yamasaki and Randall (2016) was examined for expression of ethylene pathway related genes. Briefly, in that experiment 10 day old soybean seedlings were exposed to 4°C for 0, 1, or 24 h prior to extraction of mRNA from unifoliate leaves. All treatments were performed in triplicate with $n \geq 6$ plants per replication. Three libraries were created from the replicates for a total of nine libraries. Reads were mapped and statistically evaluated as described in Yamasaki and Randall (2016). All data can be found on NCBI GEO (Accession # GSE117686). A GO analysis (Ashburner et al., 2000; Consortium, 2017) was utilized to identify ethylene genes regulated by cold treatment. The predicted protein sequences of these genes were retrieved from Soybase ver. 2.1 (Grant et al., 2010) for soybean, and TAIR (Lamesch et al., 2012) for Arabidopsis. Clustal Omega (Sievers et al., 2011) was utilized to compare protein sequence homology. A phylogenetic tree to visualize the similarities of predicted protein sequences of Arabidopsis and soybean genes was generated and annotated with a heatmap by utilizing Interactive Tree of Life (Letunic and Bork, 2016) visualizing the log2 fold change of transcripts measured in the RNA-Seq analysis for soybean and microarray data from 4°C treated aerial portions of Arabidopsis (Kilian et al., 2007).

Characterizing Ethylene Signaling Pathway Inhibition in Soybean Seedlings

The impact of silver nitrate on ethylene responsiveness in soybean cotyledons was characterized using a cut seedling/hydroponic feeding method (Curtis, 1981). Only **Figure 1** and **Supplementary Figure S1** utilized this hydroponic method. Briefly, seedlings were cut 8–10 cm from the apical bud and placed in a 15 mL plastic Falcon tube which had been cut at the 5 mL line. Tubes were filled daily with either 1.38 mM ethephon (Sigma) or water as a mock control. Leaves were sprayed until runoff daily with either 1 mM silver nitrate ($AgNO_3$, Fisher Scientific), 1 mM silver sulfate (Ag_2SO^4, Fisher Scientific), 50–300 ppm 1-Methylcyclopropene (1-MCP, AgroFresh) or water. Pre-treatment was accomplished by placing seedlings in tubes containing water and spraying with appropriate foliar sprays 24 h prior to being moved to new tubes containing either 1.38 mM ethephon or water. Cotyledon abscission was measured daily by counting the number of cotyledons that had fallen off after gentle agitation. Unifoliate leaves from individual plants were collected at various time points, frozen in liquid nitrogen, and stored at −80°C for later analysis.

Ethylene Pathway Manipulation During Cold Stress

Wildtype Williams 82 and transgenic *AtRD29A*$_{prom}$::*GFP/GUS* soybean lines (17-9, 22-23, and 28-5) were sprayed with 1 mM silver nitrate or mock control twice, 24 h before and immediately prior to transfer to 4°C. After 48 h in the cold, unifoliate leaves from 6 to 7 individual plants were collected for each replicate (18–21 total plants for three replicates for both mock and silver nitrate) and frozen in liquid nitrogen, then stored at −80°C for later analysis.

Transgenic line 22-23 seedlings of 14 days old were utilized for ethylene manipulation experiments. Seedling

[1]http://ptf.agron.iastate.edu/

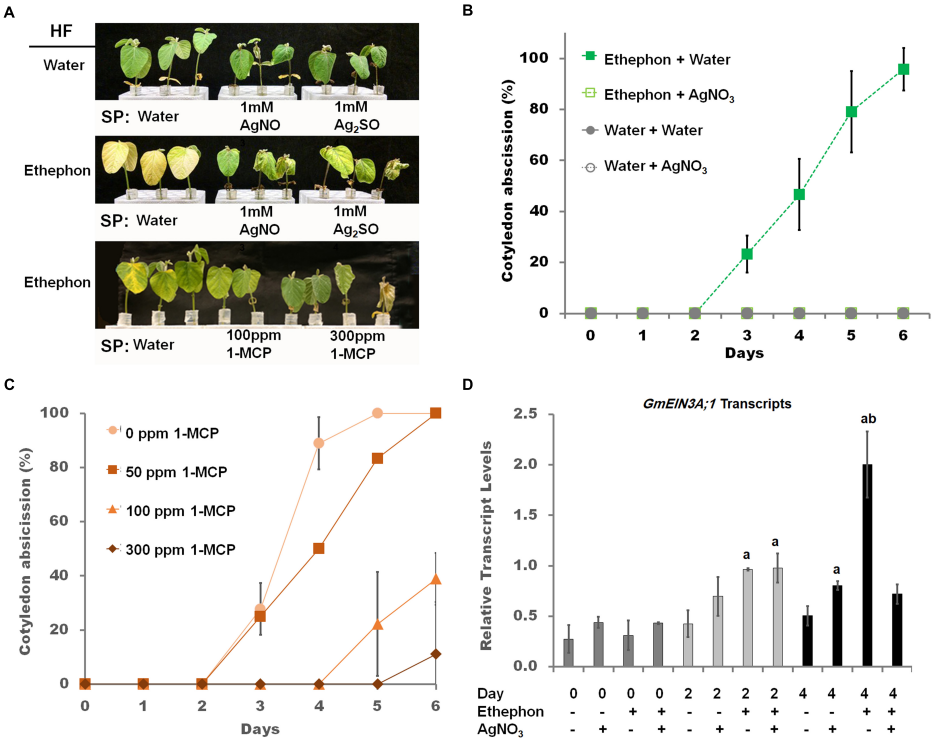

FIGURE 1 | The effect of the ethylene receptor inhibitors, silver cation and 1-MCP, on soybean seedlings. **(A)** Effect of ethylene pathway inhibitor [1 mM silver nitrate, 1 mM silver sulfate, and 100 ppm 1-MCP foliar sprays (SP)] on cut seedlings hydroponically fed (HF) water for the first 24 h then either water or 1.38 mM ethephon for six additional days. Image is representative of three independent experiments. **(B)** Cotyledon abscission for seedlings sprayed (SP) with either water (closed symbols) or 1 mM silver nitrate (open symbols) 1 day prior to exposure to HF 1.38 ethephon (squares) or HF water (triangles). Foliar sprays continued daily over the entire monitoring period. Starting at 3 days, cotyledon abscission in seedlings HF ethephon and SP water was significantly increased based on Student's *t*-test at the $p < 0.01$ level, which continued until the end of the monitoring period, $n = 9$. **(C)** Cotyledon abscission for seedlings sprayed with varying concentrations of 1-MCP starting 1 day prior to HF with 1.38 mM ethephon. Foliar sprays continued daily over the entire monitoring position, $n = 9$. **(D)** Transcript levels, determined by RT-qPCR, of *GmEIN3A;1* on days 0, 2, and 4 during 1 mM silver nitrate treatments from panel **(B)** and normalized to *GmACT11*. Two way ANOVA indicated significant impact of SP and HF along with an interaction between them at the $p < 0.01$ level (**Supplementary Table S3**). *Post-hoc* analysis (TukeyHSD) was used to compare samples, "a" indicates $p < 0.01$ comparing water (ethephon, $AgNO_3^-$) of the same day with the other treatments, $n = 3$ composed of a total of 12 plants. Error bars represent SD and those that are not visible are smaller than the symbol.

were sprayed with 1 mM silver nitrate, 100 ppm 1-MCP, 100 μM aminoethoxyvinylglycine (AVG, Sigma), 1 mM 1-Aminocyclopropane-1-carboxylic acid (ACC, Calbiochem), 1.38 mM ethephon or mock control at both 24 h and immediately prior to the start of cold treatment. Treatment concentrations for silver nitrate and 1-MCP were experimentally derived in this study, while AVG (Nukui et al., 2000), ACC (Zhang et al., 2010), and ethephon (Curtis, 1981) concentrations were obtained in the literature. Cold treatments were performed at 5°C for 48 h. The response of soybean to cold is for the plants to adopt a "sleep response" (unifoliate leaves folded down); **Supplementary Figure S3**. Time lapse photography (data not shown) showed this leaf movement response was initiated almost immediately following application of cold (only examined when cold was applied at $ZT = 4$) and was largely completed within 6 hours and was stable after that regardless of time of day or treatment until a return to control temperature. It should also be noted that silver treatment usually induced a red/purple coloration to the leaf veins and often resulted in leaf curling. The other treatments resulted in no significant differences compared to the cold control. Samples were flash-frozen in liquid nitrogen and then stored at −80°C until analysis.

Chlorophyll Content

Chlorophyll was measured using a modified Warren (2008) microplate method. Leaves were pulverized in liquid nitrogen and 0.07 g was extracted with 0.7 mL 100% cold methanol. The tube was vortexed vigorously, covered in foil, and rotated for 5 min at room temperature prior to centrifugation at 10,000 rpm at 5°C. The supernatant was then collected and saved at −20°C, while the pellet was re-extracted with 0.7 mL and both supernatants were combined before 200 μL was added to a microplate and read on SpectraMax M2® with PathCheck™ using a methanol cuvette reference (Molecular Devices). Chlorophyll *a* and *b* were calculated using the equations in Warren (2008).

Transcript Analysis

RNA was extracted via RNeasy® Plant Mini Kit (Qiagen Cat. No. 74903) and treated with DNase (Qiagen Cat. No. 79254) during extraction. The cDNA was synthesized from 500 ng of RNA using SuperScript® III First-Strand Synthesis using oligo$(dT)_{20}$ primer (Invitrogen Cat. No. 18080051). Transcript levels were quantified via RT-qPCR starting with 6.25 ng cDNA, 500 nM of each primer (**Supplementary Table S2**) and 10 μL Maxima SYBR® Green Master Mix (ThermoFisher) run on 7300 Real-Time PCR System (Applied Biosystems®) with a standard curve generated for each set of primers and normalized to either *GmACT11* or *GmUNK1* levels as described in Yamasaki and Randall (2016).

GUS Assay

The GUS activity assay was modified from Yoo et al. (2007) and Fior et al. (2009). Total protein content was determined via Bradford Assay (Bradford, 1976). To assess GUS activity levels, 10 μg of total protein was combined with 100 μL MUG (4-Methylumbelliferyl-β-D-glucuronide dehydrate) substrate [10 mM Tris-HCl (pH 8), 1 mM MUG, and 2 mM $MgCl_2$] in a black bottom 96 well plate. Fluorescence was measured every minute for 1 h at 37°C on a Spectramax M2® (Molecular Devices) with excitation at 360 nm and emission at 460 nm. GUS activity was calculated from the linear slope of the fluorescence readings in R (R Core Team, 2013).

Electrolyte Leakage

Six to eight replicates were tested for each variable with 3–4 leaf discs (1 cm diameter) randomly selected from all discs generated from 12 to 15 plants. Freezing was done in a glycerol bath (Brinkmann Lauda MGW RC 20) with temperatures starting at −1.0°C for 1 h at which time a single crystal of ice was added, and then lowered 0.5°C every 2 h until −4°C was reached then were maintained for another 2 h prior to overnight storage at 4°C. Three milliliters distilled water was added and vigorous shaking was applied for 6 h. Electrical conductivity was measured by a portable conductivity meter (Milwaukee Model MW301 EC meter). A subsequent freezing of the same samples at −80°C was used to determine 100% electrolyte leakage.

Lipid Peroxidation and Proline Levels

Lipid peroxidation was measured using the 2-thiobarbituric acid-reactive substances (TBARS) assay which measures MDA concentration (Sharmin et al., 2012). Briefly, 50 mg of soybean leaf tissue was homogenized with a motor powered pestle in 0.5 mL of 20% trichloroacetic acid, 0.01% butylated hydroxytoluene, and 0.65% 2-thiobarbituiric acid. The samples were heated at 95°C for 30 min before being put on ice for 2 min. After centrifugation at 3 kg for 10 min, samples were read at 440, 453, and 600 nm on a SpectraMax M2® microplate reader using PathCheck™ with cuvette reference (Molecular Devices). MDA concentration was calculated using the equations of Hodges et al. (1999) to adjust for sucrose interference.

Proline was measured by the ninhydrin method (Bates et al., 1973). Briefly, leaf tissue (50 mg) previously collected, flash-frozen in liquid nitrogen, and stored at −80°C was pulverized and then extracted with 15 volumes of ethanol:water (4:6) overnight at 4°C. The ninhydrin reagent (200 μL) was heated to 95°C with 100 μL of extract for 20 min. Following cooling and a centrifugal spin to remove particulates, the absorbance of a 200 μL aliquot was measured in a microplate reader at 520 nm. A standard curve was generated from 0 to 30 nmoles proline.

Photosynthetic Parameters

Chlorophyll *a* transient curves were measured using a Plant Efficiency Analyzer (Handy PEA, Hansatech). Fluorescence signal was recorded over 1 s of irradiation with an excitation light of 650 nm at 3,600 μmol m^{-1} s^{-1}. Unifoliate leaves were dark adapted for 10 min with the clips provided with the Handy PEA. Clips were placed on the right side of the midrib approximately halfway between the leaf tip and base. There were nine unifoliate leaves from nine individual plants recorded for each condition. Parameters were analyzed using the JIP test (Strasser et al., 2000).

Statistical Analysis

Two-way and one-way Analysis of Variance (ANOVA) with Tukey Honest Significant Difference *post-hoc* analysis were completed using R version 3.3.1 (R Core Team, 2013). Two-tailed Student's *t*-test was calculated in Excel (Microsoft, 2013).

RESULTS

Ethylene Responsiveness and Ethylene Pathway Inhibition in Soybean Seedlings

To measure ethylene responsiveness in soybean seedlings, several targets of ethylene, leaf senescence (Grbić and Bleecker, 1995), cotyledon abscission (Curtis, 1981), and chlorophyll degradation (Purvis and Barmore, 1981), were examined. In excised seedlings no abscission of the cotyledons occurred (**Figure 1A**, top row, **Figure 1B**). Hydroponic feeding (HF) of 1.38 mM ethephon, a bioconvertible precursor to ethylene (Murray et al., Hort sci, 1995), resulted in full cotyledon abscission and increased leaf yellowing. The concentration of ethephon used was the same as Curtis (1981). When ethylene binding inhibitors (1-MCP, silver nitrate, and silver

sulfate) were applied as foliar sprays (SP), both abscission and yellowing were diminished (**Figure 1A**, bottom two rows, **Figure 1B**). Seedlings sprayed with silver nitrate simultaneously with ethephon hydroponic feeding lead to a delay of abscission, inhibition of chlorophyll *a* loss, and a delayed reduction of *GmEIN3A;1* transcript levels (**Supplementary Figures S1A–C**). However, when silver nitrate treatment preceded ethephon by 1 day, cotyledon abscission was completely blocked (**Figure 1B**). Complete cotyledon abscission blockage was only achieved with 1 mM silver nitrate, only partial prevention of abscission was noted with 0.125, 0.5, or 0.175 mM silver nitrate (data not shown). To optimize foliar spray of 1-MCP concentrations, 50, 100, and 150 ppm were applied to ethephon hydroponically fed seedlings. Increasing concentrations of 1-MCP also increased the delay of cotyledon abscission (**Figure 1C**), 100 ppm was identified as the optimal concentration of 1-MCP (**Figure 1A** bottom row). At 4 days of treatments, when approximately 50% of cotyledons had abscissed in the ethephon treated plants; a marked impact on *GmEIN3A;1* transcript was observed. *GmEIN3A;1* transcripts were approximately four times that of the non-treated leaves and silver treatment reduced *GmEIN3A;1* levels to near control levels (1.4×, **Figure 1D**).

Changes in Ethylene Pathway Transcripts in Cold-Treated Soybeans

Several key ethylene signaling transcripts were significantly upregulated by cold (**Figure 2** and **Supplementary Table S1**). Five predicted homologs of *AtCTR* were identified in soybean, three of which (*Glyma.10g066000, Glyma.13g151100, Glyma.02g165800*) were downregulated

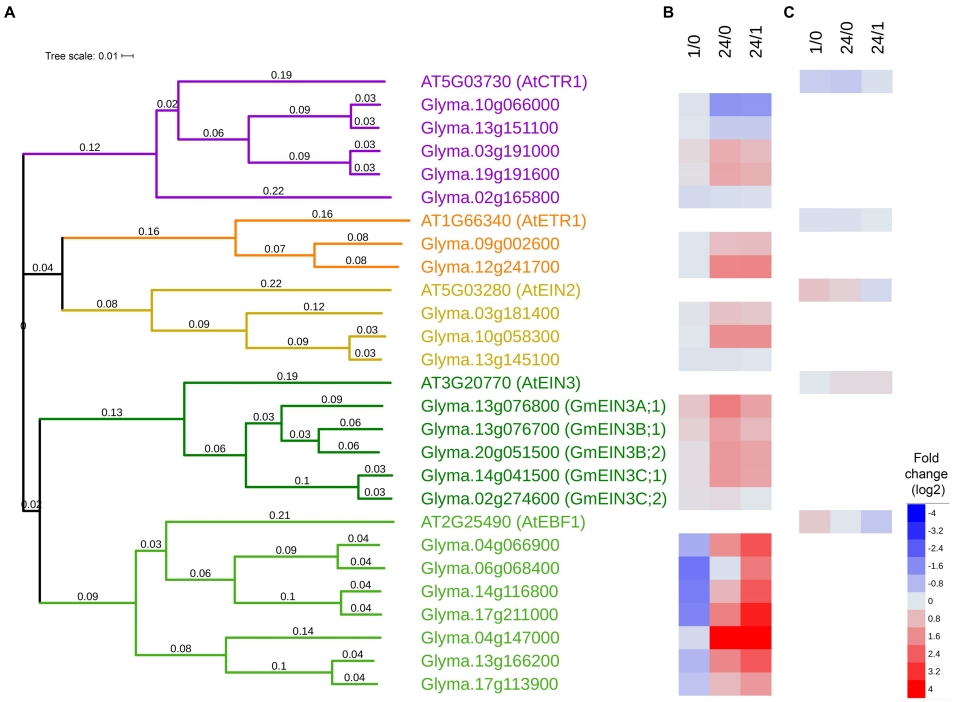

FIGURE 2 | Ethylene signaling pathway genes identified in RNA-Seq from cold treated soybean. **(A)** Phylogeny tree depicting predicted protein sequences from Arabidopsis [extracted from TAIR (Lamesch et al., 2012)] and soybean [extracted from Soybase (Grant et al., 2010; Severin et al., 2010)] homologs. The colorations on the tree reflect the protein classification with purple indicating serine/threonine-protein kinase, yellow/orange indicating membrane bound, and green indicating transcription factors. **(B)** Heatmap of log2 fold changes comparing soybean cold responses (4°C) 1 vs 0 h (1/0), 24 vs 0 h (24/0), and 24 vs 1 h (24/1) from RNA-Seq data (from Yamasaki and Randall, 2016) where blue indicates decreases and red indicates increases in comparison. The averaged read counts with SDs are in **Supplementary Table S1**. **(C)** Heatmap of log2 fold changes comparing cold responses (4°C) of the aerial portions of Arabidopsis 1 vs 0 h (1/0), 24 vs 0 h (24/0), and 24 vs 1 h (24/1) from microarray data from Kilian et al. (2007) where blue indicates decreases and red indicates increases in comparison.

and two (*Glyma.03g191000* and *Glyma.19g1916000*) were upregulated by 24 h of cold exposure. Two predicted homologs of the ethylene receptor *AtETR1* (*Glyma.09g002600* and *Glyma.12g241700*) were upregulated by 24 h of cold exposure. Of the three predicted *EIN2* homologs, two (*Glyma.03g181400, Glyma.10g058300*) were significantly increased at 24 h, where one (*Glyma13g20810*) remained unchanged. Of five predicted *EIN3* homologs, four (*Glyma.13g076800, Glyma.13g076700, Glyma.20g051500, Glyma.14g041500*) were accumulated greater than twofold after 24 h in the cold. The genes that increased in the cold were designated *GmEIN3A;1, GmEIN3B;1, GmEIN3B;2* and *GmEIN3C;1* while the one that did not increase Glyma.02g27460 was designated *GmEIN3C;2*. The significant increase of *GmEIN3* transcripts in cold treated soybean seedlings after 24 h (ranged from 2.5 to 3 fold in the three most responsive *GmEIN3* genes) is distinct from the modest effect in aerial portions of Arabidopsis (log2 0.2 or 1.2 fold; Kilian et al., 2007) or approximately 1.3 fold at 24 h in whole Arabidopsis seedlings (Shi et al., 2012). Additionally, of the seven predicted EBF1 homologs, four (*Glyma.04g066900, Glyma.06g068400, Glyma.14g116800, Glyma.17g211000*) were significantly decreased after 1 h of cold stress. After 24 h of cold exposure, six soybean *EBF* homologs were upregulated. The immediate activation of the ethylene signaling pathway in the cold is demonstrated by the upregulation of positive regulators (*EIN2* and *EIN3*) and the concomitant transient decrease of negative regulators (*EBF1*) of the pathway.

Manipulation of the Ethylene Signaling Pathway During Cold Stress

The abiotic stress reporter contains the GFP/GUS fusion protein driven by the native *AtRD29A* promoter which possesses three CRT/DRE elements, the binding site for CBF/DREB1, two abscisic acid responsive element (ABRE), one drought responsive MYB binding site (MBS) element, and two methyl-jasmonate wound responsive (CGTCA) motifs (**Figure 3A**; Sazegari et al., 2015). GUS activity varied approximately twofold among the three independent homozygous lines in the absence of stress (**Figure 3B**). GUS activity level increased in all three soybean transgenic lines during cold stress by fold 2.1, 6.4, 8.7 (line 17-9, 28-5, 22-23, respectively) after 2 days (**Figure 3B**). Pre-treatment with silver nitrate resulted in a 2.0, 3.5, 6.5 fold increase at 22°C indicating that silver nitrate alone is sufficient to upregulate the *AtRD29A* driven construct (**Figure 3B**). The addition of cold-treatment (4°C) to silver treated seedlings resulted in an additional increase (2.3, 2.4, 2.1 fold) in all lines (**Figure 3B**). To address specificity for the observed ethylene regulation of *AtRD29A*$_{prom}$*::GFP/GUS* expression, line 22-23 was further subjected to modulators of different specificity; inhibitors (1 μM AVG, 100 ppm 1-MCP) and stimulators (1.38 mM ethephon, 1 mM ACC) during cold stress (**Figure 3C**). Compared to cold stressed, mock treated soybean, treatment with ethylene inhibitors (AVG, 1-MCP, though not silver nitrate) significantly increased GUS activity (**Figure 3C**). This supports the hypothesis that the increase in GUS activity is due to release of ethylene inhibition of the cold response.

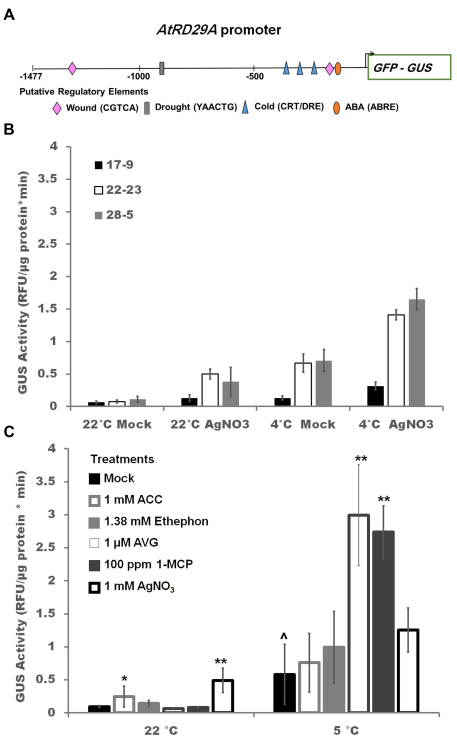

FIGURE 3 | Reporter response to ethylene pathway modulations **(A)** The *AtRD29A*$_{prom}$*::GFP/GUS* construct introduced into soybean with the major abiotic stress regulatory elements highlighted. **(B)** Effect of 1 mM silver nitrate treatment sprayed twice (–1 and 0 day) prior to exposure to cold or control temperatures for 2 days in three independent homozygous transgenic soybean lines. Two Way ANOVA showed an independent effect of temperature and treatment at $p < 0.001$ and combinatorial effect of treatment*temperature of $p < 0.01$ (**Supplementary Table S3**). **(C)** Effect of ethylene pathway stimulators (1 mM ACC, 1.38 mM ethephon) and inhibitors (1 μM AVG, 100 ppm 1-MCP, 1 mM $AgNO_3$) on GUS activity in transgenic soybean line ST164-22-23. One way ANOVA was performed for each temperature individually (**Supplementary Table S3**). *Post-hoc* analysis using TukeyHSD was performed comparing treatment with the mock from the same temperature, *$p < 0.05$, **$p < 0.01$. Comparison between cold treated and non-cold treated mocks was done using Student's *t*-test, ^$p < 0.05$. $n = 3$ composed of a total of 12 plants.

RNA-Seq analysis of soybean *GmEIN3s* indicated differential regulation of the various *GmEIN3* transcripts in the cold (**Figure 2**). Only *GmEIN3A;1, GmEIN3B;1, GmEIN3B;2* and *GmEIN3C;1* were cold induced and within those *GmEIN3A;1* had the highest cold induction of 3.6 fold after 24 h (**Supplementary Table S1**). Three cold inducible *GmEIN3s* were validated by RT-qPCR (**Figure 4**). In the cold, *GmEIN3A;1* transcripts

were increased by ethylene pathway stimulation and trended downward with ethylene pathway inhibition, though only silver nitrate treatment was significantly decreased (**Figure 4**). Conversely, *GmEIN3B;1* transcript levels were decreased by ethylene pathway stimulation in the cold, while *GmEIN3C;1* was unaffected by any ethylene pathway manipulation (**Figure 4**). A downstream target of EIN3, E*RF056* (*Glyma.15g15200*) which possesses an consensus EIN3 binding site at −976 bp, was not cold induced, but was increased significantly with ACC treatment (**Figure 4**).

Cold responsive *GmCBF/DREB1* transcripts are strongly, but transiently, accumulated in response to cold, generally declining after 10 h of cold onset, and reaching a more constant but still increased level, compared to non-cold treated plants, after several days (Yamasaki and Randall, 2016). Despite this rapid reaction, soybean does not attain significant cold tolerance until after 2 days of cold and approaches a maximum acclimation after 7 days (Robison et al., 2017). Therefore, it was decided to examine the various molecular and physiological responses at 2 days post cold treatment, especially since at least 3 days (starting with 1 day before onset of cold treatment) of silver nitrate treatment was required to impact cotyledon abscission and decreased *GmEIN3A;1* transcripts (**Figures 1B,D** and **Supplementary Figure S1C**). Transcript levels of the *GmCBF/DREB1* family were measured 2 days after cold with stimulation or inhibition of the ethylene signaling pathway (**Figure 5**). *GmDREB1A;1*, *GmDREB1A;2* and *GmDREB1B;1* were significantly cold induced after 2 days in the cold while *GmDREB1B;2* was not. *GmDREB1A:1* had the greatest (sustained) fold-increase after 2 days in the cold, as well as the most abundant transcript at 0, 1, and 24 h based on RNA-Seq (**Supplementary Table S1**) and total transcript copy number based on RT-qPCR (Yamasaki and Randall, 2016). The promoters of *GmDREB1A;1*, *GmDREB1B;1* and *GmDREB1B;2* had predicted EIN3 promoter elements (yellow stars, **Figure 5**). In the cold, ethylene pathway stimulation decreased *GmDREB1A;1* transcript levels, while ethylene pathway inhibition increased transcript levels (**Figure 5**). In the cold, *GmDREB1A;2* transcripts were

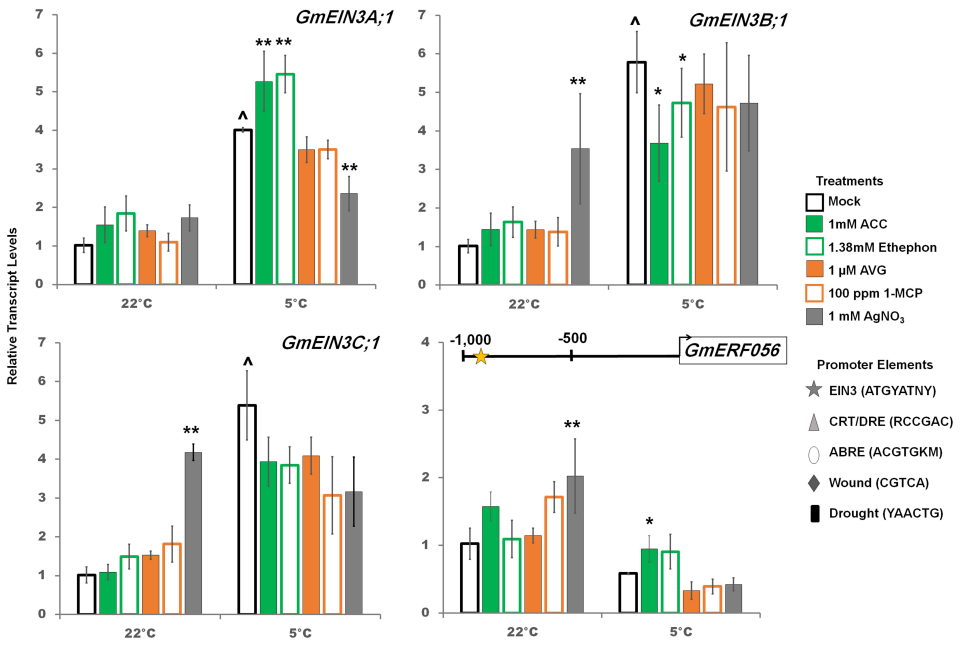

FIGURE 4 | RT-qPCR analysis of transcript levels of *GmEIN3A;1*, *GmEIN3B;1* and *GmEIN3C;1*; as well as a predicted downstream target of EIN3, *GmERF056*, with ethylene pathway stimulation (1 mM ACC, 1.38 mM ethephon) or inhibition (1 µM AVG, 100 ppm 1-MCP, 1 mM $AgNO_3$) after 2 days at either control or cold temperatures. Transcripts normalized to *GmUNK1* transcript levels. Position of the consensus EIN3 binding elements present in the promoter of *GmERF056* is displayed above the graph. All promoters depicted in **Figures 4–6** were examined for the consensus binding elements shown. Error bars represent SD. One way ANOVA was performed for each temperature individually (**Supplementary Table S3**). *Post-hoc* analysis using TukeyHSD was performed comparing treatment with the mock from the same temperature, $*p < 0.05$, $**p < 0.01$. Comparison between cold treated and non-cold treated mocks was done using Student's *t*-test, $\hat{}p < 0.05$. $n = 3$ composed of a total of 18–21 plants.

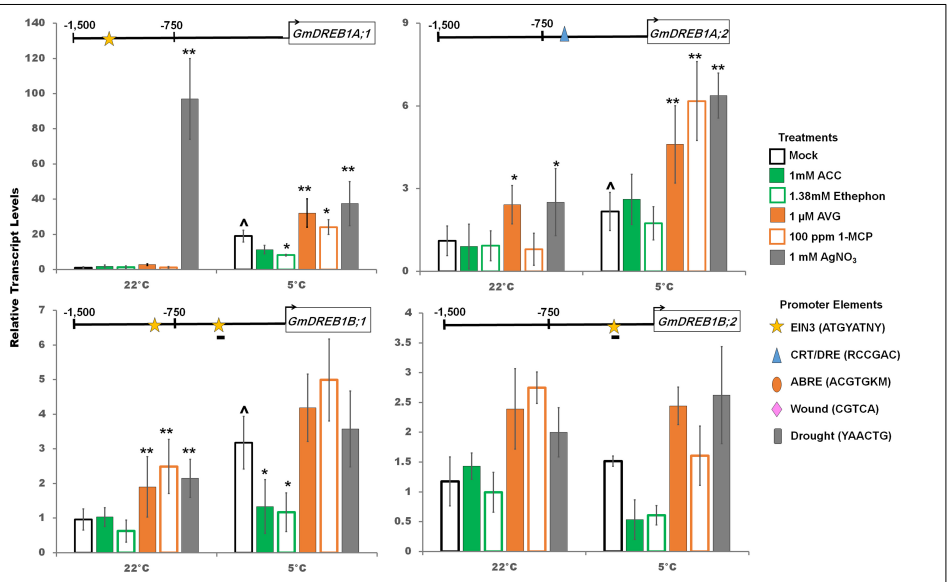

FIGURE 5 | Changes in transcript levels (RT-qPCR) of *GmDREB1A;1*, *GmDREB1A;2*, *GmDREB1B;1* and *GmDREB1B;2* by ethylene pathway stimulators (1 mM ACC, 1.38 mM ethephon) or inhibitors(1 µM AVG, 100 ppm 1-MCP, 1 mM $AgNO_3$) after 2 days at either control or cold temperatures. Transcripts normalized to *GmUNK1* transcript levels. All promoters depicted in **Figures 4–6** were examined for the consensus binding elements shown. Binding elements present in promoters displayed above the graph of each transcript. A line beneath the motif symbol indicates the motif is found on the reverse strand. Error bars represent SD. One way ANOVA was performed for each temperature individually (**Supplementary Table S3**). *Post-hoc* analysis using TukeyHSD was performed comparing treatment with the mock from the same temperature, $*p < 0.05$, $**p < 0.01$. Comparison between cold treated and non-cold treated mocks was done using Student's *t*-test, $\hat{}p < 0.05$. $n = 3$ composed of a total of 18–21 plants.

increased with ethylene pathway inhibition despite the lack of obvious EIN3 binding sequences in the promoter (**Figure 5**). However, *GmDREB1A;2* does contain a predicted CRT/DRE promoter element (blue triangle) and may be responding to the increasing *GmDREB1A;1* transcript levels (**Figure 5**). In the cold, *GmDREB1B;1* and *GmDREB1B;2* tended to decrease with ethylene pathway stimulation and increase with ethylene pathway inhibition; however, not always statistically significant at the 0.05% level (**Figure 5**).

Predicted downstream targets of *GmCBF/DREB1* were examined. Two alcohol dehydrogenase (ADH1) like soybean genes, one containing a predicted CRT/DRE promoter element (*Glyma.12g015100*) and one without (*Glyma.12g015300*) were compared as ADH is thought to play an important role in cold and freezing tolerance (Song et al., 2016). *Glyma.12g015100* transcripts were cold induced, as expected due to presence of CRT/DRE in the promoter, and treatment with ethylene pathway stimulators decreased transcript levels to non-cold treated levels. However, there was no increase when treated with ethylene pathway inhibitors (**Figure 6**). Though not cold-induced *Glyma.12g015300* was impacted by ethylene pathway manipulation, possibly due to interactions at one or more of two drought, one ABRE, and one EIN3 binding motifs predicted.

Three additional potential targets of the CBF/DREB1s, annotated as a ubiquitin ligase (Glyma.14g212200), an AP2-like transcription factor (*Glyma.05g186700*), and *GmCYP82A3* (*Glyma.19g041600*), a cytochrome P450 (Yan et al., 2016), were strongly accumulated in response to the cold (**Figure 6** and **Supplementary Table S1**). Furthermore, transcript levels of all three significantly decreased when treated with ethylene stimulator treatment in the cold (**Figure 6**). Interestingly, *GmCYP82A3* transcript levels decreased with both ethylene stimulation and inhibition compared to the cold control. The promoter for this gene, in addition to the CRT/DRE, also includes three EIN3 binding elements and a wound response element, suggesting this complex response could be due to crosstalk between these pathways (**Figure 6**).

Impact of Ethylene Pathway Modulators on Freezing Tolerance, Oxidation, Proline Levels, and Photosynthesis

The finding that the *GmDREB1A;1* and *GmDREB1A;2* transcripts increased in the presence of silver nitrate during

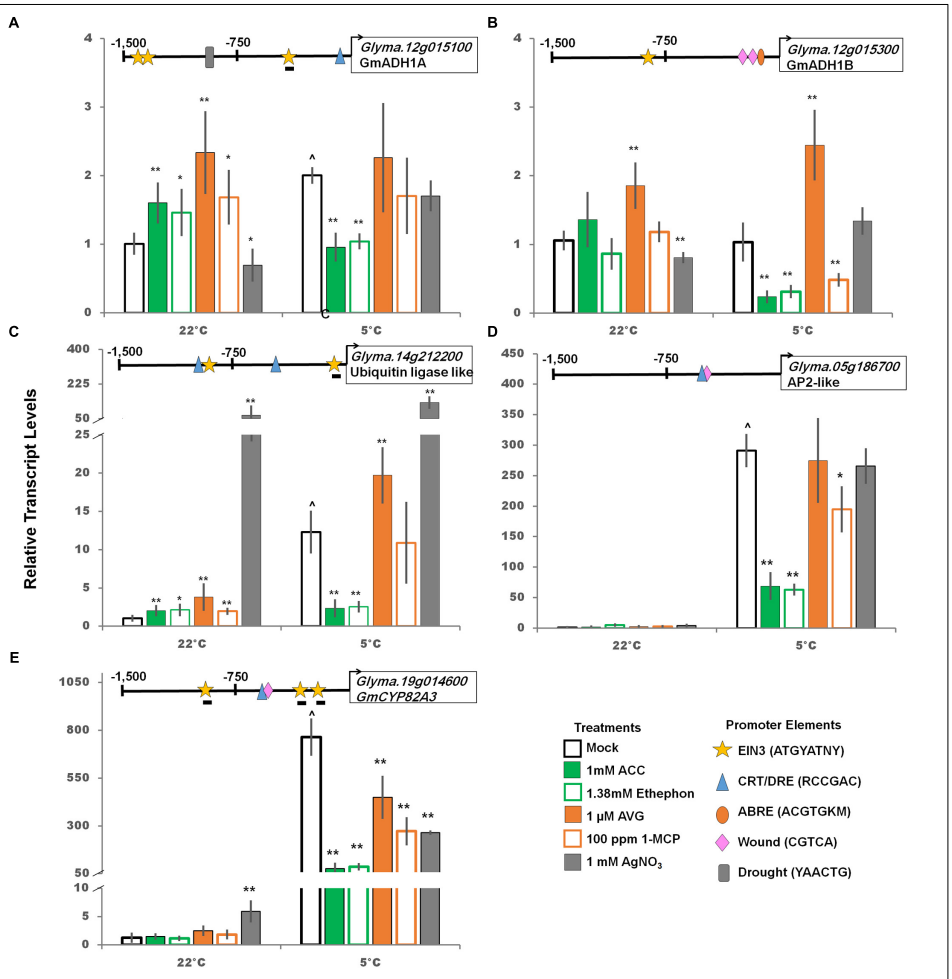

FIGURE 6 | Impact of ethylene pathway stimulation and inhibition on transcript levels of cold responsive genes (panels **A-E**, *GmADH1A*, *GmADH1B*, ubiquitin ligase-like, AP2-like, and *GmCYP82A3*; respectively) after 2 days at either control or cold temperatures measured via qRT-PCR and normalized to *GmUNK1*. All promoters depicted in **Figures 4–6** were examined for the consensus transcription factor binding elements shown. Binding elements present in promoters displayed above the graph of each transcript. A line beneath the motif symbol indicate the motif is found on the reverse strand. Error bars represent SD. One way ANOVA was performed for each temperature individually (**Supplementary Table S3**). *Post-hoc* analysis using TukeyHSD was performed comparing treatment with the mock from the same temperature, $*p < 0.05$, $**p < 0.01$. Comparison between cold treated and non-cold treated mocks was done using Student's *t*-test, $\hat{}p < 0.05$. $n = 3$ composed of a total of 18–21 plants.

cold treatment (**Figure 4**); suggested that silver nitrate treatment might enhance cold tolerance. After 2 days, non-acclimated silver nitrate treated plants had significantly better freezing tolerance between −1.5 and −3.5°C; and cold acclimated plants demonstrated a lesser though significant, impact. The LT50 for non-acclimated plants was −1.7 and −1.9°C (with and without silver nitrate, respectively) and −2.7 and −2.9°C for cold acclimated plants (**Figure 7A**). Electrolyte

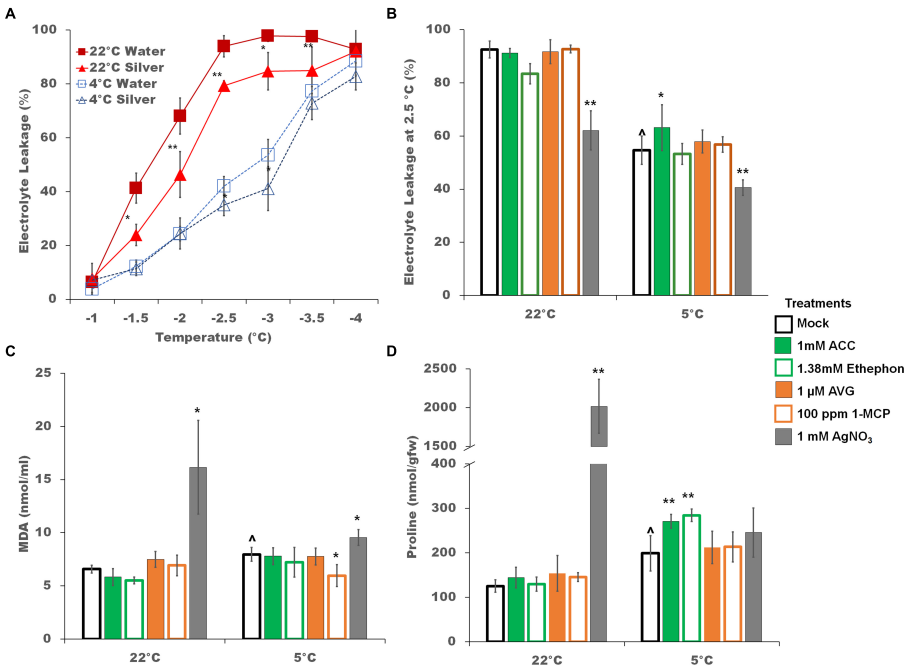

FIGURE 7 | Physiological responses to ethylene pathway manipulation during cold stress. **(A)** Freezing tolerance of soybean seedlings treated with silver nitrate (triangles) or mock controls (squares) as measured by electrolyte leakage across a range of freezing temperatures after 2 days of either control (22°C, red lines) or cold (5°C, blue lines) temperatures. **(B)** Freezing tolerance at –2.5°C of soybean seedlings during ethylene pathway stimulation or inhibition. **(C)** MDA levels of soybean seedlings during ethylene pathway stimulation or inhibition. **(D)** Free proline levels of soybean seedlings during ethylene pathway stimulation or inhibition. Error bars represent SD and non-visible error bars are smaller than the symbol. One way ANOVA was performed for each temperature individually (**Supplementary Table S3**). *Post-hoc* analysis using TukeyHSD was performed comparing treatment with the mock from the same temperature, $*p < 0.05$, $**p < 0.01$. Comparison between cold treated and non-cold treated mocks was done using Student's *t*-test, $\hat{}p < 0.05$. $n = 3$ composed of a total of 18–21 plants.

leakage at −2.5°C was tested for all ethylene pathway stimulators and inhibitors, and their impact was found to be minimal.

Oxidation of membrane lipids is a common environmental damage, typically assessed by measuring changes in MDA levels (Hodges et al., 1999). In soybean seedlings, MDA content was cold induced (**Figure 7C**). Overall, ethylene signaling pathway manipulation had no strong additional effect on lipid oxidation in cold treated plants (**Figure 7C**). At 22°C, silver nitrate induced significantly higher MDA levels (**Figure 7C**). Increases in free proline is also associated with cold tolerance in plants (Ashraf and Foolad, 2007). Increases in proline levels were cold-induced (**Figure 7D**). Ethylene pathway stimulators resulted in a further increase in free proline content, while ethylene pathway inhibitors had little effect. Interestingly, silver nitrate treatment resulted in a substantial increase in proline levels under control conditions, but not in the cold.

Manipulation of the ethylene signaling pathway altered PSII photochemistry, and the effect was more pronounced at control temperatures. Chlorophyll *a* content was not affected by a 2 days cold treatment. However, chlorophyll *a* content was reduced at both control and cold temperatures by ethylene pathway stimulators (**Figure 8A**). A 22°C, ethylene pathway stimulation lowered the quantum photosynthetic efficiency of PSII (F_v/F_m), while ethylene pathway inhibition resulted in a significant increase in F_v/F_m indicating that ethylene depresses the efficiency of Q_A reduction by captured photons (**Figure 8B**). In the cold, any manipulation of the ethylene pathway resulted in significantly lower F_v/F_m (**Figure 8B**). Time resolved transient chlorophyll *a* fluorescent curves (O-J-I-P) can be utilized to dissect the electron flow through the photosystems as each point has been correlated to a physiological state (Strasser and Srivastava, 1995). In dark adapted conditions, all PSII reaction centers are considered open, i.e., capable of accepting excited

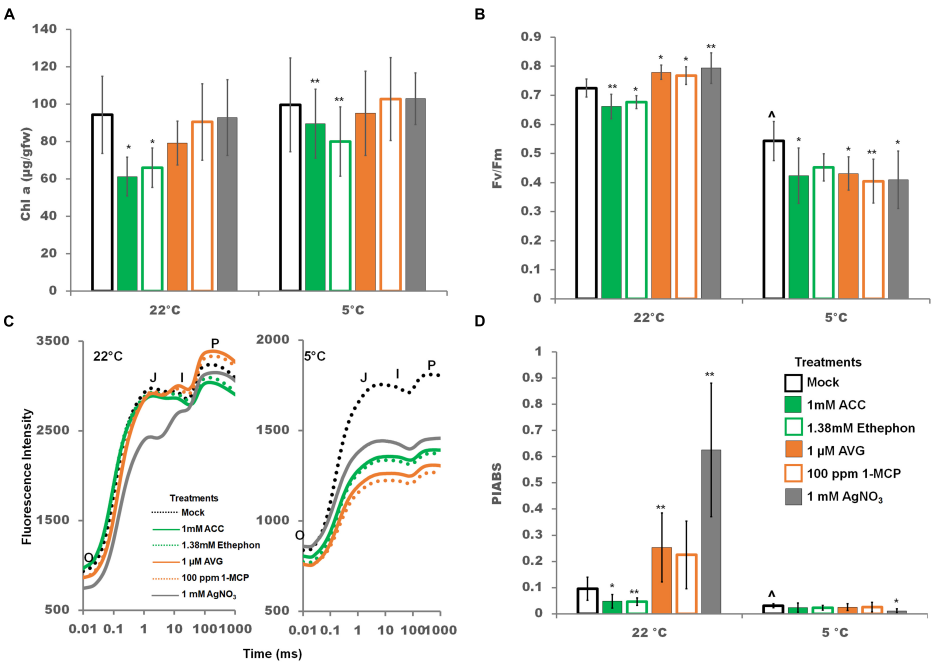

FIGURE 8 | Effects of ethylene pathway manipulation on chlorophyll *a* content and PSII chlorophyll fluorescence parameters. **(A)** Chlorophyll *a* content after 2 days of either control or cold temperatures combined with foliar sprays. **(B)** Quantum yield of photosystem II (F_v/F_m) after 2 days of either control or cold temperatures combined with foliar sprays. **(C)** Transient chlorophyll fluorescence (Kautsky curve) plotted on a logarithmic time axis after 2 days of either control or cold temperatures combined with foliar sprays. Averages are represented without error bars for clarity of the graph. **(D)** The Performance Index (PI_{ABS}) is a parameter indicating the functionality and capacity of energy capture from PSII through to reduction of PSI. Error bars represent SD. One way ANOVA was performed for each temperature individually (**Supplementary Table S3**). *Post-hoc* analysis using TukeyHSD was performed comparing treatment with the mock from the same temperature, $*p < 0.05$, $**p < 0.01$. Comparison between cold treated and non-cold treated mocks was done using Student's *t*-test, $\hat{}p < 0.05$. $n = 9$.

electrons, at point O, and closed, i.e., completely reduced and incapable of accepting excited electrons, at point P. Briefly O-J relates to the reduction of Q_A to Q_A^-, J-I the reduction of Q_B to Q_B^{2-}, and I-P the reduction of the PQ pool and electron flow into PSI (Zhu et al., 2005; Boisvert et al., 2006). In the cold, chlorophyll fluorescence transient curves were lower at all states (O, J, I, P) and flattened at the J peak to P peak suggesting disruption in the electron flow from Q_A to Q_B and beyond (**Figure 8C**).

At control temperatures, the performance index of photochemistry (PI_{ABS}), a structural and functional parameter representing the overall efficiency and capacity of light-dependent photosynthesis, was increased by ethylene pathway inhibition and generally decreased by stimulation (**Figure 8D**). PI_{ABS} was strongly decreased in the cold. Only silver nitrate treatment resulted in an additional and significant decrease during cold treatment (**Figure 8D**). These data suggest that ethylene pathway stimulation at control temperatures, cold temperatures, and silver nitrate in the cold all negatively impact overall PSII activity.

Decreases in light dependent photosynthesis functionality and efficiency were noted with ethylene stimulation at control temperatures, cold treatment, and ethylene pathway manipulation in the cold, particularly silver nitrate treatment. Theses decrease are likely being driven by a decrease in PQ pool size limiting electron flow from PSII to PSI as indicated by the shape of the OJIP curve (**Figure 8C**).

DISCUSSION

Soybean Responds Physiologically to Ethylene

The phytohormone ethylene is involved the regulation of many growth and developmental pathways in plants, including senescence and leaf abscission (Grbić and Bleecker, 1995).

Accelerated cotyledon abscission was blocked by ethylene pathway inhibitors (silver nitrate and 1-MCP). Likewise the enhanced yellowing of unifoliates caused by ethephon was reduced in presence of silver ions, showing that soybean seedlings respond to ethylene stimulation of senescence and leaf abscission similarly to other plants (Beyer, 1976; Curtis, 1981; Joyce et al., 1990).

Ethylene and Cold Pathway Crosstalk in Soybean

Ethylene treatment enhances cold tolerance in grapevine (Sun et al., 2016), tomato (Zhang and Huang, 2010), and peanut (Zhang et al., 2016), while in *M. truncatula* (Zhao et al., 2014), Bermuda grass (Hu et al., 2016), and Arabidopsis (Shi et al., 2012) ethylene treatment decreases cold tolerance. The interaction between ethylene and cold in Arabidopsis has been suggested, in the absence of a significant transcriptional response, to be mediated by a cold-stabilized EIN3 protein, which binds to the promoter of *CBF3* preventing its transcription (Shi et al., 2012). In contrast, in soybean, the ethylene signaling pathway is strongly cold-activated, resulting in accumulation of *GmEIN2* and *GmEIN3* transcripts (as well as down regulation of *GmEBF* transcripts), which ultimately results in a decrease in *GmDREB1* transcript levels. Distinctive from the Arabidopsis response (Shi et al., 2012), in soybean this decrease of a key transcription factor in the cold signaling pathway, has little to no impact on cold tolerance in soybean. While silver ions impact both *GmDREB1* transcript levels and freezing tolerance, silver is likely not exerting cold stress enhancement through the ethylene pathway as the more specific ethylene pathway inhibitors, 1-MCP and AVG, have no impact on freezing tolerance despite their strong (and similar to silver) impact on the *GmDREB1* transcripts. As suggested below in the conclusions, silver ions may be enhancing cold tolerance by an alternative mechanism, possibly by induction of an antioxidative response. While the crosstalk between cold and ethylene signaling in soybean shares some similarity with Arabidopsis, the impact on cold tolerance is much different; suggestive that the soybean cold tolerance may not be limited by the CBF/DREB1 cold response.

A putative EIN3 binding motif is present in the promoter of *GmDREB1A:1*, while two EIN3 binding motifs are predicted in *GmDREB1B;1* (**Figure 5**) suggesting that regulation by GmEIN3s is possible; consistent with the ethylene regulation observed. However, further biochemical studies must be done to demonstrate that GmEIN3A;1 indeed binds to the promoter of *GmDREB1A;1* and *GmDREB1B;1* as predicted. Interestingly, transcripts of *GmDREB1A;2*, which does not possess an obvious EIN3 binding motif, still increased under ethylene inhibition (**Figure 5**). Closer examination of the *GmDREB1A;2* promoter region revealed a CRT/DRE-like motif (Baker et al., 1994) suggesting that *GmDREB1A;1* could be regulating *GmDREB1A;2*.

Downstream Targets of GmDREB1s Are Cold Regulated and Ethylene Responsive

All four predicted downstream targets of CBF/DREB1s containing putative CRT/DRE were strongly cold-induced and three were also down-regulated by ethylene pathway stimulation. Only one, ubiquitin ligase, *Glyma.14g212200*, increased following ethylene pathway inhibition (**Figure 6**). Of the four potential CBF/DREB1 targets, *Glyma.14g212200* was the only transcript with multiple CRT/DRE motifs present in the promoter, which may explain the further enhancement of cold induction with ethylene inhibition (**Figure 6**). Further studies would be required to determine the mechanism of this regulation.

GmCYP82A3 (*Glyma.19g014600*), a homolog of the Arabidopsis cytochrome P450 enzyme AtCYP82C (AT4G31940), has been shown to increase in response to iron deficiency and is regulated by the circadian clock (Murgia et al., 2011). In soybean, *GmCYP82A3* transcripts are upregulated by salt and methyl jasmonate, decreased by drought and salicylic acid, and transiently upregulated by ethylene treatment (Yan et al., 2016). In this study, the massive cold induction of *GmCYP823A* is significantly reduced by any ethylene pathway manipulations, both stimulation and inhibition (**Figure 6**). The promoter of *GmCYP82A3* contains three predicted EIN3 like binding motifs (−148, −284, −1,093 bp) located on the non-coding strand. Each of these EIN3 like binding motifs lack the final 3′ nucleotide found in the consensus AtEIN3 binding motif, ATGYATNY (Konishi and Yanagisawa, 2008; Boutrot et al., 2010) such that these motifs are ATGTATTA, ATGTATGA, ATGTATAG, respectively. The complexity of this response may be explained by *GmCYP82A3* involvement in many abiotic and biotic stress responses and the regulation by these elements.

Two ADH like transcripts were evaluated in this study; only the one with a predicted CRT/DRE present in the promoter (*Glyma.12g015100*) was cold up regulated (**Figure 6**). In the cold, ethylene pathway activation resulted in a significant decrease for both transcripts; while ethylene pathway inhibition only impacted *Glyma.12g015300*.

Physiological of Soybean Response to Cold and the Impact of Ethylene Modulators

Soybean is minimally capable of acquiring cold tolerance (Robison et al., 2017). Evidence for increased cold tolerance include decreased electrolyte leakage (Simon, 1974) and increased proline levels (Gilmour et al., 2000). Ethylene pathway inhibition results in an increase in electrolyte leakage in grapevine (Sun et al., 2016) and tomato (Zhang and Huang, 2010) and a decrease in Arabidopsis (Shi et al., 2012), *M. truncatula* (Zhao et al., 2014), and Bermuda grass (Hu et al., 2016). In this study, electrolyte leakage was only significantly improved by treatment with silver nitrate but not other ethylene inhibitors (**Figures 7A,B**), though both AVG and silver nitrate have been implicated in improving freezing tolerance in the previously mentioned studies. This correlates well with the large singular impact of silver (other ethylene pathway inhibitors had no effect) on the increase in *GmDREB1A;1* transcripts at 22°C and in the massive increase in proline levels. This suggests that the improvement in electrolyte leakage in soybean may have more to do with increases in ROS

or other off target effects of silver ion rather than the ethylene signaling pathway.

As MDA is the final product of lipid oxidation (Leshem, 1987), it is often utilized as a proxy for general oxidative damage within plants (Jouve et al., 1993). Ethylene pathway inhibition increases MDA content during heat stress in reproductive soybean (Djanaguiraman et al., 2011). In Bermuda grass, in which ethylene negatively regulates the cold pathway, MDA content increases with ACC treatment and decreases with silver nitrate treatment (Hu et al., 2016). In this study, only 1-MCP resulted in a significant decrease in MDA; with silver nitrate doing the opposite (**Figure 7C**). In previous studies, transient increases in reactive oxygen species have been suggested to provide abiotic and biotic stress protection (Torres and Dangl, 2005; Suzuki and Mittler, 2006). Low levels of silver causes an increase of super oxide radicals, MDA content and proline levels, as well as increases in superoxide dismutase, peroxidase, and catalase activity; while higher levels decreased antioxidant enzymatic activity and oxygen radicals increased (Qin et al., 2005). The high level of silver used in the present study suggests a significant impact on reactive oxygen species generation.

Proline can play a protective role by stabilizing membranes, buffering redox potential, and as a protein chaperone (Hayat et al., 2012). In this study, proline levels increased slightly with cold. Treatments with 1-MCP and silver nitrate significantly increased proline content at control temperatures, while in the cold ACC and ethephon significantly increased proline content (**Figure 7D**).

Photosynthetic Response to Cold and Ethylene

Cold stress can lead to a decrease in the rate and efficiency of photosynthesis (Savitch et al., 2001; Tambussi et al., 2004; Ensminger et al., 2006). Chilling and cold stress effects on soybean photosynthesis have been examined only in late vegetative and reproductive stages (Van Heerden and Kruger, 2000; Van Heerden et al., 2003; Tambussi et al., 2004; Manafi et al., 2015) not in early vegetative stages such as seedlings. In reproductive soybean cold stress (8–9°C) for a 9 h dark period resulted in a decrease in overall light-dependent photosynthesis due to an uneven balance between photon trapping and electron transport from Q_A to PSI (Van Heerden and Kruger, 2000; Van Heerden and Krüger, 2002). Data on young seedlings presented here also suggests that light-dependent photosynthesis decreases during extensive cold stress (2 days, 5°C) in seedlings due to an uneven balance between photon trapping and energy transport. This is likely due to a decrease in the PQ pool size in this study leading to less electron transport through the photosystems.

Interestingly, in the cold only silver nitrate treatment significantly impacted PI_{ABS}, a structural and functional parameter representing the overall efficiency and capacity of light-dependent photosynthesis. PI_{ABS} was decreased 0.36 fold by silver nitrate treatment indicating that overall silver nitrate is more damaging than any other treatment utilized in this study to light dependent photosynthesis (**Figure 8D**). As silver nitrate treatment also resulted in a significant increase in MDA content (**Figure 7C**) it is reasonable to suggest that increased reactive oxygen species are generated by silver nitrate treatment. As photosystem II repair is very sensitive to reactive oxygen species (Nishiyama et al., 2011), we suggest that generation of reactive oxygen species by silver nitrate leads to the further decrease in PI_{ABS} in cold stress soybean seedlings.

Overall, light-dependent photosynthesis in soybean seedlings is negatively impacted by ethylene pathway stimulation at control temperatures, cold temperatures, and ethylene pathway manipulation in the cold through similar mechanisms.

CONCLUSION

The response of the *GmEINs* is complex. Soybean *EIN3A;1, EIN3B;1*, and *EIN3C;1* genes were all positively responsive to cold, but only the *EIN3A;1* levels further increased by activation of the ethylene pathway and were repressed by deactivation of the pathway (**Figure 4**). A downstream target of the EIN3's, *GmERF056*, was also clearly regulated in the cold, responding as expected in response to alterations in *GmEIN3A;1* transcript levels. The cold responsive transcription factors, *GmDREB1A;1*, and *GmDREB1B;1*, were upregulated by cold and their levels were consistently increased by ethylene pathway inhibitors or decreased (or no effect) by ethylene pathway stimulators (**Figure 5**). Gene targets with predicted cold responsive elements, CRT/DRE's, (ADH1A, CYP82A3, Ubiquitin ligase-like, and AP2-like) were indeed cold regulated, while ADH1B which lacks a predicted cold element was not (**Figure 6**). All these genes responded consistently in the cold by having strongly decreased transcript levels in the presence of stimulators of the ethylene pathway, though interestingly one of these did not have a predicted EIN3 responsive element (AP2-like); suggesting response to an indirect regulator. However, several (AP2-lke, ADH1A, and B) did not respond consistently to ethylene pathway inhibitors; suggesting they might already be at maximal levels in response to cold.

Photosynthetic parameters in soybean were strongly impacted by the cold. This is most dramatically demonstrated by the PI_{ABS} (**Figure 8D**); the Photosynthetic Performance Index, a measure of the energy conserved from absorption to reduction of PSI acceptors (**Figure 8D**) (Strasser et al., 2000). The PI_{ABS} is strongly and consistently impacted by both activators and inhibitors of the ethylene pathway, but only under control conditions. Cold conditions appear to bring PI_{ABS} to a minimum level which is little impacted by the ethylene pathway which correlates well with the indicated decreased PQ pool size (**Figure 8C**).

Not surprisingly, far downstream responses of metabolic indicators of cold stress (**Figure 7**) were a bit more variable. MDA and proline levels, common responses to cold, were moderately increased in the cold, and only small changes were induced by the presence of ethylene pathway modulators.

Interestingly, silver ions alone had a significant impact on both MDA and proline levels, increasing substantially those levels under control conditions. Likewise, silver had a moderate impact on freezing tolerance, decreasing the electrolyte leakage in both acclimated and non-acclimated soybean leaves (**Figure 7B**). Since these silver effects were not mimicked with either of the ethylene pathway inhibitors AVG or MCP, this suggests off target effects of silver ions, perhaps through its ability to generate free radicals, which can induce oxidative stress and thus oxidative stress responses (Bagherzadeh Homaee and Ehsanpour, 2016; Pradhan et al., 2017). Silver ions have been demonstrated to transcriptionally up-regulate oxidative stress responsive genes such as those encoding superoxide dismutase, cytochrome P450-dependent oxidase, and peroxidase (Kaveh et al., 2013). It may well be that cold tolerance enhancement in soybean by silver is by activating oxidative stress responses as a direct way to moderately increase the cold tolerance of soybean.

Overall, this work has shown that soybean seedlings have a typical ethylene response, indicated by ethylene induced leaf yellowing and cotyledon abscission. Additionally, the ethylene pathway is upregulated in response to cold, mediated by the sustained accumulation of transcripts encoding the transcription factor (*GmEIN3*), the increase in ethylene receptors (*GmETRs*), and the transient loss of transcripts encoding the negative regulatory F-box binding proteins (*GmEBF1s*). Ethylene modulators impact the level of an important cold responding transcription factor family, the *GmCBF/DREB1s*. Not only is the ethylene pathway upregulated in the cold; where it counters the upregulation of cold-responsive genes (*GmCBF/DREB1s*), but at normal temperatures, the cold-responsive genes also appear under negative regulatory control exerted through the ethylene signaling pathway.

Soybean is only mildly cold tolerant and has a meager acclimation response (Robison et al., 2017). Previous work (Yamasaki and Randall, 2016) demonstrated the functionality of the soybean *DREB1* genes by their activation of appropriate targets and resultant enhanced cold tolerance when expressed in Arabidopsis. The observation that up-regulation of the ethylene pathway from the RNA-Seq experiment, in particular the increase in *GmEIN3* transcripts suggested that the low ability of soybean to cold acclimate might be in part due to antagonism by the ethylene pathway. The data described here (summarized in **Figure 9**) demonstrates a clear impact of the ethylene pathway on the transcription of *GmDREB1s* and their downstream targets; with an activated ethylene pathway leading to decrease of the cold responsive pathway. We suggest that during cold stress GmEIN3A;1 is negatively regulating *GmDREB1A;1* by interaction with the EIN3 binding motif found in the *GmDREB1A;1* promoter. Inhibition of the ethylene pathway resulted in an increase in *GmDREB1A;1* transcript levels. This is quite unlike the impact of altering the ethylene pathway in Arabidopsis (Shi et al., 2012) in that soybean showed no substantial increase in freezing tolerance or cold tolerance parameters. This suggests that the initial portions of the CBF/DREB1 pathway (from cold reception to the accumulation of *GmCBF/DREB1* transcripts) are not limiting the cold responsive pathway in soybean.

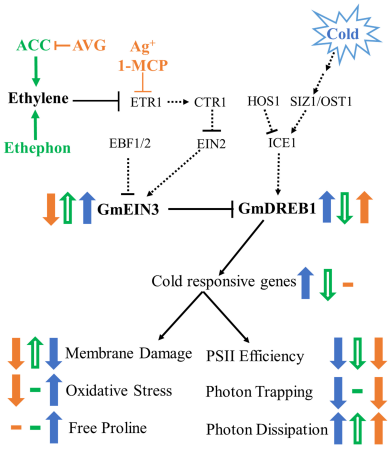

FIGURE 9 | Model of cold stress and ethylene signaling pathway in soybean seedlings. Dashed lines indicated predicted interactions based on Arabidopsis models, solid lines indicate parameters measured in this study. Changes indicated by cold are solid blue arrows, additional changes in the cold due to ethylene pathway stimulation are open green arrows, and ethylene pathway inhibition in solid orange arrows.

DATA AVAILABILITY

The datasets for the RNAseq experiments can be found on NCBI GEO (Accession # GSE117686) (https://www.ncbi.nlm.nih.gov/geo/query/acc.cgi?acc~=~GSE117686).

AUTHOR CONTRIBUTIONS

YY designed and performed the RNASeq analysis and created *AtRD29A*$_{prom}$*::GFP/GUS* construct for soybean transformation. JR isolated, characterized, and maintained transgenic soybean, designed and completed the ethylene pathway manipulation and cold stress experiments, and composed manuscript with contributions from all authors. SR supervised, designed, analyzed, and conducted experiments and edited the manuscript. All authors reviewed and edited the manuscript.

FUNDING

Funding for initiation of this project was provided by the United Soybean Board project-0238 awarded to SR, further support provided by the IUPUI Department of Biology.

Support for article processing charges fees provided by the IUPUI Open Access Publishing Fund (https://www.ulib.iupui.edu/digitalscholarship/openaccess/oafund).

ACKNOWLEDGMENTS

We wish to thank Alan Green at AgroFresh for the generous donation of 1-MCP and Tim Doyle at PP Systems for the gracious loan of the Handy-PEA utilized in these experiments. We thank Nicolas Tomeo for his feedback on early drafts of this manuscript. JR wishes to thank WAR for his general laboratory assistance.

SUPPLEMENTARY MATERIAL

The Supplementary Material for this article can be found online at: https://www.frontiersin.org/articles/10.3389/fpls.2019.00121/full#supplementary-material

REFERENCES

Ashburner, M., Ball, C. A., Blake, J. A., Botstein, D., Butler, H., Cherry, J. M., et al. (2000). Gene ontology: tool for the unification of biology. The gene ontology consortium. *Nat. Genet.* 25, 25–29. doi: 10.1038/75556

Ashraf, M., and Foolad, M. R. (2007). Roles of glycine betaine and proline in improving plant abiotic stress resistance. *Environ. Exp. Bot.* 59, 206–216. doi: 10.1016/j.envexpbot.2005.12.006

Bagherzadeh Homaee, M., and Ehsanpour, A. A. (2016). Silver nanoparticles and silver ions: oxidative stress responses and toxicity in potato (*Solanum tuberosum* L) grown in vitro. *Hortic. Environ. Biotechnol.* 57, 544–553. doi: 10.1007/s13580-016-0083-z

Baker, S. S., Wilhem, K. S., and Thomashow, M. F. (1994). The 5′-region of *Arabidopsis thaliana* cor15a has cis-acting elements that confer cold-, drought-, and ABA-regulated gene expression. *Plant Mol. Biol.* 24, 701–713. doi: 10.1007/BF00029852

Bates, L. S., Waldren, R. P., and Teare, I. D. (1973). Rapid determination of free proline for water-stress studies. *Plant Soil* 39, 205–207.

Beyer, E. M. (1976). A potent inhibitor of ethylene action in plants. *Plant Physiol.* 58, 268–271. doi: 10.1104/pp.58.3.268

Boisvert, S., Joly, D., and Carpentier, R. (2006). Quantitative analysis of the experimental O-J-I-P chlorophyll fluorescence induction kinetics. Apparent activation energy and origin of each kinetic step. *FEBS J.* 273, 4770–4777. doi: 10.1111/j.1742-4658.2006.05475.x

Boutrot, F., Segonzac, C., Chang, K. N., Qiao, H., Ecker, J. R., Zipfel, C., et al. (2010). Direct transcriptional control of the Arabidopsis immune receptor FLS2 by the ethylene-dependent transcription factors EIN3 and EIL1. *Proc. Natl. Acad. Sci. U.S.A.* 107, 14502–14507. doi: 10.1073/pnas.1003347107

Bradford, M. M. (1976). A rapid and sensitive method for the quantitation of microgram quantities of protein utilizing the principle of protein-dye binding. *Anal. Biochem.* 72, 248–254. doi: 10.1016/0003-2697(76)90527-3

Catalá, R., and Salinas, J. (2015). The Arabidopsis ethylene overproducer mutant eto1-3 displays enhanced freezing tolerance. *Plant Signal. Behav.* 10:e989768. doi: 10.4161/15592324.2014.989768

Cheng, Y.-Q. (2013). RNA-seq analysis reveals ethylene-mediated reproductive organ development and abscission in soybean (*Glycine max* L. Merr.). *Plant Mol. Biol. Rep.* 31, 607–619. doi: 10.1007/s11105-012-0533-4

Cheng, Y.-Q., Liu, J., Yang, X., Ma, R., Liu, Q., and Liu, C. (2013). Construction of ethylene regulatory network based on the phytohormones related gene transcriptome profiling and prediction of transcription factor activities in soybean. *Acta Physiol. Plant* 35, 1303–1317. doi: 10.1007/s11738-012-1170-0

Ciardi, J. A., Deikman, J., and Orzolek, M. D. (1997). Increased ethylene synthesis enhances chilling tolerance in tomato. *Physiol. Plant* 101, 333–340. doi: 10.1111/j.1399-3054.1997.tb01005.x

Consortium, T. G. O. (2017). Expansion of the gene ontology knowledgebase and resources. *Nucleic Acids Res.* 45, D331–D338. doi: 10.1093/nar/gkw1108

Cook, D., Fowler, S., Fiehn, O., and Thomashow, M. F. (2004). A prominent role for the CBF cold response pathway in configuring the low-temperature metabolome of Arabidopsis. *Proc. Natl. Acad. Sci. U.S.A.* 101, 15243–15248. doi: 10.1073/pnas.0406069101

Curtis, R. W. (1981). Light requirement for AgNO3 inhibition of ethrel-induced leaf abscission from cuttings of Vigna radiata. *Plant Physiol.* 68, 1249–1252. doi: 10.1104/pp.68.6.1249

Ding, Y., Li, H., Zhang, X., Xie, Q., Gong, Z., and Yang, S. (2015). OST1 kinase modulates freezing tolerance by enhancing ICE1 stability in Arabidopsis. *Dev. Cell* 32, 278–289. doi: 10.1016/j.devcel.2014.12.023

Djanaguiraman, M., and Prasad, P. V. V. (2010). Ethylene production under high temperature stress causes premature leaf senescence in soybean. *Funct. Plant Biol.* 37, 1071–1084. doi: 10.1071/FP10089

Djanaguiraman, M., Prasad, P. V. V., and Al-Khatib, K. (2011). Ethylene perception inhibitor 1-MCP decreases oxidative damage of leaves through enhanced antioxidant defense mechanisms in soybean plants grown under high temperature stress. *Environ. Exp. Bot.* 71, 215–223. doi: 10.1016/j.envexpbot.2010.12.006

Dong, C. H., Agarwal, M., Chang, Y., Xie, Q., and Zhu, J. K. (2006). The negative regulator of plant cold responses, HOS1, is a RING E3 ligase that mediates the ubiquitination and degradation of ICE1. *Proc. Natl. Acad. Sci. U.S.A.* 103, 8281–8286. doi: 10.1073/pnas.0602874103

Ensminger, I., Busch, F., and Huner, N. P. A. (2006). Photostasis and cold acclimation: sensing low temperature through photosynthesis. *Physiol. Plant* 126, 28–44.

Fior, S., Vianelli, A., and Gerola, P. D. (2009). A novel method for fluorometric continuous measurement of β-glucuronidase (GUS) activity using 4-methyl-umbelliferyl-β-D-glucuronide (MUG) as substrate. *Plant Sci.* 176, 130–135. doi: 10.1016/j.plantsci.2008.10.001

Gallie, D. R. (2015). Ethylene receptors in plants - why so much complexity? *F100Prime Rep.* 7:39. doi: 10.12703/P7-39

Gilmour, S. J., Fowler, S., and Thomashow, M. F. (2004). Arabidopsis transcriptional activators CBF1, CBF2, and CBF3 have matching functional activities. *Plant Mol. Biol.* 54, 761–781. doi: 10.1023/B:PLAN.0000040902.06881.d4

Gilmour, S. J., Sebolt, A. M., Salazar, M. P., Everard, J. D., and Thomashow, M. F. (2000). Overexpression of the Arabidopsis CBF3 transcriptional activator mimics multiple biochemical changes associated with cold acclimation. *Plant Physiol.* 124, 1854–1865. doi: 10.1104/pp.124.4.1854

Gilmour, S. J., Zarka, D. G., Stockinger, E. J., Salazar, M. P., Houghton, J. M., and Thomashow, M. F. (1998). Low temperature regulation of the Arabidopsis CBF family of AP2 transcriptional activators as an early step in cold induced COR gene expression. *Plant J.* 16, 433–442. doi: 10.1046/j.1365-313x.1998.00310.x

Grant, D., Nelson, R. T., Cannon, S. B., and Shoemaker, R. C. (2010). SoyBase, the USDA-ARS soybean genetics and genomics database. *Nucleic Acids Res.* 38, D843–D846. doi: 10.1093/nar/gkp798

Grbić, V., and Bleecker, A. B. (1995). Ethylene regulates the timing of leaf senescence in Arabidopsis. *Plant J.* 8, 595–602. doi: 10.1046/j.1365-313X.1995.8040595.x

Hanway, J. J., and Thompson, H. E. (1967). *How a Soybean Plant Develops*. Ames, IA: Cooperative Extension Service.

Hayat, S., Hayat, Q., Alyemeni, M. N., Wani, A. S., Pichtel, J., and Ahmad, A. (2012). Role of proline under changing environments: a review. *Plant Signal. Behav.* 7, 1456–1466. doi: 10.4161/psb.21949

Hodges, D. M., DeLong, J. M., Forney, C. F., and Prange, R. K. (1999). Improving the thiobarbituric acid-reactive-substances assay for estimating lipid peroxidation in plant tissues containing anthocyanin and other interfering compounds. *Planta* 207, 604–611. doi: 10.1007/s004250050524

Hu, Z., Fan, J., Chen, K., Amombo, E., Chen, L., and Fu, J. (2016). Effects of ethylene on photosystem II and antioxidant enzyme activity in Bermuda grass under low temperature. *Photosynth. Res.* 128, 59–72. doi: 10.1007/s11120-015-0199-5

Hughes, S. L., Schart, V., Malcolmson, J., Hogarth, K. A., Martynowicz, D. M., Tralman-Baker, E., et al. (2013). The importance of size and disorder in the cryoprotective effects of dehydrins. *Plant Physiol.* 163, 1376–1386. doi: 10.1104/pp.113.226803

Jaglo-Ottosen, K. R., Gilmour, S. J., Zarka, D. G., Schabenberger, O., and Thomashow, M. F. (1998). Arabidopsis CBF1 overexpression induces COR genes and enhances freezing tolerance. *Science* 280, 104–106. doi: 10.1126/science.280.5360.104

Janero, D. R. (1990). Malondialdehyde and thiobarbituric acid-reactivity as diagnostic indices of lipid peroxidation and peroxidative tissue injury. *Free Radic. Biol. Med.* 9, 515–540. doi: 10.1016/0891-5849(90)90131-2

Jia, Y., Ding, Y., Shi, Y., Zhang, X., Gong, Z., and Yang, S. (2016). The cbfs triple mutants reveal the essential functions of CBFs in cold acclimation and allow the definition of CBF regulons in Arabidopsis. *New Phytol.* 212, 345–353. doi: 10.1111/nph.14088

Jouve, L., Engelmann, F., Noirot, M., and Charrier, A. (1993). Evaluation of biochemical markers (sugar, proline, malonedialdehyde and ethylene) for cold sensitivity in microcuttings of two coffee species. *Plant Sci.* 91, 109–116. doi: 10.1016/0168-9452(93)90194-5

Joyce, D. C., Reid, M. S., and Evans, R. Y. (1990). Silver thiosulfate prevents ethylene-induced abscission in holly and mistletoe. *Hortscience* 25, 90–92.

Ju, C., and Chang, C. (2015). Mechanistic insights in ethylene perception and signal transduction. *Plant Physiol.* 169, 85–95. doi: 10.1104/pp.15.00845

Kaplan, F., Kopka, J., Sung, D. Y., Zhao, W., Popp, M., Porat, R., et al. (2007). Transcript and metabolite profiling during cold acclimation of Arabidopsis reveals an intricate relationship of cold-regulated gene expression with modifications in metabolite content. *Plant J.* 50, 967–981. doi: 10.1111/j.1365-313X.2007.03100.x

Kaveh, R., Li, Y.-S., Ranjbar, S., Tehrani, R., Brueck, C. L., and Van Aken, B. (2013). Changes in *Arabidopsis thaliana* gene expression in response to silver nanoparticles and silver ions. *Environ. Sci. Technol.* 47, 10637–10644. doi: 10.1021/es402209w

Kidokoro, S., Watanabe, K., Ohori, T., Moriwaki, T., Maruyama, K., Mizoi, J., et al. (2015). Soybean DREB1/CBF-type transcription factors function in heat and drought as well as cold stress-responsive gene expression. *Plant J.* 81, 505–518. doi: 10.1111/tpj.12746

Kilian, J., Whitehead, D., Horak, J., Wanke, D., Weinl, S., Batistic, O., et al. (2007). The atgenexpress global stress expression data set: protocols, evaluation and model data analysis of UV-B light, drought and cold stress responses. *Plant J.* 50, 347–363. doi: 10.1111/j.1365-313X.2007.03052.x

Konishi, M., and Yanagisawa, S. (2008). Ethylene signaling in *Arabdiopsis* involves feedback regulation via the elaborate control of EBF2 expression by EIN3. *Plant J.* 55, 821–831. doi: 10.1111/j.1365-313X.2008.03551.x

Lamesch, P., Berardini, T. Z., Li, D., Swarbreck, D., Wilks, C., Sasidharan, R., et al. (2012). The Arabidopsis information resource (TAIR): improved gene annotation and new tools. *Nucleic Acids Res.* 40, D1202–D1210. doi: 10.1093/nar/gkr1090

Lescot, M., Dehais, P., Thijs, G., Marchal, K., Moreau, Y., Van de Peer, Y., et al. (2002). PlantCARE, a database of plant cis-acting regulatory elements and a portal to tools for in silico analysis of promoter sequences. *Nucleic Acids Res.* 30, 325–327. doi: 10.1093/nar/30.1.325

Leshem, Y. Y. (1987). Membrane phospholipid catabolism and Ca2+activity in control of senescence. *Physiol. Plant* 69, 551–559. doi: 10.1111/j.1399-3054.1987.tb09239.x

Letunic, I., and Bork, P. (2016). Interactive tree of life (iTOL) v3: an online tool for the display and annotation of phylogenetic and other trees. *Nucleic Acids Res.* 44, W242–W245. doi: 10.1093/nar/gkw290

Littlejohns, D. A., and Tanner, J. W. (1976). Preliminary studies on the cold tolerance of soybean seedlings. *Can. J. Plant Sci.* 56, 371–375. doi: 10.4141/cjps76-056

Liu, Q., Kasuga, M., Sakuma, Y., Abe, H., Miura, S., Yamaguchi-Shinozaki, K., et al. (1998). Two transcription factors, DREB1 and DREB2, with an EREBP/AP2 DNA binding domain separate two cellular signal transduction pathways in drought- and low-temperature-responsive gene expression, respectively, in Arabidopsis. *Plant Cell* 10, 1391–1406. doi: 10.1105/tpc.10.8.1391

Manafi, E., Modarres Sanavy, S. A. M., Aghaalikhani, M., and Dolatabadian, A. (2015). Exogenous 5-aminolevulenic acid promotes antioxidative defence system, photosynthesis and growth in soybean against cold stress. *Not. Sci. Biol.* 7, 486–494. doi: 10.15835/nsb.7.4.9654

Medina, J., Bargues, M., Terol, J., Pérez-Alonso, M., and Salinas, J. (1999). The Arabidopsis CBF gene family Is composed of three genes encoding AP2 domain-containing proteins whose expression is regulated by low temperature but not by abscisic acid or dehydration. *Plant Physiol.* 199, 463–470. doi: 10.1104/pp.119.2.463

Miura, K., Jin, J., Lee, J., Yoo, C. Y., Stirm, V., Miura, T., et al. (2007). SIZ1-mediated sumoylation of ICE1 controls CBF3/DREB1A expression and freezing tolerance in Arabidopsis. *Plant Cell* 19, 1403–1414. doi: 10.1105/tpc.106.048397

Murgia, I., Tarantino, D., Soave, C., and Morandini, P. (2011). Arabidopsis CYP82C4 expression is dependent on Fe availablility and circadian rhythm, and correlates with genes involved in the early Fe deficiency response. *J. Plant Physiol.* 168, 894–902. doi: 10.1016/j.jplph.2010.11.020

Nishiyama, Y., Allakhverdiev, S. I., and Murata, N. (2011). Protein synthesis is the primary target of reactive oxygen species in the photoinhibition of photosystem II. *Physiol. Plant* 142, 35–46. doi: 10.1111/j.1399-3054.2011.01457.x

Nukui, N., Ezura, H., Yuhashi, K.-I., Yasuta, T., and Minamisawa, K. (2000). Effects of ethylene precursor and inhibitors for ethylene biosynthesis and perception on nodulation in *Lotus japonicus* and *Macroptilium atropurpureum*. *Plant Cell Physiol.* 41, 893–897. doi: 10.1093/pcp/pcd011

O'Kane, D., Gill, V., Boyd, P., and Burdon, R. (1996). Chilling, oxidative stress and antioxidant responses in *Arabidopsis thaliana* callus. *Planta* 198, 371–377. doi: 10.1007/BF00620053

Park, S., Lee, C.-M., Doherty, C. J., Gilmour, S. J., Kim, Y., and Thomashow, M. F. (2015). Regulation of the Arabidopsis CBF regulon by a complex low-temperature regulatory network. *Plant J.* 82, 193–207. doi: 10.1111/tpj.12796

Paz, M. M., Shou, H., Guo, Z., Zhang, Z., Banerjee, A. K., and Wang, K. (2004). Assessment of conditions affecting Agrobacterium-mediated soybean transformation using the cotyledonary node explant. *Euphytica* 136, 167–179. doi: 10.1023/B:EUPH.0000030670.36730.a4

Pradhan, C., Routray, D., and Das, A. B. (2017). Silver nitrate mediated oxidative stress induced genotoxicity of Allium cepa L. *Cytologia* 82, 183–191. doi: 10.1508/cytologia.82.183

Purvis, A. C., and Barmore, C. R. (1981). Involvement of ethylene in chlorophyll degradation in peel of citrus fruits. *Plant Physiol.* 68, 854–856. doi: 10.1104/pp.68.4.854

Qin, Y., Zhang, S., Zhang, L., Zhu, D., and Syed, A. (2005). Response of in vitro strawberry to silver nitrate (AgNO3). *Hortscience* 40, 747–751.

R Core Team (2013). *R: A Language and Environment for Statistical Computing*. Vienna: R Foundation for Statistical Computing.

Ristic, Z., and Ashworth, E. N. (1993). Changes in leaf ultrastructure and carbohydrates in *Arabidopsis thaliana* L. (Heyn) cv. Columbia during rapid cold acclimation. *Protoplasma* 172, 111–123. doi: 10.1007/BF01379368

Robison, J., Arora, N., Yamasaki, Y., Saito, M., Boone, J., Blacklock, B. J., et al. (2017). Glycine max and glycine soja are capable of cold acclimation. *J. Agron. Crop Sci.* 203, 553–561. doi: 10.1111/jac.12219

Savitch, L. V., Barker-Åstrom, J., Ivanov, A. G., Hurry, V., Öquist, G., Huner, N. P., et al. (2001). Cold acclimation of *Arabidopsis thaliana* results in incomplete recovery of photosynthetic capacity, associated with an increased reduction of the chloroplast stroma. *Planta* 214, 295–303. doi: 10.1007/s004250100622

Sazegari, S., Niazi, A., and Ahmadi, F. S. (2015). A study on the regulatory network with promoter analysis for Arabidopsis DREB-genes. *Bioinformation* 11, 101–106. doi: 10.6026/97320630011101

Schaller, G. E., and Binder, B. M. (2017). "Inhibitors of ethylene biosynthesis and signaling," in *Ethylene Signaling: Methods and Protocols*, eds B. M. Binder and G. E. Schaller (Berlin: Springer Science), 223–235.

Severin, A. J., Woody, J. L., Bolon, Y.-T., Joseph, B., Diers, B. W., Farmer, A. D., et al. (2010). RNA-Seq atlas of glyxine max: a guide to the soybean transcriptome. *BMC Plant Biol.* 10:160. doi: 10.1186/1471-2229-10-160

Sharmin, S. A., Alam, I., Kim, K.-H., Kim, Y.-G., Kim, P. J., Bahk, J. D., et al. (2012). Chromium-induced physiological and proteomic alterations in roots of *Miscanthus sinensis*. *Plant Sci.* 187, 113–126. doi: 10.1016/j.plantsci.2012.02.002

Shi, Y., Tian, S., Hou, L., Huang, X., Zhang, X., Guo, H., et al. (2012). Ethylene signaling negatively regulates freezing tolerance by repressing expression of CBF and type-A ARR genes in Arabidopsis. *Plant Cell* 24, 2578–2595. doi: 10.1105/tpc.112.098640

Sievers, F., Wilm, A., Dineen, D., Gibson, T. J., Karplus, K., Li, W., et al. (2011). Fast, scalable generation of high-quality protein multiple sequence alignments using clustal omega. *Mol. Syst. Biol.* 7:539. doi: 10.1038/msb.2011.75

Simon, E. W. (1974). Phospholipids and plant membrane permeability. *New Phytol.* 73, 377–420. doi: 10.1111/j.1469-8137.1974.tb02118.x

Song, Y., Liu, L., Wei, Y., Li, G., Yue, X., and An, L. (2016). Metabolite profiling of adh1 mutant response to cold stress in Arabidopsis. *Front. Plant Sci.* 7:2072. doi: 10.3389/fpls.2016.02072

Steponkus, P. L., Uemura, M., Joseph, R. A., Gilmour, S. J., and Thomashow, M. F. (1998). Mode of action of the COR15a gene on the freezing tolerance of *Arabidopsis thaliana*. *Proc. Natl. Acad. Sci. U.S.A.* 95, 14570–14575. doi: 10.1073/pnas.95.24.14570

Stockinger, E. J., Gilmour, S. J., and Thomashow, M. F. (1997). *Arabidopsis thaliana* CBF1 encodes an AP2 domain-containing transcriptional activator that binds to the C-repeat/DRE, a cis-acting DNA regulatory element that stimulates transcription in response to low temperature and water deficit. *Proc. Natl. Acad. Sci. U.S.A.* 94, 1035–1040. doi: 10.1073/pnas.94.3.1035

Strasser, R. J., and Srivastava, A. (1995). Polyphasic chlorophyll a fluorescence transient in plants and cyanobacteria. *Photochem. Photobiol.* 61, 32–42. doi: 10.1111/j.1751-1097.1995.tb09240.x

Strasser, R. J., Srivastava, A., and Tsimilli, M. (2000). "The fluorescence transient as a tool to characterize and screen photosynthetic samples," in *Probing Photosynthesis:Mechanism, Regulation & Adaptation*, eds U. Pathre, M. Yunus, and P. Mohanty (London: Taylor Francis), 445–483.

Street, I. H., and Schaller, G. E. (2016). Ethylene: a gaseous signal in plants and bacteria. *Annu. Rev. Cell Dev. Biol.* 16, 1–18.

Sun, Z., Zhao, T., Gan, S., Ren, X., Fang, L., Karungo, S. K., et al. (2016). Ethylene positively regulates cold tolerance in grapevine by modulating the expression of ETHYLENE RESPONSE FACTOR 057. *Sci. Rep.* 6:24066. doi: 10.1038/srep24066

Suzuki, N., and Mittler, R. (2006). Reactive oxygen species and temperature stresses: a delicate balance between signaling and destruction. *Physiol. Plant* 126, 45–51. doi: 10.1111/j.0031-9317.2005.00582.x

Tambussi, E. A., Bartoli, C. G., Guiamet, J. J., Beltrano, J., and Araus, J. L. (2004). Oxidative stress and photodamage at low temperatures in soybean (Glycine max L. Merr.) leaves. *Plant Sci.* 167, 19–26. doi: 10.1016/j.plantsci.2004.02.018

Thomashow, M. F. (1999). Plant cold acclimation: freezing tolerance genes and regulatory mechanisms. *Annu. Rev. Plant Physiol. Plant Mol. Biol.* 50, 571–599. doi: 10.1146/annurev.arplant.50.1.571

Torres, M. A., and Dangl, J. L. (2005). Functions of the respiratory burst oxidase in biotic interactions, abiotic stress and development. *Curr. Opin. Plant Biol.* 8, 397–403. doi: 10.1016/j.pbi.2005.05.014

Van Heerden, P. D., Tsimilli-Michael, M., Kruger, G. H., and Strasser, R. J. (2003). Dark chilling effects on soybean genotypes during vegetative development: parallel studies of CO2 assimilation, chlorophyll a fluorescence kinetics O-J-I-P and nitrogen fixation. *Physiol. Plant* 117, 476–491. doi: 10.1034/j.1399-3054.2003.00056.x

Van Heerden, P. D. R., and Kruger, G. H. (2000). Photosynthetic limitation in soybean during cold stress. *South Afr. J. Sci.* 96, 201–206.

Van Heerden, P. D. R., and Krüger, G. H. J. (2002). Separately and simultaneously induced dark chilling and drought stress effects on photosynthesis, proline accumulation and antioxidant metabolism in soybean. *J. Plant Physiol.* 159, 1077–1086. doi: 10.1078/0176-1617-00745

Wang, K. L.-C., Li, H., and Ecker, J. R. (2002). Ethylene biosynthesis and signaling networks. *Plant Cell* 14(Suppl.), S131–S151. doi: 10.1105/tpc.001768

Warren, C. R. (2008). Rapid measurement of chlorophylls with a microplate reader. *J. Plant Nutr.* 31, 1321–1332. doi: 10.1080/01904160802135092

Xin, Z., and Browse, J. (1998). Eskimo1 mutants of Arabidopsis are constitutively freezing-tolerant. *Proc. Natl. Acad. Sci. U.S.A.* 95, 7799–7804. doi: 10.1073/pnas.95.13.7799

Yamasaki, Y., Koehler, G., Blacklock, B. J., and Randall, S. K. (2013). Dehydrin expression in soybean. *Plant Physiol. Biochem.* 70, 213–220. doi: 10.1016/j.plaphy.2013.05.013

Yamasaki, Y., and Randall, S. K. (2016). Functionality of soybean CBF/DREB1 transcription factors. *Plant Sci.* 246, 80–90. doi: 10.1016/j.plantsci.2016.02.007

Yan, Q., Cui, X., Lin, S., Gan, S., Xing, H., and Dou, D. (2016). GmCYP82A3, a soybean cytochrome p450 family gene involved in the jasmonic acid and ethylene signaling pathway, enhances plant resistance to biotic and abiotic stresses. *PLoS One* 11:e0162253. doi: 10.1371/journal.pone.0162253

Yoo, S.-D., Cho, Y.-H., and Sheen, J. (2007). Arabidopsis mesophyll protoplasts: a versatile cell system for transient gene expression analysis. *Nat. Protc.* 2, 1565–1572. doi: 10.1038/nprot.2007.199

Zarka, D. G., Vogel, J. T., Cook, D., and Thomashow, M. F. (2003). Cold induction of Arabidopsis CBF genes involves multiple ICE (Induce of CBF Expression) promoter elements and a cold-regulatory circuit that is desensitized by low temperature. *Plant Physiol.* 133, 910–918. doi: 10.1104/pp.103.027169

Zhang, J., Chen, N., Zhang, Z., Pan, L., Chen, M., Wang, M., et al. (2016). Peanut ethylene-responsive element binding factor (AhERF6) improves cold and salt tolerance in Arabidopsis. *Acta Physiol. Plant* 38:185. doi: 10.1007/s11738-016-2201-z

Zhang, W., Hu, W., and Wen, C.-K. (2010). Ethylene preparation and its application to physiological experiments. *Plant Signal. Behav.* 5, 453–457. doi: 10.4161/psb.5.4.10875

Zhang, Z., and Huang, R. (2010). Enhanced tolerance to freezing in tobacco and tomato overexpressing transcription factor TERF2/LEERF2 is modulated by ethylene biosynthesis. *Plant Mol. Biol.* 73, 241–249. doi: 10.1007/s11103-010-9609-4

Zhao, M., Liu, W., Xia, X., Wang, T., and Zhang, W.-H. (2014). Cold acclimation-induced freezing tolerance of *Medicago truncatula* seedlings is negatively regulated by ethylene. *Physiol. Plant* 152, 115–129. doi: 10.1111/ppl.12161

Zhu, X.-G., Govindjee, Baker, N. R., deSturler, E., Ort, D. R., and Long, S. P. (2005). Chlorophyll a fluorescence induction kinetics in leaves predicted from a model describing each discrete step of excitation energy and electron transfer associated with Photosystem II. *Planta* 223, 114–133. doi: 10.1007/s00425-005-0064-4

Conflict of Interest Statement: The authors declare that the research was conducted in the absence of any commercial or financial relationships that could be construed as a potential conflict of interest.

VITA

VITA

Jennifer D. Robison

Education

Doctorate of Philosophy in Biology, 2019

Indiana University Purdue University Indianapolis

PI: Dr. Stephen Randall

Research: Domestic soybean (*Glycine max*) is capable of mild cold acclimation. The ethylene signaling pathway negatively regulates cold tolerance in soybean

Masters of Science in Marine Biology and Biochemistry, 2006

University of Delaware

PI: Dr. Mark Warner

Research: An investigation of the photophysiology of symbiotic dinoflagellates (*Symbiodinium* spp.) under varying light and thermal conditions and the implications for coral bleaching.

Bachelors of Science in Biology, 2003

Dickinson College

Chemistry minor, Magna Cum Laude, Dept. Honors.

Research Advisor: Dr. Carol Loeffler

Research: Examining the impact of environmental factors on the life histories of two invasive wildflower species, *Alliaria petiolata* and *Hesperis matornalis*.

Teaching Experience

Manchester University

Visiting Assistant Professor, 2018 - present

Courses taught: 313 Microbiology, 313L Microbiology Laboratory, 431 Immunology, 365 Cellular Biology, 106L Principals of Biology laboratory.

Indiana University Purdue University Indianapolis

Graduate Teaching Assistant, 2013 - 2018

Courses taught: K103 Concepts of Biology II lab 6 semesters, K323 Genetics lab 2 semesters, K325 Cellular Biology lab 2 semester.

ITT Technical Institute

Adjunct Instructor, 2010 - 2013

Courses taught: SC2730 Microbiology 13 quarters, SC1130 Survey of the Sciences 7 quarters, AP2535 Anatomy & Physiology 1 4 quarters, GS1145 Strategies of the Successful Professional 4 quarters.

Global Learning Solutions

Course Writer, 2011-2013, 2015

Courses: SC2730 Microbiology, SC1130 Survey of the Sciences, GRT1 Biochemistry

Teaching Awards and Certification

- Certificate in College Teaching, IUPUI Center for Teaching and Learning August, 2017
- Center for the Integration of Research, Teaching, and Learning Associates Certificate May, 2017
- Teaching Assistant Award School of Science IUPUI April, 2017

- IUPUI Student Athlete Favorite Professor Fall, 2017
- Instructor of the Quarter , ITT Technical Institute Fort Wayne Campus June 2010

Peer-Reviewed Publications

- **Robison**, J. D., Y. Yamasaki, S. Randall, 2019. The Ethylene Signaling Pathway Negatively Impacts CBF/DREB-Regulated Cold Response in Soybean (*Glycine max*). Frontiers in Plant Science, 20:121.
- **Robison**, J. D., N. Aurora, Y. Yamasaki, M. Saito, J. Boone, B. Blacklock, S. Randall, 2017. Cold Acclimation Potentials of *Glycine max* and *Glycine soja*. Journal of Agronomy and Crop Science, 203:553-561.
- **Robison**, J. D., M. E. Warner, 2006. Differential impacts of photoacclimation and thermal stress on the photobiology of four different phylotypes of *Symbiodinium* (Pyrrhophyta). Journal of Phycology, 42:568-569.
- Warner, M. E., T. C. LaJeunesse, J. D. **Robison**, R. M. Thur, 2006. The ecological distribution and comparative photobiology of symbiotic dinoflagellates from reef corals in Belize: Potential implications for coral bleaching. Limnology and Oceanography, 51:1887-1897.

Invited Research Presentations

- **Robison**, J. D., P. Gentry, N. Berbari, A. Rao, 2018. Writing Scientist Biographies Increases Students Awareness of Diversity in Genetics. American Society of Plant Biology Annual Meeting, July 15, Abstract #CS-2-2, Montreal, Quebec.

- **Robison**, J. D., S. Randall, 2017. The Ethylene Signaling Pathway Negatively Regulates Cold Tolerance in Soybean. Invited Speaker: ASPB Environmental and Ecological Plant Physiology Section Meeting, June 27, Abstract #1, Honolulu, Hawaii.

- **Robison**, J. D., 2017. Let it Snow! Increasing the cold tolerance of Soybean. Spring Arbor University Biology Department Seminar, Spring Arbor MI, April 21. `https:\www.youtube.com/watch?v=zfVnWQlea68`

- **Robison**, J. D., Y. Yamasaki, S. Randall, 2016. Ethylene Signaling Negatively Impacts Cold Stress Responses in Soybean. Platform Presentation: SOY2016 Molecular and Cellular Biology of the Soybean 16th Biennial Conference, August 8, Abstract # S15, Columbus, OH.

- **Robison**, J. D., 2005. Photobiology of the symbiotic dinoflagellate *Symbiodinium* during coral bleaching. Dickinson College Biology Invitational Seminar, Carlisle PA, Mar. 10.

Invited Educational Workshop Facilitator

- **Robison**, J. D., C. Kassab, 2017. Active Learning Strategies for Teaching STEM Labs. Teaching for Graduate Students and Postdocs Series, Center for Teaching and Learning IUPUI, Sept. 27.

- **Robison**, J. D., P. Gentry, 2017. Teaching Laboratory Sessions in the Biological Sciences. IUPUI TA Orientation, Center for Teaching and Learning IUPUI, Aug. 17.

- Rao, A., J. D. **Robison**, 2017. CIRTL Advancing Learning Through Evidence-Based STEM teaching MOOC Centered Learning Community. Co-facilitator. Center for Teaching and Learning IUPUI, Spring 2017.

- **Robison**, J. D., G. Shaker, 2016. Graduate Student Professionalism: Time and Classroom Management. Invited Presentation: 2016 IUPUI TA Orientation, Center for Teaching and Learning IUPUI, Aug. 19.

- **Robison**, J. D., R. Clark, 2015. Managing your Time as a Graduate Student: How to Get It All Done and Stay Sane. Educational Training for Teaching Assistants, Center for Teaching and Learning IUPUI, Aug. 21.

- **Robison**, J. D., K. Badertscher, 2014. Managing your Time as a Graduate Student: How to Get It All Done and Stay Sane. Educational Training for Teaching Assistants, Center for Teaching and Learning IUPUI, Aug. 22.

Presentations and Posters

- **Robison**, J. D., S. Randall, 2018. Alterations of the ethylene pathway impact the cold response in soybean Poster: American Society of Plant Biologist Plant Biology Meeting, July 14-18, Abstract #1100-011, Montreal, Quebec.

- **Robison**, J. D., P. Gentry, N. Berbari, A. Rao, 2018. Writing Scientist Biographies Increases Students Awareness of Diversity in Genetics. American Society of Plant Biology Annual Meeting, July 14-18, Abstract #100-006, Montreal, Quebec.

- **Robison**, J. D., P. Gentry, N. Berbari, A. Rao, 2018. A Simple Intervention to Increase Inclusive Pedagogy in a Biology Laboratory. Presentation: 133rd Annual Indiana Academy of Science Meeting. March 24, Indianapolis, Indiana.

- **Robison**, J. D., S. Randall, 2017. The Ethylene Signaling Pathway Negatively Regulates Cold Tolerance in Soybean. Poster: American Society of Plant Biologist Plant Biology Meeting, June 25-26, Abstract #1100-143, Honolulu, Hawaii.

- **Robison**, J. D., S. Randall, 2017. The Ethylene Signaling Pathway Negatively Regulates Cold Tolerance in Soybean. Presentation: American Society of Plant

Biologists Midwestern Sectional Meeting, Feb. 5. Abstract # T20, Purdue University, West Lafayette, IN.

- **Robison**, J. D., Y. Yamasaki, S. Randall, 2016. Ethylene Signaling Negatively Impacts Cold Stress Responses in Soybean. Poster: SOY2016 Molecular and Cellular Biology of the Soybean 16th Biennial Conference, August 8, 2016, Abstract # P007, Columbus, OH.

- **Robison**, J. D., Y. Yamasaki, S. Randall, 2016. Ethylene Signaling Negatively Impacts Cold Stress Response in Soybean. Poster: American Society of Plant Biologists Plant Biology Meeting, July 10, 11, Abstract # 1100-059-Z, Austin, TX.

- **Robison**, J. D., M. Saito, S. Randall, 2016. Domestic (*Glycine max*) and Non-domesticated (*Glycine soja*) Soybean are Capable of Cold Acclimation. Presentation: Indiana Academy of Sciences 131st Annual Meeting, Mar. 26, JW Marriott, Indianapolis IN.

- **Robison**, J. D., Y. Yamasaki, S. Randall, 2015. Investigation into the CBF cold pathway in Soybean. Presentation: American Society of Plant Biologists Midwestern Sectional Meeting, Mar. 21. Abstract # T3, Donald Danforth Plant Science Center, St. Louis, MO.

- **Robison**, J. D., Y. Yamasaki, S. Randall, 2014. Investigation into the CBF cold pathway in Soybean. Presentation: Indiana Academy of Sciences 129th Annual Meeting, Mar. 15, JW Marriott, Indianapolis, IN.

- **Robison**, J. D., M.E. Warner, 2006. Differential impacts of photoacclimation and thermal stress on the photobiology of four phylotypes of symbiotic dinoflagellates. Poster: American Society of Limnology and Oceanography Ocean Sciences meeting, Feb. Abstract #OS26G-01, Honolulu Convention Center, Honolulu, HI.

- **Robison**, J. D., M.E. Warner, 2005. Dissecting the pathways of thermal and light stress in different symbiotic dinoflagellates. Poster: American Society of Limnology and Oceanography Aquatic Sciences meeting, Feb. 23. Abstract #GS09-64, Salt Palace Convention Center, Salt Lake City, UT.
- **Robison**, J. D., C. Loeffler, 2003. Investigations on the life histories of two invasive species: *Alliaria petiolata* (M. Bieb.) Cavara & Grande and *Hesperis matronalis* L. Poster; Pennsylvania Academy of Sciences Annual Meeting, April.

Professional Activities

- Twitter Manager, PlantingScience July 2017 present
- Community Catalyst, ASPB Plant Biology Meetings May 2018 present
- Social Media Manager, ASPB Plant Biology Meeting Honolulu June 2017
- Social Media Manager, Central Indiana Science Outreach May 2016 present
- Publications Manager, Midwest section ASPB July 2016 present
- American Society of Plant Biologist member Jan 2015 present
- National Science Teachers Association member March 2012 present
- Graduate Advisor, IUPUI Center for Teaching and Learning Advisory Board August 2017 2019

Research Awards, Fellowships, and Grants

- PlantingScience Digging Deeper Fellowship Recipient July, 2017
- ASPB Travel Grant Recipient June, 2017
- Outstanding Oral Presentation 3rd place ASPB Midwest Section Meeting February, 2017

- ASPB Midwest Travel Grant Recipient March 2015
- Elizabeth K Tunnel Memorial Fellowship for Research Diving, Beneath the Sea March, 2004
- Spencer Fullerton Baird Prize for Excellence in Biology, Dickinson College Spring, 2003
- Paul Burkholder Biology Prize for Research, Dickinson College Spring, 2002

Outreach Experience

- Scientist Liaison/Mentor for PlantingScience `https:\plantingscience.org`. Mentored middle, high school, and undergraduate students who were engaging in inquiry based plant sciences. Mentor 12 groups and Liaison 3 classroom. September 2016 to present.
- Scientist Penpal for Letters to a Pre-Scientist `http:\www.prescientist.org/`. Two penpals from December 2016 to present.
- Exploring Plants hands on demos at Celebrate Science Indiana, Indiana State Fairgrounds, Indianapolis, IN. First Saturday in October 2014 2018.
- Social Media for Scientists Invited Panelist Member, discussions on how to effectively utilize social media as scientists to engage the public, Indiana State Museum, March 18, 2017.
- Cell-fie Science YouTube channel consisting of brief self-produced videos about various plant biology topics. Launched August, 2016: `https:\www.youtube.com/channel/UCh8KPAsLVDqiHY2bfKoAZbA`.
- Leaf Anatomy hands on demo and activity booklet in Mr. Stephen Lockes 2nd grade class at Arthur C Newby Elementary School, Speedway, IN. May 4, 2016.
- Chemical identification for Forensic Bear Badge experiments with Bear den from Cub Scout Pack 504 March 7, 2016.

- Super Science Bear Badge demonstrations and experiments with Bear den from Cub Scout Pack 504 March 14, 2016.

- #TeamAutotroph Commandeers @RealScientists host of rotating Twitter account @RealScientists on plant stress biology. February 27 March 5, 2016.

- Jen Talks Plants host of rotating Twitter account @Biotweeps on various aspects of plant stress biology. October 19 24, 2015.

- Plant Biology: A Behind the Scenes 5 part video series for Mr. Stephen Lockes 2nd grade class at Arthur C Newby Elementary School, Speedway, IN. January February, 2015.

- Breathing Plants: Discovering Stomata hands on demo in Mr. Stephen Lockes 2nd grade class at Arthur C Newby Elementary School, Speedway, IN. February 6, 2015.

- Warner′s Wonderful World of Coral Reefs hands on demo and activity booklet at Coast Day, University of Delaware, Lewes, DE. First Sunday in October 2003 2006.